Optimized Firefighting Aircraft

DSE - Final Report

Group 19 – June 2025

César Iglesias Olloqui	5706947	Eliot Azoulay	5761158
Jorge Perez Ruano	5758777	Darío Díez Zarraga	5677882
Maximiliano Comenge	5714672	Nicolás Nogueiras García	5683408
Simon Caron	5529808	Marcos Carrera Valle	5682525
David Julian Hasler	5687187	Syméon Verstraete	5763452

Delft University of Technology

TU Delft

Optimized Firefighting Aircraft

DSE - Final Report

by

Group 19 – June 2025

César Iglesias Olloqui	5706947	Eliot Azoulay	5761158
Jorge Perez Ruano	5758777	Darío Díez Zarraga	5677882
Maximiliano Comenge	5714672	Nicolás Nogueiras García	5683408
Simon Caron	5529808	Marcos Carrera Valle	5682525
David Julian Hasler	5687187	Syméon Verstraete	5763452

Project duration: April 22, 2025 – June 27, 2025
Tutor: Dr. Marta Ribeiro
Coaches: Dr. Tercio Lima Pereira,
Dr. Calvin Rans
Group TA: Hanna Niemczyk
Institution: Delft University of Technology
Course : AE3200 Design Synthesis Exercise

Cover image credit: 3DExperience

TU Delft

Executive Overview

The Final Report of the Wildfire Optimised Firefighting Aircraft, named W-132, sums up the work of Group 19 of the Design Synthesis of Delft University of Technology. From the 22nd of April to the 27th of June, ten students worked on this project under the supervision of Dr. Marta Ribeiro. The goal of this project is to develop a firefighting aircraft capable of meeting the demands of a market that lacks purpose-built aircraft and faces an ever-increasing threat. The W-132 is capable of making precise, targeted drops thanks to its high manoeuvrability, whilst maintaining a very high cruise speed and payload relative to its competitors. This report includes logistics, operations, sustainability, design process, feasibility, risk and cost analyses, providing a thorough overview of the team's achievements.

An image of the final design can be seen below.

Figure 1: *Final Design of W-132, 3DExperience*

Project Objective Statement

To design a next-generation, purpose-built aerial firefighting aircraft optimised for European wildfire conditions. The aircraft will be developed for its specific landscape - vegetation, water sources available and complex terrain, with mission-driven requirements including high manoeuvrability, volume of water drop rate and rapid turnaround. The COLOSSUS SoS X Grand Challenge will be used as a tool to support validation, but it is not the primary design driver. The concept will target an entry into service around 2035, incorporating advanced technologies where feasible.

Mission Need Statement

The growing threat of wildfires across Europe demands rapid, flexible, and high-performing firefighting solutions to reduce the increasing risk of large-scale damage caused by the rising frequency and severity of forest fires. Current aerial firefighting platforms—often adapted from previous designs—are not purpose-built for Europe's specific geographic, environmental, and operational context, limiting their effectiveness.

The aim of designing an operational aircraft by 2035 is critical to take a step back and look at a broader picture of the design process. Strategic planning and fleet composition must be analysed alongside the technical development of the aircraft to ensure successful mission-specific design. This will ensure that the design meets real-world demands instead of something already in the market.

Market Gap Analysis

A critical market gap in the European aerial firefighting market was identified, namely the absence of a high capacity purpose-built aircraft that is optimised for European geography and operational constraints. Existing aircraft either fall short in the established performance requirements or are aging and becoming increasingly unreliable, which specifically applies to larger fixed wing firefighting aircraft. The market analysis revealed a niche for a lightweight, high-performance aircraft designed specifically to integrate into current European fleets. Through a trade-off a large fixed wing scooper aircraft was demonstrated as being the most optimal choice, over VTOL and helicopters. The W-132 addresses this market gap by focusing on improving performance parameters that are most critical aerial firefighting in the European market.

Operations and Logistics

The W-132 has been designed to provide the most performance gain within European countries with the fewest number of aircraft. The main use case of the W-132 is to be purchased using half of the RescEU budget and provide the largest coverage over Europe. It is also designed to operate well within current and future European risk areas. The aircraft's design also complies with requirements set to ensure that it is capable of integrating well into European firefighting infrastructure, both in the air and elsewhere, where an overview of the complete operational lifecycle of a firefighting aircraft is provided from pre to post-mission maintenance. Furthermore, the timeline, from the detection to the extinction of fire, is broken down showing how the existing aircraft fits into the chronology of a firefighting process,

The strategies used for the three mission types that the W-132 will conduct are designed for the European market and ensure the aircraft was designed with high-performance targets even in conservative mission parameters.

Sustainable Development Strategy

The aircraft's design prioritizes performance while incorporating sustainable innovations wherever they complement operational capabilities. A representative mission scenario was developed to quantify the emissions saved by the W-132 and compare them with those of its main European competitor, the CL-415. The analysis, which is carried out for a specific scenario, demonstrates that the W-132 emits more emissions per mission due to its design characteristics. However, these provide better firefighting capabilities, leading to a greater saving of fire emissions. Adding both effects, the W-132 achieves significantly greater net emission reduction in the proposed scenario, of up to 1172 tonnes of CO_2 per mission.

Aircraft Design

The overall performance parameters of the aircraft are shown in Table 1.

Table 1: *W-132 Performance parameters*

Parameter	Value	Unit	Parameter	Value	Unit
Maximum take-off weight	39780	kg	Fuselage length	20.2	m
Payload	13200	L	Fuselage width	2.0	m
Cruise speed	741	km/h	Wing area	140.5	m^2
Stall speed	120	km/h	Aspect ratio	9	-
Mission range	688	km	Hybrid-assisted take-off distance	1300	m
Ferry range	2450	km	Take-off distance	1800	m

This DSE focused on performing a feasibility study for a firefighting aircraft. Hence instead of focusing on many small details of the aircraft, only the critical aspects of the design were investigated. Namely, the wing overall design, the wing box, the empennage, the fuselage, water tanks, and propulsion were sized here.

Wing Group

An innovative approach was carried out when designing the wing. To make it a fully purpose-built aircraft, manoeuvrability was a top priority given the frequency of scooping and releasing manoeuvres in aerial firefighting. As a result, the design was adapted to maximise efficiency at low speeds rather than cruise conditions.

By implementing double slotted flaps, slats, and a blown flap boundary layer control mechanism in a NACA 4412 airfoil, stall speeds as low as 120km/h can be achieved. This facilitates precision and altitude of water dropping, effectively increasing the amount of useful water dropped on the fire.

The wing box was sized to withstand the loads acting on the wing, in the worst case scenario of the limit load of 4g that was determined from the V-n diagrams. The wingbox configuration was optimized for the lowest weight while still withstanding the critical failure stress, identified to be skin panel buckling. The overall weight of the wing group (without the engine) turned out to be 5066 kg.

Propulsion

The W-132 features an innovative parallel hybrid electric propulsion system with an in-house designed internal combustion engine, the WE-3000, built specifically for use in a hybrid parallel system. Through discussions with an expert a novel configuration where the internal combustion engine is optimised for one power setting and the hybrid system serves to provide additional power where needed was designed. This configuration allows for versatile mission profiles and increased firefighting capabilities through increased efficiency and manoeuvrability.

Empennage

The empennage faced the challenge of having to provide a large correction moment with a small tail arm. For this, the decision of placing part of the empennage beyond the aft end of the fuselage was made. This allowed to provide sufficient stability without an excessive tail size.

A T-tail configuration is used with symmetrical airfoils, yielding dimensions slightly larger than that of the CL-415. Additionally, ventral and dorsal fins ensure optimal low speed behaviour and spin recovery, allowing for aggressive manoeuvres during firefighting missions.

Fuselage

The fuselage is designed using 2 main design philosophies. The first being that the exterior must be hydrodynamically stable to allow the aircraft to perform scooping mechanisms during missions. The second is that the aircraft must be purpose built so as to minimise unnecessary weight.

Through these design decisions, a compact unpressurised fuselage design is chosen so as to limit the volume of unused space. The choice of an unpressurised fuselage is done as most of the firefighting mission is done within breathable atmosphere while relatively light oxygen tanks can be used during the completion of the ferry range. This slender fuselage design also allows for a minimisation of the water slamming forces, thereby reducing the weight of the necessary structural reinforcements.

The choice of a carbon fibre reinforced polymer based fuselage is also done as this leads to weight savings of the fuselage. Thanks to the "snowball" effect, this leads to massive weight improvements

of the entire structure.

Storage Subsystems

The storage subsystems encompass the water tanks, foam concentrate tank and oxygen tanks. Although the majority of the space is taken by the water tanks as the foam can be stored as a concentrate, greatly reducing their volume and the oxygen is stored in very high pressure, rendering the volume negligible.

The water tanks are made such that they reduce slushing through the use of baffles. The dispensation mechanism utilises a coupled actuator to avoid unequal water drops and as such high instability in case of failures.

Verification and Validation

Verification and validation of requirements, numerical model and final design was performed thoroughly to ensure the validity of the design. To verify requirements, inspection, analysis, demonstration or test methods were used. For the numerical model, unit tests of multiple functions and files was done, together with an overall sensitivity study to validate the model against expected outcomes. Finally, external tools such as Colossus, flight route simulations or water drop simulations validated that the W-132 can be a valuable asset in the European firefighting market.

Aircraft Subsystem Logistics

The aircraft uses modern avionics so as to optimise the amount of information available to the pilots. This is done to reduce the risk of the aircraft and increase the success rate of the mission. In addition to conventional aircraft equipment, this design utilises water tank related controls and sensors as well as high degrees of redundancy.

Cost Analysis

The price of the aircraft was found to be $50.6 million, after a sensible cost analysis, consisting of RDT&E analysis, making use of Raymer, and DAPCA IV CERs methods[1], then using a production learning curve and break-even ROI analysis, the price was found. Finally, operating costs were estimated to be in the range of $2-7 millions per year. A possibilty for European funding to drive down costs was also looked into.

Risk Assessment and Contingency Plan

To identify the most major threats of the mission, a risk analysis and contingency management was carried out. 37 different risks were identified across 7 different mission phases. 19 of them are reduced in level of risk either by their severity or their likelihood through the contingency management while 17 of them are fully mitigated. The result of this contingency management was eight new requirements used as a way to further constrain the design and create its "design space". Furthermore, the RAMS (Reliability, Availability, Maintainability, Safety) of the aircraft is assessed. The reliability of the W-132 is qualitatively assessed through the redundant methods applied to different subsystems. The availability is considered significant considering that the aircraft can be integrated into existing European fleets and also has very quick response times. Then in terms of maintenance, certain subsystems such as the wing and empennage will require longer term but periodic and heavy inspections while other subsystems will require more in detail routine visual, borescope, functional and operational checks such as the engines. Finally, significant safety measures have been adopted by mitigating risks such as failed battery charging, propeller blade failures, blocked water intakes and overheating from the fire.

Future Development

This DSE W-132 project sets the foundation for a potential fully operational aircraft by 2035. For this the design should first be further detailed, after which it could be manufactured and certified under the CS-25 regulations. The aircraft could then finally be distributed. Due to its low production volume, the aircraft parts should be produced in already existing facilities around Europe to diminish the fixed production costs, and take advantage of existing expertise.

Contents

1

Introduction

The W-132 has been developed in direct response to the escalating threat of wildfires across Europe's coastal and southern regions, where rising temperatures and prolonged dry seasons have intensified due to the frequency and severity of fires. These wildfires endanger both urban and rural areas, placing immense pressure on ecological systems, infrastructure, and public safety. In response, the European Union has expanded its firefighting fleet, currently consisting of 28 fixed-wing aircraft and 4 helicopters [2]. However, this expansion has not been accompanied by significant technological innovation. Most notably, no major advancements have been made since the introduction of teh Canadair CL-415, itself being a redesign of the 60-year-old CL-215, which is why mission specific firefighting aircraft are needed.

The W-132 scooper firefighting aircraft, produced as part of the AE3200 Design Synthesis Exercise, aims address this gap by optimising for operational efficiency, cost-effectiveness and tactical deployment. Developed as part of the COLOSSUS SoS Exploration Grand Challenge, the aircraft is intended to enter service by 2035. It will enable the EU to strengthen its wildfire response while staying within the financial constraints of the 600 million euro RescEU budget. The design will target a unique niche: a high-capacity platform capable of outperforming existing solutions in wildfire suppression missions through purpose-built performance and adaptability. The W-132 will be designed to meet strict targets: a cruise speed of 250 km/h, a 10,000-litre water payload, a maximum take-off weight of 40,000 kg and a 500 km range—based on the needs of stakeholders like RescEU and CAL FIRE, supported by market and fleet analyses. Large aircraft may be prioritized given their strategic value. A key goal, tied to the COLOSSUS Sos Exploration Grand Challenge, is to develop an operational strategy for its use in coordinated firefighting fleets, evaluating both homogeneous and mixed configurations through simulations using the COLOSSUS SoSID toolkit.

The report is organized in the following manner. First, Chapter 2 provides an overview of the functions the aircraft has to fulfil and a flow diagram demonstrating their interconnectedness. Chapter 3 underlines a major market gap. Chapter 4 defines the use case and gives an overview of the operational framework. Then, Chapter 5 provides a sustainable plan for the W-132 design and its environment impact. Subsequently, Chapter 6 begins by highlighting the results of the preliminary class 1 and 2 weight estimations together with manoeuvre and gust load analysis. These sections are then followed by the propulsion system design, an extensive aerodynamic analysis of the wings and a drag estimation. Moreover, the wing design is carried out together with it's structural and material analysis. Additionally, the CG excursion along with the stability and control analysis is carried out leading to the final sections of this chapter with the empennage, fuselage and undercarriage designs. Chapter 7 features the final design characteristics and budget analysis. Also, Chapter 8 addresses the verification and validation methods that are carried out to justify the reliability of the design. Chapter 9 portrays system connectivity, software block and data handling block diagrams. Chapter 10 assess the potential mission threats and risks with their respective mitigation processes. Then, Chapter 11 carries out a cost analysis providing a final return on investment of the W-132. Finally, Chapter 12 demonstrates the future development after the preliminary design of the W-132.

2

Functional Analysis Overview

Two diagrams found in Section A.1 show all functions that the aircraft must perform throughout its life cycle, from conceptual design to decommissioning. The Functional Flow Diagram, which presents functions in a temporal sequence, and the Functional Breakdown Diagram, which organizes functions hierarchically. These diagrams provide a comprehensive overview of the aircraft's tasks, ensuring that no aspect of its life cycle is overlooked.

2.1. Functional Flow Diagram

The functional flow diagram orders the aircraft's functions in a temporal sequence and presents a high level of detail for all the top-level functions the aircraft shall perform such as design, manufacture, distribute, operate and retire.

While this design synthesis exercise focuses primarily on designing for the operation part, rather than the manufacturing or the retiring phase, the functions cover all these aspects of life cycle of the aircraft, as they may still lead to the derivation of new significant requirements.

First, the five main functions are decided upon, which are later on grouped into three main areas of Pre-Operation, Operation and Post-Operation as can be seen in the Flow Diagram. These were each divided into subfunctions consisting of levels 0, 1 and 2. Given that some of the processes are non-linear, several functions are then related to other ones with the use of decision blocks, clearly showing how the whole process is followed.

2.2. Functional Breakdown Diagram

The functional breakdown diagram proposes the same functions but orders them clearly in a hierarchical structure. This way, each function can be traced back to its parent function. This is useful to understand where each function is derived from. If all subfunctions are performed, the parent function is by definition also performed. Similarly to the functional flow diagram, the FBD also helps identify new requirements by looking at their hierarchy and their interdependency. It can also be seen in Section A.1.

3

Market Gap and Analysis

This chapter identifies the current aerial firefighting situation in Europe in order to target demands that are currently not met to tailor the design of the W-132. To do so a market analysis is carried out, analysing existing firefighting aircraft and the European market, followed by user requirements and a trade-off where the plane is selected as final concept based on the above. Finally, a sensitivity analysis is carried out to define key parameters.

3.1. Market Analysis

The market analysis evaluates several aircraft and helicopter models against the three main user requirements and examines the influence of geography in the European market's needs for firefighting.

3.1.1. Existing Firefighting Aircraft

There are four main user requirements that define the performance targets for this aircraft. Though these are not set in stone, they serve as a guideline for what can be expected from this aircraft and a point of comparison with others in the market. These requirements are:

- Cruise speed shall be equal to or larger than 250 km/h.
- The aircraft shall be able to carry at least 10,000 L.
- The operational range shall be at least 500 km.
- The maximum take-off weight (MTOW) shall be below 40 tons.

Performing an analysis of current aircraft in the market that are still operational shows that no fixed wing aircraft and only one helicopter matches them.

None of the fixed wing aircraft manage to reach these requirements, but some get close namely the RJ-85 and the Beriev Be-200 also it is important to mention that the CL-415 is also not too far from reaching these requirements as it is the primary comptetitor for aerial firefighting in Europe. From these only two are scooping aircraft, the Be-200 and the CL-415. The Be-200 is no longer accessible for countries within the European Union, while the CL-415 flew for the first time in 1993, 32 years ago, so it is safe to estimate that its design process began 40 years ago. Many of the CL-415 in European fleets are old and are becoming an unreliable tool for aerial firefighting.

Regarding aircraft types, the market analysis reveals an interesting trend. Very Large Air Tankers (VLAT) are perhaps unnecessarily large, causing them to have poor manoeuvrability and inefficient in fighting the problem of water evaporation. On the other hand, Single Engine Air Tankers (SEAT) are too small to carry the amount of water needed. Nonetheless, fleet compositions cannot be discarded. This decision will also depend on whether tankers or scoopers are selected.

Table 3.1: *Market analysis of air-planes versus performance requirements [3–8]*

Aircraft Models	Type	Cruise speed (km/h)	Capacity (L)	MTOW (tons)	Operational range (km)
DC-10	VLAT	563	35583	259	9493
Boeing 747-400	VLAT	724	68137	413	13700
RJ-85	LAT	563	11356	42	2037
Lockheed EC-130Q	LAT	563	15142	70	3800
Boeing MD-87	LAT	563	11356	68	4630
Lockheed C-HC-130H/J	LAT	370	11356	75	2963
de Havilland Canada Q400	LAT	600	7000	30	2040
Embraer C-390 Millenium	LAT	870	12000	87	6240
McDonnell Douglas MD-87	LAT	830	15000	65	5000
Air Tractor 802	SEAT	322	3028	7	982
PZL-Mielec M-18 Dromader	SEAT	200	2200	4.2	970
Canadair CL-415	Scooper	322	6132	19	2427
Air Tractor Fire Boss	Scooper	274	2650	7	982
Beriev Be-200	Scooper	560	12000	42	2100
ShinMaywa US-2	Scooper	480	13610	48	4700
Target		**>250**	**>10000**	**<41**	**>500**

However, modern fleets not only contain air-planes. Helicopters are crucial in European firefighting missions and are hence also explored as a possible solution to the problem.

Table 3.2: *Market analysis of helicopters versus performance requirements [3]*

Helicopter Models	Type	Cruise speed (km/h)	Capacity (L)	MTOW (tons)	Operational range (km)
Sikorsky/Erickson S-64E/F	Type 1	212	9464	19	370
Boeing CH-47 "Chinook"	Type 1	282	11356	25	740
Boeing CH-46E 'Sea Knight'	Type 1	222	4164	11	265
Kaman K-1200	Type 1	145	2574	3	560
Airbus H215/225 NG	Type 1	257	3785	9	851
Bell 205/210, Bell UH-1	Type 2	195	1893	4.3	556
Bell 212 HP	Type 2	212	1325	5	439
Bell 412	Type 2	225	1363	5.4	980
Airbus H125 NG	Type 3	253	984	2.4	630
Bell 407 NG	Type 3	245	1022	2.7	246
Bell 206 L3/4	Type 3	204	852	1.5	220
Target		**>250**	**>10000**	**<41**	**>500**

The analysis demonstrates that only type 1 helicopters would be able to reach the set performance requirements. These helicopters are large tanker helicopters that employ snorkeling devices to refill

internal tanks. These helicopters face longer refill times than scooping aircraft and usually have large evaporation in the droppping manoeuvre but have significantly improved access to water sources. The Boeing CH-47 is the only helicopter matching the requirements, however it is a military helicopter that is not purpose-built for firefighting, which invites the possibility of having a large room for improvement with a mission optimised helicopter.

A further commercial market analysis is performed in order to identify the market niche that the design can fulfil. This is done by first identifying the stakeholders and categorising them by influence and interest in the outcome of the project. Identifying their needs and wants allows for a more in-depth and complete market study.

This deeper market study reveals the market niche of lightweight high capacity aircraft, unfulfilled by any competing this designs. It is estimated that this is due to the fact that there does not exist any modern, specialised and adapted to European cases firefighting aircraft. Producing this design could therefore prove to secure an advantageous market position.

Following this, a commercial analysis is performed to determine a reasonable asking price for the out of factory aircraft. Due to the premium characteristics and innovative design, a competitive price of 30 million USD is deemed reasonable as it is slightly less than its closest competitor the CL-415.

Synthesising all of these points is done through SWOT (strength, weakness, opportunity, threats) analysis to summarise and categories the discovered traits of the design. This analysis is of the form of the following table :

STRENGTHS	**WEAKNESSES**
• Design fulfils an extremely competitive niche in the market from a performance point of view. • No aircraft are close in performance to the design and as such there are no direct competitors.	• Unproven design which might not end up being feasible. • Low groundwork set for the design of such specific aircraft. • Very lightweight firefighting aircraft seem much more price efficient and might overtake an already narrow market.
OPPORTUNITIES	**THREATS**
• Due to the identified strengths, this design could establish itself as a cornerstone of the market leading to high demand. • Thanks to the innovations, this design could also afford to be sold at a premium but competitive price.	• The requirements might end up being killer and as such lead to a completely failure of the design. • The market niche fulfilled by the design might prove too specific and as such the customer base could be too restrained.

Another important aspect of a firefighting aircraft for the European market is to fit within the existing fleets rather than try to replace all the aircraft in them. Each aircraft type has its own strength and weaknesses for aerial firefighting and combining them together is what will lead to the most optimal performance. The most popular fixed wing firefighting aircraft are the CL-415 and the Fire

Boss while the Sikorsky S-64, Chinook and Bell 412 are the most popular helicopters [9][10][11][12]. The Fire Boss, Chinook and Bell 412 are all still currently manufactured [12][13], so small fixed wing aircraft as well as small and large helicopters are all already well established within the European market. On the other hand, while Europe may have a lot of CL-415s they are becoming difficult to operate and are often unable to complete their missions due to maintenance problems, according to Wissam Chalabi an expert on aerial firefighting. This presents a clear opportunity to present an aircraft that serves a similar role to the CL-415 while also covering the role of large and very large air tankers and being optimised specifically for the European market.

3.1.2. European Market

The European continent has a diverse geography, particularly in the Mediterranean, which is the most affected area by wildfires. It is a region with high elevation changes close to the sea, demanding a high rate of climb. Manoeuvrability is a key factor when accessing lakes and inland water sources as many are located in mountainous regions, though access to the sea in the region is the case most times. In other cases water bodies will need to be used for refilling, while available data on water bodies is difficult to find for Europe estimates can be made for standard values to use for designing based on previous missions. On the other hand data on airports and airfields within Europe is accessible and thus derive values for expected distance between airfields and fires to base the design upon. Furthermore, data on these airports respective lengths are also available. All the findings from this market research are summarised in Table 3.3.

Design Consideration	**Relevant Value**
Distance to snorkeling water body from fire	10 [km] [14]
Distance to large scoop-able water body from fire	25 [km] [14]
Maximum distance to fire from airports	200 [km] [15]
Percentage of runways longer than 1800 [m]	87% [15]
Percentage of runways longer than 1300 [m]	98% [15]

Table 3.3: *European Market Analysis Results*

This data shows that an aircraft employing using 1800 [m] long runway will be able to use an already significant amount of runways in Europe. Furthermore, a design that under normal conditions takes-off from these larger runways but is able to land at the smaller runways if one is nearer to fires would allow for a much more versatile mission profile. The data also allows for the definition of a standard design mission for fixed wing aircraft, where the plane would fly 200 [km] to the fire, conduct drops using a water source 25 [km] from a fire and then return to its original airport of deployment if that is the closest airport.

The values shown in Table 3.3 are taken from looking into previous cases, looking at maps and making judgements on reasonable values to design for instead of over designing for maximum values. However, further work could be conducted analysing distance of areas of high risk in Spain to water bodies using different European available datasets. Conducting a more detailed analysis on the geometries of water bodies in Europe as well as their surrounding area (i.e. are they in a valley, a mountainous area or a plain) could allow for an understanding of how tweaking scooping time/distance or manoeuvrability would improve access to water bodies and thus fire fighting performance.

3.2. User Requirements and Trade-off

From the following user requirements, Figure 3.1, which were later on divided into mission and system requirements, certain sub-system requirements showed to have an impact on the trade off and hence, these subsystem requirements were then detailed as much as possible.

In some cases, these requirements were too constraining and had to be re-evaluated with the customer. An example can be "The aircraft shall be able to refill water tanks using a snorkel device", where it ended up being removed, given that the most practical method for the aircraft design was having a scooping mechanism.

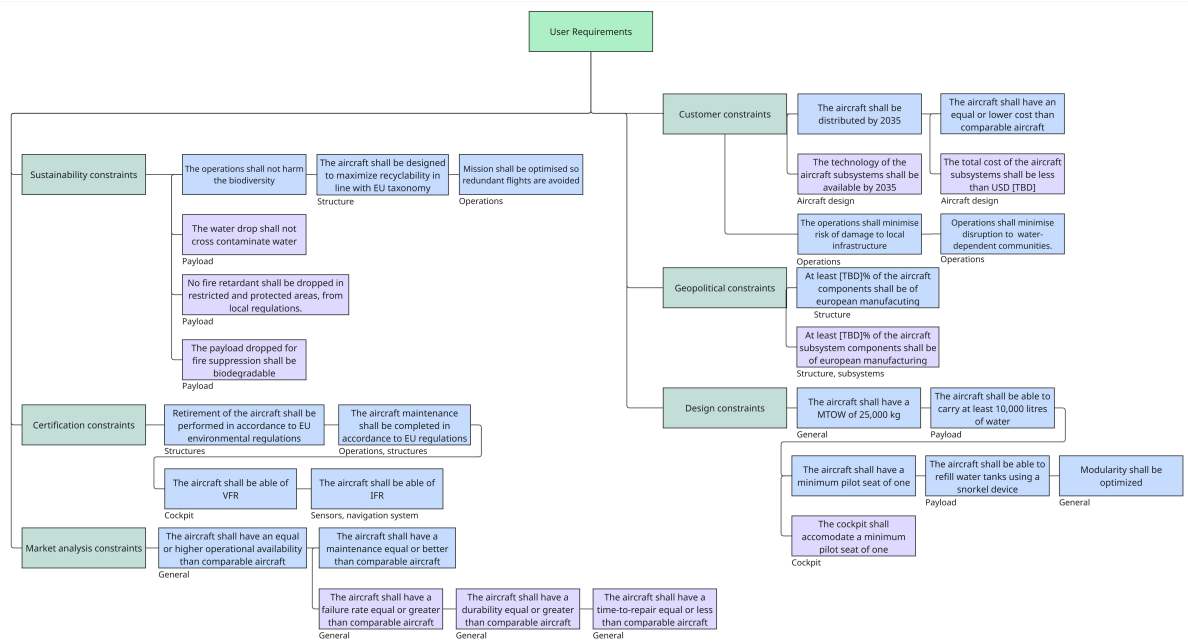

Figure 3.1: *User Requirements*

From these further developed requirements, the trade-off was performed as can be seen in the table below.

Table 3.4: *Comparison of VTOL, Helicopter, and Plane: Performance and Operational Criteria*

Criteria	Weight	Sub-Criteria	Weight	VTOL 1	Helicopter	Plane
Cost	0.3	Acquisition	0.25	0.88	1.00	0.70
		Operation	0.6	0.37	0.79	1.00
		Maintenance	0.15	0.50	1.00	0.50
Firefighting capabilities	0.5	Water drop rate	0.7	1.00	0.87	0.80
		Airport accessibility	0.1	1.00	1.00	0.75
		Response time	0.2	0.78	0.53	1.00
Sustainability	0.1	Life-time	0.5	0.90	0.90	1.00
		Emissions	0.5	0.75	0.50	1.00
Risks	0.1	Development	0.5	0.75	0.50	1.00
		Operational	0.5	0.75	1.00	1.00
Performance				**79%**	**81%**	**87%**

After thorough tradeoffs for all three Helicopters, VTOL and Planes were carried out, one design was chosen for each. Following these selections, the final trade-off is performed using a set of criteria organised into four main categories: cost, firefighting capabilities, sustainability, and risk. The cost category includes acquisition, operation, and maintenance costs. Firefighting capabilities are assessed based on water drop rate, airport accessibility, and response time. Sustainability is evaluated in terms of life-cycle impact and emissions. Finally, the risk category considers both development/ knowledge risks and operational risks.

The plane concept emerges as the best overall design, ranking highest in operational cost, response time, sustainability, and risk, while still maintaining a relatively high water drop rate compared to the other concepts. Although the results appear conclusive, a sensitivity analysis is performed to ensure a fair comparison by varying the weights of the different criteria to observe whether the outcome changes. A critical scenario is also considered, in which emissions and development risk are excluded from the evaluation. Even in this case, the plane concept, consistently remains the top-performing option.

3.3. Sensitivity Analysis for Key Design Parameters

As a large scooping aircraft configuration was chosen it is important to analyse which parameters of design for such an aircraft could be improved to achieve the most performance gain. This analysis must be conducted taking into account existing fleets to ensure that performance gains will actually lead to an improved performance overall rather than cases where the aircraft operates alone. For this Spain was chosen as data on their firefighting resources is available Figure 3.2)[16]. Furthermore, out of the countries most currently affected by wildfires it has a large amount of fires not within a 50km radius from the sea and thus presents a more challenging case. This paired with with the risk data presented by EFFIS (European Forest Fire Information System) [17] which assesses the risk of a spatial cell when modelling wildfires and as well as other types of vegetation allows for analysis into which parameters will best improve performance in high risk areas (can be seen in Figure 4.2b).

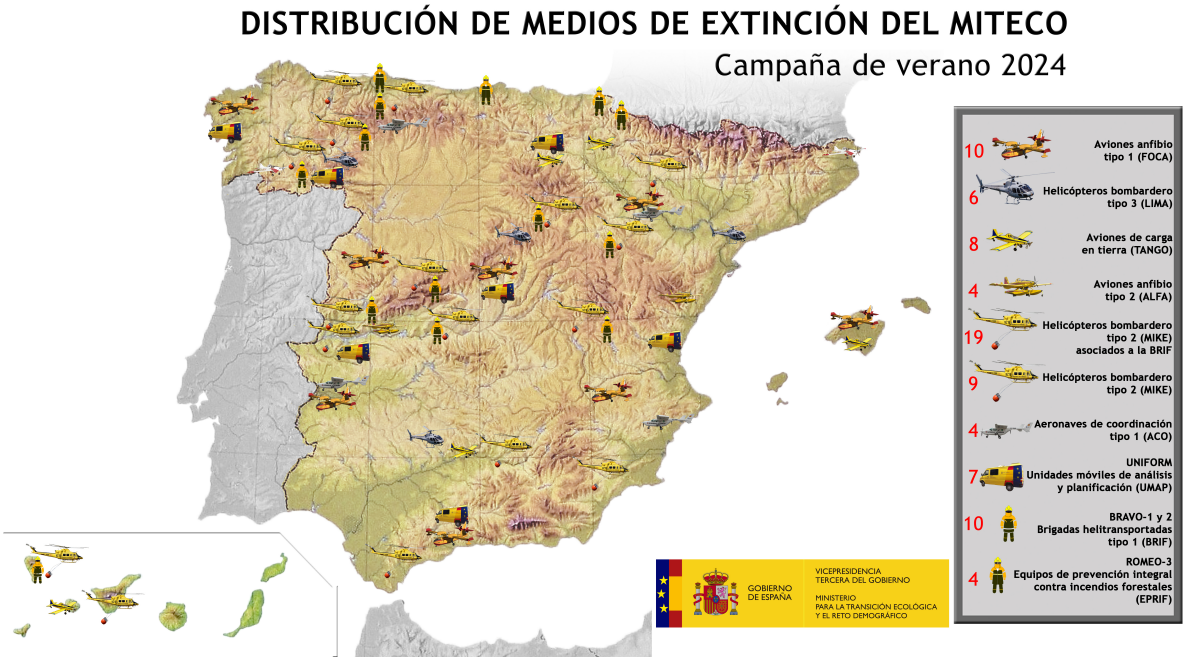

Figure 3.2: *Available firefighting resources in Spain [10]*

From speaking with an external expert who has worked on many similar projects two key aspects were identified in terms of firefighting performance, namely the response time and the water flow rate. The response time represents the time taken to reach the fire after detection, and it is critical as wildfires spread exponentially meaning that even a few minutes more could mean the fire is significantly larger. Next the water flow rate represents how much water can be dropped on an area per area and is significant as being able to drop more water per hour means being able to put more fire out or make a larger area of land less prone to burning. Note that this analysis takes into account the water dropped that reaches the ground and not just the total water dropped. These two criteria can be combined with the risk score the EFFIS database creating the risk score and impact score presented in Equation 3.1 and Equation 3.2 respectively.

$$\text{risk score} = \text{risk} \cdot \text{response time} \tag{3.1}$$

$$\text{impact score} = \text{water dropped per hour during one mission} \cdot \text{response time} \tag{3.2}$$

Using the CL-415 as the baseline as it is already integrated into the Spanish fleet its performance parameters were increased individually (or decreased in the case that a lower parameter is more beneficial such as reducing time to warm up) by 10%.

Table 3.5: *Risk Score Sensitivity*

Parameter Changed	Mean Risk Score [Min]	Improvement From Baseline (%)
Standard CL-415	19.9	N/A
10% Reduction in Ground Time	19.7	1.1
10% Increase in Cruise Speed	19.5	2.3
10% Increase in Rate of Climb	19.8	0.5

Table 3.6: *Impact Score Sensitivity*

Parameter Changed	Impact Score [L/hr]	Improvement From Baseline (%)
Standard CL-415	43500	N/A
10% Reduction in Ground Time	43600	0.2
10% Increase in Cruise Speed	47800	9.9
10% Increase in Rate of Climb	44300	1.8
10% Reduction in Stall Speed	44300	1.8
10% Increase in Payload	46000	5.7

The results of the study are show in Table 3.5 and Table 3.6, and demonstrate clearly that cruise speed is the most important parameter to improve upon as well as payload while improving ground time can help with response time but not much with the mass flow. However, it is important to note that it is not possible to just increase a parameter like cruise speed while keeping all other aspects of the design the same. For example greater cruise speeds than the CL-415 are achievable but usually at a cost of extra operational empty weight. These results provide a guideline for moving forward and as a way to balance out choices and reason out design decisions.

Similarly to Subsection 3.1.2 the analysis conducted here can be further expanded to allow for better optimisation of the design. First the simulation uses a set distance for the distance between the fire and a water body, incorporating Spanish water body data would allow for a better understanding of

how changing the parameters would actually influence performance. Furthermore, the EFFIS risk data is available for the entirety of Europe so obtaining data like is available for the Spanish fleet for other European states would allow for an expansion of the analysis to the entirety of Europe. This would help ensure that the aircraft is not over designed for Spain. Finally manoeuvrability is not fully taken into account within the simulation, including its effect on drop altitude, water body availability, and performance in complex geographies could provide insight on the benefits of improving on an area where similarly sized aircraft usually struggle.

Table 3.7 demonstrates how the findings in this section were used when designing the W-132. The parameters of high impact identified were used for decisions throughout the decision, though certain parameters of similar impact were improved upon by different amounts due to feasibility. For example, it would have been extremely constraining to try to further reducing the stall speed of the W-132, whereas increasing the rate of climb proved to not constrain the design too much through the use of boundary layer control.

Table 3.7: *Parameter Improvement of the W-132*

Parameter Changed	**CL-415**	**W-132**	**Improvement (%)**
Ground Time	420	378	10
Cruise Speed	92.5	205.9	122.6
Rate of Climb	8.1	11	35
Stall Speed	35	33.5	4.3
Payload	6137	13200	115

4

Operations and Logistics

This chapter details the use case the aircraft falls into and the expectorated mission & operation profiles and operations. This reveals that the aircraft's design is driven by the idea of providing the firefighting performance increase using as little resources as possible.

4.1. Use Case

The W-132 has been designed to provide the most performance gain within European countries with the fewest number of aircraft. With a focus on European collaboration this aircraft was designed so that the European Union could purchase a reasonable amount of W-132 from its 600 million euro RescEU budget. It is unreasonable to assume that RescEU would spend its entire budget on one aircraft type as it will also need the resources to purchase smaller helicopters and planes as well as other firefighting resources such as gear and equipment for the fleet. Thus it will be assumed that at most 300 million euro of its budget can be spent on the W-132. To achieve the greatest performance gains, the design must focus on optimising its coverage of current and future European risk areas, guaranteeing a quick response time as well as a significant increase in water flow on the high risk areas.

From this use case different requirements were derived to drive the design. These requirements are summarised in Table 4.1. The method of how requirement compliance is assessed is explained in Subsection 6.1.1.

Table 4.1: *Requirements Derived From Use Case*

Requirement ID	Description	Compliance	Verification Method
REQ-MIS-1	The aircraft shall have a ferry range of at least 2450 km.	✓	Analysis, verified
REQ-MIS-2	The aircraft shall be able to conduct the ferry mission with discharged batteries.	✓	Demonstration, not verified
REQ-MIS-3	The aircraft shall be able to complete its ferry mission in less than 5 hours.	✓	Analysis
REQ-MIS-4	The aircraft shall cost at most 51 € million.	✓	Analysis, verified
REQ-MIS-5	The aircraft shall be able to fly at least 620 km in 1 hour after a fire is detected.	✓	Analysis, verified
REQ-MIS-6	The aircraft shall be able to drop 80,000 L after reaching a fire 1 hour away, with a water source 25 km away.	✓	Analysis

A ferry range of 2450km ensures an excellent cover of Europe that allows the W-132 to always be at

the disposal of EU members as can be seen in Figure 4.1.

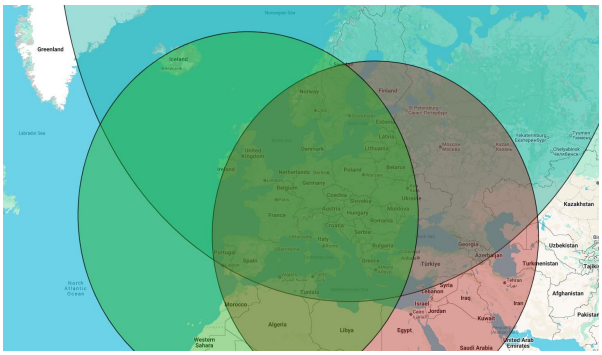

Figure 4.1: *Ferry Range of 2450km over Europe (Green circle centered in Madrid, Blue circle centered in Stockholm, Red circle cetered in Athens)*

Allowing for the ferry mission to be conducted with no battery usage ensures that the aircraft is always able to get within the mission range with full batteries thus allowing it to instantly perform the mission. This also allows the aircraft to use all of its charge during the mission without having to conserve them for the return phase. Furthermore, although the destination airport may have the appropriate batteries in stock, enabling a quick replacement, this is unlikely, as the designated refuelling point could be a small airfield with limited resources. Being able to conserve the battery usage for manoeuvre intensive missions is therefore a priority. Ensuring the ferry mission is completable in at most five hours guarantees the W-132 to be at the disposition of countries in need as soon as possible, this is also much better than the CL-415 which is the main competitor to the W-132.

Aircraft like the W-132 usually do not fly more than an hour to a fire and thus requirements REQ-MIS-1.4, REQ-MIS-1.5 & REQ-MIS-1.6 come from ensuring that using 300€ million leads to adequate coverage of every high risk area in Europe. Furthermore, these ensure that the aircraft will also be able to drop enough water to slow down a large fire by creating a perimeter around it. Figure 4.2a shows the cover of Europe with a mission range while Figure 4.2b shows the EFFIS risk data thus demonstrating that 620km provides sufficient coverage over Europe. Finally the aircraft will be able to conduct at least 10 drops during this ultimate distance mission which with a payload of 13200 L will ensure more than 80000 L are dropped on fires one hour away. This value was chosen as a value representing enough water to set up a 15 meter perimeter on a rapidly growing fire that has had 1 hour to spread and was chosen upon discussion with another group's research.

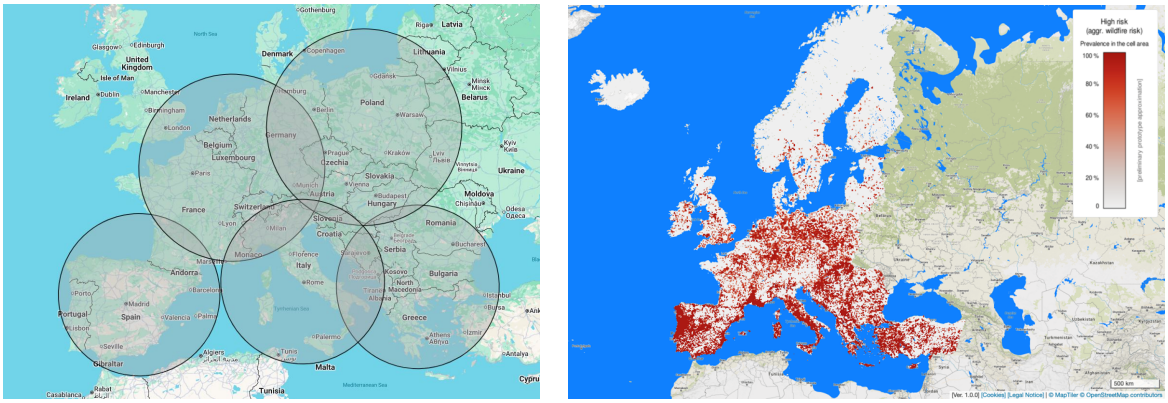

(a) *Mission range map*

(b) *Fire risk map of Europe*

Figure 4.2: *Comparison of mission range with 5 aircraft over Europe with risk map of Europe from EFFIS dataset [18]*

4.2. Requirements

In order to fully describe and understand the operations and logistics of the aircraft, their driving constraints and requirements must be determined. These are shown in Table 4.2. The method of how requirement compliance is assessed is explained in Subsection 6.1.1.

Table 4.2: *Requirements regarding operations and logistics*

Requirement ID	Description	Compliance	Verification Method
REQ-OPS-1	Mission shall be optimised so redundant flights are avoided	✓*	Analysis, not verified
REQ-OPS-2	Retirement of the aircraft shall be performed in accordance to EU environmental regulations	✓*	Demonstration, not verified
REQ-OPS-3	The aircraft maintenance shall be completed in accordance to EU regulations	✓*	Demonstration, not verified
REQ-OPS-4	The operations shall minimise risk of damage to local infrastructure	✓*	Analysis, not verified
REQ-OPS-5	Operations shall minimise disruption to water-dependent communities	✓*	Analysis, not verified
REQ-OPS-6	The aircraft shall have an equal or higher operational availability than comparable aircraft	✓*	Inspection, verified
REQ-OPS-7	Water sources that undershoot the minimum dimensions shall be rejected	✓*	Inspection, verified

The main mechanism used to adhere to all of these requirements is the use of established aircraft firefighting methods. These are, in order, mark every water body the aircraft is capable and authorised to utilise to avoid cross contamination, determine the optimal flight path through specialised trained personnel or using specialised software. This information is then given and displayed to the pilot, beginning the mission.

The maintenance and retirement requirements are adhered to by using conventional and verified methods. The major difference with commercial aircraft is that, because of the manoeuvre intensive and unfavourable environment, much higher maintenance frequencies are necessary during fire seasons. Necessary maintenance checks are therefore necessary at the end of every major operation.

Regarding verification, most of the requirements have not been verified. Requirements needing demonstration cannot be verified until the aircraft is manufactured. REQ-OPS-4 and 5 require the aircraft to be operated to assess the result of the verification. Finally, REQ-OPS-1 has not been verified yet as there is no software available to do this as of now.

4.3. Operational and Infrastructure Descriptions

In order to comprehend the process of operations and logistics of a firefighting aircraft from its deployment all the way through to its maintenance, two diagrams have been thoroughly planned out. The first diagram covering the Concept of Operations (ConOps), Figure 4.3, focuses on the operations part of the Aircraft's life cycle. This includes water collection, fire impression and post-mission maintenance. The second diagram, Figure 4.4, outlines the connectivity that the whole procedure entails by taking a step back and showing the connections from the aircraft with the

ground firefighting teams, drones, satellites helicopters, other planes and command centres. Then, presenting an even bigger picture, a timeline of Operations from detection to post-fire recovery shows how the W-132 should fit into and be designed for efficient uses in time-sensitive operations. Together, these diagrams and the timeline show the whole process of how firefighting aircraft are used all the way from the start of a fire to its extinguishment.

4.3.1. Concept of Operations

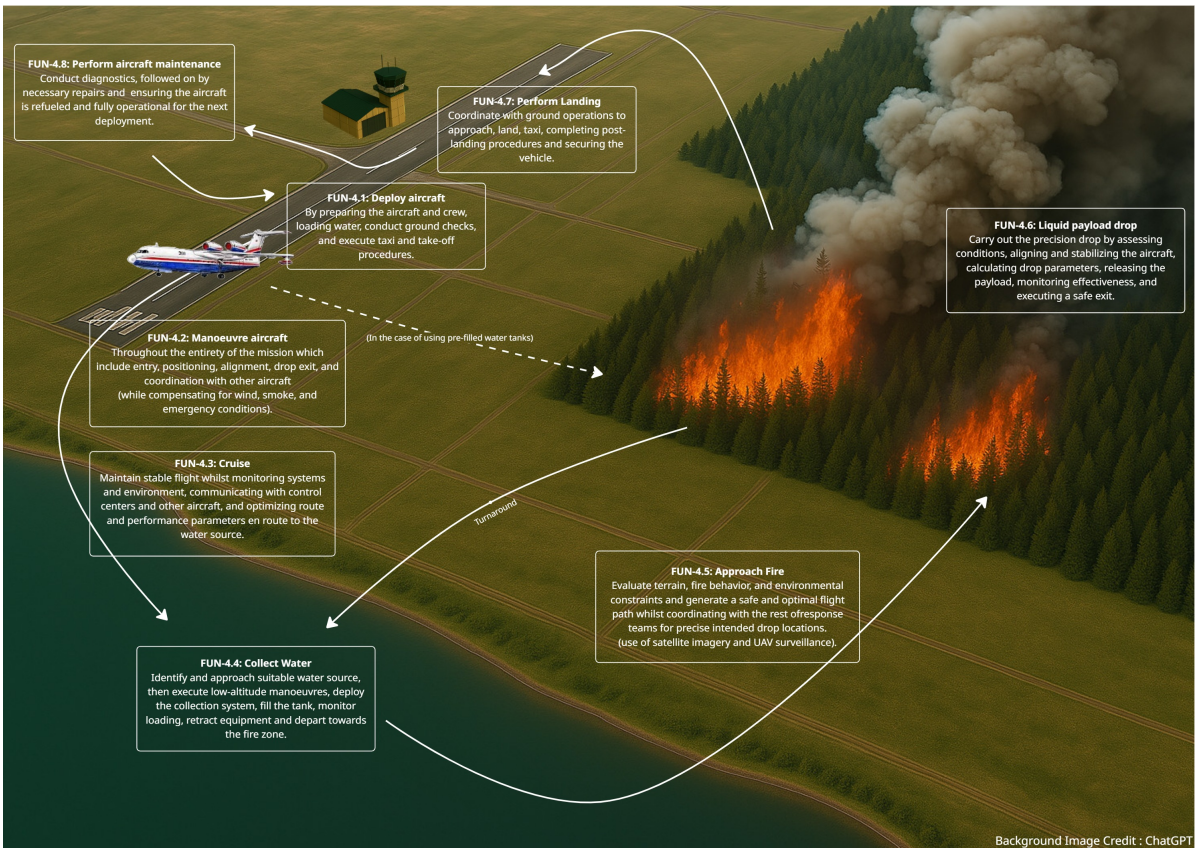

Figure 4.3: *Concept of Operations, own work*

The ConOps diagram shows an overview of the complete operational lifecycle of a firefighting aircraft by highlighting each phase in detail from pre to post-mission maintenance, following from the use the defined functional flow diagram as a starting point. As can be seen, it is broken down into eight main operation procedures, where in some cases these are loops that depend on independent outcomes. For example, after the water body is chosen and the most optimal route is determined, the payload is dropped and the aircraft needs to turn around for more water collection; only when the help of the aircraft firefighter is not needed anymore will it return back for inspection and maintenance.

It is important to point out that the background image is not realistic as both the airport body of water and the forest fire are very close to each other, unlike in most real-life occasions.

This diagram reveals the importance of certain key parameters, these are the airport accessibility, decided by the runway length accessibility, take-off procedure time and the time required to reach the point of interest. Through the use of electric hybrid engines, the take-off length can be reduced by allowing for temporary increase in power, as such the aircraft performs well in this domain especially while empty - which it should be during refuelling parts of the mission. The take-off clearance

time is higher than small aircraft such as the AT-802 in major part due to the necessary authorisations required, this time should not be higher than any other large scooper however. The response time is also compensated by larger speeds reached by the aircraft thanks to its powertrain structure.

4.3.2. Integration into Existing Infrastructures

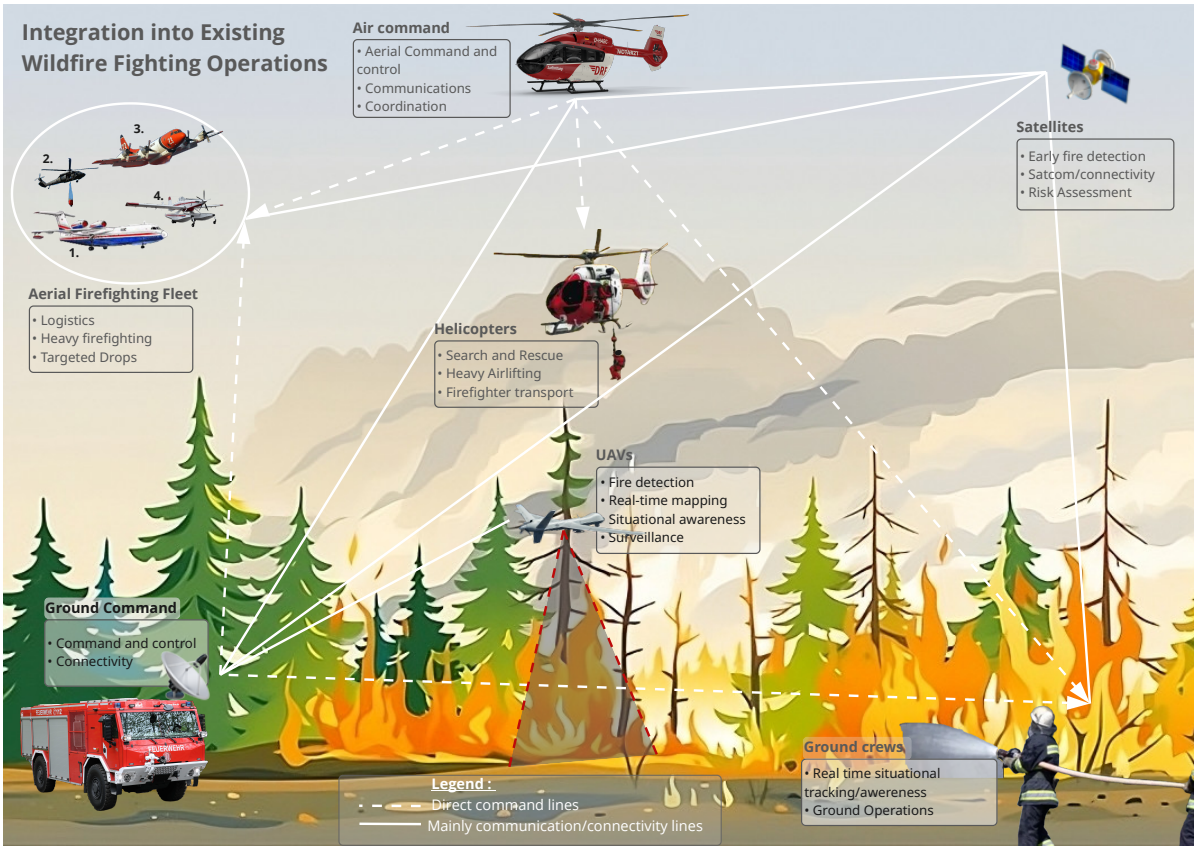

Figure 4.4: *Infographic for integration of the aircraft into existing infrastructures, own work.*

This second infographic is meant to show the existing infrastructure in order to better understand how the chosen design can integrate within it. As can be seen, aerial firefighters mainly depend on orders given by the ground and air commands [19], each of those receiving diverse inputs and information from ground crews, satellites, and UAVs.

An integral part of the project, outside of designing the aircraft itself, is to design a specialized fleet that would be custom-made for the European market. When looking at W. Chalabi's work [3], it can be seen that different combinations of tanker and scooper aircraft in the same situation is not always the best choice to cover intense wildfire fighting, and algorithmic methods can be used to calculate the best paths and combination of tanker/scooper to use per specific situations. Understanding that the designed aircraft will not be used on its own is of the utmost importance. In order to make it competitive, it will be part of a diverse fleet, composed of a possible combination made up of these possible aircraft (seen in the top right-hand corner of Figure 4.4):

1. In the picture, the Beriev Be-200 represents the very large scooper concept chosen in the present report.
2. Helicopters with scooper buckets are used for precision drop and quick response.
3. Very large air tankers are used to drop fire retardant as an emergency preventive measure to

stop fire spread.

4. Small scoopers are more agile and perform better on smaller ranges.

It is essential to highlight the roles of newer technologies in the field and how they can be used in unison with the chosen concept aircraft. These include surveillance drones, that are being increasingly used by first response teams or even pre-emptively as a way to detect fire during the high risk seasons. They enable accurate real-time mapping and close situational updates of the terrain, are also used for catching perpetrators of wildfire of human origin and searching for possible people in distress. Real time drone data is then used to more accurately manoeuvrer the aircraft, for better reliability and facilitates more precise drops.

Satellites, such as those used in the Copernicus program which has a wildfire-specialized arm, are also an application of newer technologies. For example, real-time satellite maps are added to the avionics bay of the design contrarily to currently used designs which do not integrate this, as seen in the CL-415 cockpit in Figure 4.5a. In comparison, in Figure 4.5b a new avionics system already exists, with more interconnectivity in mind.

(a) *CL-415 Old avionics panel*

(b) *CL-415 improved future avionics panel*

Figure 4.5: *CL-415 old/new cockpit configurations*

This integration into existing infrastructure is also an aspect covered in the use case. Indeed, as it can be seen the fleet is composed of versatile aircraft each specialised in performing best in certain situations. As the aircraft is designed to cover large risk areas, it must be complemented with fast response units such as single engine scoopers and helicopters capable of limiting the spread of the fire while it arrives. Reciprocally, the W-132 design fulfils the role "relaying" these aircraft, which are incapable of containing the fire on large scales due to their limited speeds and tank capacities. In this sense, the W-132 aims to replace fleets of tankers and other large scoopers such as the CL-415 by improving on their driving performance factors.

4.4. Timeline

To properly understand the required design of the chosen concept, it is useful to examine how it integrates into the broader timeline of firefighting. A. Passero, an Italian forest firefighter, was consulted and provided insight into the sequence of operations involved in wildfire response, from early detection to post-fire recovery. This helps with understanding the general timeline of wildfire response. It is essential when designing a firefighting aircraft, because it defines how, when, and under what conditions the aircraft is used. Each phase comes with its own requirements, from quick deployment and fast scooping cycles during initial response, to precise drops and coordination with other units during escalation. Designing with a full picture in mind ensures the aircraft isn't just capable on paper, but actually useful in real-world operations where speed, adaptability, and integration with ground teams, drones, satellites, and command centres are key.

1. **Detection** After the fire has started, smoke starts being spotted from either the public, satellite detection or forest surveillance drones. It is important to note that the earlier the detection, the faster the response and less damage is provoked.
2. **Reporting** If spotted by the public, they call 112 and the location and evaluated size of the fire is reported to local fire management authorities, if done trough drones or satellite, data is cross-referenced and forwarded to ground teams to confirm the fire's presence and dispatch resources accordingly.
3. **Initial Response** At first, local firefighters units are deployed to the fire location and firefighters go to the fire by a land vehicle and evaluate the situation. If the fire is small enough it is taken care of by first response teams. Otherwise, bigger units and flying units might be called in while quick containment strategies are put in, and search and rescue missions begin to take place. At this step, drones are being set up, ready to fly, while early warning can be issued to the local populations.
4. **Preventive Measures (during fire)** Several approaches can be taken in order to prevent or mitigate fire. Using hand crews or bulldozers, bigger fire lines are made by clearing strips of land to prevent future fire spread. Another common measure is to start controlled burns ahead of fire or clearing vegetation in order to remove possible fuel.
5. **Escalation Measures** After the arrival of the ground teams, reinforcements are called if the fire is; hard to reach with a land vehicle (one of the main reason why air vehicles are used), a crown fire, too big, too fast or close to houses. These consist of fixed-wing aircraft or helicopters, which are coordinated via command centres and satellite tracking.
6. **Containment and Suppression** The fire is contained by first dropping water at the head of the fire front seen in Figure 4.6, which cools down the flames, allowing ground crews to step in and extinguish the fire. The left and right front are then dealt with in order of risk to closest human settlements. These steps are not set in stone, as forest fire can be very unpredictable and wind can change in a matter of minutes. For final containment, the fire is completely surrounded using expanded fire lines and aerial retardant or water drops. Hotspots are monitored to avoid reigniting and are extinguished, this is also where the use of drones is put in place to help locate remaining heat sources that can further start a new fire.

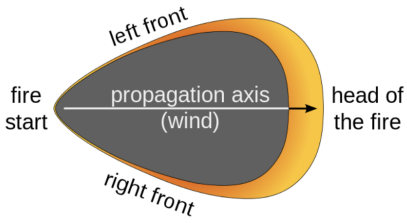

Figure 4.6: *Fire Propagation Diagram*

7. **Full Extinction and Post-Fire Recovery** After the fire is deemed to be extinguished; this is, all visible flames are out, no hot spots remain, even underground (e.g., smouldering roots or peat) and the fire shows no signs of re-ignition under normal weather conditions, then the fire crews declare it "out". After that, damage assessment, soil stabilization (to prevent erosion), and reforestation efforts begin while public safety communications continue if a risk of mudslides or flooding exists.

4.5. Mission

4.5.1. Mission Profiles

The W-132 will need to conduct three different expected mission profiles that will then be used to design and size the aircraft. These missions were identified in Subsection 3.1.2 and in Section 4.1.

The flight profile for the ferry mission can be seen in Figure 4.7. Since the ferry mission must be able to be completed with discharged batteries it can not take-off from runways shorter than 1800 [m]. Furthermore, no phases of the flight employ the hybrid electric system. The aircraft then completes its 3000 [km] of travelling before landing or loitering if needed.

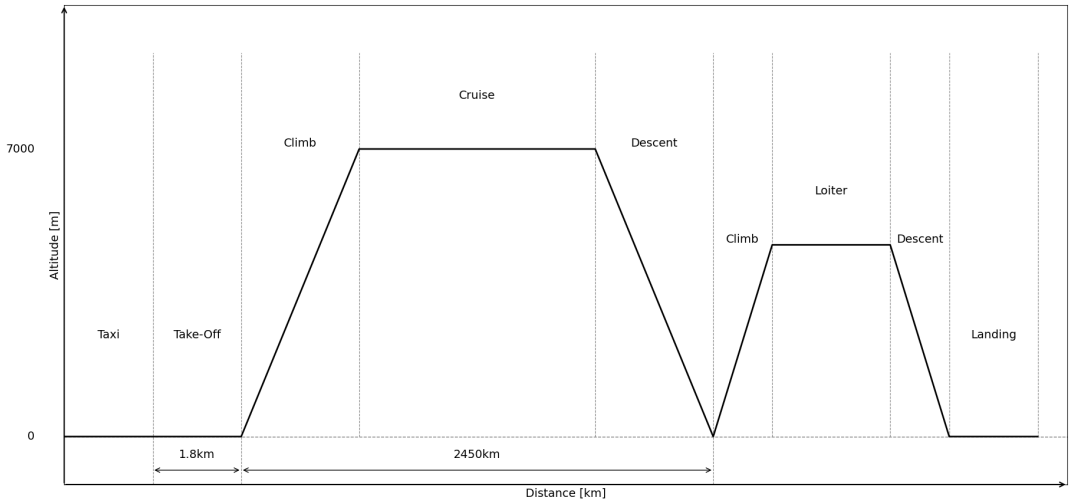

Figure 4.7: *Ferry Mission Flight Profile*

The flight profile for the standard mission described in Subsection 3.1.2 can be seen in Figure 4.8. The blue rectangle represents the firefighting section of the mission and is expanded in Figure 4.9. In both figures, phases where the hybrid propulsion system will be engaged have been made green. Note that the take-off phase for the standard mission only needs to use the hybrid system if the aircraft is being deployed from an airport with a runway shorter than 1800 [m]. Furthermore if an airport is closer than the airport of deployment then it should be employed over the one of origin which could lead to the aircraft being able to conduct additional loops before needing to land.

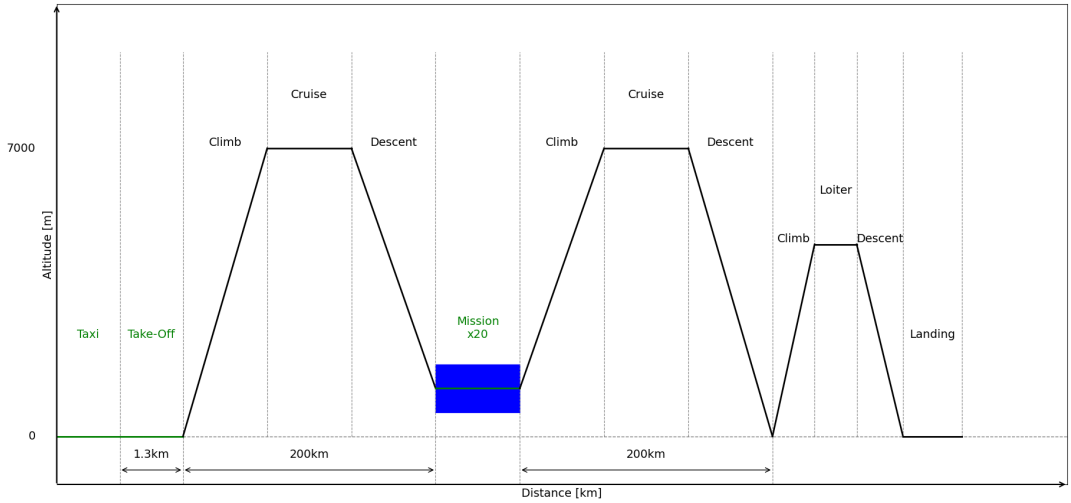

Figure 4.8: *Standard Mission Flight Profile*

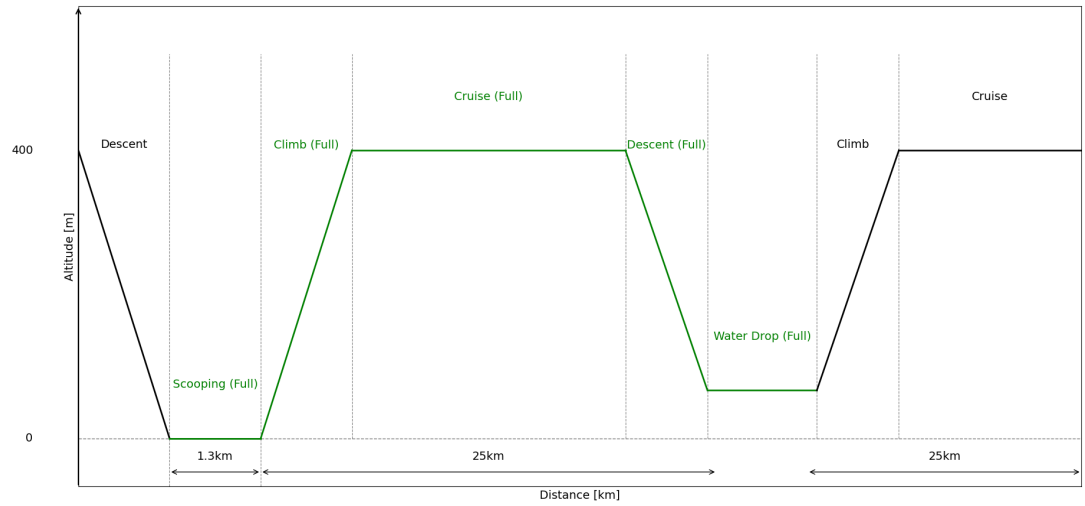

Figure 4.9: *Firefighting Mission Flight Profile*

An important aspect to note about Figure 4.9 is that in the case of a hybrid system failure the aircraft is able to complete the required phases to return to an airport at least 200 [km] away. If the aircraft is full during a hybrid system failure it will need to drop the water before proceeding to an airport. This 200 [km] distance was also used to determine the amount of reserve fuel to include in the aircraft.

Finally there will be times where the aircraft will need to travel long distances and still complete some firefighting loops due to being the only available aircraft. This ultimate distance mission has the aircraft reach the water source 1 hour after being alerted of the fire. After this the aircraft should complete at least 10 loops of the firefighting mission profile (see Figure 4.9). Finally the aircraft will then return to a nearer airport instead of its airport of origin for refuelling, this airport should be at a maximum of 200km from the fire. The mission flight profile for this can be seen in Figure 4.10.

As described in Section 4.1 the aircraft must be able to conduct a mission travelling for one hour to reach the fire, conduct 10 drops and then fly to an airport at most 200 [km] away. This ultimate distance flight profile can be seen in Figure 4.10, where green phases are ones that require the hybrid system.

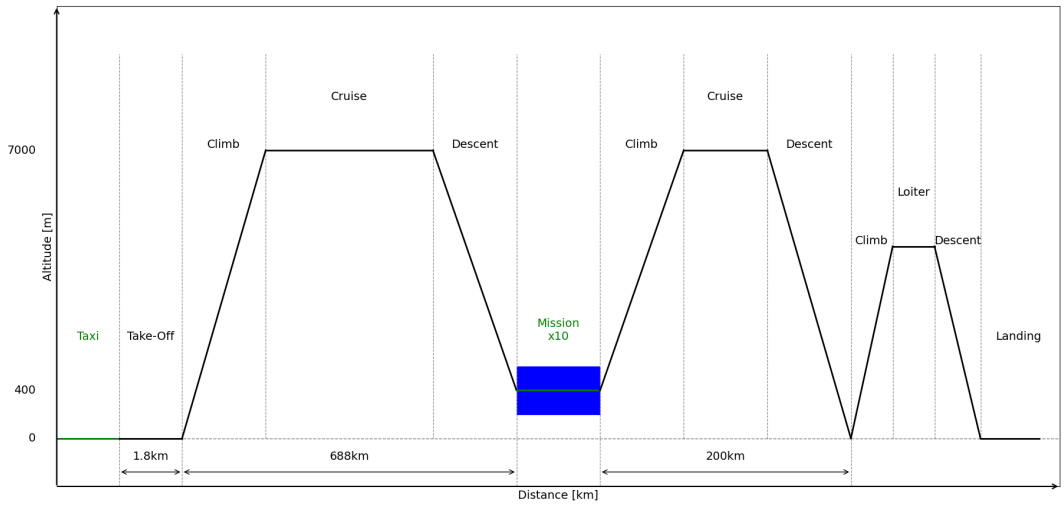

Figure 4.10: *Ultimate Distance Mission Flight Profile*

4.5.2. Hybrid system logistics

Regarding the hybrid design of both electric and conventional fuel-based systems for propulsion, it is important to take into consideration that it takes way longer to charge a battery than conventional kerosene refuelling of the W-132. That being the case, ideally there will be more than one battery in the airports where the aircraft is stationed, given that the aircraft will be positioned as previously mentioned in separate regions and different countries of the southern part of the European Union.

With this, first, the aircraft will always be ready to take off with the battery in use already charged. Then, when sent to its mission, the extra battery will be taken to the closer airport possible with other means of transport such as small planes or helicopters used for the transport of materials. When the battery has been drained and the aircraft also needs to be refuelled, instead of spending a large amount of time charging these, the batteries will be swapped, ensuring that the time taken to change them will always be less than that of refuelling. This is also because charging a battery requires specific equipment that may not be available at many airports, given that the use of batteries in aircraft is recent. In addition, even though changing a 4 ton aircraft battery at an airport requires specialised equipment, given the size of airports W-132 will land on, these are all equipped with machinery capable of lifting heavier than 4 ton objects.

5

Sustainability

The growing frequency and intensity of wildfires in recent years have caused a substantial increase in atmospheric CO_2 emissions. As a result, the aircraft's design prioritizes performance while incorporating sustainable innovations wherever they complement operational capabilities. A representative mission scenario was developed to quantify the emissions saved by the W-132 and compare them with those of its main European competitor, the CL-415. The analysis demonstrates that, due to its purpose-built design and optimized performance, the W-132 achieves significantly greater emission reductions. In this chapter, the emissions analysis will be conducted, while the main performance and innovations' impact on it are explained.

5.1. Requirements

Before explaining the strategy regarding sustainability, the requirements associated with it must be recalled. This is shown in Table 5.1. The method of how requirement compliance is assessed is explained in Subsection 6.1.1.

Table 5.1: *Requirements regarding sustainability*

Requirement ID	Description	Compliance	Verification Method
REQ-SUS-1	The aircraft shall be designed to maximize recyclability in line with EU taxonomy sustainability criteria.	✓	Analysis, verified
REQ-SUS-2	The water drop shall not cross-contaminate water	✓*	Analysis, not verified
REQ-SUS-3	No fire retardant shall be dropped in restricted and protected areas, from local regulations.	✓*	Demonstration, not verified
REQ-SUS-4	The payload dropped for fire suppression shall be biodegradable	✓*	Test, not verified
REQ-SUS-5	Water sources exceeding certain pollutant threshold shall be rejected	✓*	Anlaysis, not verified

Three requirements have not been verified. This is due to the limited time resources. Building a database of the composition of the water sources, restricted areas and testing retardant was deemed unnecessary in the scope of this project and is recommended for further steps of the design of the aircraft.

5.2. Emission Analysis per Mission

This analysis aims to compare the operational life cycle emissions of the W-132 and compare them to the CL-415's, since it is the main competitor within the European market. To do this, the emissions produced by each of the aircraft per mission will be calculated, as well as the emissions avoided per mission, which will yield on the net CO_2 emissions per mission of each aircraft.

Aircraft Specifications

During the design phase of the W-132, sustainability was taken into account in two different ways in order to verify REQ-SUS-1. On one hand, the design choices that are explicitly focused on sustainability but also enhance performance, such as the propulsion system choice, which includes a hybrid-electric engine. On the other hand, some design choices and targets influence greatly the sustainability of the mission, but they do not influence the sustainability of the aircraft directly. Some of these parameters are the high water capacity, verifying REQ-SUS-4, cruise, and stall speed. These characteristics are improved with respect to the CL-415s, and the values for the two aircraft for these parameters can be seen in Table 5.2:

Table 5.2: *Comparison of parameters between W-132 and CL-415 [20]*

Parameter	W-132	CL-415
Water capacity (L)	13200	6140
Cruise speed (km/h)	741	333
Stall speed (km/h)	120.6	126

In the case of the cruise speed, it influences sustainability in a positive way because it reduces the time that the aircraft needs to get to the fire, but comes with a cost, the fuel consumption. The W-132 has a fuel consumption of 1440 kg/hr, while the CL-415's fuel consumption is 672 kg/hr [20]. Nevertheless, this is balanced out by the higher speed of the W-132, resulting in a much faster response time, which is a critical parameter for the scope of the mission as it prevents the fire from spreading as fast, therefore reducing emissions.

Methodology and Results

To carry out this analysis, a specific scenario has been used to enable a quantification of the sustainability impact of both aircraft. For this case, a fire in the Pyrenees will be simulated. Both aircraft take-off from the same airport, and the fire is located at 150 km from the airport. Once on fire, the closest water body accessible for both aircraft is located at 50 km from the fire. For this analysis, several assumptions are used:

- From the actual fire, there are 235.35 tonnes of CO_2 emissions released per hectare, based on the type of forest of the Pyrenees [21][22].
- Based on the payload drop volume of each aircraft, the effective number of hectares suppressed per drop are 0.4 for the CL-415 and 0.7 hectares for the W-132 [23].
- The standard value of 3.16 kg of CO_2 emitted per kg of fuel burnt is used.
- The cruise speed is used when going from the airport to the fire and back.
- The stall speed is used when going from the fire to the water source and back.
- For the range of the mission, 70% of the ferry range of each aircraft (2427 km for the CL-415 and 3000 km for the W-132) is used, taking into account scooping manoeuvres, reserve fuel, and dropping manoeuvres.

Using all of the stated assumptions and the values used in Table 5.2, the number of drops per mission can be estimated, and the total CO_2 emissions saved per mission, CO_2 emissions emitted per mission, and CO_2 emissions per mission can be calculated:

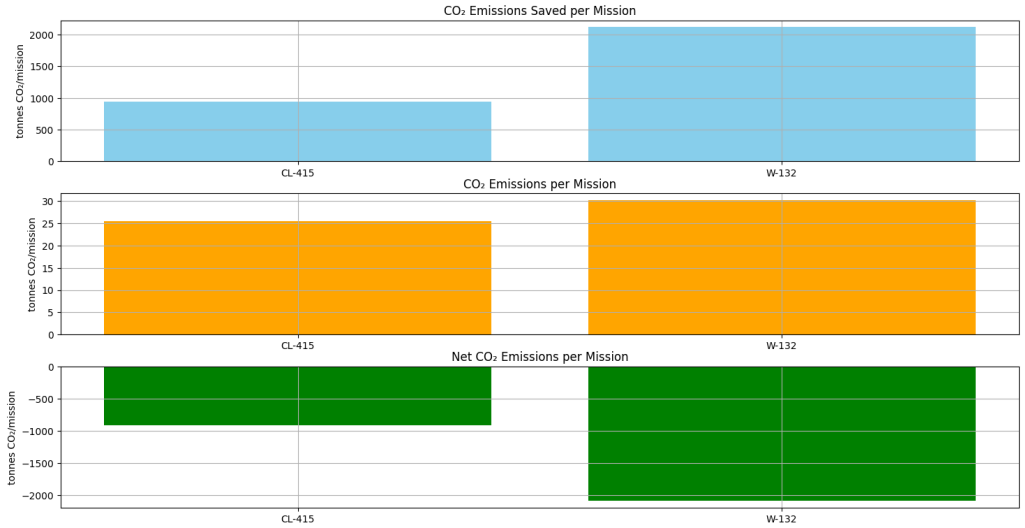

Figure 5.1: *Net CO_2 emissions per misson W-132 vs CL-415*

As observed in the results displayed in Figure 5.1, the W-132 produces more emissions during every complete mission, but the net reduction of CO_2 emissions is much greater than that of the CL-415, over 1150 tons per mission, due to the increased capabilities in speed and water drop capacity of the W-132. This shows that the small penalty in emissions of the aircraft per mission is greatly compensated by the overall emissions saved, which was the primary objective of the W-132 design.

Future Steps

The analysis presented in this chapter is the main section of a Life Cycle Assessment (LCA). An LCA has the objective of evaluating the environmental impacts of the aircraft across its entire lifecycle, from raw material extraction to the end-of-life process. The analysis performed in this chapter focuses mainly on the operational life of the aircraft, by analysing the net emissions per mission, which was the main focus of the design. However, there are several aspects that could be analysed for further development of the LCA of the aircraft, such as the raw material extraction process, the manufacturing process, and the end-of-life process.

The implementation of these would provide a wider overview of the total emissions of the aircraft lifecycle. These analysis could include assessment of the energy used and emissions produced during the first two phases mentioned before, emissions resulting from maintenance activities, such as facilities energy use and spare part production. Moreover, an extensive analysis of end-of-life procedures should be conducted. These should include dismantling and recycling rates, and potential waste disposal estimations. Moreover, recycling processes to recycle CFRP should be included to estimate the amount of material that could be reused for further use, and battery disposal impacts should also be considered.

Finally, REQ-SUS-2, REQ-SUS-3, and REQ-SUS-5 will be verified using relevant regulations and with the use of real time mapping and mission planning to avoid the restricted areas and water sources.

6

Aircraft Characteristics

The conceptual design phase plays a critical role in shaping the overall configuration and performance of an aircraft. It involves iteratively estimating weight, geometry, and system requirements while ensuring compliance with mission objectives and constraints.

This chapter begins with an overview of the top-level aircraft requirements that drive the design, followed by the estimation methods used to derive key performance and weight parameters. Section 6.2 and Section 6.3 detail the Class I and II sizing methods used for early mass and performance estimates. Section 6.3 presents the structural load envelope through V-n diagrams.

The main subsystems are designed in the following sections, including the propulsion system, wing group, empennage, fuselage, storage and under carriage. The final configuration and performance characteristics resulting from this design process are presented in the next chapter.

6.1. Requirements

In line with the systems engineering approach, the design is driven by the requirements. Hence, throughout this report, requirements are presented before the design method. This emphasizes the importance of these requirements. However before discussing the aircraft requirements, an overview of how requirements are presented and compliance is checked must be explained.

6.1.1. Compliance of requirements

Requirements are presented in tables which include the requirement ID, description, compliance and verification method. The requirement IDs have been simplified in comparison to the baseline report, for readability. However the descriptions have not been change.

During the analysis of requirements throughout this report, compliance of the requirements will be evaluated and explained in each individual section. Requirements that have been complied with have a tick (✓). The justification of why the requirement has been met will be explained during the design, and the tick marks have a hyperlink to the relevant section. Requirements that have not been met will be noted with a (✗) and the explanation as to why this is the case will be done after its requirements table. Finally, a tick with an asterisk (✓*) means that the requirement is expected to be met, but in the given design phase, this cannot be verified yet.

The method of verification is also mentioned in the table, but a more detailed explanation on this is presented in Appendix B.

6.1.2. Aircraft Requirements

To derive the aircraft requirements, the stakeholder requirements are analysed, and new user requirements are derived if considered necessary, as shown in Figure 3.1. From the user requirements and the use case, the mission requirements are developed. This procedure is explained in the baseline report of this project. From the mission requirements, the subsystem requirements are defined.

These requirements are the objectives throughout the design phase, and the system is deemed verified as long as the individual subsystem requirements are met.

Although there are over 180 requirements, some requirements apply to all subsystems. Such requirements are classified as system requirements and are presented in Table 6.1. It can be assumed that these requirements apply to every subsystem.

Table 6.1: *Requirements regarding aircraft subsystems and technical specifications*

Requirement ID	Description	Compliance	Verification Method
REQ-SYS-1	The technology of the aircraft subsystems shall be available by 2035	✓	Inspection, verified
REQ-SYS-2	The total cost of the aircraft subsystems shall be less than 56 € million.	✓	Analsysis, verified
REQ-SYS-3	At least [TBD]% of the aircraft components shall be of European manufacturing [1]	✓*	Inspection, not verified
REQ-SYS-4	The aircraft shall have a MTOW no larger than 40,000 kg	✓	Analysis, verified
REQ-SYS-5	Critical subsystems shall be protected from water ingress	✓	Inspection, verified
REQ-SYS-6	Subsystems exposed to water shall be corrosion resistant	✓	Inspection, verified

All requirements are complied with or expected to be complied with. The first requirement REQ-SYS-1 is complied as throughout the design stage, complexity and maturity of technology is considered throughout the various trade-offs. Regarding REQ-SYS-3, the supplier of parts has not been decided yet, but it is expected to be of European manufacturing and hence will be complied. As it has not been investigated yet, it has also not been verified. The remaining requirements have been verified through analysis or inspection.

With the systems requirements defined, the aircraft design can be presented.

6.2. Aircraft Estimation Method

Due to the cyclical nature of the calculations, several loops where multiple iterations were performed were created. The design process was inspired by the N2 chart. The pseudocode for the code program can be seen in Figure 6.1.

From the diagram, two main loops can be identified. The first loop begins after inputting the initial parameters from the `Parameters.json` file and calculating the statistical values for the Class 1 estimation. This loop cycles through the preliminary design estimations until a 0.1% convergence in MTOW is achieved and at least 15 iterations are completed. The second condition ensures that not only does the weight converge, but also all other parameters stabilise. Following the preliminary phase, a detailed design of the most critical subsystems is carried out, followed by an analysis of stability, control, and centre of gravity (CG) excursion. This process is then repeated in the second loop, where the final design is iterated until convergence according to the same criteria. All important parameters are saved a file.

[1] The % of the components of EU manufacturing has not been defined yet, and it is impossible to define until a later design stage. Hence it is left as [TBD]

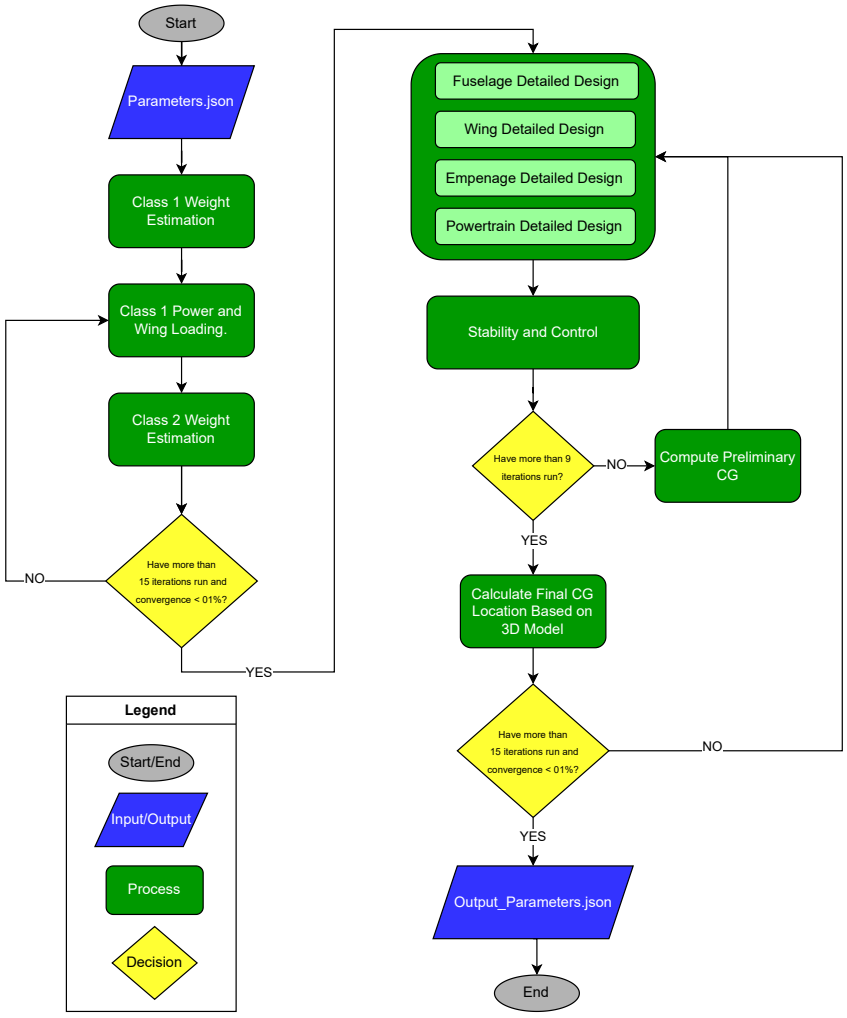

Figure 6.1: *Pseudocode Diagram*

6.3. Initial Estimations

This section details the initial estimations of the aircraft design, this contains the very high level statistical estimations obtained from class I methods. This then leads into the class II estimations that, while still statistical, analyse the weight of the individual subsystems, leading to a more accurate estimation.

6.3.1. Class I

Class I estimations encompasses both a preliminary statistical weight estimation as well as a initial power and wing area estimations. These power and wing area estimations are obtained from physical relations and as such are accurate enough that the method is used beyond class I.

6.3.1.1. Weight Estimation

Class I estimations aim to offer a statistical upper bound to the system weights of the design. As such this is based strictly on high level parameters dictated by the requirements of the aircraft. These parameters are statistical operational empty weight (OEW) to maximum take-off weight (MTOW) ratios, statistical fuel fractions supplemented with the fuel needed for cruise, dependant on range and engine efficiency.

The statistical data is obtained from similar scooping aircraft, however due to the specialisation of these aircraft, the sample size may lead to imprecisions. Furthermore, these aircraft may not necessarily be specialised modern designs, this weight would therefore not incorporate the innovative design decisions and as such the weight saving. The engine characteristics are taken from the PW-150 as it fits the appropriate weight class for this initial design.

This results in a MTOW of 57.7 tons and an OEW of 34.3 tons. These far exceed the goals set for the design, mostly explainable by the use of statistical fuel fractions obtained from data for cargo aircraft due to the lack of information available for scooping aircraft. These result in a high fuel weight of 10 tons, leading to these results. Although an overestimation, these values serve as a starting point for the design to converge to a more realistic design.

6.3.1.2. Power and Wing estimations

Class I estimations also incorporate initial power and wing estimations through the creation of a power and wing loading diagram. This diagram is based mostly on mathematical and physical relations rather than statistical, as such these values are deemed relevant throughout the design.

This process takes into account the power and wing size requirements at different critical steps of the flight. These are at stall, landing, cruise, rate of climb (ROC) and climb gradient. These calculations are based off of Raymer [24] as well as simple aircraft statistical force analysis. In addition to these conventional situations, 2 take-off requirements are taken, the first being that aircraft must be able to take-off full from a runway of 1800m. This is to model a situation where the aircraft is stored with full payload in an airport and must quickly be deployed. The second situation is one where the aircraft must quickly refuel during a mission, as such airport accessibility is a priority, the runway length is therefore 1300m, to compensate, the aircraft is assumed to have empty payload as it is coming back from a drop. The first iteration of this process results in the following graph :

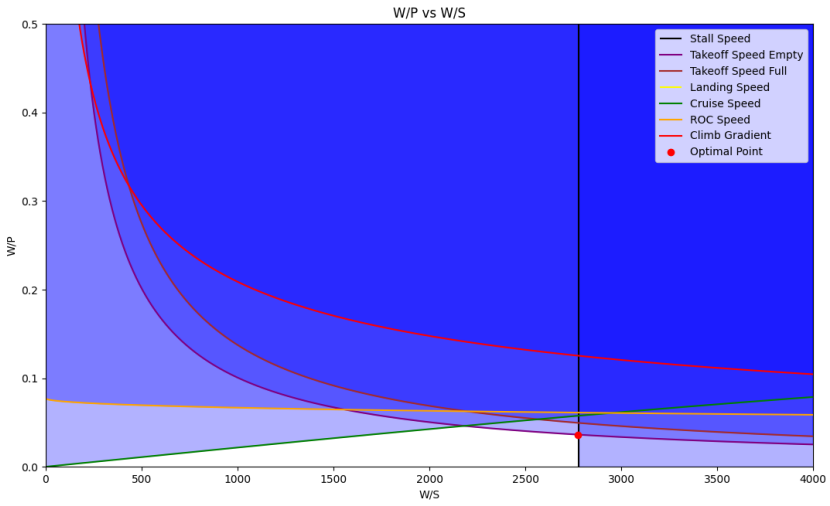

Figure 6.2: *Wing and power loading graph*

Here the aircraft weight to wing area ratio is 2778 N/m^2. and the aircraft weight to power ratio is 0.0362 N/W. These values are not constant however as throughout the iterations certain input parameters are modified, leading to slight differences.

6.3.2. Class II

The class II method is used to determine the weight of the individual subsystems of the aircraft based on high level input parameters that can be derived from requirements. This method is therefore used to obtain the weight of the fuselage, engines, wing, empennage, landing gear and fixed equipment.

The fuselage weight is obtained using the method for large transport aircraft from Roskam's Aircraft Design part 5 [25]. This method uses the wetted area of the fuselage, obtained by assuming the fuselage as a rectangular prism. The other parameters such as the length are obtained by assuming that the aircraft is purpose built and as such does not waste unnecessary volume. A factor is applied on this to account for the fact that it is an amphibious aircraft.

The engine weight is obtained using the power requirement obtained in class I. Indeed, this gives the required engine type as well as the amount needed. For this, it is assumed that PW-150 engines are used. Although this is not representative of the final design as the system is hybrid in reality, this does offer a target weight that the hybrid powertrain should aim to achieve.

The wing and empennage weight is obtained in a similar manner with the addition of the use of Roskam's Aircraft Design part 3 [26], a more detailed analysis on the obtaining of the parameters required for this can be found in their respective section.

The landing gear also uses the Roskam method, with the additional use of Aircraft Design part 4 [27], this weight estimation is exclusively dependant on the MTOW of the aircraft.

The final subsystem sized in this manner is the fixed equipment of the aircraft, accounting for the flight control, hydraulic, pneumatic and electrical systems, the avionics and their instrumentation, the air conditioning, the paint, the auxiliary power system and the oxygen. Some of these values were modified however so as to account for the uniqueness of the design. As the design is one of an unpressurised aircraft, the value of the weight of the air conditioning and pressurisation unit was divided by 12 as it is assumed that half of that weight is for pressurisation and only a sixth of the fuselage requires air conditioning. Similarly, the weight of the oxygen system is increased by a factor 2 as it is critical to this mission as the cruise altitude is unbreathable. A more precise estimation for the required oxygen and its weight is done in later sections.

6.4. V-n diagrams

Sizing the wing starts with identifying the loads the aircraft will be subjected to. This is done by building the manoeuvre load and gust load diagrams. For this, the method of chapter 4 from Roskam book 5[25] was followed. From this analysis, the limit load according to which the aircraft should be designed for will be found.

For the gust load diagrams, Roskam proposes different aircraft categories to size the different gust velocities. There, the FAR 25 aircraft category is selected, because it corresponds to larger aircraft, such as commercial or cargo transport, the closest to W-132 MTOW. Roskam suggests a few numbers for this aircraft category, for the gust velocities or the limit load according to which the aircraft should be designed.

The different gust velocities in the diagram correspond to the worst case scenario that is expected to occur during the flight phase. For instance, gust velocities of 15.2 m/s during cruise is something

extremely unlikely to happen, but that the aircraft should still be able to withstand in that worst case scenario. All these values are given for FAR 25 aircraft, but a critical look should be given at them to ensure they still are relevant in the context of a firefighting aircraft. Vertical velocities wind gusts are expected to range between 6-10m/s above a fire [28], but those gust speeds of 15m/s are extremely rare[29]. So these gust velocities at cruise speed for the loading diagram were considered reasonable in this case, particularly because the aircraft will not be cruising above fires. The phases where the aircraft would be subjected to the vertical gusts due to convection of air during the forest fire would be the water drop manoeuvres, where the airplane would fly at much slower speeds.

Hence building the corresponding V-n diagram for the W-132 yields Figure 6.3:

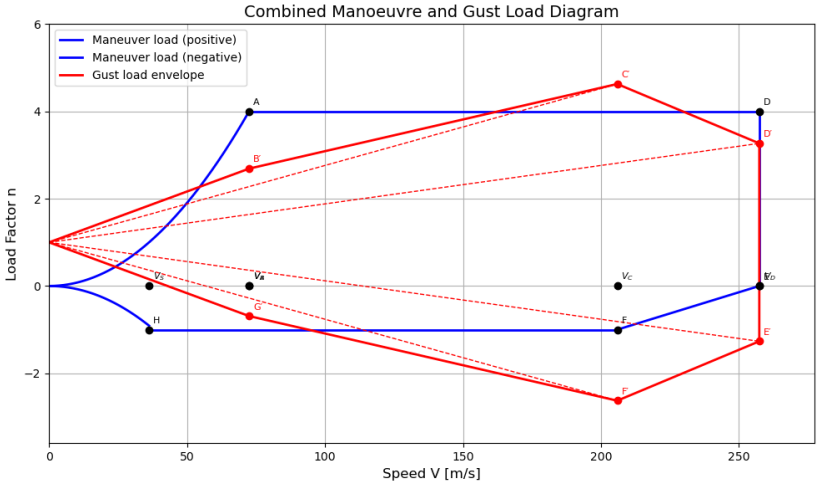

Figure 6.3: *Combined Manoeuvre and Gust Load Diagram for W-132*

Here the limit load that the W-132 should be designed after, was set to be at 4. While the cruise gust velocities could indicate that the aircraft should be able to sustain higher loads of up to 4.6, a limit load of 4 was set for the W-132. This was done Roskam specifies that the limit load should be set to a maximum of 3.8. While this is for regular FAR25 aircraft, a firefighting aircraft will be enduring stronger loads which is why 4 was chosen. Regarding the negative limit load, Roskam suggests to set it to 0.4 times the limit load that was found, hence -1.6. The limit load of 4 was also arbitrarily chosen by considering the limit load of the CL415 being 3.25 [30].

Understanding better Figure 6.3, the load factor due to the gust velocities at V_C is particularly high in this case due to the large cruise speed V of the W-132. The formula for it is given by Equation 6.1

$$\Delta n = \frac{\rho V U_{de} a_s}{2W/S} \tag{6.1}$$

In this analysis, the load factors from the waterscooping or water drop manoeuvres were not considered, as they would not be greater than the ones from the manoeuvres or the gusts. For the CL415, the 'vertical' loads during scooping reach typically 1.3 during water scooping, and 1.6 during the water drop phase [31].

6.5. Propulsion System

The W-132 features an innovative parallel hybrid electric propulsion system with an in-house designed internal combustion engine, the WE-3000, built specifically for use in a hybrid parallel system. This configuration features a novel approach where the internal combustion engine is op-

timised for one power setting and the hybrid system serves to provide additional power where needed. The propulsion system features two large turboshaft engines each providing 2.77 MW of power. Each engine is connected to a gearbox driving a propeller, each gear box also connects to an electric motor capable of delivering 1MW of power. To complete its firefighting missions the W-132 will have 5850 [kg] of fuel as well as two batteries weighing a combined 3900 [kg], this gives a total subsystem dry weight of 4567 [kg] and a wet weight of 10417 [kg] .

6.5.1. Requirements

Before the design phase, the requirements associated with the propulsion system must be recalled. This is shown in Table 6.2.

Table 6.2: *Requirements of the propulsion system*

Requirement ID	Description	Compliance	Verification Method
REQ-PROP-1	The fuel tank shall have a capacity of at least 7300 litres	✓	Analysis, verified
REQ-PROP-2	The propulsion system shall be at least 7 MW of Power	✓	Inspection, verified
REQ-PROP-3	The aircraft shall have a fuel consumption of at most 0.3 kg/kWh	✓*	Analysis, not verified
REQ-PROP-4	The engines shall maintain stable engine performance in extreme environments	✓*	Test, not verified
REQ-PROP-5	The propulsion system shall provide power no less than 7 MW during water take-off	✓	Analysis, verified
REQ-PROP-6	The approach speed during water scooping shall not exceed 60 m/s	✓*	Demonstration, not verified
REQ-PROP-7	The water scooping distance shall not exceed 1300 metres	✓*	Demonstration, not verified
REQ-PROP-8	The water take-off distance shall not exceed 2500 metres	✓*	Demonstration, not verified
REQ-PROP-9	The aircraft shall have a ferry range of at least 2450 km.	✓	Analysis, verified
REQ-PROP-10	The aircraft shall be able to conduct the ferry mission with discharged batteries.	✓	Demonstration, verified
REQ-PROP-11	The aircraft shall be able to complete its ferry mission in less than 5 hours.	✓	Analysis, verified
REQ-PROP-12	The aircraft take-off distance using its hybrid system shall not exceed 1300 km .	✓	Analysis, verified
REQ-PROP-13	The aircraft take-off distance using only its combustion engines shall not exceed 1800 km .	✓	Analysis, verified

6.5.2. Assumptions

A parallel hybrid electric system is a novel concept and thus assumptions had to be made when designing it. These assumptions are based on expected values for the year 2035 from research and discussions with Dr. Reynard de Vries who has conducted a lot of research on the topic and also is currently the Director of Design and Engineering of an electric aircraft company. All of these

requirements are critical to the design and thus should they not be met or not be expected to be met by 2035 the hybrid propulsion subsystem should be eliminated and the back-up conventional configuration discussed in Subsection 6.5.4 should serve as a replacement. Note that the impact of switching to the conventional configuration is not investigated beyond the weight of the propulsion system and could have further impact on the aircraft's performance which must also be investigated if necessary. These assumptions and their current confidence levels as of 2025 are expressed in Table 6.3. The confidence levels used in Table 6.3 are assigned with high confidence meaning that the values are based on current existing products, medium coming from multiple sources or expert discussions and finally low confidence representing values which have some literature but with no clear 2035 time frame. Values only with medium or high confidence were taken to reduce likelihood of the system being unfeasible.

Table 6.3: *Propulsion System Assumptions*

Code	Assumptions	Confidence
AS-PP-01	625 Wh/kg batteries [32]	Medium
AS-PP-02	0.8 Cell to pack mass ratio [32]	High
AS-PP-03	16 kW/kg Specific power of the electric motor [33]	High
AS-PP-04	0.259 kg/kWh Specific fuel consumption of the turboshaft engines [34]	High
AS-PP-05	10.4 kW/kg Specific power of the turboshaft engine [34]	High
AS-PP-06	65 $/kWh specific cost of the battery [2]	High
AS-PP-07	Engine is done being designed [32]	High
AS-PP-08	Engine is done being tested [32]	Medium
AS-PP-09	Engine is certified [32]	Medium

6.5.3. Hybrid Propulsion

Hybrid propulsion systems provide unique advantages to aircraft such as; greater efficiency, improved manoeuvrability thanks to reduced transient responses, greater reliability and decreases in noise amongst others [35][36]. There exist three main ways to implement hybrid propulsion on an aircraft, these are presented in Figure 6.4. The W-132 uses its hybrid system for additional power "boosts" during flight phases requiring large amounts of power, the configuration most suited to this type of performance is the Parallel-Hybrid Variant 1 [35].

[2] prnewswire.com

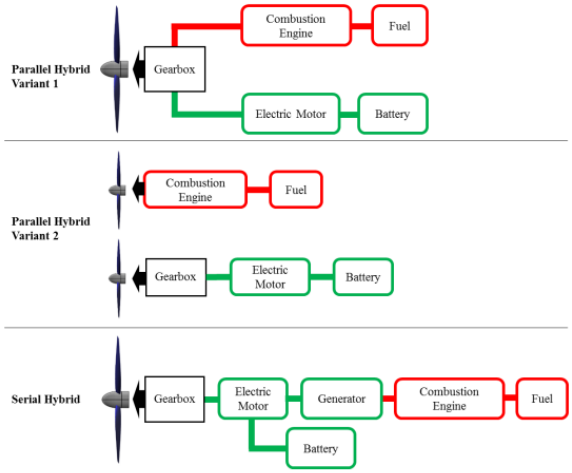

Figure 6.4: *Hybrid-Electric Powertrains [35]*

Furthermore, upon discussion with Dr. de Vries it was determined that there could be substantial efficiency and performance gains from attempting to designing and build an engine in house rather than using an existing engine. This would allow the engine to be designed for one power state which it maintains throughout the mission while the hybrid system turns on when additional power is required. The full powertrain architecture of the W-132 can be seen in Figure 6.5.

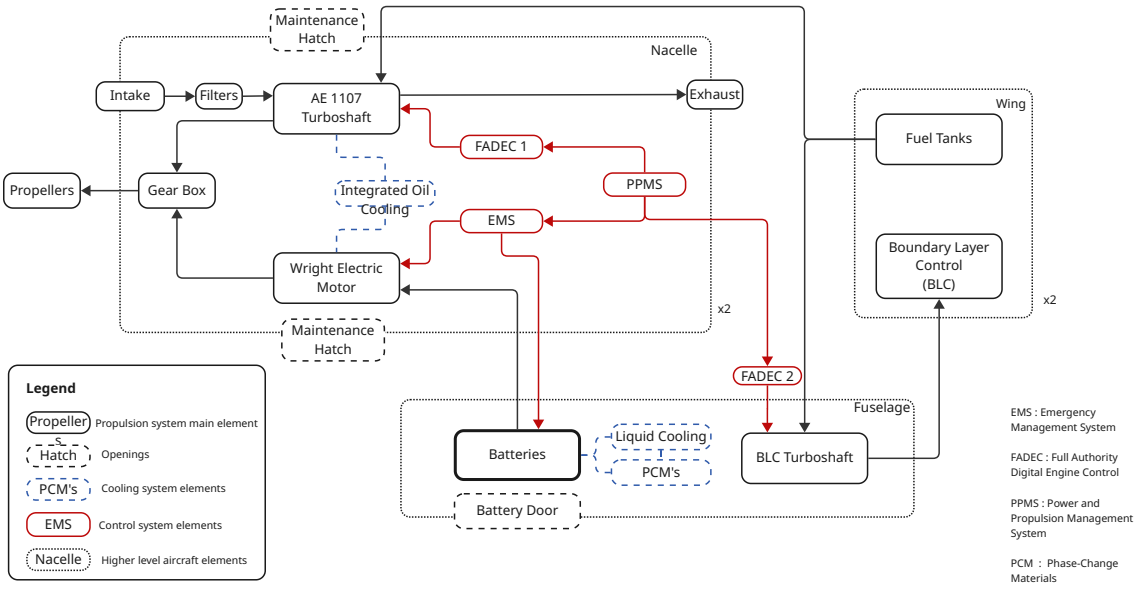

Figure 6.5: *Propulsion System Architecture*

6.5.4. Configuration Sizing

Using Figure 6.2 power requirements for the W-132 can be determined, and then to comply with REQ-MIS-1 all power required for the flight phases of a ferry mission (see Figure 4.7) must be entirely powered by internal combustion while all additional power needs can be driven by the hybrid system. Figure 6.6 shows the power required for the flight phases and how much of it should come

from the hybrid system.

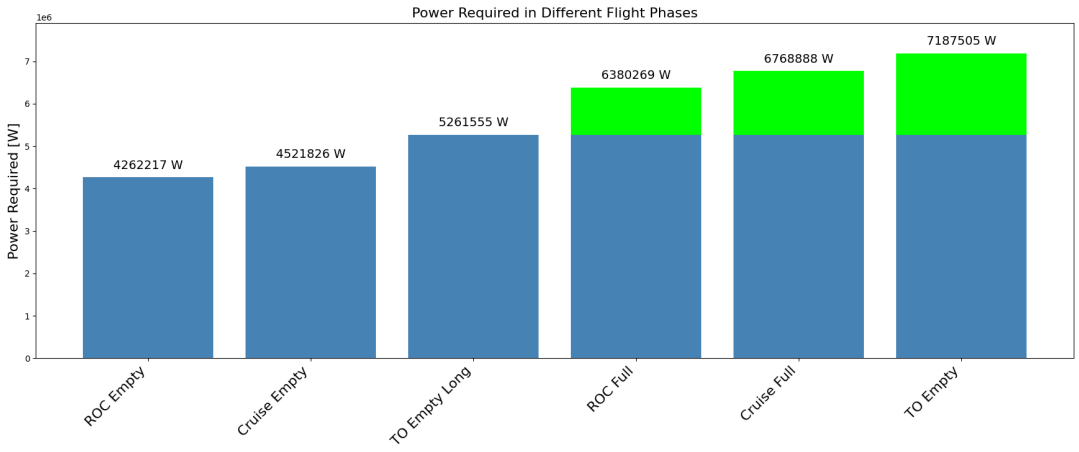

Figure 6.6: *Power Requirements for Different Flight Phases With Hybrid Threshold*

With a maximum power required of 7.2MW the hybrid and purely internal combustion configurations can be drawn up:

- 4x Pratt & Whitney 127 turboprop engines, each providing 2050 kW of power.
- 2x in house WE-3000 engines each providing 2630 kW of power in parallel with two Wright electric motors each providing an additional 0.95MW powered by two electric batteries in the fuselage.

A summary of different characteristics of the items listed above can be found in Table 6.4, these characteristics will be used for analysis further in the present section.

Table 6.4: *Propulsion Systems' Items Characteristics*

Item	Max Power (kW)	Dry Weight (kg)	Dimensions (mm)	Cost (M$)	Energy Density (Wh/kg)
PW127	2050 [37]	480 [37]	2100x660x840[37]	2-4 [38]	-
WE-3000	2630 [34]	253 [34]	890-diameter [34]	∼2.1 [39]	-
Wright Electric Motor	1040 [33]	68 [33]	640-diameter [33]	3-6 [33]	-
Battery Pack	-	3925	1333x757x1250	0.13	625 [32]

Trade-Off

To ensure that the hybrid system's benefits outweigh its possible downsides a trade-off was conducted. The propulsion system trade-off follows the same logic as the ones found in the midterm report, namely, giving a score of "1" to the best option and showing the other option as a fraction of that value when performing with exact values, whereas qualitative analysis makes use of the table present in the previous report shown in Table 6.5. The results can be found in Table 6.6, measured using four criteria; sustainability, risk, manoeuvrability, and mass of the whole system.

Table 6.5: *Qualitative analysis conversion*

Description	Value
Very Poor	0.00
Poor	0.25
Adequate	0.50
Good	0.75
Very Good	1.00

Table 6.6: *Propulsion System Trade-Off*

Criteria	Weight	4x PW127	2x WE 3000 + 2 Electric Motors + Battery
Sustainability	0.1	0.9	1
Risk	0.1	1	0.5
Maneuverability	0.5	0.75	1
Mass	0.3	1	0.85
Total Performance		0.87	0.9

Criteria

- **Sustainability** there is a clear difference in fuel usage when looking at a conventional engine design versus a hybrid system, leading to a decreased amount of CO_2 emissions. Thus, it is necessary to add the present criteria to highlight the beneficial difference between the two systems. And as sustainability is a key aspect of any modern aircraft design, it has to be put into account for the present trade-off
- **Risk** As seen in Table 6.3, there is a number of assumptions taken for the propulsion system, and a greater number of those relate to the batteries and motor as they are still in a prototype phase. Consequently, it is necessary to compare the risks that come with designing a new system that has only been conceptualised and prototyped as of today to a conventional engine system that has been flying for more than two decades.
- **Manoeuvrability** it is measured using the response time of the aircraft's engines, which is defined as the as the time from the pilot's input to the change in power level. A smaller response time leads to a better manoeuvrability and thus to better performances on the terrain and a possibility to increase the geographical reach of the W-132 by allowing it to climb faster in more mountainous areas, or to scoop smaller water bodies. It is then clear that, considering its massive impact on the mission, the manoeuvrability performance of the plane should be the most important weight.
- **Mass** between four engines and two engines with an electric system, it can be unclear which is the one that will perform the best in relation to mass. Considering how the mass of the propulsion is quite limiting since it is resting on top of the wings, however that is not the only way to consider weight. Since the hybrid fuel saves a fair amount of fuel, it is also taken into account for the mass trade-off. For these reasons, mass is the second most weighted criteria.

Score Explanation

The trade-off was conducted in parallel of the sizing of the hybrid propulsion system, as found in Subsection 6.5.4. While the values for the PW150A engine were easily found and calculated, the hybrid system, due to its modernity, had to be first estimated then refined through iterations, as explained later on.

In terms of **sustainability**, the addition of the electric system resulted in a fuel saving of 1000 kg compared to the baseline fuel consumption of 6850 kg from the four PW127 engines . This corresponds to an estimated 15% reduction in CO_2 emissions[40], assuming a direct proportionality with fuel burn. Other considerations for sustainability where not approached, such as batteries end-of-life, and life cycle assessment considerations for the sake of simplicity.

Risk was assessed considering the available literature and confidence in the assumptions, furthermore, while the lithium-sulphur battery and Wright electric motor have greater development risks, they would offer better performances in terms of operational risks since electric propulsion is generally considered more reliable than conventional propulsion systems due to the reduced number of mechanical components, this also offers easier maintenance [41]. On the other hand, the hybrid gearbox presents even more unknown risks due to the difference in power levels between the gas turbine and the electric motor that needs to be accommodated for. This leads to difficult-to-quantify risk scenarios, which is why it was qualitatively assessed, giving a score of "very good" (1)" to the Pratt & Whitney and "adequate (0.5)" for the new hybrid system.

Manoeuvrability is quantified, using the response time of the propulsion system, from pilot input to change of state of the aircraft. For turboprop engines, it can be estimated to be in the region of 1-2 seconds, whereas for electric propulsion it is near instantaneous. As explained further on in the present section, since the electric part of the propulsion system is solely use for manoeuvrers, this means that all of the change of state of the aircraft would save as much as 2 seconds. This could mean a difference of 200 to 400 meters that can be shaved off from it's scooping distance, granting the aircraft even smaller water bodies and permitting access of more mountainous regions of Europe. This can be translated into a "very good" (1.00) score for the hybrid system's manoeuvrability and ""good" (0.75) for the combustion engine.

Mass of the systems can be split into the dry mass and the fuel mass to get the total wet mass. The dry mass of the PW127 system is calculated using the known dry weight of the system from the engine's EASA certification document [42], this gives a dry mass of 1920 [kg]. For the hybrid system using the assumptions established in Table 6.3 a dry weight for the motors plus the engines is 642. The battery also counts towards the dry weight but is sized through the same process as the fuel.

Sizing the fuel mass requires identifying the critical flight profile in terms of fuel/energy needs. The three flight profiles can be analysed using the power requirements of the aircraft in its different phases of flight . The fuel mass can be determined using the 0.259 kg/kWh specific fuel consumption discussed in Table 6.3.

Table 6.7: *Fuel and Electrical Energy Required for the Different Flight Profiles*

Flight Profile	Fuel Required [kg]	Electrical Energy Required [kWh]
Ferry Mission	**5850**	0
Maximum Distance	4600	815
Standard Mission	5300	**1605**

Table 6.7 shows that the ferry mission is the critical profile for fuel requirements and that the standard mission is critical for the electrical energy requirements. However, the number of drops in the firefighting mission profiles is a minimum and more drops would be beneficial for the missions. Therefore, by assuming that the aircraft begins each mission profile with 5850 kg of fuel the firefighting profiles could conduct more drops for more electrical energy.

Table 6.8: *Fuel and Electrical Energy Required for the Different Flight Profiles With Full Fuel Tanks*

Flight Profile	Fuel Required [kg]	Electrical Energy Required [kWh]
Ferry Mission	**5850**	0
Maximum Distance	**5850**	1368
Standard Mission	**5850**	**1950**

Using the full fuel will allow for seven more drops during the maximum distance mission and four more drops during the standard mission allowing for improved firefighting capabilities. A pack mass of 3950 [kg] is found by using the specific energy of batteries and the cell to pack mass ratio discussed in Table 6.3 1950 [kWh]. By using the specific fuel consumption of the PW127 engine (0.279kg/kWh) [43], in place of that of the WE-3000, and converting the electrical energy requirement into an equivalent fuel mass, the resulting fuel weight is estimated at 6850 kg.A summary of the corresponding system weights is presented in Table 6.9.

Table 6.9: *Fuel and Electrical Energy Required for the Different Flight Profiles With Full Fuel Tanks*

Flight Profile	Hybrid System	PW127
Dry Weight (Includes battery) [kg]	4560	1920
Fuel Weight [kg]	5850	6850
Total wet weight [kg]	**10345**	**8770**

6.5.5. Secondary Subsystems

6.5.5.1. Cooling Systems

When flying batteries over a fire, one might think that they might expect extreme case of overheating, however, when looking at the strategies used by firefighting airplanes to combat forest fire, it can be seen that the temperatures are not very limiting when comparing to a conventional aircraft. Thus, the cooling system used can be conventional as well, and inspiration can be taken from prototype electric or hybrid aircraft. Consequently, the W-132 will make use of 3 different cooling systems, in blue in Figure 6.5, each having distinct functions, integrated oil cooling for the gas turbine and electric motor. Then liquid cooling in combination with phase-change materials (PCMs) constantly and actively cooling the battery. Finally, the PCMs used as a fail-safe mechanism in case of severe over-heating.

6.5.5.2. Foreign Debris Mitigation

One critical consideration to take into account when designing a propulsion system for a wildfire fighting aircraft is the cinder and ashes that stem from the burning wood. Such lighter-than-air components can cause engine damage that creates lasting impacts and increases both risk and maintenance costs. Therefore, a mitigation mechanism in the form of filters is used. The best fit for such an environment is initial particle separators, in the form of a centrifugal (vortex) separator, which uses the greater inertia of particles such as cinder or ash to trap them in tight turns, these do not get clogged as easily and are already used as the newest most efficient solutions for helicopters in sandy regions [44]. All for negligible amount of power than can be inputted from the APU system.

6.5.5.3. Battery Type

While various lithium-based batteries were considered, lithium–sulfur (Li–S) was ultimately selected due to its higher theoretical specific energy and relatively low projected weight at pack level.

Initial estimates were based on commercially available prototypes and lab data, which indicate specific energies in the range of 250–600 Wh/kg for battery packs, depending on configuration and maturity level [32]. A specific energy of 625 Wh/kg was retained for the sizing phase, as exposed in the assumptions.

Operationally, Li–S offers significant benefits. Its low cell weight and ability to fully discharge make it a favourable option in mission profiles where energy needs to be delivered quickly and at relatively constant power, such as during manoeuvres or loitering above target zones. Additionally, the use of sulfur, a byproduct of petroleum refining, provides advantages in terms of material availability and sustainability, although battery end-of-life and recycling processes were not considered in this phase. While Li–S technology presents greater development risks due to its relatively lower technology readiness level compared to lithium-ion, its expected improvement in cycle life (up to 1500 cycles) and high energy density justify its selection for this use case, especially given the weight constraints associated with aerial firefighting operations [32].

6.5.5.4. Boundary Layer Control

In Subsection 6.6.3, a high-lift device in the form of a Boundary Layer Control system (BLC) is chosen. To power such a mechanism it was chosen to follow the ShinMaywa US-2, by using a turboshaft engine housed in the upper part of the fuselage. However, the W-132's BLC would necessitate around 200-300 kW of power, much less than the Japanese aircraft power needs. Thus, a smaller Pratt & Whitney 206 turboshaft, whose power output is corresponding closely to the power needs of the BLC, can be used for W-132, a summary in Table 6.10 presents the main characteristics of this engine for proper sizing.

Table 6.10: *PW206B characteristics*

Item	Max Power (kW)	Dry Weight (kg)	Dimensions (mm)	Cost (k$)
PW206B	321 [45]	118.9 [45]	1.04 x 0.52 x 0.73 (L x W x H) [45]	18 [46]

6.5.5.5. Controls of the Propulsion System

Fianlly, the control of the hybrid system can be seen in red in Figure 6.5. It can be seen that it works with a power and propulsion management system (PPMS) which acts as a master to the two lower level control systems, the Full Authority Direct Engine Control (FADEC) that is part of the gas turbine and the Energy Management System (EMS) dealing with the electric part of the hybrid system. A summary of the different functions and which system they relate to can be seen in the following Table 6.11

Table 6.11: *Functional Allocation of Hybrid-Electric Propulsion Control Systems [47] [48] [49] [50]*

Function	PPMS	EMS	FADEC
Overall power flow coordination	Primary control	Provides input on battery availability	Not involved
Power source switching (thermal vs. electric)	Primary control	Supports based on battery state	Responds to required power settings
Battery charge and discharge control	Supervisory commands	Full control	Not involved
Battery health and thermal monitoring	Not involved	Full responsibility	Not involved
Battery state-of-charge (SoC) management	Not involved	Full responsibility	Not involved
Turbine thrust and power control	Provides power setpoints	Not involved	Full authority
Engine fuel flow, ignition, and component control	Not involved	Not involved	Full authority
Redundancy and fault management	System-level coordination	Battery-side fault handling	Engine-side fault handling
Phase-specific power distribution (e.g., takeoff/cruise)	High-level scheduling and control	Delivers power as commanded	Modulates engine performance accordingly
System-wide energy efficiency optimization	Central coordination	Contributes via battery usage strategy	Optimizes engine operation within constraints
Pilot input interpretation and dispatching	Interfaces with pilot controls and automation	Indirect; responds to power requests	Indirect; executes engine commands via PPMS

6.6. Wing Group

This chapter section details the design of the wing group subsystem, which follows from the general aircraft requirements presented in Table 6.1. The wing uses a NACA 4412 airfoil with double slotted flaps, slats and a blown flap boundary layer control system. It results in a wingspan of almost 36 metres and area of 140.5m^2. The wing contains differential ailerons for roll manoeuvres, a wing box structure, and tip floaters for water stability.

6.6.1. Requirements

To define aerodynamic design targets, the requirements dependent on it must be recalled. These are shown in Table 6.12.

Several requirements have been flagged as "not verified" due to the current level of design detail. Nonetheless, there is proof that such requirements can be complied with by extrapolating from previous aircraft. In addition, conservative assumptions and safety margins were applied when necessary to justify compliance. However, because such requirements are not yet formally satisfied, they are left for future work.

Table 6.12: *Aerodynamic requirements*

Requirement ID	Description	Compliance	Verification Method
REQ-AER-1	The control surfaces shall adapt to manoeuvring loads to maintain stability	✓	Analysis, not verified
REQ-AER-2	The control surfaces shall adapt to gust loads to maintain stability	✓*	Analysis, not verified
REQ-AER-3	The control surfaces shall provide sufficient force to keep the aircraft stable	✓*	Analysis, not verified
REQ-AER-4	The control surfaces shall maintain roll within [2]° of commanded values	✓*	Demonstration, not verified
REQ-AER-5	The aerodynamic surfaces shall be optimized to minimize drag at the cruise speed	✓	Analysis, verified
REQ-AER-6	The stall speed shall not exceed 40 m/s under extreme conditions	✓*	Analysis, not verified
REQ-AER-7	The wing shall withstand the highest loads of 4g to be expected during flight	✓	Analysis, verified

6.6.2. Airfoil Selection

The firefighting mission must always be the driving factor when designing the airfoil. A main selling point of the aircraft is being purpose-built, and thus the airfoil selection shall reflect that. For that reason, the airfoil selection takes a different approach by optimising the airfoil for low speed manoeuvres and high-lift device compatibility, resulting in the NACA 4412. Flying at a cruise Mach number of 0.6 means transonic effects should not be considered, according to Roskam [51]. This section dives into the approach taken to reach this conclusion.

The first step is to define the objectives, from which a trade-off can be generated. These are:

- High $C_{l_{max}}$ with high deflection flaps to achieve lowest possible manoeuvre speeds.
- Delayed stall angle of attack to allow high rates of climb, with high deflection flaps considered.
- Provide $0.25C_L$ at clean, cruise configuration for M=0.6 and $\alpha = 0$.
- Sufficient thickness to store all fuel in the wing and reduce wing structural weight.
- Drag shall be minimised in cruise conditions.

Naturally, there is no way of achieving all of these objectives without penalising on others.

Several candidates were evaluated based on the criteria detailed above. Due to software limitations, only NACA airfoils were considered. The software XFLR5 was used to determine the following values, explained in Table 6.13. Preliminary trial and error with various airfoils yielded the following six candidates. 5-digit NACA airfoils were also considered but not selected due to poor cruise performance.

To calculate $C_{l_{max}}$ and α_{stall}, a simple flap modelled in XFLR5 with 30 degrees of deflection is used. Low speed analysis was done with $Re = 4.0 \times 10^6$ and $M = 0.1$. High speed analysis was done with $Re = 5.5 \times 10^7$ and $M = 0.6$.

A simple calculation can already rule out the first two airfoils due to killer cruise performance, because of their C_{l_0} too low. Using a simple, fully loaded, $L = W$ equivalence in cruise conditions, and assuming a flight altitude of 7000 metres gives a C_L of 0.25 is required. With a C_{l_0} of 0.30 in the

Table 6.13: *Airfoil performance parameters*

NACA Airfoil	$C_{l_{max}}$	α_{stall}	C_{l_0}	t/c	C_{d_0}
2212	2.15	12.0	0.28	0.12	0.0050
2312	2.11	12.5	0.30	0.12	0.0048
4410	2.04	9.5	0.63	0.10	0.0045
4412	2.10	14.5	0.64	0.12	0.0047
4415	2.08	14.0	0.65	0.15	0.0051
5212	2.16	10.0	0.70	0.12	0.0056

best case, considering the loss of lift when converting to the 3D case, there is not enough margin to ensure a safe cruise.

A trade-off between the remaining airfoils is conducted. To do so, weights to each criteria shall be assigned. Given the mission objective and the market gap that this aircraft is targeting, high manoeuvrability at low speeds is necessary and thus $C_{l_{max}}$ is given 30%. Achieving a high rate of climb is also a major priority to maximise the number of places the aircraft can scoop from, so α_{stall} is given 25% weight. Then the remaining cruise lift, thickness and drag are all given 15%. This results in Table 6.14.

Table 6.14: *Airfoil selection trade-off*

Airfoil	Weight	4410	4412	4415	5212
$C_{l_{max}}$	0.30	0.25	0.75	0.50	1.00
Stall	0.25	0.25	1.00	0.75	0.50
Cruise	0.15	0.25	0.50	0.75	1.00
Thickness	0.15	0.50	0.75	1.00	0.75
Drag	0.15	1.00	0.75	0.50	0.25
	Total Performance	0.40	0.78	0.68	0.73

The scores were primarily based on Table 6.13. A qualitative trade-off was carried out, providing normalised scores from Very Poor to Very Good to each airfoil, as per Table 6.5. As a result, the NACA 4412 was selected, being the best performer overall for the weights considered. This shows compliance with REQ-AER-5 from Table 6.12. Its properties are summarised in Figure 6.7.

In Figure 6.7, the cruise state of the airfoil is shown in yellow, whereas the manoeuvre state (assuming a simple flap) is shown in brown. The respective Reynolds and Mach numbers are considered. In cruise conditions, the C_l/C_d against α plot shows laminar flow until 4°, reaching 190 C_l/C_d. An angle of attack larger than 4 is not expected in cruise conditions, so the aircraft can fly efficiently in such conditions. However, the aircraft shall fly around the design lift coefficient of 0.25, which coincides with the minimum drag value of the airfoil at 0°.

In the flapped condition, an increase in $C_{l_{max}}$ of 0.3 can be observed with respect to the clean configuration at those flow conditions. This comes at a large drag penalty and decrease in efficiency, as well as a decrease in the stall angle. It indicates that a further development of the high-lift device (HLD) system shall be done to minimise the stall speed of the aircraft and reduce power consumption.

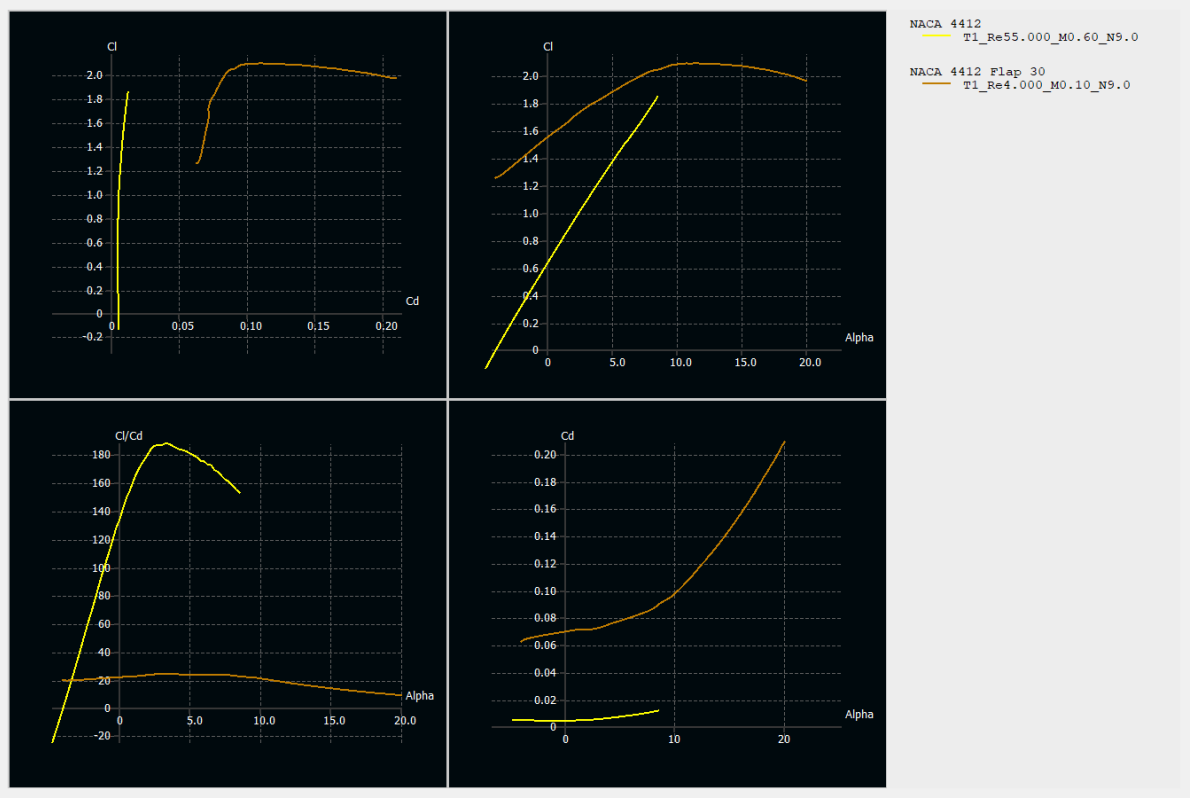

Figure 6.7: *NACA 4412 (yellow) against NACA 4412 with 30º flap deflection (brown) polars at respective Reynolds and Mach numbers*

6.6.3. High-Lift Devices

This aircraft will include double slotted flaps, slats and a "blown flap" boundary layer control mechanism. To decide on the high-lift device systems required in this aircraft, certain targets are set. The most limiting case for C_L is assumed to be at maximum take-off weight (MTOW) and sea-level conditions, which corresponds to dropping maximum payload whilst being fully loaded. As a reference, the ShinMaywa US-2 has a stall speed of 90 km/h, and the Canadair CL-415 of 126 km/h [52][53]. Naturally, these aircraft manoeuvre at a higher speed, but the airfoil must be designed to fail at the target stall angle. The minimum C_L that this aircraft must provide, given by the scenario being assumed and a manoeuvre speed of 130 km/h, is 3.50. This manoeuvre speed fits the market analysis from Chapter 3 and is a design target of the aircraft.

Clearly, from Figure 6.7, the airfoil itself with a simple flap is not able to provide this. At least double the amount of airfoil lift is required to reach that wing lift, so an aggressive flap configuration is needed. Double slotted flaps have been chosen as a solution to this, precisely due to their large increase in lift and proven viability in firefighting contexts. For example, the ShinMaywa US-2 uses double slotted flaps [52] in the trailing edge to achieve this increase in lift. Due to limitations in software, complex flaps can not be modelled with the resources available, but estimations can be used. Estimations show that the increase in airfoil lift coefficient from double slotted flaps are $\Delta C_{l_{max}} = 1.6 \cdot c'/c$ [54].

Furthermore, slats are added in the leading edge to enhance this effect. Slats are able to provide more lift than leading edge flaps, Kruger flaps or slots, and are widely used in a variety of airplanes. They are also necessary when using slotted flaps to delay the stall angle, as slotted flaps decrease this value significantly. Ailerons in the outer wing can not contain flaps, so the difference in lift between the inner an outer wing causes a strong rolling moment during stall. This is mitigated with

the implementation of slats. Estimations show the increase due to slats is $\Delta C_{l_{max}} = 0.4 \cdot c'/c$ [54].

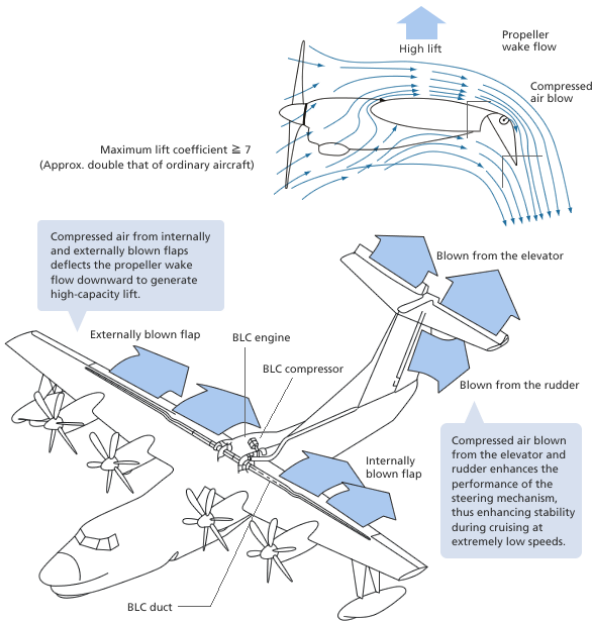

Figure 6.8: *Boundary layer control system in the ShinMaywa US-2 [55]*

Finally, the main innovation in the high-lift devices subsystem is the boundary layer control. Boundary layer control involves manipulating the flow near a surface to improve performance and efficiency. By blowing high speed bleeding air through the joint between the upper slotted flap and airfoil, the flaps are able to generate much more lift than previously. This is because flow separation has already begun after the airfoil, but re-energising the boundary layer causes it to attach to the surface. Such air can come from the compressor of the engine or a separate power system. Quantifying this increase in lift is very application dependent, and it is out of the scope of this project to design this mechanism. However, reports suggest an increase in lift of 150-250%. Fortunately, boundary layer control in the form of blown flaps has already been applied to firefighting aircraft. This technology is what allows the ShinMaywa US-2 to achieve a stall speed of 90 km/h, reaching C_L values of more than 7, as shown in Figure 6.8 [55]. The ShinMaywa US-2 also has blown flaps on the elevator and rudder, but these will not be considered in this aircraft. However, in order to have a highly conservative estimate, only a 50% increase will be assumed.

From this, and selected proportions of wing surface area covered by flaps and slats shown in Table 6.15, a value of the maximum lift coefficient can be provided using Equation 6.2 [54]. Such areas have been revisited so that the roll rate provided by ailerons is sufficient to fit requirements, and can be observed in Figure 6.9. An angle of attack of 10° is assumed as a conservative estimate given that greater angles of attack may not always be reached in manoeuvres. The results are presented in Table 6.15.

$$\Delta C_{L_{max}} = 0.9 \Delta C_{l_{max}} \frac{Swf}{S} \tag{6.2}$$

To determine the c'/c of the double slotted flaps, a flap deflection of 50° is assumed, reasonable when observing Figure 6.8 as the boundary layer control system allows for increased flap deflections. This yields a value of 1.245 [54]. For slats, c'/c is assumed to be 1.

In manoeuvres with full payload, all high-lift devices are needed. When the aircraft has no payload, like in take-off, boundary layer control is not needed and can be deactivated to save power.

Table 6.15: *Airfoil to wing lift coefficient comparison*

Component	C_l	C_L	$\frac{Swf}{S}$
Airfoil	1.50	1.35	-
Flaps	1.99	1.08	0.6
Slat	0.40	0.25	0.7
BLC	1.95	1.34	0.6
Total	**5.84**	**4.02**	

A C_L of 4.02 corresponds to a stall speed of 120 km/h. Given that a highly conservative estimate has been used for the boundary layer control system lift increase, a manoeuvre speed of 130 km/h can be established to include a $0.5C_L$ margin between stall and manoeuvre. This is the minimum speed at which the aircraft can drop water safely. Furthermore, this analysis also excludes the lift generated by the empennage as a conservative estimate. Because REQ-AER-6 considers extreme conditions and these are not well defined, it is marked as "Pending Analysis". However, given that stall speed under normal conditions is 33 m/s, it is assumed that the requirement can be fulfilled with further analysis.

6.6.4. Wing Sizing

This section will deal with the several design choices that were made regarding wing dimensional parameters. These are summarised in Table 6.16 and depicted in Figure 6.9.

Table 6.16: *Wing parameters*

Parameter	**Value**	**Unit**
Positioning	High	-
Sweep	0	deg
Aspect Ratio	9	-
Area	140.5	m^2
Wingspan	35.56	m
Taper ratio	0.75	-
Root chord	4.61	m
Tip chord	3.46	m
Twist	-6	deg
Dihedral	3	deg

The first choice made was the wing positioning with respect to the fuselage. A high wing was chosen as any other configuration would cause interference with water during scooping manoeuvres. It also facilitates engine clearance during runways and scooping. This is consistent with all other scooping aircraft in the market [51].

For a subsonic airfoil with thickness-to-chord ratio of 0.12, like the NACA 4412, flying at a maximum cruise speed of 0.6 Mach does not cause drag divergence at any point of the airfoil [56]. This has a direct impact on sweep angle: the main advantage of sweep is to increase the critical Mach number to avoid supersonic flow in the airfoil, but this is not necessary in this context. Given that sweep is not necessary for compressibility drag purposes, the advantages of no sweep outweigh the disadvantages. These include low structural weight, good control at stall and a high lift curve slope, opposed to worse turbulence control [51]. Therefore, zero sweep was selected for this aircraft. This is consistent with relevant firefighting aircraft in the market, like the Canadair CL-415 or ShinMaywa

US-2 [57][52].

The wing surface area depends on many other factors of the aircraft, so a target area was not set. However, an aspect ratio of 9 was chosen to define the wingspan as a function of the surface area. The scooping and dropping manoeuvres are very recurrent in firefighting missions, these can occur on average every 6 minutes as per Chapter 3. High-lift devices are deployed very often, leading to high C_L values and induced drag. A high aspect ratio reduces this induced drag significantly. For example, for a $C_L = 4$, increasing the aspect ratio from 6 to 9 causes a $\Delta C_D = 0.18$. This leads to a greater wing weight and a high wingspan, but a greater lift-curve slope that becomes useful when climbing. This is again consistent with relevant firefighting aircraft, whose aspect ratios range from 8 to 10 [51].

Wing lift distributions are generally elliptical and thus require less surface area to generate lift in the tip, introducing the solution of a taper ratio to save unnecessary area and thus weight. However, a too aggressive taper ratio can rapidly lead to tip stall [51]. Due to the nature of firefighting missions, water drops can occur at very low speeds and thus many measures must be taken to prevent stall. For such reasons, a taper ratio of 0.75 was selected, in line with competitor aircraft [56]. Additionally, this aircraft shall also store fuel in the wing. For a taper ratio of 0.75, the amount of volume available for fuel storage is 28.6m^3 [56].

Wing twist is added to the wing design, once again, to reduce the likelihood of tip stall under low speed manoeuvres. This leads to an induced drag penalty, but for -6° this is negligible, in the order of $\Delta C_D = 3 \times 10^{-4}$ [54].

A positive dihedral of 3° was chosen for this aircraft for ground and water clearances, both during take-off or landing and scooping. The large propeller blades create a need for a substantial dihedral despite being wing-mounted. This also increases spiral dynamic stability, and is sufficient to not cause dutch roll instability [51].

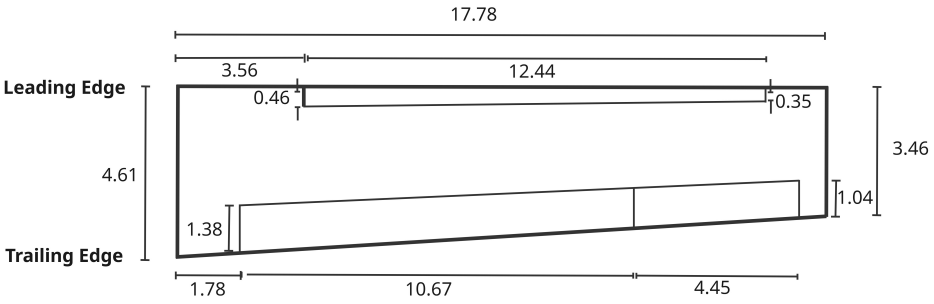

Figure 6.9: *Wing Top View*

6.6.5. Drag Estimation

In this drag estimation, two parallel drag estimations have been done. One applies for high Reynolds numbers, corresponding to cruise, and the other for low Reynolds numbers corresponding to manoeuvres. The latter includes high-lift devices. The drag estimation has been separated into eleven different components. Landing gear drag has been assumed to be negligible as it is retractable and thus is only deployed during take-off and landing. Numerical analysis was not carried out for any component. A component drag build-up method was used for the zero-lift drag, as shown in Equation 6.3[54].

$$C_{D_0} = \frac{1}{S_{ref}} \sum_c C_{f_e} \cdot FF_c \cdot IF_c \cdot S_{wet_c} + C_{D_{misc}} \tag{6.3}$$

This is then converted to total drag by adding lift induced drag, as per Equation 6.4.

$$C_D = C_{D_0} + \frac{C_L^2}{\pi Ae} \tag{6.4}$$

The result of this is shown in Table 6.17. Form factors (FF_c) and interference factors (IF_c) were taken from literature. These include shape factors that were taken as a function of lengths and diameter of the respective part. Skin friction coefficients were calculated assuming different percentages of laminar and turbulent flow per component, based upon suggestions by Cervone [54].

Table 6.17: *Drag build-up per component for cruise and manoeuvre conditions*

		$\Delta C_{D_{\text{cruise}}}$	**% of total**	$\Delta C_{D_{\text{manoeuvre}}}$	**% of total**
Component	Wing system	0.0102	29.5	0.0105	2.3
	Tail system	0.0036	10.4	0.0046	1.0
	Fuselage	0.0079	22.8	0.0101	2.2
	Engines	0.0017	4.9	0.0022	0.5
	Floaters	0.0007	2.0	0.0009	0.2
Miscellaneous	Upsweep	0.0004	1.2	0.0004	0.1
	Base	0.0054	15.0	0.0054	1.1
	HLDs	-	-	0.0622	13.4
	Wave	0.0020	5.8	0.0020	0.4
	Excrescence	0.0007	2.0	0.0069	1.5
	Induced	0.0022	6.4	0.3574	77.3
	Total	**0.0349**	**100**	**0.4624**	**100**
	L/D	**7.15**		**8.69**	

A large difference can be observed between cruise and manoeuvre drag, due to the high lift coefficients needed for the firefighting mission and the resulting induced drag. For future works, induced drag is the target for drag reduction at low speeds, potentially by increasing aspect ratio. Interestingly, the boundary layer control mechanism leads to a higher lift-to-drag ratio for the flapped configuration than for the clean configuration.

The influence of blown flaps on the drag coefficient is unclear and very application dependent [58]. The lift-to-drag ratio is proven to increase significantly, however quantifying the drag for this particular aircraft is out of the scope of this project and left for future improvements. A reason for this is that, by energising the boundary layer, delaying flow separation. This counteracts the drag caused by the boundary layer control mechanism, in the form of leakage and interference. Therefore, the decision to leave this for future research was done based on the proven increase in lift-to-drag ratio.

Winglets are implemented in the wing design to increase the effective aspect ratio of the aircraft and reduce the induced drag. For this, several parameters such as winglet height and airfoil had to be decided. These were inspired by the A320neo "Sharklets". According to Scholz, the drag reduction of winglets justifies the increase in weight [59]. The reduction in induced drag caused by the winglets amounts to $\Delta C_D = 0.037$, or about 7% of the total drag at low speeds. This is included within the

wing system drag in Table 6.17. In comparison, the increase in weight due to the winglets and in consequence reinforced wing structure amounts to 2% of the aircraft's empty weight [59].

Table 6.18: *Winglet parameters*

Parameter	Value	Unit
Root chord	3.457	m
Tip chord	1.502	m
Taper ratio	0.434	-
Airfoil	NACA 4412	-

6.6.6. Aileron Design

Differential ailerons with a maximum deflection of 20°, a c_A/c ratio of 0.3 and a length of 4.45m equal to 25% of the wingspan were chosen, as shown in Figure 6.9. The ailerons were designed based on a target deflection angle consistent with comparable aircraft [51]. Differential ailerons were chosen to counteract the Dutch roll cause by the ailerons, such that the down going wing deflects less than the up going wing. A typical ratio for this is 0.75 [54]. The deflection angle is then given by Equation 6.5.

$$\delta_a = \frac{1}{2}(\delta_{a_{down}} + \delta_{a_{up}}) \tag{6.5}$$

These ailerons were designed to achieve the maximum roll rate possible at manoeuvre speeds, which is the firefighting condition where the aircraft must be able to roll the most. This is limited by the amount of surface area the ailerons can cover, as the trailing edge also contains flaps, and the deflection angle of the ailerons. This results in a roll rate of 0.65 rad/s, or 37.2deg/s, from Equation 6.6. Data publicly available is very limited for roll rates of comparable aircraft, so this roll rate is accepted. In the event that it were not, more deflection of the ailerons is possible.

$$P = -\frac{C_{\ell_{\delta a}}}{C_{\ell_p}}\delta_a\left(\frac{2V}{b}\right) \tag{6.6}$$

$C_{\ell_{\delta_a}}$ and C_{ℓ_p} are a function of geometric parameters of the wing and 2D airfoil characteristics, like c_{ℓ_a} and c_{d_0}. These were calculated using Equation 6.7 and Equation 6.8, respectively. Aileron effectiveness, τ, is dependent on the control-surface-to-lifting-surface chord ratio and is equal to 0.6 [54].

$$C_{\ell_{\delta a}} = \frac{2c_{\ell_a}\tau}{S_{ref}b}\int_{b_1}^{b_2} yc(y)dy \tag{6.7}$$

$$C_{\ell_p} = -\frac{4(c_{\ell_\alpha} + c_{d_0})}{S_{ref}b}\int_0^{b/2} y^2 c(y)dy \tag{6.8}$$

Because the aileron design follows existing designs, the feasibility and requirement compliance of these control surfaces is very high, though not proven. Therefore, the requirements REQ-AER-1, REQ-AER-2, REQ-AER-3 and REQ-AER-4 from Table 6.12 regarding control surfaces are marked as "not verified".

6.6.7. Floater Design

Tip floaters mounted in the wing were design to provide stability in water conditions, and therefore, their design is driven by this aspect. The volume of the floater is determined based on the required displacement of water in kilograms that the floater must be able to sustain. This value is 65% of the weight of the half wing that the floater is attached to[60]. With the value of the volume required for each tip float, its length and diameter dimensions can be obtained[60]. Furthermore, the mass of the tip floater is obtained with an empirical formula based on the MTOW of the aircraft[60]. Finally, the spanwise location of the floaters was decided to be 79% of the semi-span of the wing [60]. This is in the conservative side of the recommended range, due to the value of the span of the aircraft and the loads it has to sustain.

6.6.8. Internal Wing Structure

In order to carry out the interior design of the wing, the sizing and placement of its components an analysis of the loads on the wing was made. Given that the aircraft configuration consists of a high wing profile with 2 wing-mounted engines, wing-mounted landing gear, and wingtip floats, half of the wing structure that was modelled required the combination of distributed and point loads, which led to internal force, buckling and shear diagrams.

6.6.8.1. Wing Structural Load Analysis

Given the very large wing area calculated for this aircraft, along with its maximum take-off weight (MTOW), high cruise speed, low stall speed, and the substantial loads experienced during flight and scooping maneuvers, the wing will be subjected to significant forces. Therefore, its structural design must ensure it can withstand these loads. To properly design the wingbox, the exact load distribution along the wing span must be determined.

First, in order to account for the lift distribution, an elliptical profile was used to simulate the real aerodynamic loading. This approach revealed the spanwise variation of lift and enabled the subsequent calculation of the shear force and bending moment diagrams.

Next, the weight of the components acting on the wing was evaluated. The wing skin weight was estimated from the total area, skin thickness, and the chosen material, which was initially kept as a parameter until a proper trade-off study for material selection was completed. The fuel weight was assumed to be uniformly distributed along half the inboard portion of the span, taking into account the space required for the landing gear and avionics. The engines, floats, and main landing gear were modeled as point loads, with their positions determined based on their inboard locations.

To construct the cumulative shear force distribution in the wingbox, the *limit load case* was considered—meaning all forces acting on the wing were multiplied by the limit load factor n_{lim}. Based on this, the cumulative shear force was calculated and is shown in Figure 6.10.

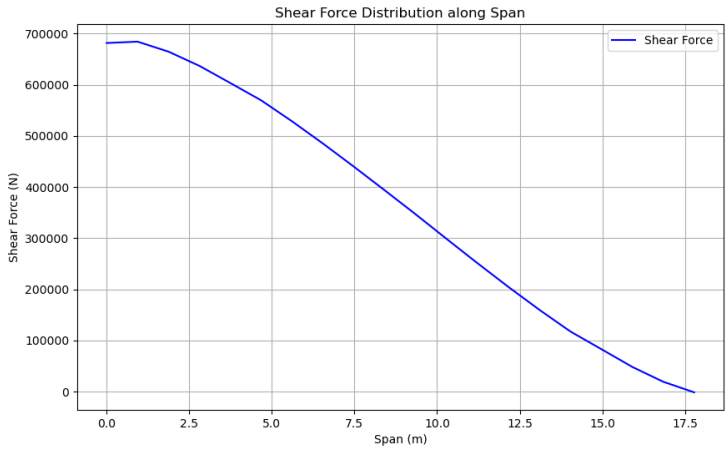

Figure 6.10: *Shear force distribution along the wing*

From the shear force distribution, the bending moment distribution is found out by integrating the shear force from the wing tip to the root chord. This is pictured in Figure 6.11 .

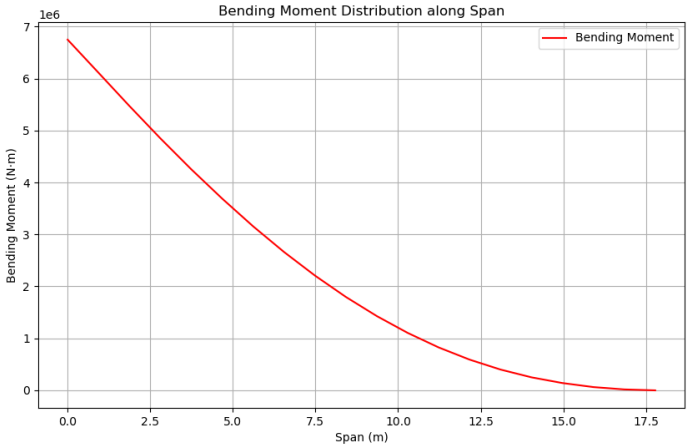

Figure 6.11: *Bending moment distribution along the wing*

6.6.8.2. Wingbox Sizing

The most critical forces that the aircraft would be subjected to were identified in Subsubsection 6.6.8.1, and this chapter will design a light wing box capable of withstanding these conditions.

Design Assumptions

In order to simplify this wing box feasibility study, the wing box will be sized under the assumption that its structure will be carrying the entirety of the loads acting on the wing. This assumption is conservative as the skin of the wing also will be carrying some normal stress and shear, reducing thus the actual loads that would be carried by the wing box.

The wing box was assumed to start at 15% of the chord, and end at 60% of the chord [61, Chapter 7.4.3]. This allows for the airfoil to curve in front of the wing box, and leave enough place for the high lift devices, hydraulics, and boundary layer control system at the aft part of the wing. Then to simplify the analysis further, the wing box was assumed to have a symmetric trapezoidal shape,

where the height of the front spar is the long base, and the rear spar is the short base. A visualization of the wing box in the airfoil is presented in Figure **??**, and a visualisation of the idealised wing box is given in Figure 6.13.

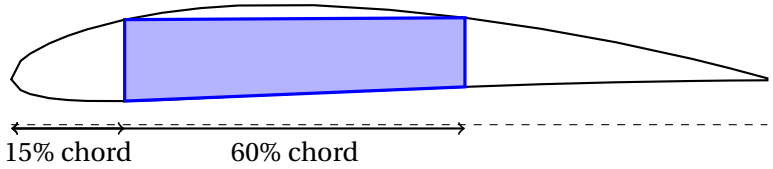

Figure 6.12: *Wingbox in the airfoil representation*

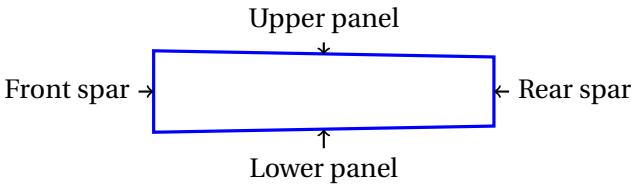

Figure 6.13: *Simplified wingbox geometry*

Failure Modes Considered

The wing box was sized, such that it is able to withstand three failure modes: material yielding, skin panel buckling, and shear failure. The formulas for each are given below.

$$\sigma = \frac{M \cdot y}{I_{xx}} \tag{6.9}$$

Where σ is the normal stress at a position y for a cross section with I_{xx} and a moment M acting on the cross section along the x-axis. The symmetric assumption of the cross section allows for not considering I_{xy} and simplifying the above equation. If σ_{max} in the structure were to be larger than σ_y (yield strength) of the material, the structure would fail by material yielding.

$$\tau = \frac{q}{t} = \frac{V \cdot Q}{I_{xx}} \tag{6.10}$$

Where τ is the shear stress, for a shear flow q flowing through a thin cross section of thickness t. If the largest shear stress τ_{max} were to be larger than τ_y, this would indicate that the structure fails by shear failure.

$$\sigma_{buckling} = C \cdot \frac{\pi^2 \cdot E \cdot t_{web}^2}{12 \cdot (1 - \nu^2) \cdot b^2} \tag{6.11}$$

For the buckling calculations, the skin panels were modelled as "buckling rectangles" bounded by stringers and ribs, which define the panel dimensions. In Equation 6.11, the buckling coefficient C is taken from Figure 6.14, where the case with four simply supported edges (SSSS) was selected.

This choice is justified by the boundary conditions present in the actual structure: the panel edges are attached to both stringers (along the longitudinal direction) and ribs (along the spanwise direction). These attachments strongly restrain out-of-plane displacements but allow for some limited rotation at the edges, which is closer to a simply supported condition rather than fully clamped

or free. Since the stringers and ribs provide relatively stiff support in displacement but less so in rotation, the SSSS assumption provides a conservative estimate of the critical buckling stress.

For panels with aspect ratios a/b larger than 2 (which applies here, as the stringer spacing was always less than half of the rib spacing), the coefficient C for SSSS conditions approaches a constant value of 4. This allows the use of $C = 4$ consistently throughout the analysis. The choice of SSSS is conservative because more realistic partially clamped boundaries (SSCC or SSCS cases) would result in higher buckling coefficients and thus higher allowable stresses. Therefore, this assumption yields safe lower-bound estimates for panel sizing.

In this context, E and v are the Young's modulus and Poisson ratio of the skin material, t is the panel thickness, and b is the stringer spacing. If the normal stress calculated with Equation 6.9 exceeds the critical buckling stress from Equation 6.11, skin panel buckling is assumed to occur.

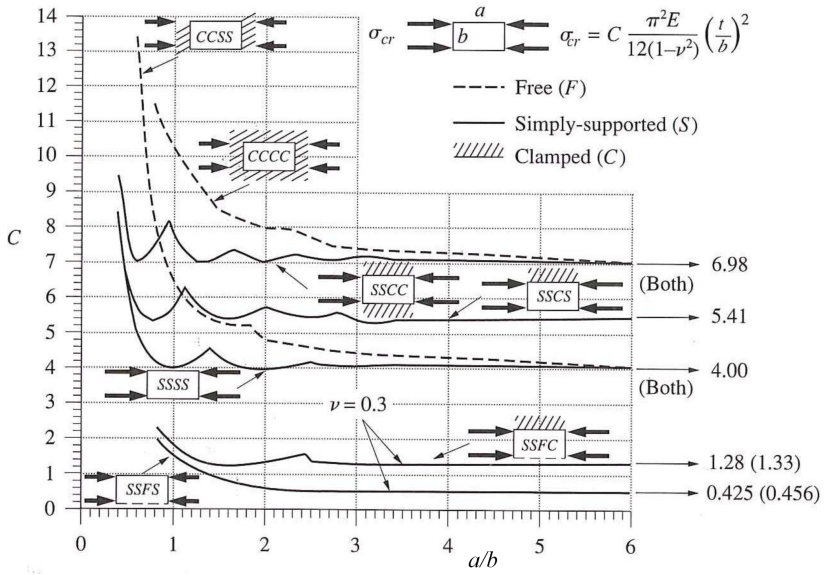

Figure 6.14: *Graph of the Buckling Coefficient*

Preliminary Failure Mode Analysis

The critical failure mode was identified to guide the design process.

Figure 6.15 presents, for a selected cross section made of CFRP, the calculated failure stresses for both buckling and yielding. The calculations were performed using the following parameters: Young's modulus (for buckling) of 55.00 GPa, stringer pitch (mean value) of 0.050 m, web thickness of 3 mm, and yield stress of 800 MPa.

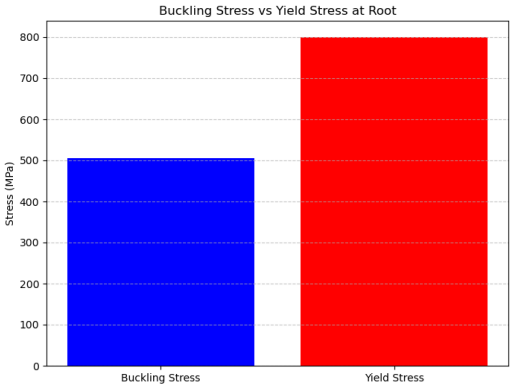

Figure 6.15: *Buckling versus Yield Stress for the Selected Cross Section*

From this figure, it can be concluded that buckling is the governing failure mode for this design, even for much smaller stringer spacing or higher web thicknesses. Shear failure was not considered in this analysis, as it primarily determines the spar web thickness and is not directly dependent on the global bending stiffness (e.g., I_{xx}), so it was not considered as the failure mode driving the design of the cross section.

With this in mind, the following approach was taken to designing the lightest wing box capable of withstanding skin panel buckling, shear failure and material yielding. First, the spar web thickness was sized to prevent shear failure, after which the rest of the cross section was designed to prevent skin panel buckling, as buckling had been identified as the critical failure mode.

Spar Web Sizing for Shear Loads

The spar web is here sized for preventing the shear stress from overcoming the maximum shear stress the material can withstand. For this, the shear flows, q, in the walls of the cross section must be analysed.

In order to find these shear flows, a preliminary analysis of the cross section was carried out, simplifying the structure using the idealised structure approach [62]. For the initial evaluation, the cross section was idealised by concentrating the structural areas into four booms positioned at the corners of the wing box [62].

This idealisation led to several conservative consequences: the bending stiffness was underestimated due to neglecting the skin's contribution; as a result, the maximum normal stress was overestimated because of the lower calculated bending stiffness. But simultaneously, the maximum shear flow was underestimated, as it was assumed to remain constant between booms. This underestimation of the shear flow was not considered problematic, since it was demonstrated that shear failure is not the critical failure mode for this design.

What this idealisation allowed to do is reduce the shear flows due to the vertical shear force in the upper and lower panels to zero[62]. The analysis then becomes very simple, with the situation presented in Figure 6.16. Following the idealised cross section assumption, the shear flow is evaluated in the front and rear spar of the wing box.

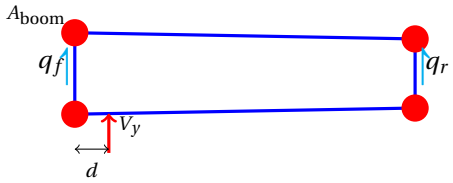

Figure 6.16: *Shear flows and vertical force in wing box*

Following force and moment equivalence, the value for shear flow in the front and rear spar is found using Equation 6.12 and 6.6.8.2.

$$q_r = \frac{V_y \cdot d}{h_r \cdot w} \tag{6.12}$$

$$q_f = \frac{V_y - q_r \cdot h_r}{h_f} \tag{6.13}$$

Where V_y corresponds to the shear force at the considered cross section, and d is 10% of the chord, based on the assumption that the force acts at the quarter-chord (25% of the chord), while the front spar is located at 15%, yielding $d = 25\% - 15\% = 10\%$.

To these shear flows from the shear force, the contribution of the torque from the pitching moment of the airfoil must be added.

Finding the contribution to the torque of every section of the wing is done with Equation 6.14:

$$\delta M = C_{m0} \cdot q_\infty \cdot c^2 \tag{6.14}$$

The $C_{m0} = -0.1032$ was found for the NACA4412 in airfoil tools [63], this was under the assumption that the angle of attack is 0°. Similarly q_∞ was found assuming V to be at cruise speed, and ρ to be at sea level as the airplane will be flying close to the ground. Integrating from the tip to the root of the wing yielded the internal torque the structure should be able to withstand. The final internal torque within the wingbox is shown in Figure 6.17:

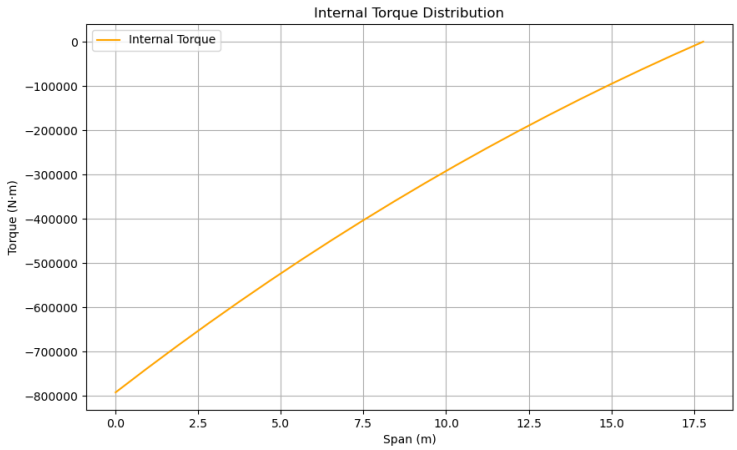

Figure 6.17: *Wingbox internal torque*

The contribution of the torque to the shear flow is found with Equation 6.15.

$$q_{torque} = \frac{T}{2 \cdot A_m} \tag{6.15}$$

Because the shear flow was assumed to point up in Figure 6.16, and that the torque creates a counter clockwise shear flow in the cross section, the final shear flows in the front and rear spars are shown in Equation 6.16 and 6.17:

$$q_{r_{final}} = q_r + |q_{torque}| \tag{6.16}$$

$$q_{f_{final}} = q_f - |q_{torque}| \tag{6.17}$$

Then using Equation 6.10 and setting τ equal to the τ_y of the material, the minimum thickness required can be found. The largest thickness found from q_r and q_f was applied to both spar webs for simplicity purposes. This decision is conservative as it will just make the spar with lower shear flow stronger. In order to make the design more manufacturable, a minimum thickness for the spar was set to be 1mm.

Skin Panel, Stringer and Boom Sizing

With the spar web thickness figured out, the skin web panel thickness, the amount of stringers and the boom area still need to be calculated. Here the boom area mentioned would correspond to the area on the flanges of the vertical spar. As investigated previously, it is buckling that will occur first in this cross section, and it will be sized accordingly.

The approach used for sizing the different parameters was as follows. A skin panel thickness and a stringer cross-sectional area, both tapering along the wing span, were initially defined. The skin panel thickness was assumed to decrease from 3 mm at the wing root to 1 mm at the wing tip. The stringer cross-sectional area was assumed to vary from 120 mm^2 at the root to 60 mm^2 at the tip. This stringer area correspond to L-shaped stringers, with dimensions ranging from 40 mm width and 1.5 mm thickness at the root, down to 30 mm width and 1 mm thickness at the tip.

With these parameters set, the buckling stress was calculated for a range of stringer counts, where the maximum number of 35 stringers was limited by a minimum spacing distance of 10 cm at the wing tip, where the stringers are closest to each other. This minimum spacing was selected to ensure sufficient attachment area on the wing box skin panel and to avoid overlap between adjacent stringers.

For each number of stringers, the corresponding buckling stress σ_{buckling} was then inserted into Equation 6.9, which allowed determining the required area moment of inertia I_{xx} such that the maximum normal stress in the structure remains equal to the calculated buckling stress (i.e., ensuring that the structure reaches, but does not exceed, its buckling limit). With the web thickness and number of stringers fixed, the required boom area needed to achieve this I_{xx} was subsequently calculated. When computing the boom area, a minimum area of 1000mm^2 was set to ensure manufacturability. The boom area required along the span is therefore plotted in Figure 6.18:

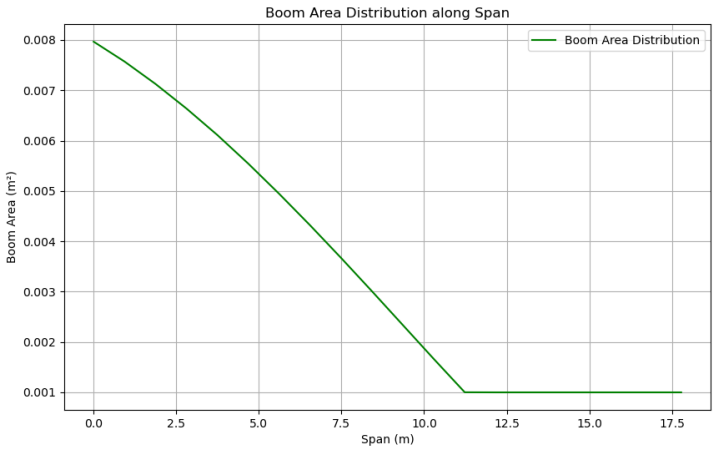

Figure 6.18: *Boom area distribution along the wing*

The boom area distribution, shown in the figure, exhibits particularly large values at the wing root, reaching approximately $0.008 m^2$. This results from the high bending moments at the root, which require a large area moment of inertia to reduce the normal stress in the cross section, and thus avoid buckling. In the current sizing, these boom areas represent simplified equivalent spar caps located at the top and bottom of the spar web. However, this design represents a very conservative preliminary estimation. In reality, by optimizing the spar cap geometry, using more efficient cross-sections than the circular booms assumed here, it is possible to achieve the required moment of inertia with less total material. This will ultimately allow for a reduction in cross sectional area, and a corresponding decrease in wing structural weight. A visual representation of the wingbox is shown in Figure **??**, where the boom areas and stringer areas ar not to scale, for clarity purposes.

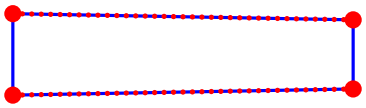

Figure 6.19: *Final wing box representation (point areas not to scale)*

For each iteration of amount of stringers, the corresponding wing box weight was computed, and the configuration resulting in the lowest total weight was selected as the final design. Finally, a safety factor of 1.5 (from the FAR 25 regulations) was applied to the calculated boom areas, and the spar web thickness, impacting the Ixx, normal stress and thus the final weight.

A graph showing the weights of the wing box for the different stringer amount, using carbon fiber-reinforced plastic is shown in Figure 6.20:

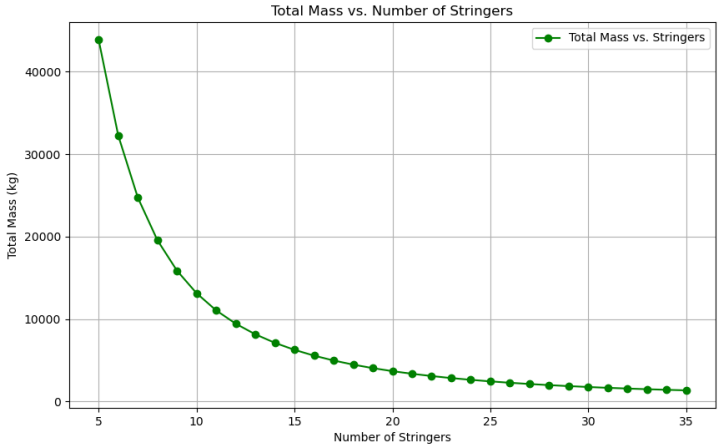

Figure 6.20: *Wing box mass for different amounts of stringers*

Wing Weight Estimation

Once the wing box was designed, the total wing weight was estimated. For this purpose, both the wing skin weight and the rib weight were calculated.

The wing skin weight was computed by assuming a constant thickness of 3 mm along the entire span. Although this value is higher than typically used for conventional aircraft, it was selected as a conservative estimate to account for the significant loads and demanding operating conditions that the aircraft is expected to encounter. The total wing skin weight was then calculated by multiplying the skin area by its thickness and the material density.

The rib weight was estimated by extrapolating the rib density (i.e., average number of ribs per meter of span) from the CL-415 aircraft. This rib density was then applied to the W-132 wing span to determine the total number of ribs per wing. Assuming a rib thickness of 3 mm (Value from visual inspection of ribs at the Aircraft Collection of TU Delft aerospace faculty, + margin), and finding the area of the airfoils along the span from an image measurement tool [3], the total rib weight was subsequently calculated.

To provide an estimation of the total wing weight, the weight rest of the components of the wing should be estimated. Namely the boundary layer control system, the high lift devices, the ailerons, hydraulics, wing skin stringers and miscellaneous other components should have their weight estimated. No source regarding the weight distribution amongst the different components could be found in aircraft design books or online, so it was evaluated that the wing box + ribs + wing skin weight would amount to 80% of the total wing weight.

Material Selection

With the code for the whole aircraft set up, different potential materials with their properties were tested to see the overall aircraft weight. The carbon fiber-reinforced plastic (CFRP) led to the overall lowest aircraft weight. Subsection 6.9.3 investigates further the whole material selection and analysis. For the wingbox, due to all the loads acting in all directions, a quasi isotropic CFRP (0, $\pm$ 45, 90) was used. Its characteristics used here were 60 MPa for the τ_{max} (from Chapter 6.8.4 of [64], ρ= 1550 kg, ν= 0.3, E for compression (buckling) = 55 GPa [4].

[3] Image measurement tool: https://imagemeasurement.online/image/select.

[4] Gonçalo Fonseca, *Carbon Fiber Quasi-Isotropic Laminate*, Scribd, available at https://www.scribd.com/document/76975806/Carbon-Fiber-Quasi-Isotropic-Laminate.

This therefore yielded a weight of **5066 kg** for the whole wing group. As the wing box was sized to be able to withstand the highest loads, coming from the limit load of 4g, the REQ-AER-7 is verified.

6.6.8.3. Further Development of the Wing Structure

This section served as a feasibility study for the wing designed. This analysis could be improved in the future by considering some of the following points.

The column buckling of the stringers was not analysed, nor was the buckling of the wing skin, the crippling of spar caps, and stringers. Including them in the analysis could lead to stricter failure modes, constraining the design further.

The boom (spar cap), and stringers were left as point areas while their shape should be defined. This should help with improving the I_{xx}, reducing the area needed there, and thus reducing the overall weight.

The contributions of the thrust of the engine and the drag of the floater could be included to increase the accuracy of the internal torque distribution. Their omission in the present study was not critical, as the pitching moment of the airfoil already alleviates part of the shear flow in the front spar. Accounting for the engine and floater would further reduce even more the shear flow in the front spar while increasing it in the rear spar. Nevertheless, the resulting changes in spar web thickness would be expected to remain limited and would not significantly affect the overall wing weight.

Other structural aspects should be considered as well, such as the link between the engine or the floater and the wingbox, to ensure efficient load transfer.

Due to the high loads at the wing root, the structural elements are particularly large in this region. Adding more stringers or introducing an additional spar extending over one third of the wing could allow for a lighter and more efficient structure.

An rough value of the wing weight as used in the load analysis for shear. In the future, a loop should be done to include the newly calculated wing weight in the vertical loads acting on the wing.

One load case that was not considered is analysing the force of the wing in the horizontal direction. So looking at the drag's impact on the cross section, as well as the case where one floater would touch the water during the scooping manoeuvre, hence creating a very large moment along the y-axis at the wing root. However, the current design can already be considered as quite good as I_{yy} is probably very large due to the fact that the wing box is quite "slender", meaning that a lot of area is far away from the y-axis. With the large boom areas that were found out, this should already be able to sustain some relatively high loads along the x-axis.

6.7. Stability and Control

6.7.1. Requirements

Before explaining the approach on stability and control, the requirements associated with it must be recalled. This is shown in Table 6.19.

Table 6.19: *Requirements regarding stability and control*

Requirement ID	Description	Compliance	Verification Method
REQ-S&C-1	The center of gravity shall remain within limits when the tank is full	✓	Analysis, verified
REQ-S&C-2	The c.g range shall be limited to a maximum value of 0.5 m	✓	Analysis, verified
REQ–S&C-3	The aircraft shall maintain control and stability in extreme environments	✓*	Analysis, not verified

REQ–S&C-3 has not been verified because a dynamic stability analysis should be conducted to verify this requirement. To simulate extreme environments, a dynamic stability analysis that models eigenmotions such as phugoid, short-period, dutch roll, and aperiodic roll would have been the next step in the stability and control analysis. However it is expected for this requirement to be met in future development stages.

6.7.2. CG Excursion

In order to calculate the CG position of the aircraft, a preliminary CG excursion is carried out. First, the aircraft components are subdivided into two groups, the fuselage group and the wing group. For instance, the propulsion system is considered part of the wing group due to its wing-mounted engine design. Subsequently, the weights of each specific subcomponent are obtained from the Class II weight estimation. Then, an initial estimation of the OEW CG position is chosen, and the CG positions of the subcomponents within the fuselage are estimated to compute it. Table 6.20 demonstrates these initial estimates.

Table 6.20: *Center of Gravity (CG) locations of aircraft components and groups*

Description	Location Expression
Wing center of gravity (CG) location	40% of wing chord at 40% span
Fuselage CG location	38% of fuselage length
Empennage CG location	Given directly as empennage CG
Propulsion system CG location	25% of mean aerodynamic chord (MAC)
Fixed equipment CG location	38% of fuselage length
Operating empty weight (OEW) CG	25% of mean aerodynamic chord (MAC)
CG of fuselage, empennage, and fixed equipment	Weighted average of individual CGs
CG of wing and propulsion systems	Weighted average of individual CGs

These locations, together with the OEW estimate, lead to the longitudinal position of the LEMAC (Leading Edge Mean Aerodynamic Chord) which is computed using Equation 6.18

$$X_{\text{LEMAC}} = X_{\text{FCG}} + \bar{c}\left[\left(\frac{x}{c}\right)_{\text{WCG}} \frac{M_w}{M_F} - \left(\frac{x}{c}\right)_{\text{OEWCG}} \left(1 + \frac{M_w}{M_F}\right)\right] \tag{6.18}$$

This formula gives the initial longitudinal position of the wing. Then the OEW CG location can also be calculated using:

$$X_{\text{CG}} = \frac{\sum M_i X_i}{\sum M_i} \tag{6.19}$$

The resultant OEW CG location is then used in an iterative procedure where a new XLEMAC is computed to update the OEW CG location. This process is repeated until the difference between successive OEW CG locations is less than 1%, starting with an initial value of 8.1 m in the first iteration. Once this convergence criterion is met, the variation in CG due to fuel and payload weights is analysed. The fuel CG is assumed to be located at 25% of the MAC, while the payload CG is assumed to coincide with the CG location of the OEW + fuel configuration, satisfying both REQ-S&C-1 and REQ-S&C-2. After nine iterations, final CG calculations are performed using the exact component locations derived from 3D drawings and detailed design data. Based on these refined values, the aircraft loading diagram is constructed as follows:

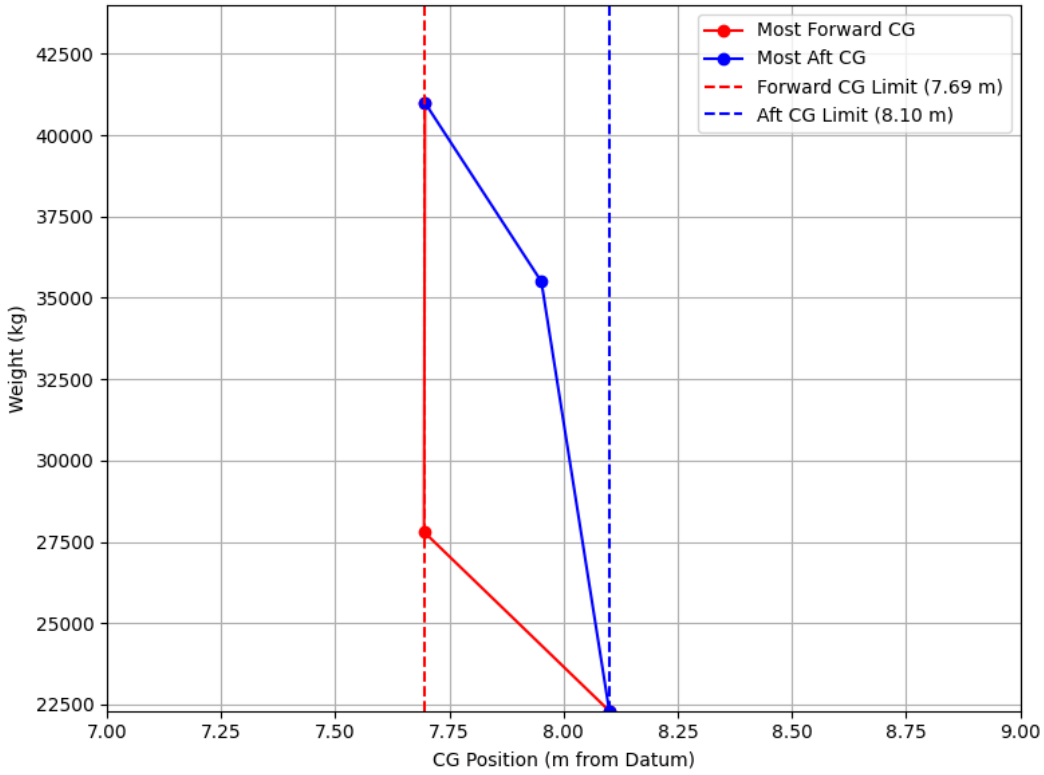

Figure 6.21: *Initial loading diagram with initial CG limits*

Figure 6.21 demonstrates the maximum range of CG locations for an initial calculation of the wing position, as shown by the vertical lines. It can also be noted that the change in CG by the water drop remains minimal, ensuring secure drops. The process described above will be iterated throughout the whole design phase with the updated values. The CG excursion explained above is dependent on the value of the LEMAC, so the same procedure is carried out through a series of iterations, where the longitudinal position of LEMAC is varied, to calculate the shifted CG range of each iteration. The result of this operation is shown in Figure 6.22:

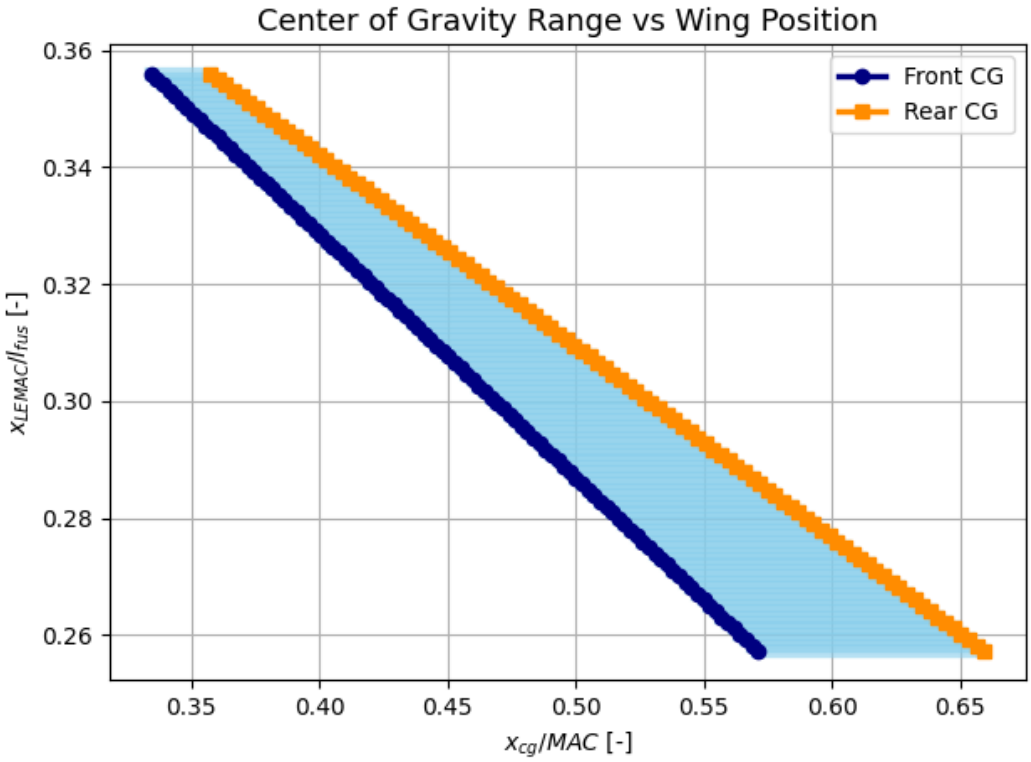

Figure 6.22: *CG range vs wing position*

This graph shows the different CG ranges for different wing positions. To select the most optimal wing position, this plot is superimposed onto the scissor plot of the aircraft. The scissor plot demonstrates the curves for stability and controllability of the W-132 expressed by Equation 6.20 and Equation 6.21.

$$\bar{x}_{c.g.} = \bar{x}_{a.c.} + \frac{C_{L_{\alpha_h}}}{C_{L_{(A-h)_h}}}(1 - \frac{d\varepsilon}{d\alpha})\frac{S_h l_h}{S\bar{c}}(\frac{V_h}{V})^2 - S.M. \tag{6.20}$$

$$\bar{x}_{c.g.} = \bar{x}_{a.c.} - \frac{C_{m_{ac}}}{C_{L_{A-h}}} + \frac{C_{L_h}}{C_{L_{A-h}}}\frac{S_h l_h}{S\bar{c}}(\frac{V_h}{V})^2 \tag{6.21}$$

After calculating and obtaining all of the necessary parameters to calculate these curves, the scissor plot of the aircraft can be obtained and superimposed on the CG range versus wing positioning plot. This final plot is used to determine the necessary sizing for the horizontal stabiliser. This minimum value of area for the horizontal stabiliser will ensure that the aircraft is stable and controllable enough within the CG ranges that it can achieve throughout the mission. As shown in Figure 6.23, the minimal required S_h/S for the aircraft to be able to restore any disturbance and provide enough force for manoeuvring is $S_h/S = 0.24$. Raymer [1] states that a stability margin between 10% and 10% should be used, so a stability margin of 10% has been used to ensure stability under all conditions.

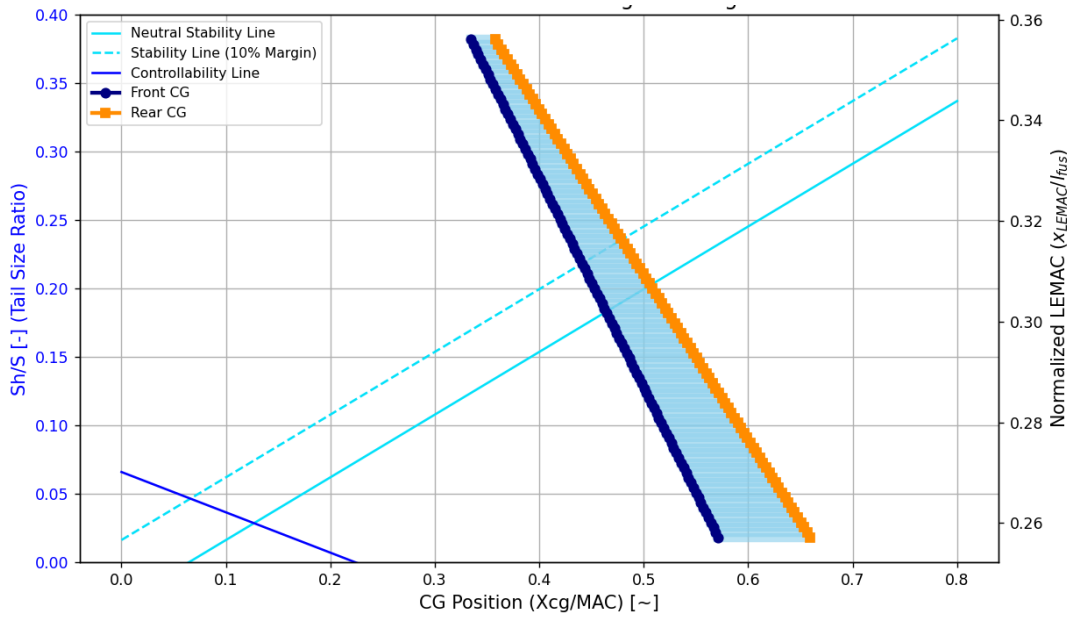

Figure 6.23: *Final scissor plot with CG range vs wing position plot*

From Figure 6.23, it can be concluded that the limiting factor in this case is stability. This means that the horizontal stabiliser size is driven by the stability requirement, which is needed so that the aircraft is able to restore any disturbances appropriately in every flight condition.

Finally, the final longitudinal position of the LEMAC is calculated from the graph, using the right-hand axis, leading to a final X_{LEMAC} of 6.4m, and final CG limits of 8.42 m and 8.74 m for the most forward and most aft CG positions, respectively. These are the final values after all the iterations throughout the design phase with the final values.

6.8. Empennage Design

The empennage provides stability and control in pitch and yaw, ensuring safe and balanced flight. In this design, the empennage is slightly larger than typical market examples. This compensates for the aircraft's shorter tail arm, maintaining the required control authority and stability. Table 6.21 presents the geometric and aerodynamic characteristics of the final design. Figure 6.24 illustrates the geometry of the empennage.

Table 6.21: *Geometric and aerodynamic properties of empennage components*

Property	Horizontal Tail	Vertical Tail	Ventral Fin	Dorsal Fin
Airfoil	NACA0012	NACA0012	NACA0012	NACA0012
Moment Arm (m)	12.04	9.99	9.99	–
Area (m^2)	34.94	25.66	3.70 (6.98) [5]	
Aspect Ratio	4	1.2	0.31	0.63
Taper Ratio	0.8	0.6	–	0
Span (m)	11.82	5.55	1.47	1.09
Average Chord (m)	2.96	4.62	4.77	1.74
Sweep angle (deg)	2	30	30	75
Control Surface Span Ratio	0.9	0.8	1.0	–
Control Surface Chord Ratio	0.25	0.3	0.3	–

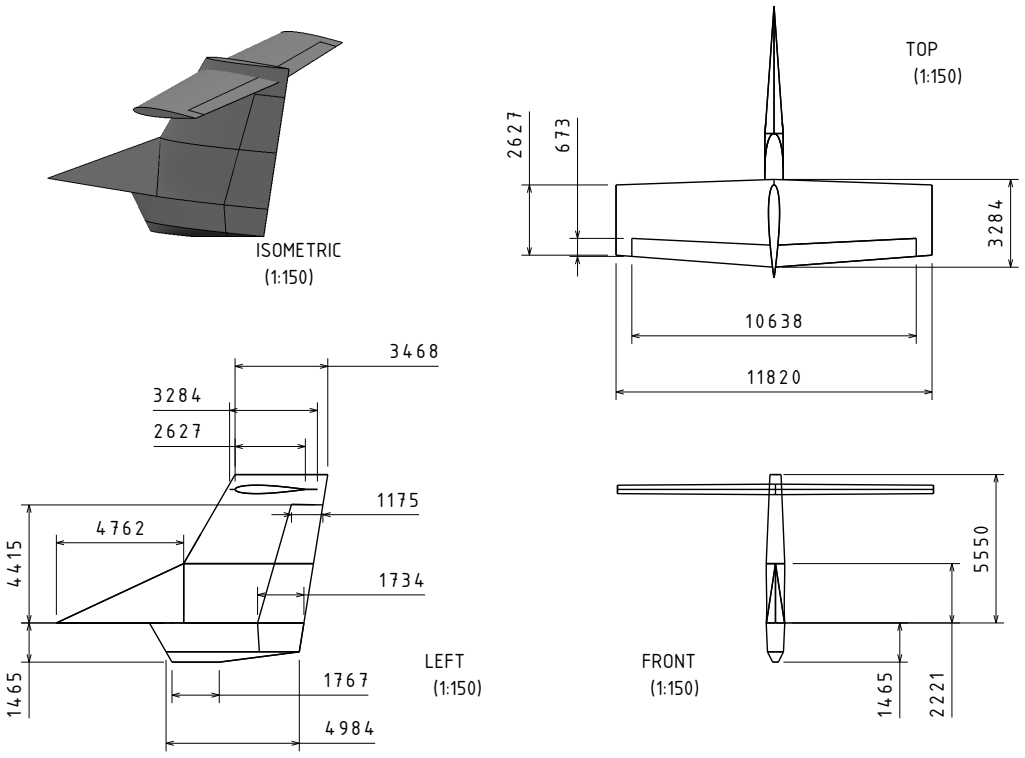

Figure 6.24: *Technical Drawing of the Empennage (units in mm)*

6.8.1. Requirements

The design of the empennage is driven by the mission requirements. The empennage follows the general aircraft requirements presented in Table 6.1. Additionally, the mission requirements associated with the empennage have been used to derive the following empennage requirements: Table 6.22.

While the design can fulfil all stated requirements, the compliance is pending analysis due to the current level of design detail. The sizing and positioning were performed using established methods from Raymer and Roskam, which offer statistically validated starting points. However, test flight demonstrations, methods like detailed aerodynamic modelling and analysis of the stability and control derivatives are still required to confirm compliance.

[5]The ventral fin has an area of 6.98 m^2, of which 3.70 m^2 is exposed to airflow

Table 6.22: *Requirements of the empennage*

Requirement ID	Description	Compliance	Verification Method
REQ-EMP-1	The aircraft shall take off in wind conditions of up to 20 knots ([65], pg. 46)	✓*	Demonstration, not verified
REQ-EMP-2	The aircraft shall land in wind conditions of up to 20 knots ([65], pg. 46)	✓*	Demonstration, not verified
REQ-EMP-3	The aircraft shall reduce its vertical oscillations during extinguishing manoeuvres	✓*	Analysis, not verified
REQ-EMP-4	The control surfaces shall adapt to gust loads to maintain stability	✓*	Analysis, not verified
REQ-EMP-5	The control surfaces shall adapt to manoeuvring loads to maintain stability	✓*	Analysis, not verified
REQ-EMP-6	The control surfaces shall provide sufficient force to keep the aircraft stable	✓*	Analysis, not verified
REQ-EMP-7	The control surfaces shall maintain pitch within ±2° of commanded values	✓*	Demonstration, not verified
REQ-EMP-8	The control surfaces shall maintain yaw within ±2° of commanded values	✓*	Demonstration, not verified

6.8.2. Preliminary Design

The preliminary sizing of the empennage forms the foundation of the tail design process and aims to define the overall geometry and positioning required to ensure adequate stability and control. This phase begins with the selection of the tail configuration. Once this is established, key design constants are defined, guided by statistical data and practices outlined in Roskam's methodology. Finally, an iterative class II sizing and positioning is performed to define the location and dimensions of the tail, as well as the weight.

6.8.2.1. Tail Configuration

The selection of the empennage configuration is a critical early step in the design of the tail. According to Raymer's *Aircraft Design: A Conceptual Approach*, multiple tail types are available ([1], pg. 99). For this project the most feasible tail configurations considered where the conventional tail, T-tail, cruciform tail and H-tail. Other configurations such as twin-boom and V-tails were excluded due to their incompatibility with the aircraft's mission profile and unfamiliarity.

A trade-off analysis was conducted to objectively evaluate the remaining tail configuration options using the following five criteria, each weighted according to its importance in the context of the mission. The criterion and weights are as follows:

- **Structural weight (0.3)**: Assesses the impact of the tail configuration on aircraft mass.
- **Integration with high-wing configuration (0.3)**: Measures how effectively the tail configuration avoids aerodynamic interference from the wing's wake.
- **Complexity (0.2)**: Simpler solutions are favoured for cost and reliability.
- **Deep stall susceptibility (0.1)**: Evaluates the risk of entering a deep stall condition, where the tail gets blanketed by the wing at high angles of attack.
- **Water clearance (0.1)**: How well the tail is protected from water spray during scooping (In

compliance with REQ-SYS-5).

Each tail configuration was scored from 0 to 1 for each criterion, based on assessments drawn from Raymer and engineering judgement. Scores were then multiplied by their respective weights to determine a final, weighted total score for each option.

Table 6.23: *Tail configuration trade-off*

Tail Type	Weight	Conventional	T-Tail	Cruciform	H-Tail
Structural Weight	0.30	0.9	0.6	0.8	0.4
High-wing Integration	0.30	0.2	0.9	0.8	0.6
Complexity	0.20	0.9	0.8	0.6	0.5
Deep Stall	0.10	0.9	0.3	0.5	0.9
Water Clearance	0.10	0.2	1	0.8	0.3
	Total Performance	0.62	0.74	0.73	0.52

The T-tail configuration achieved the highest total score of 0.74, primarily due to its superior integration with the high-wing design of the aircraft. By placing the horizontal stabilizer atop the vertical fin, the T-tail avoids aerodynamic interference from the wing's wake, ensuring cleaner airflow over the control surfaces, which is essential during critical flight conditions such as low-speed maneuvering and water drops.

The cruciform tail performed almost as well, and it provides important advantages over the T-tail, most notably a reduced structural weight as the bending loads on the fin are smaller. However its structural complexity penalizes it, as the horizontal tail root must fit within the vertical tail without intersecting the rudder. However this option may be necessary if the deep stall behaviour of the T-tail is deemed insufficient in a more detailed analysis (Subsubsection 6.8.3.3).

In conclusion, the T-tail configuration presents the best compromise among the evaluated criteria, and the following design phases will proceed with this tail layout.

6.8.2.2. Preliminary Positioning and Sizing

The preliminary sizing process is part of a broader iterative loop used to estimate aircraft geometry and weights during the conceptual design phase. The code sequentially executes Class I and II weight estimations following Roskam's methodology, integrating the wing, fuselage, and tail subsystems. These elements are recalculated in each iteration until convergence is achieved.

Within this framework, a tail sizing function computes the position and size of the horizontal and vertical stabilizers. Firstly, several parameters are assumed and constant (aspect ratio, taper, leading edge sweep angle, volume coefficient) and taken from statistical relationships from similar aircraft. The tail arms are then calculated from estimated chord lengths and the centre of gravity position. Finally, the required tail areas are calculated ensuring sufficient longitudinal and directional stability following equations 8.1 and 8.2 in Roskam's *Airplane Design Part II* ([56], pg. 190).

The resulting tail dimensions are used to estimate tail weight using Torenbeek's method for commercial transport airplanes ([66], pg. 74). This data is then reintegrated into the aircraft model to update total mass properties and center of gravity, feeding into the next iteration of the sizing loop. This ensures that the empennage is not only properly dimensioned but also harmonized with the rest of the aircraft's structure and aerodynamic layout.

6.8.2.3. Design Integration Issues

During the initial design iteration of the empennage, a significant convergence issue was encountered. When the tail was positioned such that the trailing edge of the tail root aligned with the end of the fuselage, the sizing iteration diverged. The divergence arose from a self-reinforcing loop: increasing the empennage area to meet stability needs shifted the leading edge forward, shortening the tail arm. A shorter tail arm required an even larger surface to maintain the same moment, further reducing the tail arm. This is shown in the following figures:

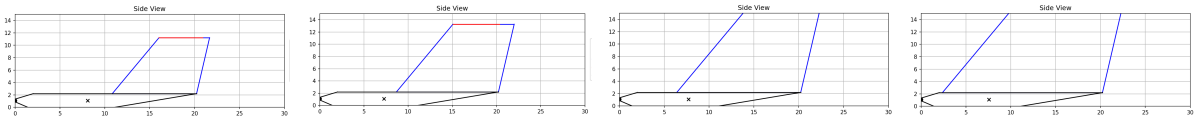

(a) *First Iteration* **(b)** *Second Iteration* **(c)** *Third Iteration* **(d)** *Fourth Iteration*

Figure 6.25: *Tail Area Diverging*

To break this cycle and achieve convergence, it became necessary to position the empennage rearward, beyond the original fuselage boundary. A series of configurations were tested where increasing fractions of the tail chord were placed outside the fuselage. These variants were labelled WA-132-0.25, WA-132-0.5, WA-132-0.75, and WA-132-1, indicating that 25%, 50%, 75%, and 100% of the empennage chord extended aft of the fuselage, respectively.

For each case, the tail arm increased due to the more rearward position of the aerodynamic centre, which allowed the tail surface area to decrease. The results are summarized in Table 6.24:

These results are compared to the current market. As can be seen, the tail arm of the aircraft is very small as compared to similar aircraft, and moving the empennage rearwards corrects this anomaly (Figure 6.26a). From this graph, it can be seen that model WA-132-0.75 fits the best to the current market. Moreover, because the tail arm is so small, this is compensated by a large surface area of the tail (Figure 6.26b). As the empennage is moved rearwards, this is made smaller, and models WA-132-0.75 and WA-132-1 seem to be the most similar to the current market.

Table 6.24: *Effect of empennage position on tail sizing and weight estimation*

Parameter	WA-132-0.25	WA-132-0.5	WA-132-0.75	WA-132-1
S_w [m^2]	150.95	148.2	146.9	146.1
S_h [m^2]	47.3	39.4	34.8	31.6
S_v [m^2]	45.3	35.0	29.8	26.4
x_h [m]	11.32	13.22	14.77	16.1
x_v [m]	8.59	10.83	12.57	14.1
MTOW [kg]	42700	41900	41600	41300
OEW [kg]	22000	21400	21100	20900

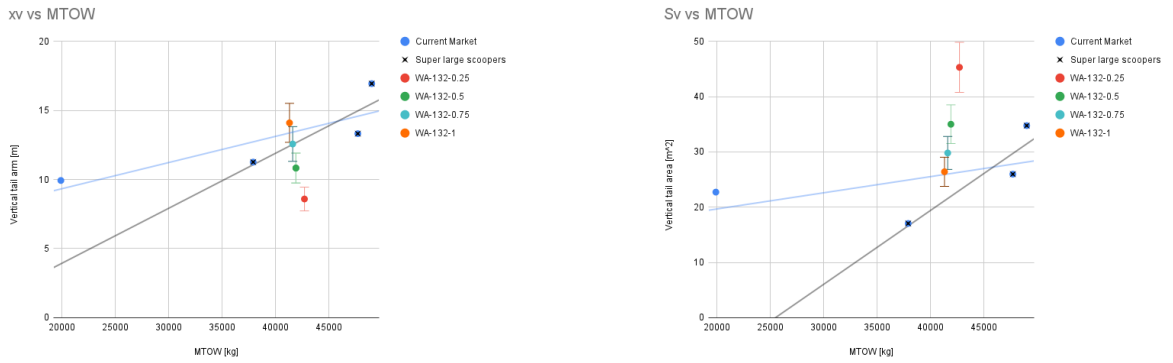

(a) *Tail Arm Comparison* **(b)** *Tail Area Comparison*

Figure 6.26: *Comparison of results to current market*

From the results, it becomes evident that placing the empennage further aft leads to a more compact and realistic tail design, as well as reducing the aircraft's weight. The trade-off, however, is structural and geometric: the feasibility of mounting the empennage further aft must be examined carefully. This involves analysing the internal structure of the vertical tail.

Vertical Tail Structure

The vertical fin is built around two main spars. According to Raymer, rudders and elevators are typically located in the final 25-50% of the tail chord ([1], pg. 162). This means that spars are located in the initial 50-75% of the tail chord. As these are the attachment points to the fuselage, a spar configuration located close to the tail chord leading edge is preferred. Hence, the spars will be located at 20% and 50% of the vertical tail chord. The rudder will be mounted in the final 35% of the chord, running from 90% of the fin tip to the base. Internal ribs and stiffeners will support the skin and maintain airfoil shape, playing a secondary role in load transmission. With this configuration, at most 55% of the vertical tail chord can be located rearwards of the fuselage, hence this configuration is selected. The rib placement can be seen in Figure 6.27.

In order to make the empennage aerodynamically efficient, this design has to modified. The following figure shows the possibilities to do this. A trade-off is done between both options to select which option is best (See Table 6.25).

(a) *Option A: Make Fuselage longer* **(b)** *Option B: Make Empannage Larger (Ventral Fin)*

Figure 6.27: *Tail Integration Possibilities*

Table 6.25: *Empennage extension trade-off*

Criterion	Weight	Option A: Longer Fuselage	Option B: Ventral Fin
Structural Complexity	0.2	0.8	0.4
Weight Impact	0.4	0.6	0.5
Tail Effectiveness	0.3	0.0	1.0
Payload	0.1	1.0	0.0
	Total Score	0.50	0.58

From this trade-off, Option B is clearly preferred. While it introduces a moderate weight and complexity penalty, it increases the tail area by around 12%. The slightly oversized tail area introduces redundancy, ensuring sufficient control margin even under off-nominal conditions or potential future growth in aircraft size or weight. Moreover, the use of a ventral fin mitigates the impact of wake interference at high angles of attack, where the wing can blanket the vertical tail.

6.8.2.4. Preliminary Design Results

With these design issues resolved, the preliminary sizing and positioning can be finalized, and the empennage weight can be calculated using equations 5.19 to 5.21 of Roskam's *Airplane Design Part V- Component Weight Estimation*. The results are shown in Table 6.26. Note that for now, the ventral fin is not taken into account and its contribution will be discussed in Figure 6.29a.

Table 6.26: *Geometric and aerodynamic properties of the empennage components*

Component	Horizontal Stabiliser	Vertical Stabiliser
Moment Arm (m)	12.88	10.44
Area (m^2)	40.64	36.46
Span (m)	12.75	6.61
Chord (m)	3.19	5.51
Aspect Ratio	4.0	1.2
Sweep (deg)	7	30
Taper Ratio	0.8	0.6
Weight (kg)	1051	983

Validation through weight estimation:

In Roskam's Airplane Design Part V book, three examples of Class II weight estimates are performed [66], (pg. 46). These results can be taken to calculate what percentage of the operational empty weight the empennage weight account for. This yields an average value of 4.92%. Given the small tail arm, and hence large tail area, of this aircraft with respect to conventional ones, it is expected that this percentage to be higher. The empennage weight estimation is deemed valid as long as it does not surpass 10% of the OEW. The current OEW of the aircraft is 21500 kg, hence the empennage weight should be no larger than $21500 \cdot 0.1 = 2150$ [kg]. The current empennage weight is 2034 kg, which is just below this limit, hence for now, the empennage weight is valid. However the preliminary design serves only as a foundation, and a more detailed design must be done to calculate final values for the empennage sizing and positioning, which are expected to yield a more realistic weight. This is done in the next section.

6.8.3. Detailed Design

The detailed design of the empennage refines the initial geometry established during preliminary sizing, focusing on aerodynamic performance, stability and control requirements. This stage begins with the selection of appropriate airfoils for the stabilizing surfaces, followed by detailed sizing of the horizontal and vertical tails. Additional components such as control surfaces, dorsal and ventral fins are incorporated to enhance stability. The section concludes with a summary of final dimensions and performance parameters.

6.8.3.1. Airfoil Selection

The selection of an appropriate airfoil is a fundamental step in the aerodynamic design of the tail surfaces. For the empennage, where stability and control effectiveness are priorities, the airfoil must be capable of generating sufficient lift while maintaining low drag and structural simplicity.

A symmetric airfoil is chosen for the tail surfaces to ensure that the airfoil produces zero lift at zero yaw angle and to function effectively in both positive and negative yaw angles. Symmetric airfoils also avoid introducing any unintended pitching moments. Several symmetric NACA four-digit airfoils are evaluated: NACA 0009, 0010, 0012, and 0015. These profiles differ primarily in thickness, which affects both structural weight, drag and lift performance. The following table summarizes their key aerodynamic characteristics, analysed with XFLR5.

Table 6.27: *Aerodynamic characteristics of selected NACA symmetric airfoils at* $Re = 10 \times 10^6$, $M = 0.6$

Property	NACA0009	NACA0010	NACA0012	NACA0015
C_{D_0}	0.00495	0.00507	0.00533	0.00571
$C_{L,\max}$	0.8683	0.9369	1.0757	1.2172
$(C_L/C_D)_{\max}$	108.96	112.61	117.59	118.26

High lift capabilities are prioritised in the selection, as the current preliminary design has a very large surface area and it is necessary to decrease it. The NACA 0012 airfoil is selected as the most suitable option for the tail surfaces. It provides a good balance between aerodynamic efficiency and structural feasibility. While the NACA 0015 offers slightly higher lift and C_L/C_D performance, the drag penalty is deemed too high. The same NACA 0012 airfoil is considered for both the horizontal and vertical tail surfaces to simplify the design process. However, future work will involve separate, detailed analyses using CFD to evaluate the suitability of this airfoil for each tail component under their respective flow conditions.

6.8.3.2. Vertical Tail Sizing

The sizing of the vertical tail is primarily driven by the requirement to maintain directional stability in the event of an engine failure. In such a scenario, the vertical tail must generate sufficient yawing moment to counteract the asymmetric thrust from the operative engine.

Since the propellers are counter-rotating, there is no critical engine, and the specific engine failure case is not crucial to the analysis. To keep the vertical tail yaw contribution positive, the scenario analysed will be the case where the left engine fails. The sum of yawing moments about the aircraft's centre of gravity can be expressed as: $N = N_{\text{wing}} + N_{\text{ailerons}} + N_{\text{fuselage}} + N_{\text{vertical tail}} - N_{\text{engine}}$.

Several simplifying assumptions are made:

- Propeller drag (D) is negligible.
- Yawing moments from the wing and fuselage are small and neglected.

- Only the yaw moment contributions from the ailerons, the vertical tail side force (F_{V_y}), and the engine thrust (T) are considered.

In the event of engine failure, the aircraft is expected to operate at or near minimum airspeed, approximately 36 m/s. The available power from one engine is 2.8 MW, and from this, the thrust generated by the operative engine is estimated. The resulting yawing moment due to asymmetric thrust is $N_{\text{engine}} = T \cdot Y_p = 272{,}223\,\text{Nm}$.

To assist with yaw control, a maximum aileron deflection of 20° is assumed. This causes the left wing to produce more lift, and consequently more induced drag, resulting in a positive yawing moment. Using XFLR5, the lift generated is estimated, and from the lift-to-drag ratio at the corresponding angle of attack, the induced drag is computed. The yaw moment contribution from the ailerons is then calculated as $N_{\text{ailerons}} = 3{,}730\,\text{Nm}$. This value accounts for both wings, using the average moment arm from the ailerons to the aircraft centreline.

The remaining yawing moment must be balanced by the vertical tail. The yawing moment generated by the vertical tail is given by $N_{VT} = q \cdot S_v \cdot C_{L_{v_{max}}} \cdot l_h$, where q is the dynamic pressure at stall speed, S_v is the vertical tail surface area, $C_{L_{v_{max}}}$ is the maximum vertical tail lift coefficient (estimated using XFLR5 with flap deflection), and l_h is the tail arm. Solving this equation yields a minimum required vertical tail area of 29.85 m^2.

Accounting for the contribution of the ventral and dorsal fin, which is estimated to increase the effective surface area by approximately 15%, the vertical tail design is considered adequately robust and redundant to ensure safe engine-out operation and other scenarios. Hence, it is assumed that REQ-EMP-1 and REQ-EMP-2 are complied.

6.8.3.3. Horizontal Tail Sizing

The horizontal tail is sized based on longitudinal stability and controllability requirements. An analysis of controllability and stability has already been explained in the previous section. The scissor plot shows the relationship between the horizontal tail's surface area and the aircraft's centre of gravity limits.

From the scissor plot, a tail area ratio of $S_h/S = 0.24$ is determined, where S_h is the horizontal tail area and S is the wing reference area (Figure 6.23). This corresponds to a horizontal tail surface area of 34.94 m^2.

The sizing of the horizontal tail is driven by the stability requirement, which is needed so that the aircraft is able to restore any disturbances appropriately. It is assumed that this design ensures REQ-EMP-3 is complied.

Deep Stall

As discussed in Table 6.23, T-tail configurations are susceptible to deep stall, a condition in which the tail becomes immersed in the wing's wake during high angles of attack. This is particularly problematic for an aircraft expected to perform aggressive pitch manoeuvres, such as those encountered during aerial firefighting operations. To make sure that the current design is not prone to this phenomenon, the positioning is checked so that it is placed in a safe region. This is illustrated in Figure 6.28. The red airfoil represents the geometry and positioning of the horizontal stabiliser.

In the current design, the T-tail would not be blanketed by the wing wake under these high-angle-of-attack conditions. This configuration is acceptable as long as the wing is a type II wing as stipulated by K. P. Spreeman ([67], pg. 90). Investigating this is an action point for further development.

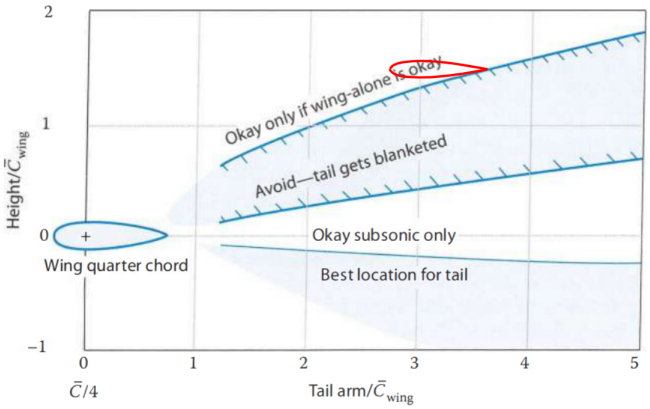

Figure 6.28: *Aft tail positioning [1], pg. 102*

6.8.3.4. Dorsal and Ventral Fin

To enhance directional stability and delay rudder stall, dorsal and ventral fins are employed.

Dorsal Fin

The dorsal fin is particularly effective in improving stability during high side-slip conditions by delaying the flow separation over the vertical stabiliser, thus postponing rudder stall. This is especially important during engine-out scenarios.

For this preliminary design, the dorsal fin is sized using the method proposed by P. Barua et al. ([68], pp. 95–98). Based on empirical trendlines, a surface area of approximately 1.90 m^2 is obtained. This value aligns well with proportions seen in comparable aircraft and is considered reasonable at this stage. The layout is shown in Figure 6.29b.

Ventral Fin

The ventral fin serves to increase the vertical tail surface area when the vertical stabiliser alone is insufficient, such as when the wing blankets the rudder during high angle of attacks. This ensures that at least 1/3 of the rudder is unblanketed to maintain lateral controllability during such manoeuvres ([1], pg. 110).

A critical design constraint is ensuring the ventral fin does not violate the required scrape angle. To satisfy this, the fin is constructed as follows: the ventral fin leading edge is drawn with the same sweep angle as the vertical stabiliser, extending downward until it reaches point A in Figure 6.29a. From point A, a horizontal segment is drawn to point B, representing the tip of the ventral fin. From point B, the profile is extended upward following the scrape angle limit until it intersects at point C. Finally, point C is connected to the trailing edge of the vertical tail, forming the aft portion of the ventral fin. The exposed area of the ventral fin is 3.70m^2.

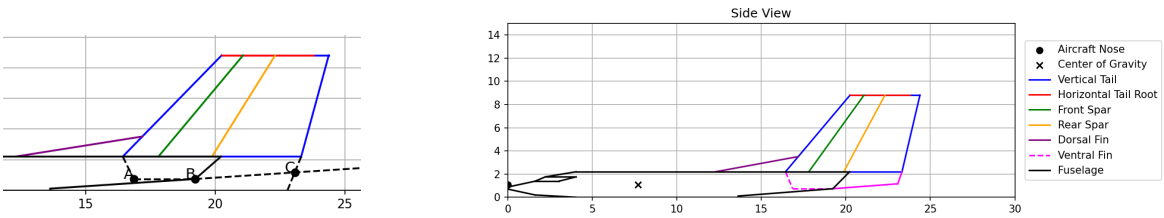

(a) *Construction of ventral fin*

(b) *Layout of dorsal and ventral fins*

Figure 6.29: *Aircraft side view with dorsal and ventral fins*

6.8.3.5. Control Surfaces

The control surfaces of the empennage, namely the rudder and the elevator, are essential for ensuring the aircraft's ability to rotate about the yaw and pitch axes, respectively.

Due to time constraints, a detailed aerodynamic and structural sizing of these surfaces has not been conducted. Instead, a preliminary sizing approach has been adopted, based on the empirical method proposed by Raymer ([1], pg. 162).

According to this method:

- The rudder is assumed to occupy the final 30% of the vertical tail chord.
- The elevator occupies the final 25% of the horizontal tail chord.
- The rudder spans from the base of the ventral fin up to 80% of the vertical tail span. This limited extent accounts for the fact that the rudder starts lower due to the ventral fin and avoids interference with the horizontal tail, located at 90% of the height of the vertical fin.
- The elevator spans from the root of the horizontal stabiliser (or as close as structurally permissible) out to 90% of the span.

These estimations serve as a first iteration for defining the control surfaces' geometric properties. A more refined design, including deflection limits, hinge moments, and actuator sizing, should be developed in subsequent design phases. For now, it is assumed this method ensures that REQ-EMP-4 to REQ-EMP-8 are complied.

The final tail with all components integrated is shown in Figure 6.30.

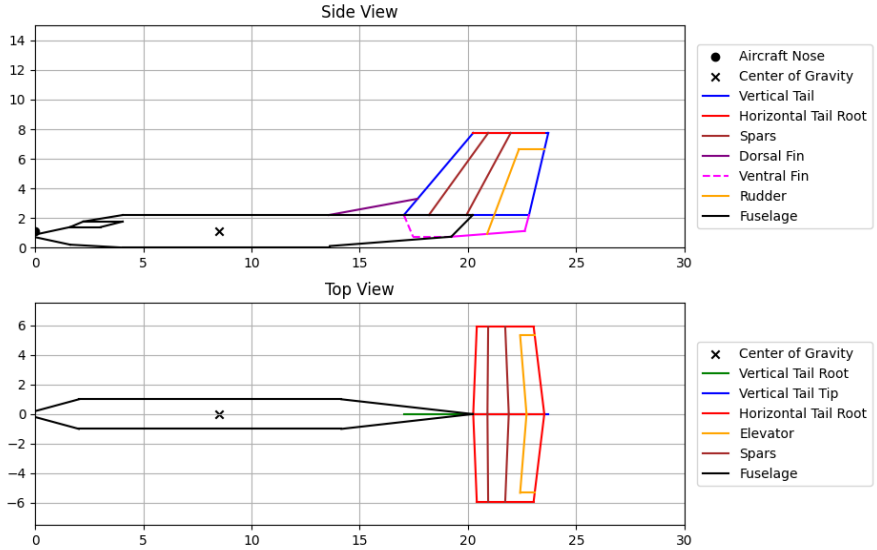

Figure 6.30: *Final Integration of the Tail*

6.8.3.6. Final Empennage Validation

To validate the sizing of the empennage, four comparative plots have been constructed:

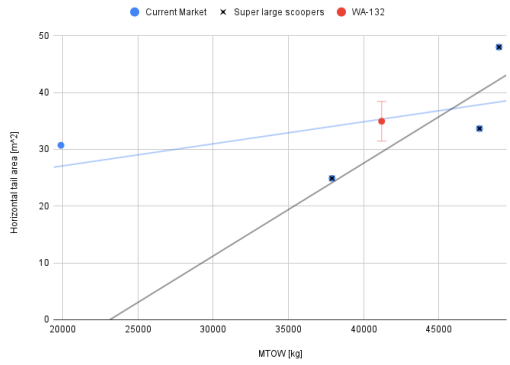

(a) *Horizontal tail area vs MTOW*

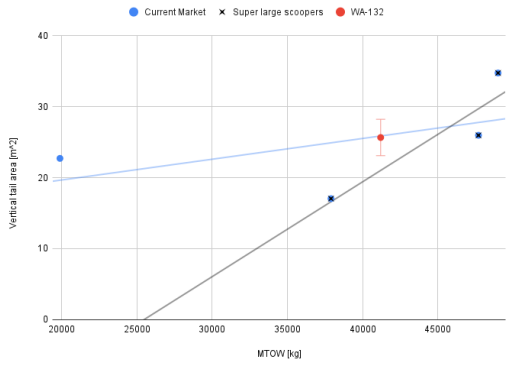

(b) *Vertical tail area vs MTOW*

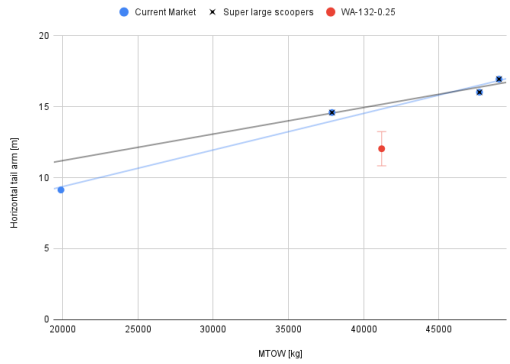

(c) *Horizontal tail arm vs MTOW*

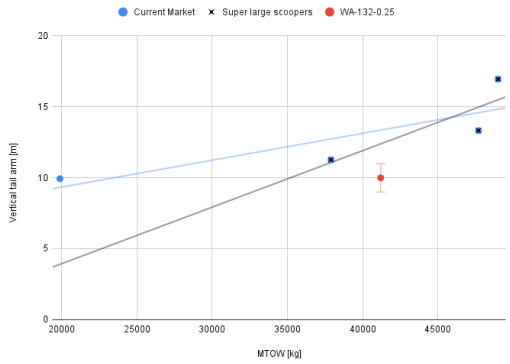

(d) *Vertical tail arm vs MTOW*

Figure 6.31: *Empennage sizing validation plots based on statistical comparison with similar aircraft*

Each plot includes data from four similar aircraft within the same class and mission profile. The plotted surface area values for the design are found to be slightly above the trend lines but remain within the expected envelope when accounting for error bars and variance. This is consistent with the fact that the moment arms in this design are slightly shorter than average, needing marginally larger tail surfaces to achieve the required stability and control effectiveness.

Moreover, the tail weight can be validated, as has been done in Subsubsection 6.8.2.4. As mentioned, the tail weight should account for around 5% of the OEW, and given the small tail arms of this design, a larger value is expected. A value smaller than 10% is considered realistic. The current percentage is $\frac{1510}{20760} = 7.27\%$. This value is much more realistic, and although it is still above average, it is justified by the short tail arm.

Overall, the tail configuration lies well within the validated design space. The regression-based comparison and weight comparison confirms the validity of the final design.

6.9. Fuselage

This section details the design of the fuselage so as to determine the weight necessary to sustain all the loads of the aircraft. This leads to a fuselage having the following characteristics:

Table 6.28: *Fuselage Parameters Table*

Parameter	Value	Unit	Parameter	Value	Unit
Type	Amphibious	(-)	Weight	4680	kg
Length	20.2	m	Longeron Weight	230	kg
Height	2.2	m	Skin and Stringer Weight	2500	kg
Width	2	m	Frame and Flooring Weight	870	kg
Material	Carbon Fibre	(-)	Local Reinforcement Weight	1080	kg

The weight of this fuselage is smaller than that of amphibious aircraft of comparable maximum take-off weight, as it is unpressurised while having optimal dimensions, minimising empty space.

6.9.1. Requirements

Before the design phase, the requirements associated with the fuselage must be recalled. This is shown in Table 6.29.

Table 6.29: *Requirements of the fuselage*

Requirement ID	Description	Compliance	Verification Method
REQ-FUS-1	The aircraft shall be capable of VFR (Visual Flight Rules)	✓	Inspection, verified
REQ-FUS-2	The cockpit shall accommodate a minimum of one pilot seat	✓	Inspection, verified
REQ-FUS-3	The engines shall have visibility in extreme conditions	✓	Inspection, verified
REQ-FUS-4	The aircraft shall withstand waves of up to 1.5 m	✓	Analysis, verified
REQ-FUS-5	The aircraft refuelling port shall support a minimum flow rate of 2000 L/min	✓*	Analysis, not verified
REQ-FUS-6	The structure shall withstand rough landing loads of 3g	✓	Analysis, verified
REQ-FUS-7	The structure shall withstand manoeuvring loads of 4 g	✓	Analysis, verified
REQ-FUS-8	The fuselage paint shall be of high contrast colours	✓	Inspection, verified
REQ-FUS-9	The structure shall withstand water landing loads of 3.3 MN	✓	Analysis, verified
REQ-FUS-10	The water tanks shall be refilled in less than 14 seconds	✓	Analysis, verified
REQ-FUS-11	The aircraft shall be able to refill water tanks using a scooping device	✓	Inspection, verified

The fuselage is designed such that it adheres to these requirements. In depth explanations and of the concepts behind them can be found in the following sections. All of these requirements are verified through inspection, by performing measurements using the computational model of the aircraft, or by analysis through the use of simplfied models. REQ-FUS-5 has not been verified as the refuellin port has not been detailed.

6.9.2. Fuselage Exterior

The aircraft exterior part was design following Roskam's Aircraft Design (Part 3) [26]. Specifically the hull, bottom part of the aircraft. The way this was designed was by using the value for the width of the body, b, and the length of the after body, La. This measurements are shown in Figure 6.32:

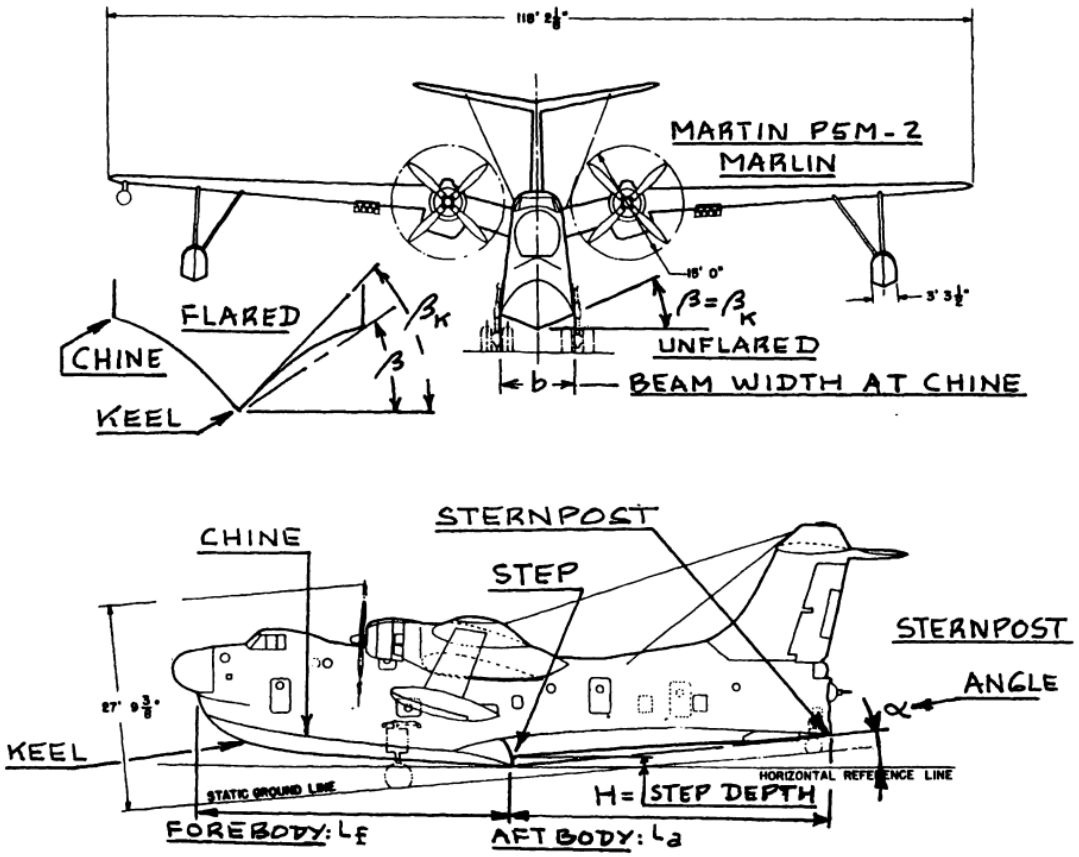

Figure 6.32: *Typical Flying Boat and Hull Geometry,[26]*

Based on the initial parameters and multiple graphs from Roskam illustrating the effects of hull geometry on the stability of water landings, the aircraft was determined to exhibit stable characteristics. The following parameters were obtained: step depth (H), sternpost angle (α), deadrise angle (β), and the maximum wave height at which water scooping is feasible. This design is therefore able to scoop in rough seas with waves 1.66m high or less.

The fuselage exterior is also designed to satisfy conventional aircraft requirements, namely the ability to fly using visual flight rule (VFR), encompassing complete visibility requirements. As such, the nose and cockpit windows are placed in such a way that the pilot has adequate ground and engine visibility.

The final look of the exterior of the aircraft can be seen in Figure 6.33 and the values in Table 6.30.

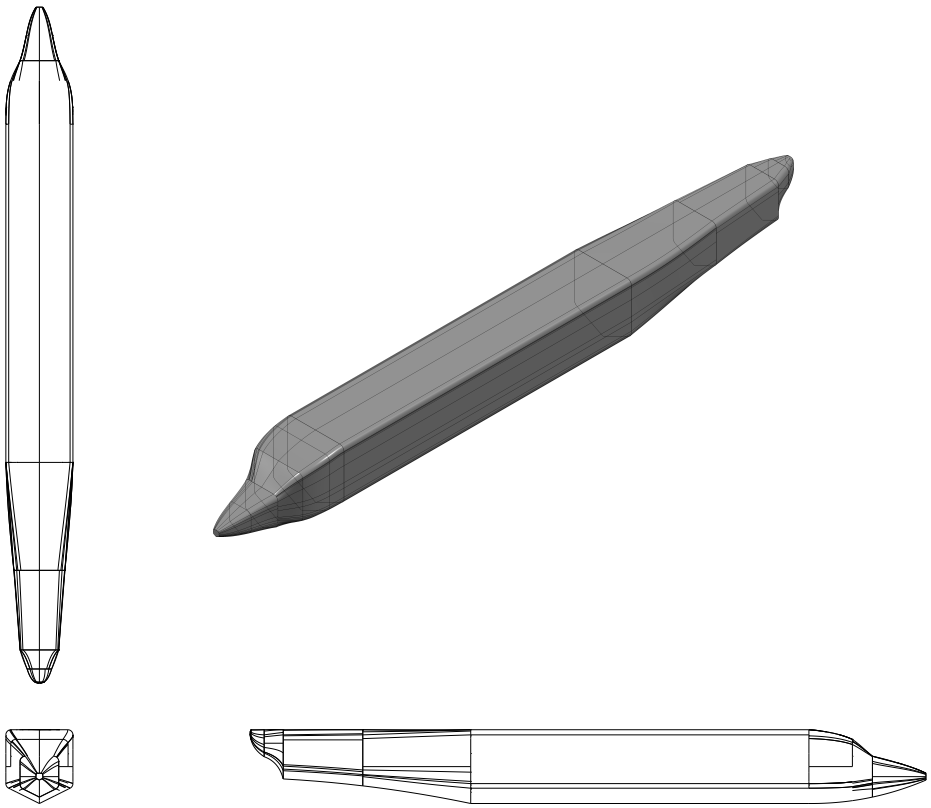

Figure 6.33: *Fuselage Drawing*

Table 6.30: *Parameters and their values*

Parameter	Value	unit
Step Depth	0.106	m
Sternpost Angle	6.40	deg
Deadrise Angle	26.5	deg
Wave Height	1.68	m

6.9.3. General Fuselage Characteristics

The fuselage is designed to be rectangular so as to optimise its structural integrity. This is because, as it is not pressurised, it does not need to sustain any pressure loads. This decision is made as during firefighting missions which represents most of its use, the aircraft will be in flight at levels of breathable atmosphere and during cruise, an oxygen system is sufficient to counteract any adverse effects of low pressure, although major redundancy systems are required [69] [70]. The length of the fuselage is given a lower bound limit by the required space for the cockpit, water tank and after-body. Increasing the size can increase the tail arm and, as such, reduce its size, presenting a trade-off. The height and width of the fuselage are obtained by analysing their effects on the fuselage weight, as the following graph shows their correlation :

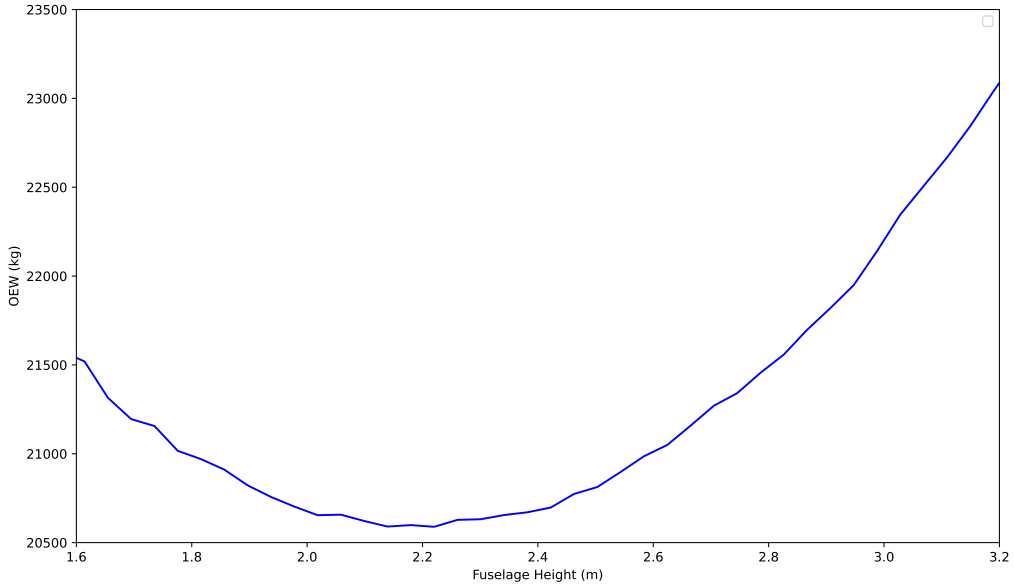

Figure 6.34: *Plot of the Operational Empty Weight (OEW) against fuselage height*

As can be seen, for a fixed volume of the aircraft, the minimum operational empty weight is obtained for a fuselage height of 2.2 meters. This is therefore the height taken for the design.

The fuselage material is also a critical parameter in determining the weight and capabilities of the fuselage. This material must take many considerations into account, not only does it need to comply with regular aircraft functions, being lightweight while having high yield stresses and strength, it must also be able to sustain large amounts of corrosion and eventual heat. As such, the material of the aircraft is chosen between 3 proven options: high strength aluminium alloys such as the 2024 T3 Al-alloy, fibreglass composites such as GLARE and carbon fibre reinforced polymers.

Corrosion resistance is critical for this mission as the aircraft will operate in maritime environment especially while scooping the sea. Each of these material present different properties with regard to corrosion, each with its benefits and limitations. Aluminium alloys are very susceptible to corrosion as although pure aluminium itself is strongly resistant to corrosion, the commonly used aircraft alloys introduce impurities, increasing the corrosion susceptibility. They can however be coated to reduce this effect with materials such as Alclad, this will ultimately lead to a lower fatigue life but this is not critical as due to the nature of the mission it will have low usage compared to conventional aircraft. Glass fibre reinforced composites do not suffer from corrosion as they are non metallic, however the salt water can lead to resin degradation, this is not critical as these materials are often used in maritime applications. Carbon fibre reinforced polymers share similar properties, in addition to the galvanic corrosion they could cause in combination with aluminium alloys. As such, a mix of both aluminium alloys and carbon fibres should be avoided for this aircraft.

Considerations concerning the heat sustained by the structure must also be taken, analysis reveals that heat experienced in fire plumes comparable to forest fires can reach $35 W/m^2 K$ [71] which translates to changes in temperature of at most 25°C in materials with heat capacities of $900 J/kgK$ which is the case for both aluminium and the composites, this should therefore not be critical for the mission. Both of these factors should therefore not be limiting while designing the aircraft, as such, the material leading to the lowest fuselage weight can be taken. The following table shows

the properties taken for each material and their resultant weight using the method described in the following sections :

Table 6.31: *Material Properties and effects*

Material	$\rho\ (kg/m^3)$	E (GPa)	$\sigma_{max}\ (MPa)$	$\tau_{max}\ (MPa)$	MTOW $(tons)$
Aluminium 2024-T3	2780	73.1	483	283	43.3
GFRC	2100	45/15	500/40	80	45.8
CFRP	1580	135/10	1000/60	90	39.8

While taking only the unidirectional longitudinal properties of the composite materials causes an overestimation of their benefits, and while pressurisation, which is lacking here, is the main transverse force usually found in aircraft, drag and other parasitic forces will need to be resisted by the structure. As such, here it is assumed that 30% of the fibres are out of plane. This is because drag can reach values up to 20% of lift and an extra 10% is allocated for any other transversal forces such as the friction of the water on the fuselage. This values is conservative as in reality most of these fibres would be oriented in the $\pm 45^{\circ}$ direction, contributing to the normal stress resistance. Furthermore, the fibres are also much more susceptible to fatigue [72] [73], they will therefore require a safety factor of 2 against 1.5 for the aluminium . Furthermore here the σ_{max} and τ_{max} are the yield strengths for the metal. However as the composites do not yield, they fail brittlely, and their ultimate tensile strength is used. This leads to the following qualitative trade-off table :

Table 6.32: *Material choice trade-off table*

Criteria	**Weight**	**Al-Alloy**	**GFRP**	**CFRP**
Corrosion Resistance	0.2	Susceptible to corrosion but can be mitigated (0.5)	High corrosion resistance (1)	High corrosion resistance (1)
Heat Resistance	0.1	Very high heat resistance (1)	Low heat resistance (0.25)	Low heat resistance (0.25)
Aircraft Weight	0.5	Average (0.75)	Largest (0.5)	Lowest (1)
Price	0.2	Low material and manufacturing costs (1)	Low material but high manufacturing cost (0.75)	High material and manufacturing costs (0.5)
	Total Performance	0.775	0.625	0.825

In this trade-off table, the corrosion resistance is given a weight of 0.2 as although this is an important factor because the aircraft will operate in close proximity to salt water, this can be completely mitigated for all of these materials. Similarly, while heat resistance is important, here the temperatures should not be critical and as such it is given a small weight. The aircraft mass is given a weight of 0.4 as this is the most important criterion, as it is a major factor in the design decisions of the aircraft. Finally, the cost is also an important criterion as the aircraft should be competitive with similar aircraft and is therefore given a weight of 0.2. This therefore leads to the choice of the carbon fibre reinforced polymer in major part thanks to its weight saving benefits, as this greatly decreases the weight of the entire aircraft, thanks to the snowball effect. It also ensures REQ-SYS-6 is complied with.

Although carbon fibres are typically a black material, these must be painted yellow and red to comply with firefighting aircraft regulations. This requires specialised surface coatings and paint but should not lead to drastically increased price nor weight compared to metal paintings.

The following sections cover the sizing of the most critical fuselage components used to obtain these results, however all of these calculations do not account for local reinforcements due to stress concentrations, any secondary load paths or fatigue weakening, as such a conservative factor of 30% is applied to the final weight of the fuselage obtained from this method. An example of local load concentrations is the fuel inlet, located within the fuselage, which must be able to sustain the loads of high flow refuelling to reduce the deployment time, critical to mission success. [74]

6.9.4. Load Cases

The aircraft is modelled over three cases determined to be critical as their loads are determined to be the highest. These are during a hard landing for which it is expected that the aircraft can have an effective weight of 2.6g [75], so as to simulate a worse case scenario a value of 3g is taken. The second critical load case is during its largest manoeuvres, which are obtained from the gust load diagram as $n_{limit} = 4$. The final case is specific to amphibious aircraft as it is the force experienced during the instantaneous contact with the water during landing and scooping manoeuvres. This is a slamming force given by the following :

$$F_s = \frac{1}{2}\rho V^2 A C_s \tag{6.22}$$

Here ρ is the density of water, A is the area in contact with the water and is therefore the step of the aircraft, and V is the speed of the aircraft relative to the water, assumed to be stall. The slamming coefficient C_s is assumed to reach values up to 10 [76], leading to values up to six times the MTOW.

6.9.5. Beam analysis

So as to obtain an estimate of the weight of the fuselage, it is modelled using simple beam analysis to obtain the longitudinal internal bending moments and shear forces expected. For the final design of the aircraft, this results in the following shear force and bending moment graphs for the 3 situations :

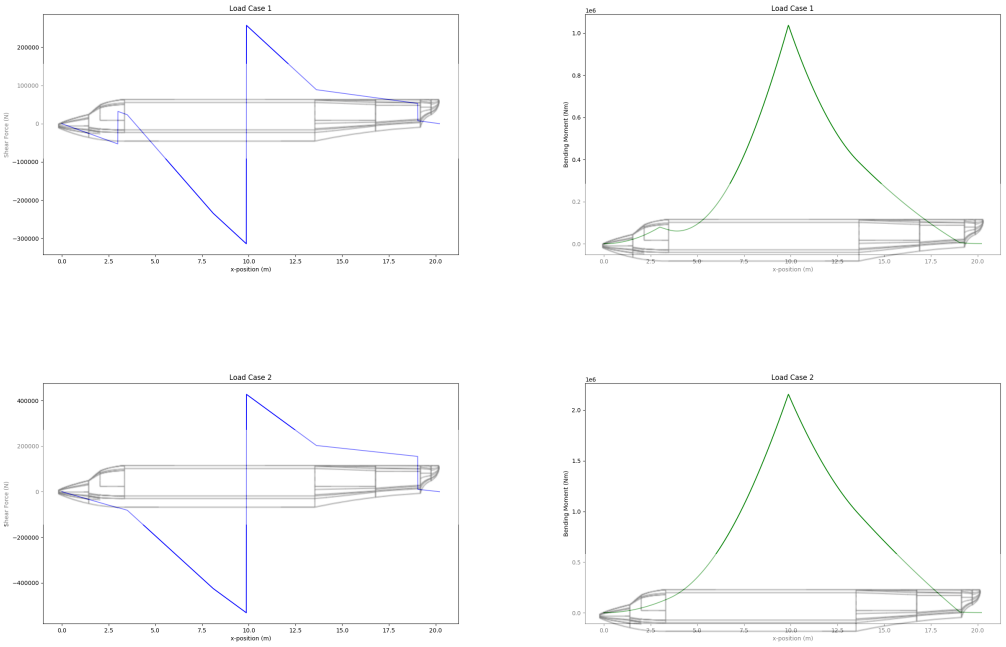

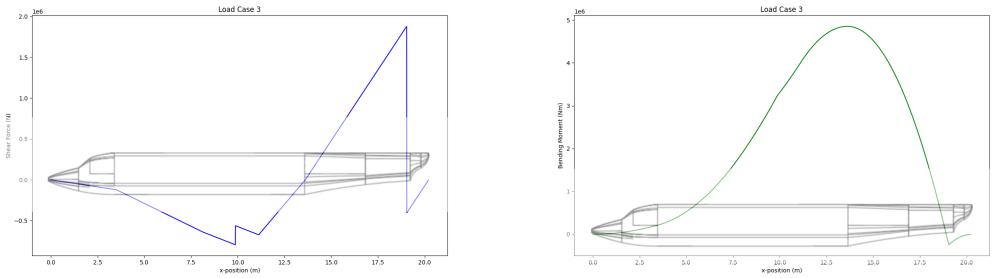

Figure 6.35: *Internal force analysis for hard landing (1), highest load factor (2) and water slamming (3)*

Using these, the internal stresses due to bending and shear can be determined. The shear stress is calculated using standard static stress analysis practices. This analysis covers shear stress and bending stresses as well as buckling of the aircraft skin. The buckling coefficient is obtained from Figure 6.14, assuming it to be simply supported so as to obtain conservative estimates.

6.9.6. Internal Fuselage Structure Sizing

The primary structural components of the fuselage are sized by assuming a general structure and determining their required area and quantities. A guiding design of the structure is the following :

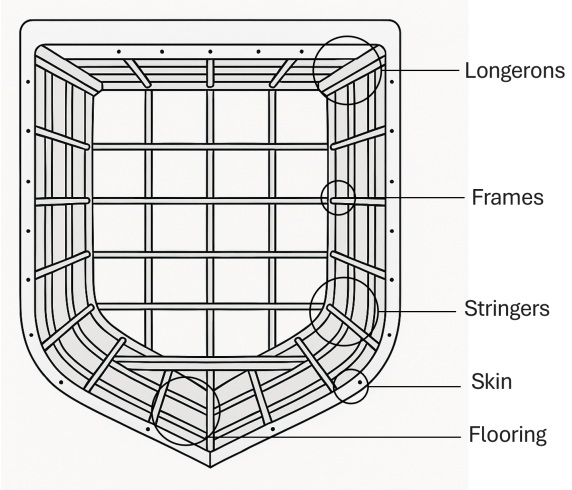

Figure 6.36: *Example internal structure of the aircraft*

It has 4 longerons with 1 in each corner, as well as skins and stringers responsible for carrying most of the stresses. It is also composed of flooring and frames to introduce and sustain the loads of the internal payload, composed of the tanks and batteries, into the structure.

To calculate the influence of the longerons on the bending stresses, they are assumed as point areas so as to reach a conservative estimate. So as to obtain the most accurate value, the longeron area is increased incrementally until the stresses become lower than the yield stress for the section. Following this, the skin thickness and stringer spacing can be obtained from the buckling.

Using these forces and stresses, the required skin thickness, stringer area and their amount can be determined. Furthermore, so as to avoid immensely over sizing these factors, the fuselage is split into 12 sections, each having a distinct skin thickness and stringer area, however the minimum thickness is not allowed to be lower than half of the maximum one so as to avoid over-fitting to the

simple model. The amount of stringers stays constant throughout the entire structure.

This entire process is iterated for different values of the amount and size of the stringers in order to converge to an optimal value, indicated by the lowest combined skin and stringer weight.

As the fuselage is unpressurised, the frames are designed to be a load path between the cargo and the entire aircraft. The fuselage has the following interior cargo structure :

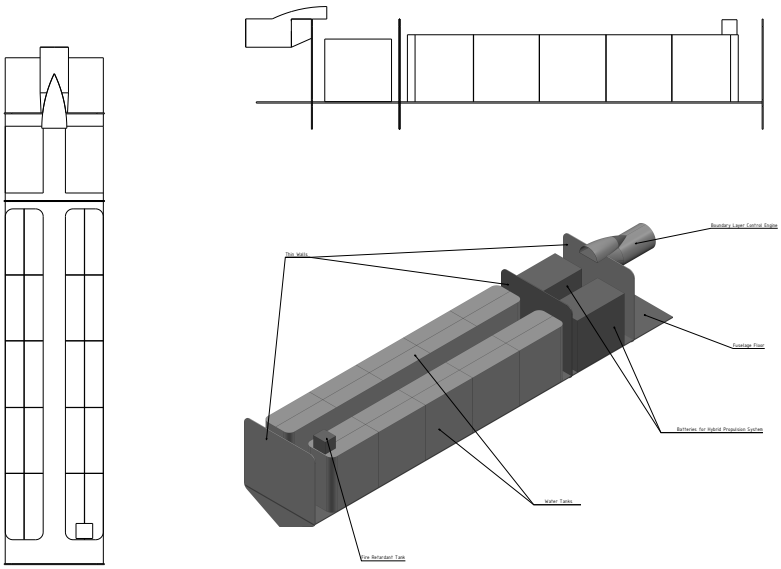

Figure 6.37: *Fuselage interior drawing*

The frames and flooring are designed such that they can sustain the mass of the water, the tanks, the batteries and any personnel present for maintenance or inspection. The frames are assumed to be thin structures made of carbon fibre, while the flooring is made in a honeycomb aluminium structure as these allow for weight savings of about 36% [77]. Aluminium is used here as isotropic materials properties are needed for this part of the structure. In order to avoid contact between the aluminium and carbon, which would cause galvanic corrosion, glass fibre reinforced inserts are used in order to isolate the material. The aluminium must also be coated in a corrosion resistant material such as Alclad. This would slightly increase maintenance complexity however the weight benefits are non-negligible.

6.9.7. Scooping Inlets

The scooping inlets were designed so that the aircraft completely refills its tanks during the time it spends scooping. To achieve this, the required refill rate was first calculated. Then, the area needed for the inlets was obtained by dividing this rate by the scooping velocity and a factor accounting for water loss, which was assumed to be 0.6. This resulted in a total inlet area of $0.0306\,m^2$. Dividing this area into two inlets and applying a height-to-width ratio of 1:2, the final scooper inlet dimensions

are 0.175 m wide and 0.0874 m high. A general view of this mechanism can be seen in Figure 6.38.

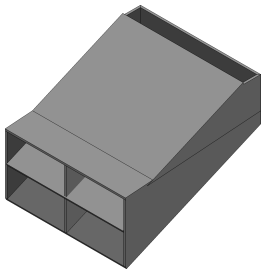

Figure 6.38: *Isometric Drawing Scooper Inlets*

6.10. Storage Subsystems

This section details the sizing and design of the firefighting payload tanks as well as the oxygen tanks. These are critical as the water tanks are the core and purpose of the firefighting design while oxygen tanks are critical lifeline equipments as the aircraft is unpressurised. These subsystems must adhere to the following requirements

Table 6.33: *Requirements of the tanks*

Requirement ID	Description	Compliance	Verification Method
REQ-TANK-1	The aircraft shall cancel dropping the water if the flight is unstable	✓*	Demonstration, not verified
REQ-TANK-2	The aircraft shall be able to carry at least 13,200 kg of water	✓	Analysis, verified
REQ-TANK-3	The tanks shall prevent noticeable slushing	✓*	Demonstration, not verified
REQ-TANK-4	The aircraft shall not be destabilised due to uneven water distribution	✓*	Demonstration, not verified
REQ-TANK-5	The aircraft shall provide enough oxygen for the entirety of the ferry range with redundancy	✓	Analysis, verified
REQ-TANK-6	Modularity shall be optimized	✓	Inspection, verified

The adherence to these requirements is detailed in the following sections. The verification of requirements 1, 3 and 4 has not been done as they require advanced fluid modelisation or a physical demonstration.

6.10.1. Firefighting Payload Tanks

The tanks are a multi-purpose part of the structure as they not only serve as a means of storing the water and as such sustain the hydrostatic loads, they also serve as input/output points for the water, as such they must be designed in such a way that they can be easily filled and depleted. Furthermore, so as to avoid major shifts in the centre of gravity of the aircraft, the tanks must be equipped with anti-slushing mechanisms. The following list of risks with regard to the tank can be derived :

- The tank fails due to hydrostatic loads.
- The tanks are too difficult to maintain
- The aircraft becomes unstable/uncontrollable due to shift in centre of gravity because of slushing.
- Failure of one of the scoopers leads to an unequal filling and therefore causes a moment about the longitude of the aircraft.
- Failure of one of the release mechanisms causes one of the tanks to stay full during a dropping sequence leading to an unstable moment.

The tank must therefore be designed in such a way that these risks are mitigated. The first risk can simply be mitigated by designing a tank with the necessary thickness to withstand the 13.2 m^3 of water, the pressure caused by the hydrostatic loads can be obtained from the following relation [78]:

$$P = \rho a h \tag{6.23}$$

With a the acceleration, in steady flight h is simply the height of the tank and a the gravitational acceleration. This formula can be extrapolated for different cases however, as during longitudinally accelerating manoeuvres, a becomes the longitudinal acceleration and h becomes the effective length of the tank. This can also be done for laterally accelerating manoeuvres. Performing a simple shear and bending beam stress analysis can then be done such that the container does not yield nor buckle. This leads to a thickness of 3mm, taking into account a safety factor and extreme flight situations where inertial forces would amplify these stresses. This calculation also takes into account the stress concentrations that occur in the corners due to the rectangular shape of the tanks. The width is obtained by assuming that there would be 2 tanks, split span-wise so as to allow for any maintenance workers to easily access them. The height is then taken as the maximum resulting space in the fuselage, while accounting for any spare space needed for cables or secondary flight subsystems. Due to this, the tanks are not necessarily required to be filled with water, other firefighting payloads may be used, increasing the modularity.

The slushing is prevented through the use of baffles, these are internal compartments to the tank with cutouts so as to limit the flow within the tank and as such the slushing that can happen within. These present the limitation of greatly reducing the longitudinal flow within the tanks and as such they must be filled from above.

Preventing any unequal fill levels is done through the use of 2 distinct mechanisms by addressing the possible causes of these disparities. The first possible source of this failure would be due to the failure of one of the scoopers, so as to mitigate this risk, the scooping systems are coupled in such a way that they can fill both tanks if necessary. The second possible source of this issue would be if one of the dropping gates fails, both are therefore mechanically coupled in such a way that one can only open if the other can too. The water and tank system can be seen in the following diagram :

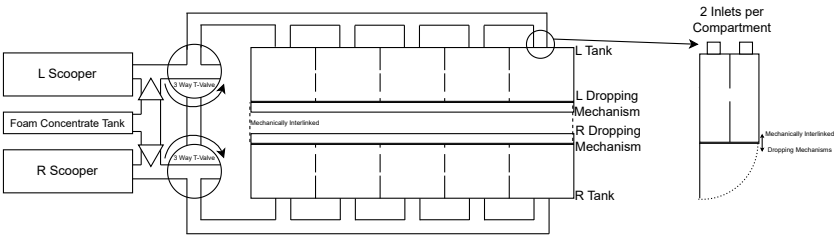

Figure 6.39: *Diagram of the water system connections*

This diagram shows a simplified view of the water connections of the aircraft. Both tanks have 2 inlets per compartment for a total of 10 inlets per tank. All of these are placed above the tanks as flow within the tank is limited because of the baffles.

The diagram also shows that 3 way T-valves are used, these allow for a simple connection during normal use while also allowing for even distribution in case of the failure of one of the scoopers by rotating. One-way valves are also used to connect the foam concentrate solution tank to the water flow. These solutions are used to increase adhesion and endurance of the dropped water. These are used in very small concentrations of 0.1 to 1% and as such should not have a consequential impact on the mass and volume of the structure. [79], therefore a simple tank with dimensions of $0.3 \times 0.3 \times 0.33 m^3$ can be taken. The one-way valves also serve as attachment points for pumps as although they are not necessary to distribute the water as this is done by the ram pressure while scooping, pumps must still be used to introduce the foam concentrate into the water system.

The dropping mechanism is highly reinforced as it would be prone to local stress concentrations and it is flush mounted to avoid discontinuities in the structure of the fuselage. This mechanism also opens outwards to avoid any contact between both and to allow the water payloads to concentrate into one mass and as such reduce the surface area in contact with air, thereby reducing evaporation rates. This mechanism is also hydraulically actuated such that it can resist the pressure of the water and close during a drop if it must be cancelled.

The baffles of this design have the following structure :

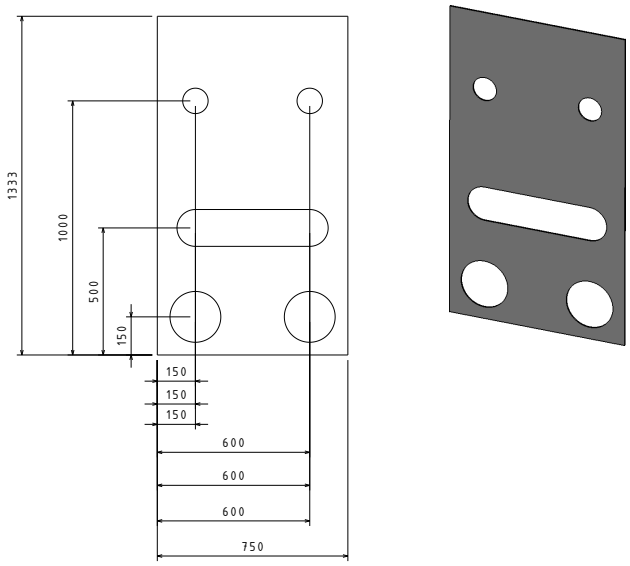

Figure 6.40: *Drawing of the span-wise baffle compartment*

As it can be seen, large cutouts are placed at the bottom to allow the water to stay level and small cutouts are placed higher up to allow for some flow to reduce the stress on the baffle. This baffle is repeated 4 times inside of the tank. This structural addition should completely eliminate any noticeable longitudinal slushing unless the water level is so low that it can all go through the lower cutouts, in which case the shifts in centre of gravity should not be noticeable. A longitudinal baffle is also included in each of the tanks with the following design :

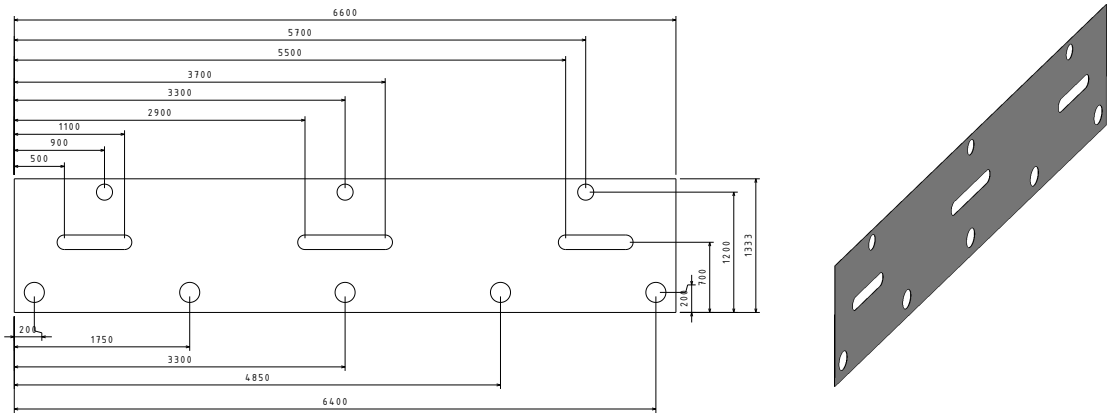

Figure 6.41: *Drawing of the longitudinally aligned baffle compartment*

Only a single longitudinal baffle is included in each tank as the tanks are much longer than wide and the longitudinal acceleration is larger than the lateral acceleration. The lateral centre of gravity is also a less critical parameter as the scale of the moment arm is much smaller. No vertical baffle is included the load path between the bottom of the tank and the rest of the structure is direct it would impede the flow rate during dropping manoeuvres. Furthermore, shifts in vertical centre of gravity are negligible terms to the stability and control of the aircraft.

Beyond reducing the slushing of the water within the tank, these baffles have the added benefit of reducing the "height" of water impacting the sides of the tank during acceleration manoeuvres. This therefore greatly reduces the hydrostatic pressure caused by inertial forces that the sides of the tank must sustain. This compartmentation of the tank is therefore a multi-purpose solution that should offset all of the risks posed with the water storage choice.

6.10.2. Oxygen System

As the aircraft is unpressurised, oxygen tanks must be sized such that the pilots can breath for the entirety of the ferry range. To determine the amount of oxygen necessary, regulatory body guidelines are used [80], these are that people use 1LPM (Litre per minute) per 10000ft of altitude. Furthermore there are only 2 pilots on board and the cruise altitude is of about 23000ft, as such the amount of oxygen can be estimated from the following relation :

$$V_{oxygen} = n_{passenger} \frac{h_{cruise}}{10000} * t_{cruise} \tag{6.24}$$

The time taken to complete the cruise portion of the ferry range is estimated to be about 4 hours, leading to an oxygen volume of 1104L. This volume is for sea level conditions, however as it is stored

in standardised pressurised containers, it can be greatly reduced. Indeed, instead standard D tanks are used, which can compress 425L of oxygen into 0.23L and only weigh about 2kg or 2.7kg when full of oxygen. For redundancy in these estimations, 4 tanks are equipped as although the regulations already provide conservative estimates, inadvertently running out of oxygen could cause a catastrophic failure of the missions. Furthermore, since these tanks are relatively light, this should not be noticeably detrimental to the entire mass budget.

6.11. Under Carriage

The design and position of the landing gear for the aircraft are carried out in this section. Two main landing gear struts with two wheels each and a single nose landing gear with double wheels are used. All the ground stability requirements are used to determine the final positioning of the main landing gear, which is retracted to a podded compartment within the fuselage.

6.11.1. Requirements

Before explaining the design of the undercarriage, the requirements associated with it must be recalled. This is shown in Table 6.34.

Table 6.34: *Requirements of the undercarriage*

Requirement ID	Description	Compliance	Verification Method
REQ-UCA-1	The aircraft shall perform ground manoeuvres on rough terrain	✓	Analysis, verified
REQ-UCA-2	The aircraft shall land on water of depth equal or smaller than 2 metres	✗	Analysis, not verified
REQ-UCA-3	The landing gear shall absorb shock loads from rough terrain	✓	Analysis, verified
REQ-UCA-4	The landing gear shall withstand loads of up to 6044 kg	✓	Analysis, Verified

REQ-UCA-2 has not been verified yet, but analysis simulating the angle of approach to the water bodies using the full aircraft will verify this model.

6.11.2. Sizing

After the market analysis and the derived expected airports, the surfaces that the W-132 is expected to land on are well maintained concrete runways. These runways restrict the maximum allowable tire pressure to 8.5 - 14 kg/cm^2. In compliance with REQ-UCA-1 the lower bound of tire pressure is taken for the aircraft to be able to perform ground manoeuvres on rough terrain. Then, using Roskam's provided statistical data, the MTOW of the W-132 best compares to the McDD DC-9/10 aircraft which has a tire pressure of 9.07 kg/cm^2 and an LCN of 39 with a MTOW of 41140.8 kg. Here, the tire pressure falls within the previous range as expected.

$$N_{nw} = W_{TO}/60000 = 443608/120000 = 3.69 \tag{6.25}$$

With this equation the value must be rounded to the nearest multiple of 4 with a minimum of 4. Rounding off the former gives a total main landing gear quantity of 4. For the landing gear layout a standard twin (dual) setup with 2 wheels is used per strut. Also, the conventional tricycle gear arrangement is chosen because of its ground stability and ability to land at a significant "crab" angle

which refers to the nose not being aligned with the runway. Also forward visibility is improved and it provides good steering characteristics which are beneficial considering the mission needs for quick response time. Additionally, the landing gear has a retractable mechanism so as to seal it within a compartment below the root of the wing and prevent any water contact. According to Roskam, two wheels per strut is a reasonable quantity for aircraft that fall in the range 22680 - 68040 kg which complies with the W-132's MTOW. Now, calculating the nose and main landing gear weights per strut is as follows;

$$P_{mw} = 0.85\frac{M_{TO}}{N_{mw}} \tag{6.26}$$

also;

$$P_{nw} = 0.15\frac{M_{TO}}{N_{nw}} \tag{6.27}$$

From these values it is possible to calculate the equivalent single wheel load (ESWL) as follows; $ESWL = \frac{P_n}{2}$ or $\frac{P_m}{2}$ yielding 2133 and 6044 kg which is compliant with REQ-UCA-4.

Based on the previous calculations, a type VII tire will be used for extra high pressure. This type of tire is almost universal across military, civil jets and turboprops. Further details are presented in Table 6.35

Table 6.35: *Tire Specifications*

Parameters	Acronym	Value	Units
Type	[-]	III	[-]
Max Outside Diameter	D_0	1.077	m
Section Width Max	W	0.38862	m
Max Shoulder Diameter	Ds	0.955	m
Max Shoulder Width	Ws	0.33	m
Unloaded Inflation Pressure	[-]	6.32763	kg/cm^2
Maximum Speed	V_{max}	160	mph
Weight	W	58.967	kg
Maximum Loading	[-]	9207	kg

6.11.3. Placement

Two constraints need to be respected for the landing gear sizing; the pitch and roll angles. The pitch angle is constrained mainly by the tip back angle which has to be above 6°according to Roskam. Also, the angle β demonstrated in Figure 6.42b is required to be at least 10 - 15 % behind the most aft CG with the aim of preventing the aircraft from tipping back, however, this limits lift off ability. Thus, 10 % is used to not hinder lift off too much but respect tip back requirements. Also, the load on the nose landing gear has to be at least 8% of the aircraft weight and at most 15%. After an iteration process it becomes clear that the minimum nose loading for the current weight distribution is 9%, otherwise the front landing gear creates too much moment about the most aft CG to maintain static stability. Hence, to leave some clearance, the distance to the nose landing gear is placed at approximately 1.5 meters from the front of the aircraft which leads to 11% loading.

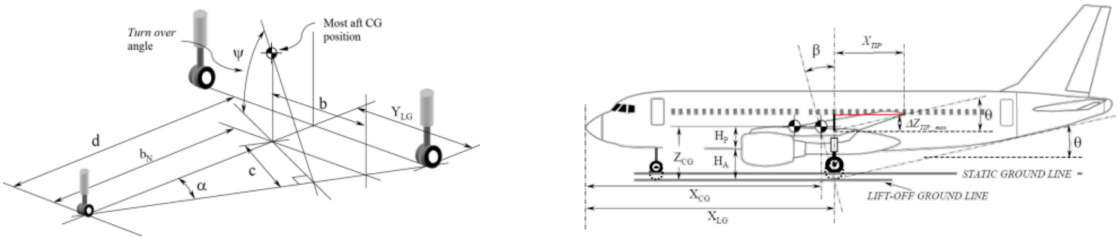

(a) *Turnover Angle Geometry [81]*

(b) *Tip Back Angle [81]*

Figure 6.42: *CL-415 old/new Cockpit Configurations*

For lateral stability, the turnover angle Ψ as demonstrated in Figure 6.42b has to be below $\Psi < 55^\circ$. To determine this angle as a function of known parameters a set of equations are required. Here, $b_N = X_{CG_{aft}} - X_{nw}$. Also, for a preliminary estimate of Ψ the length Y_{LG} is given an initial estimate of 1.2 m. From these values it is possible to determine $\alpha = \arctan\frac{Y_{LG}}{d}$ and thus, $c = b_N \sin\alpha$. The final value for the turnover angle is calculated using Equation 6.28.

$$\Psi = \arctan\frac{Z_{CG}}{c} \tag{6.28}$$

This results in a final turnover angle of 68.5°which surpasses the requirement. After a few iterations the required length Y_{LG} is altered to 2.23 m to attain a turnover angle of 55°in compliance with REQ-UCA-5.

6.11.4. Sealing Mechanism

Since the struts of the aircraft cause significant increments in drag, they are retracted into a podded compartment within the fuselage. The reason for the fuselage location for the retraction of the landing gear is due to the tip-back requirement, which results in a main landing gear placement that is more aft than the required position for it to be retracted into the wing. The compartment is also sealed to prevent any salt water contact with the landing gear in case of salt water scooping maneouvres. The same rubber and elastomeric seals used for the CL-415 around the perimeter of the compartment will be used for the sealing mechanism. Specifically, Teflon, nitrile or fluorocarbon materials are used for its sealing. Nitrile is very commonly used in the aviation industry due to its high resistance to hydraulic fluids, while fluorocarbon is generally a strong suit for high temperature requirements [82]. A combination of these, using a mix of both nitrile and fluorocarbon will provide the necessary sealing and resistant properties to prevent landing gear contact with salt water. This ensure REQ-SYS-5 is complied.

7

Final Design

7.1. Final Aircraft Configuration

The final design can be seen in all four views in Figure 7.2.

7.2. Performance Parameters

Table 7.1: *General Aircraft Characteristics*

Parameter	Value	Unit
Maximum Takeoff Weight (MTOW)	39,783	kg
Operating Empty Weight (OEW)	20,755	kg
Maximum Landing Weight (MLW)	33,000	kg
Max Zero Fuel Weight (MZFW)	28,200	kg
Payload Capacity	13,200	kg
Fuel Weight	5,827	kg

Table 7.2: *Aerodynamics & Flight*

Parameter	Value	Unit
Wing Area (S)	140.5	m^2
Wing Span (b)	35.56	m
Wing Aspect Ratio	9	–
CL_{max}	3.5	–
L/D (Cruise)	7.15	–
C_D (Cruise)	0.0349	–

Table 7.3: *Performance & Mission Parameters*

Parameter	Value	Unit
Cruise Speed	206	m/s
Stall Speed	33.6	m/s
Rate of Climb (ROC)	11	m/s
Cruise Altitude	7,000	m
Range (Max Payload)	1,500	km
Max Range (Ferry)	2,450	km
Time to Refill (Water)	12	s
Water Payload	13,200	kg
Scooping Speed	60	m/s

Table 7.4: *Propulsion & Battery System*

Parameter	Value	Unit
Total Cruise Power (Full)	6.77	MW
Takeoff Power (Full)	7.88	MW
Propulsion System	Hybrid	–
Number of Engines	2	–
Engine Efficiency	85	%
SFC	0.259	kg/kWh
Battery Weight	3,964	kg
Specific Energy	500	Wh/kg
Battery Volume	2.48	m^3

Table 7.5: *Takeoff & Landing*

Parameter	Value	Unit
Takeoff Distance (MTOW)	1,800	m
Landing Distance	1,100	m

Table 7.6: *Stability & Control*

Parameter	Value	Unit
CG Range (Forward–Aft)	43–48	% MAC
Tail Volume Coefficients (V_h / V_v)	0.8 / 0.07	–
CG (MTOW)	8.42	m

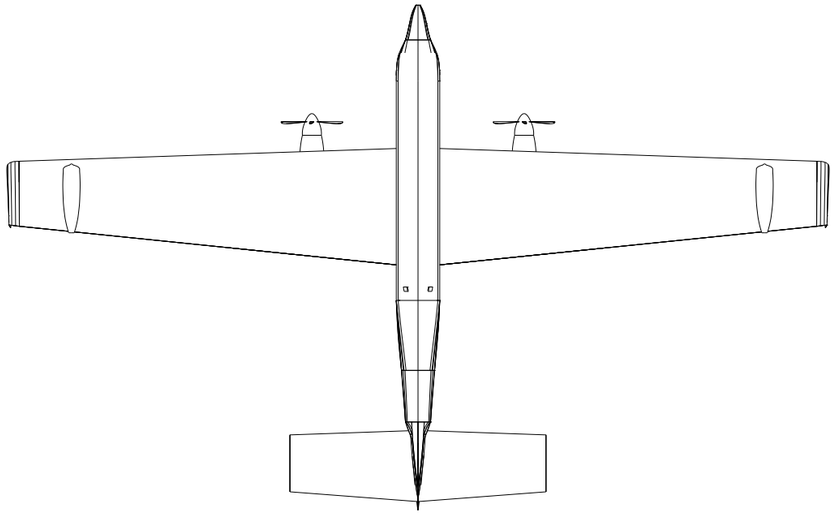

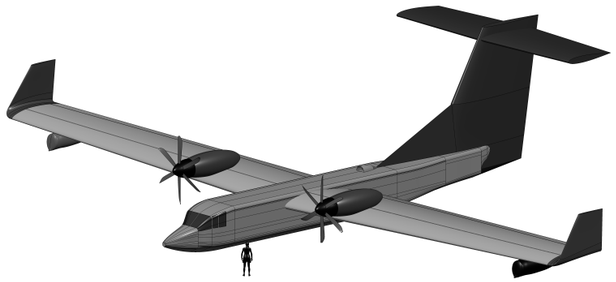

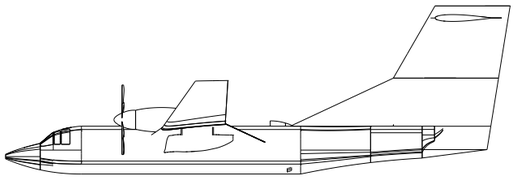

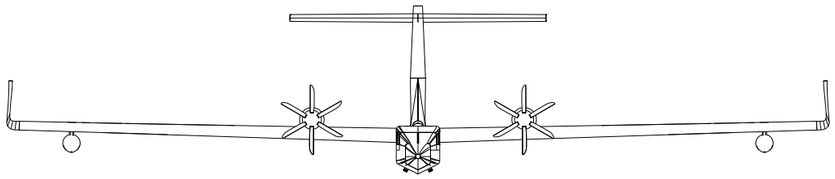

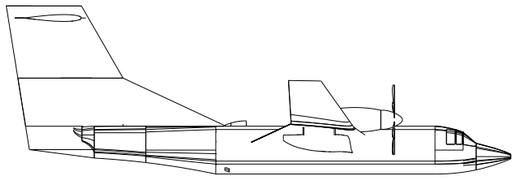

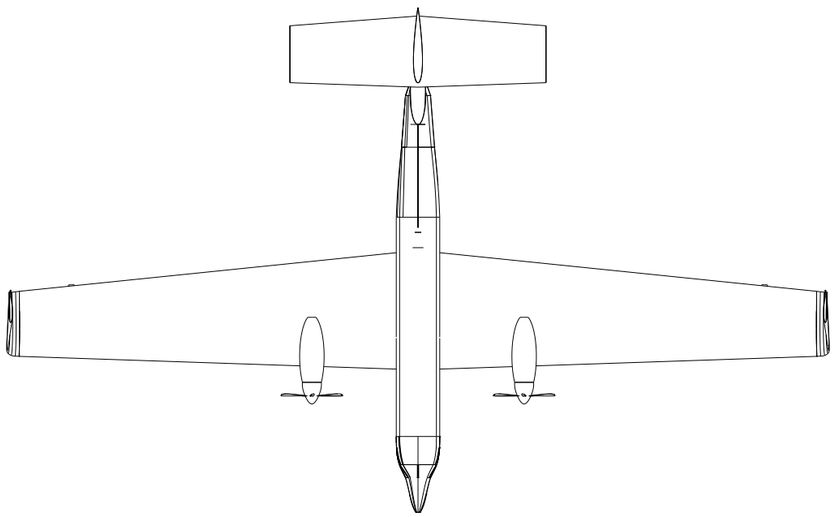

7.3. Mass and Volume Budgets

The distribution of the mass and volume of the aircraft can be easily determined when divided into its different subsystems and components. Together, these create a general budget analysis. Values for the mass budget estimates were attained directly from the computed code while the values for the volume budget estimates were either attained through the CAD model that was created or through basic geometric calculations. Due to uncertainty in the volumetric values, they have been given an approximation margin of 5%.

Table 7.7: *Volume and Weight Budget*

Component	Volume Budget (m^3)	Weight Budget (kg)
Fuselage	69.10 ± 3.46	4787.30
Wings	27.62 ± 1.38	5065.80
Empennage	15.73 ± 0.79	1509.15
Engines	2.2 ± 0.11	1080.29
Landing Gear Main	1.80 ± 0.09	1425.56
Nose Landing Gear	0.9 ± 0.05	284.80
BLC	0.5 ± 0.03	143.00
Fixed Equipment	N/A	2495.62
Batteries	4.90 ± 0.25	3963.97
Fuel	5.92 ± 0.30	5921.41
Payload	13.2 ± 0.66	13200.00

7.4. Power Budget

For the power budget, the distribution of power across subsystems is easily analysed due to the electrical systems on board. An APU auxiliary power unit mainly the BLC engine located at the back of the fuselage helps turn the aircraft on to taxi. When in flight, the hybrid engines take over and proide 300 kW of power to the avionics of the aircraft.

7.5. Time Budget

Lifetime Budget

The lifetime of the aircraft can be estimated by dividing it into 5 different time phases and allocating a time for completion. Figure 7.1 demonstrates the design phase, manufacturing, distribution, operation and retirement phases which have been approximated using past firefighting experiences and example cases of scooper air planes such as the CL-415. First, the design phase is carried out until a design freeze is attained resulting in a final design idea taking approximately 6 - 18 months. Then the manufacturing of the design is carried out for 36 - 42 months [83] which is followed by the distribution of the aircraft across markets for 16 - 32. Finally, the aircraft is put in operation for approximately 30 years [84] to then enter the retirement phase at the end of its lifetime where the aircraft cannot be operated any more and must be disposed of for 4 - 8 months [85]. Figure 7.1 demonstrates that the leading phase in the aircraft's lifetime will be operations. It is important to also acknowledge the retirement duration which represents around one percent of the lifetime but will still be essential when considering sustainability and proper decommissioning of materials and parts.

Figure 7.1: *Design and Mission Lifetime*

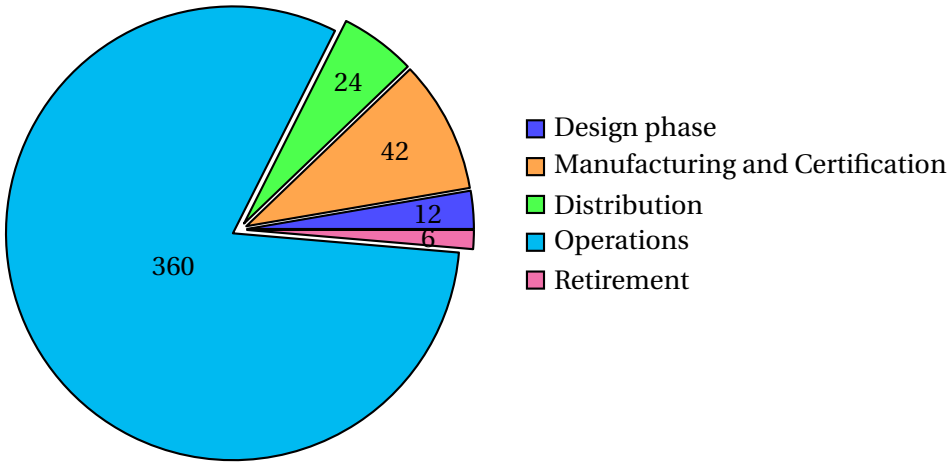

Schedule Budget

Diving into the design phase, the time allocated to different areas is essential in attaining a proper and effective design. Table 7.8 lays out the time budget allocated for the team in the previous two months. The numbers are taken from the created Gantt chart Section 12.2. Phase 4 is broken down into its subdivisions as it engulfs the majority of the design phase. Furthermore, the table clearly lays out the time allocated to different design phases. These constraints should were closely monitored by the project manager to complete the milestones and deadlines in a timely manner.

Table 7.8: *Schedule Budget*

Design Phases	**Time (hrs)**	**Man Hours**	**%Total Time**
Phase 1 : Project Planning and Requirement definition	520	52	14.8
Phase 2 : Capability Study	120	12	3.4
Phase 3 : Concept Development and Selection	680	68	19.3
Phase 4 : Preliminary Design and Feasibility Assessment	1200	120	34.1
4.1 Weight Estimation	300	30	8,5
4.2 Interface Definition	30	3	0,9
4.3 Design of Subsystems	300	30	8,5
4.4 RAMS	20	2	0,6
4.5 Verification and Validation	50	5	1,4
4.6 Strategy	30	3	0,9
4.7 Return on Investment/ Opportunity Cost	50	5	1,4
4.8 Determine Final Aircraft parameter	380	38	10,8
4.9 Assembly	40	4	1,1
Phase 5 : Implementation of Final Model	1000	100	28.4

8

Verification & Validation

After having developed the detailed design of the W-132, the requirements that were set at earlier stages of the project that would drive the design have to be verified and validated. This has been done following the V&V plan presented in the Midterm Report [86]. This plan was decided such that all the design procedures would converge in a final design that met the stated requirements for the W-132, as well as verifying that the used procedures and models for the design have been correctly implemented. Additionally, the final W-132 design has been validated using external tools, which enabled the analysis of the design's performance within specific scenarios.

8.1. Verification of Requirements

To properly verify each of the requirements, four different verification methods will be used:

- **Inspection (I):** A visual or manual check confirming compliance with requirements—ideal for qualitative or easily measured items like dimensions, labels, finishes, or configurations.
- **Analysis (A):** Uses models, simulations, or theoretical evaluation (e.g., Colossus X Challenge, FEM, CFD) to verify requirements when physical testing is impractical or costly.
- **Demonstration (D):** Shows system performance under specific conditions without detailed measurement, used when normal operation confirms requirements.
- **Test (T):** A controlled process applying specific inputs to measure outputs against requirements, best for quantitative and performance-based validation.

Each of the requirements will be verified with one of these four methods. The final table with the specific verification procedure carried out for each of the requirements can be found in **??**. For verification procedures that fall into the category of inspection and testing, it is assumed that the aircraft will be manufactured and assembled, allowing for the performance of tests and visual inspections.

8.2. Verification of Design Models

The software Python 3.11 was used to perform all the necessary calculations for the preliminary and detailed design phases of the W-132. The code was structured into different subsystems and procedures. Since every subsystem depends on other subsystems, a main iteration file was used. Moreover, a main dictionary for all the parameters was set up, where their initial estimations were input to enable the calculations to start, but once each parameter was calculated in one of the other files, its value was updated for the rest of the files and iterations.

The steps to set up the main iteration file were as follows. First, Class I and Class II weight estimation were carried out. At the same time, different subsystems were being developed using initial estimations, and their preliminary and detailed design were carried out. With the values obtained, the weight estimations can be iterated with the updated values from the different subsystems until convergence. In this section, the verification methods used to verify each of these subsystems and

iterations' code are explained. Moreover, all calculation procedures involving formulas with know values were checked and verified by performing hand calculations. Each person was responsible for performing the necessary hand calculations to verify that the code implemented in their functions was correct and did not have any errors. A function was not implemented in the main iteration until it was verified and checked so that it outputted the correct value.

8.2.1. Main iteration

The main iteration of the code consists of a file that calls all the functions from the Class I and II weight estimations, and preliminary and detailed design calculations. This is done to iterate through the design process to end up with final values after the convergence of the design.

Table 8.1: *Verification of main iteration file*

File name	Verification Method Description	Result
main.py\ parameters .json	Check that the values are correctly extracted from the parameters dictionary	The values from the parameters dictionary are correctly extracted and inputted in each of the functions in main.py
main.py	Track that the parameters calculated in the functions are used in subsequent functions	The values calculated in a function are used and updated in the subsequent functions
main.py	Check if the functions are properly implemented and output the numeric outputs and plots of all functions	Each function prints and plots the expected outcomes
main.py\ Output_ parameters .json	Check that the values are correctly outputted after being calculated in the functions to the output parameters dictionary	The values printed from the functions are the same as the values in the Output_parameters.json file
main_pre.py	Use assertions to ensure that key parameters such as MTOW, OEW, or CG values exist and stay within reasonable ranges	All tests passed and no error messages appeared.
main_pre.py	Check that the MTOW converges and the loop does not fail	The MTOW converged to the desired less than 0.1% difference between consecutive iterations and the loop does not fail at any point

8.2.2. Class I and II weight estimations

A Class I weight estimation was carried out, using statistical data, which gave as an output an initial value for the MTOW and OEW of the aircraft. After this was finished, a Class II weight estimation was performed using initial estimations of geometrical parameters of the aircraft. The Class II weight estimation gave as an output the weight of the individual components and a new MTOW and OEW.

Table 8.2: *Verification of Class I and II weight estimations*

File name	Verification Method Description	Result
WI.py\WII.py	Manually check that the past aircraft data was correctly inputted into the dictionary	The past aircraft data is the same as the data found from the sources
WI.py\WII.py	Check that the parameters file is correctly inputted and the values from the dictionary are correctly extracted	The parameters from the dictionary were printed and checked that they were extracted correctly
WI.py\WII.py	Check visually and numerically that the plots obtained are realistic	The plots were examined, and it was confirmed that the correct plots were obtained
WI.py\WII.py	Input base values for a known scenario in the formulas to verify the numerical and visual outputs	The plots and numerical values obtained matched the known scenario results

8.2.3. Subsystem detail designs

The main subsystems were designed with models that iterated through the design procedure. In subsystems such as the wing, several models were used, such as the main wing, ailerons, floaters, wing loading models. Many of the verification methods for these models consisted of hand calculation verification mentioned before, as a considerable number of formulas had to be used for the design. The verification methods used to verify these models are shown in:

Table 8.3: *Verification of subsystem design files*

File name	Verification Method Description	Result
All files	Check that the values are correctly extracted from the parameters dictionary	The values from the parameters dictionary are correctly extracted and inputted in each of the functions in main.py
All files	Check that the values are correctly outputted after being calculated in the functions to the output parameters dictionary	The values printed from the functions are the same as the values in the Output_parameters.json file
All files	Check that all parameters used come from the dictionary and not from a local variable	All variables used are extracted from the parameters dictionary
All files	Input base values for a known scenario in the formulas to verify the numerical and visual outputs	The plots and numerical values obtained matched the known scenario results
All files	Check that the functions created in each of the files are correctly called and linked in the main iteration file	All the functions are implemented without any errors and run correctly
All files	Check that the values and results obtained are realistic and fall within the expected ranges	All values were printed when first calculated to verify their correct implementation and all were verified
All files	Check that the units used in all calculations are coherent	All units were checked by checking the units of the inputs and performing test calculations

8.3. Sensitivity study

To validate the general model, certain inputs can be varied to analyse whether the output matches expected trends. These can be done for separate subsystems or general parameters. Three subsystems will be shown as examples of the sensitivity study: wing, propulsion and fuselage. Materials also performed a sensitivity study, integrated into Table 6.31. However, with an integrated and interdependent design it can become difficult to track where certain changes come from, so basic aircraft trade-offs will be explored.

Wing

The wing is one of the most mission-adapted subsystems of the aircraft, and many aspects depend on it. To visualise this, the influence of a key parameter like the aspect ratio on MTOW, wing weight and manoeuvre lift-to-drag ratio is shown. Aspect ratio is chosen for this sensitivity study as it is a fixed parameter from the early design phase, equal to 9.

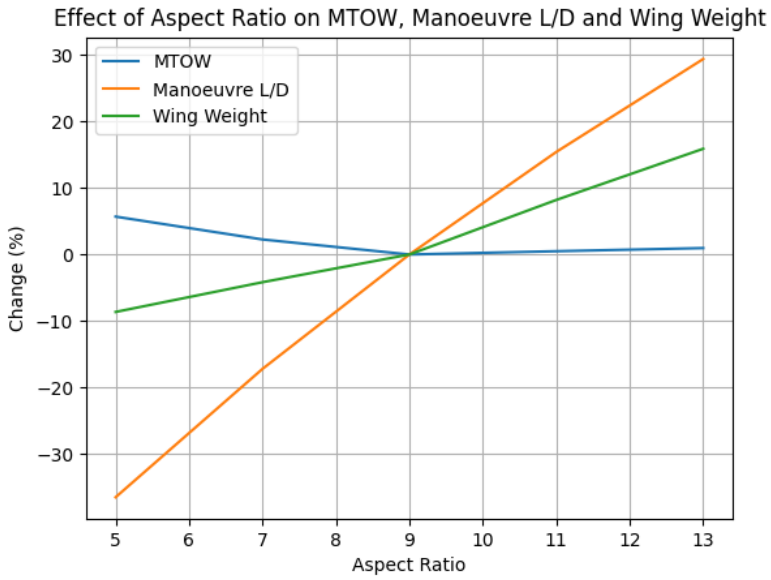

Figure 8.1: *Aspect ratio against MTOW, manoeuvre L/D and wing weight*

Figure 8.1 shows that an aspect ratio of 9 is the value that minimises MTOW, justifying the design choice. Increases in aspect ratio make the wing slender and increase aerodynamic efficiency, which is measured by the lift-to-drag ratio. This is shown in the model exactly as expected. However, it is not a reason to increase the aspect ratio as much as possible, there are structural considerations against this. The wing weight curve depicts this: increasing aspect ratio leads to a greater wing weight. As the wing is made longer, there is a larger bending moment and hence the structure needs a greater reinforcement, leading to a compromise between aerodynamic efficiency and structural weight.

The influence of aspect ratio on MTOW is less clear, but helps define the optimal point for the trade-off between aerodynamic efficiency. On one hand, a greater wing weight leads to a greater overall weight. However, improved aerodynamic efficiency reduces the fuel needed in the mission. In this model, the influence of both factors seem to cancel each other out almost perfectly, but an increase of 2% in MTOW can snowball rapidly into a much heavier aircraft. Therefore, this validates the

model and justifies the choice of aspect ratio.

Propulsion

The propulsion system is undoubtedly one of the most important features of the aircraft. Specific fuel consumption is a key parameter linking propulsion and engine characteristics to overall aircraft performance, making it a valuable focus for the sensitivity study aimed at validating the code against expected results.

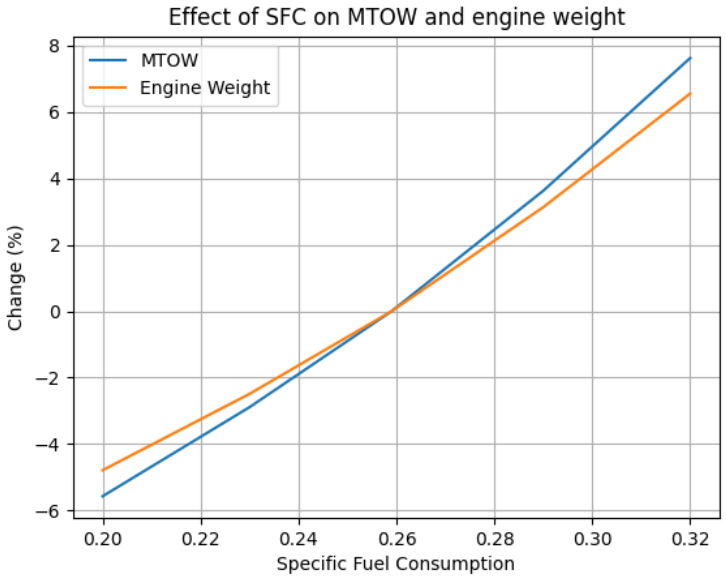

Figure 8.2: *Specific fuel consumption against MTOW and engine weight*

Figure 8.2 shows that an increase in specific fuel consumption leads to increases in engine weight and MTOW. Here, a key design feature is shown: the engines are in use for this aircraft are modified, and thus the engine weight is not a fixed value from existing engines in the market. A larger specific fuel consumption should lead to a greater engine weight, as more fuel is needed to produce the same amount of thrust, leading to a greater engine. This increase in engine weight also increases the MTOW. However, the increase in MTOW is even greater. This is due to higher structural wing weight, as the engines are wing-mounted, and a bigger fuel mass. The numerical model of this aircraft is able to display this effectively, validating the propulsion system implementation.

Fuselage

This aircraft has a very innovative design that has multiple implications on other subsystems. The fuselage must carry pilots, payloads and integrate the wing, empennage and others. A defining design feature of the aircraft is the requirement of a pilot, as this sets a minimum width and height for the cockpit. The impact of the fuselage width on fuselage weight and MTOW is explored.

Figure 8.3 shows the expected relationship between width and weight: the bigger the former, the bigger the latter. This is a simple connection that is expected in the code. However, this can be used to validate the proportions of the numerical model. The change in MTOW is proportionally smaller than the change in fuselage weight, in line with the proportion between fuselage and total weight. Furthermore, the magnitude of the values is reasonable, as the change in MTOW does not exceed 5% in absolute terms.

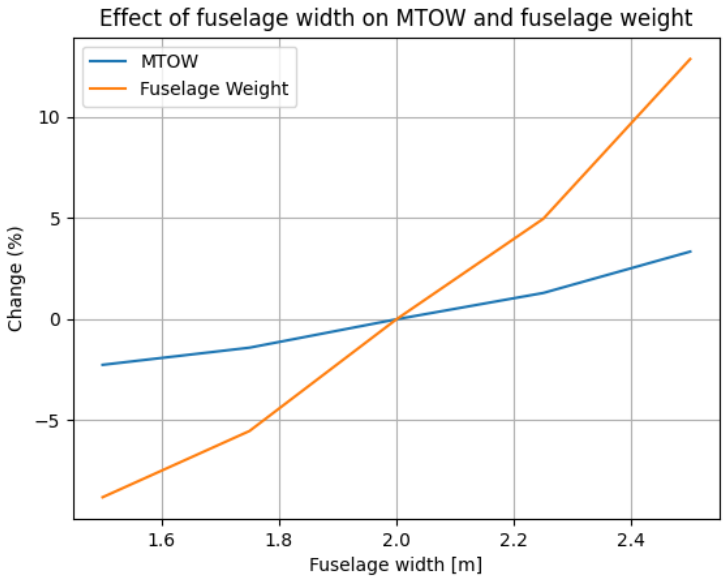

Figure 8.3: *Fuselage width against fuselage weight and MTOW*

8.4. Validation of the Final Design

To ensure the W-132 meets its objectives, the final design must be validated using several tools for validating the different aspects of the design. First the Colossus Grand Challenge software allowed to assess the overall performance of the W-132. The Optimisation Flight Route Simulation assessed the operational efficiency looking at flight paths and cooperation with other aircraft. Additionally, a tailored response time and water drop simulation was conducted to evaluate the aircraft's fire-fighting effectiveness and deployment speed. Together these softwares provide confidence in the aircraft's capability to achieve its missions.

8.4.1. Colossus Grand Challenge Simulation

In order to proceed with the validation process, the Colossus simulation was used to compare the W-132 with the current fleet and see how well it would perform in three different imaginary scenarios. Each of them is characterised by different conditions, such as being further away from the sea, or water bodies only accessible by VTOL. The fleet was made with a budget of 100 million euros, and it consists of 2 fire bosses, 1 Chinook and 1 large scooper. This fleet was analysed with the W-132 aircraft as the large scooper and compared with a control case where the DHC-515 -the new version of the CL-415, was used. The results for each scenario are presented in the Table 8.4:

Table 8.4: *Comparison of fire suppression performance metrics for W-132 and DHC-515 across different regions*

Region	Aircraft	Burnt Area (m²)	CO_2 Emissions (tons)	Burnt Area Cost (€)	Ops Cost (€)	Mission Time	MOE
Salamis	W132	763,000	65,000	1,460,000	2,260	1:28:20	0.677
	DHC515	978,000	68,800	1,540,000	1,460	1:54:21	0.675
Pyrenees	W132	39,900	10,900	228,000	1,020	0:38:20	0.698
	DHC515	40,900	8,980	188,000	556	0:40:28	0.699
Palysades	W132	83,700	115	6,790,000	821	0:35:08	0.699
	DHC515	149,000	83.8	1,290,000	564	0:55:45	0.699

Furthermore an illustration of what the suppressed area looks like for each fleet can be seen in Figure 8.4:

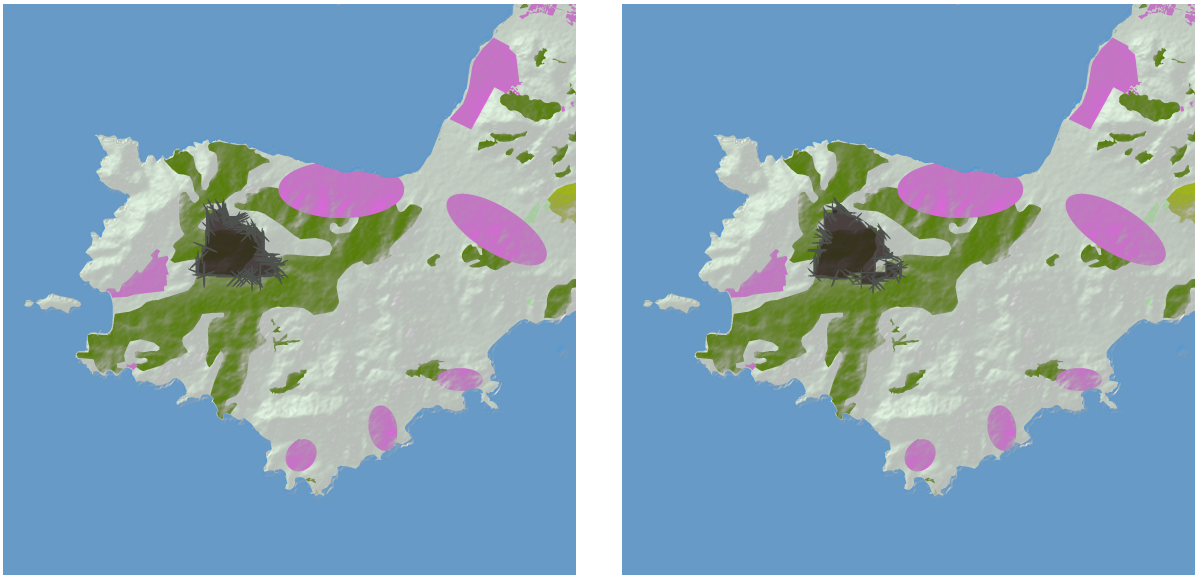

(a) *W-132* **(b)** *DHC-515*

Figure 8.4: *Comparison of fire suppression scenarios in Salamis.*

From the measure of effectiveness (MOE) values alone, no definitive conclusion can be drawn, as each fleet performs better in some scenarios and worse in others. However, a closer examination of the data in Table 8.4 reveals a noteworthy inconsistency: the burnt area cost for the W-132 is significantly higher relative to the actual burnt area. This discrepancy can be attributed to two main factors. First, the model assumes a straight-line drop pattern that is not aligned tangentially to the fire line, which limits suppression efficiency. Second, in real-world operations, firefighting tactics are far more dynamic and adaptive, often changing in response to evolving fire behaviour — something the current model does not fully capture.

Despite these limitations, it is important to emphasise that the W-132 achieves a substantial reduction in both burnt area and mission time—two critical performance indicators. Furthermore, considering that the W-132 already demonstrates superior results even without accounting for advanced tactical deployment, it is reasonable to expect even greater effectiveness in real operations, outperforming current fleets such as the ones composed with DHC-515.

The limitation of the proposed design within the program is that for fires that are either not significantly large or not nearby, the benefit of using a larger aircraft is negligible, making the use of smaller aircraft more efficient.

8.4.2. Optimised Flight Route Simulation

The design is also validated using an aerial firefighting vehicle routing solver [3]. This software allows for the determination of the optimal time taken to reach a fire given a ratio of tanker aircraft and scooper aircraft. This software optimises the firefighting tactics used and as such should eliminate the variance of the results obtained in the colossus Grand Challenge code results due to the unadapted tactical difference. This also allows for a more accurate simulation of the effect of water tank capacity as this model correctly takes into account the effect of water tank capacity on fire extinguishing effectiveness.

So as to further increase the accuracy of the model for the W-132 use case and as such increase the validation accuracy, this code has been slightly modified such that it can take into account multiple types of scoopers as well as allow for different type of water sources, accessible only by certain aircraft.

These modifications allow the modelisation of a fleet similar to the one used in the Colossus Grand Challenge code with 2 small firefighting aircraft such as the Air Tractor AT-802, 1 Firefighting helicopter with specifications similar to the Chinook and the W-132 or DHC515 to offer a point of comparison. Similarly, the use of a larger fleet of smaller aircraft could also be an option as such a fleet of 4 Air Tractors and 1 helicopter is analysed, this number is obtained from the cost of the aircraft, as 1 W-132 is equivalent to 10 Air Tractors. However as these have less than 30% of the range and much smaller cruise speeds and as such will be less available and, on average, will reach the fires slower. It is therefore assumed that only 2 of these are immediately available for every fire. Furthermore, a maximum simulation computational time of 5 minutes is given so as to model the time available for real operators [3]. This results in the following values :

Table 8.5: *Table of the time to latest arrival for both fleets*

Fleet Type	Objective Time (in mins)
Incl. W-132	119.56
Incl. DHC515	145.01
Incl. 4 AT-802	126.69

As it can be seen, using the W-132 leads to an objective time improvement of 25.45 minutes, or about 18% against the DHC515. This confirms that the increase in speed and water tank capacity greatly increases the firefighting efficiency even within the context of a fleet. This therefore confirms that within the context of an optimal firefighting mission with a typical fleet, the W-132 should be the most optimal design.

The optimised flight route simulation has also revealed that there exists better suited solutions for very localised and predictable fires. Indeed, the comparison with a fleet of smaller aircraft assumed that they would be spread about a large distance, and as such only 20% would make it to the fire at the same time as the W-132. However if the fires are concentrated in a smaller predictable area, such as the case of French territory where as the fires are all found within the same region, this availability can go up to 50%. Within the code, this translates to an objective time of 85.54 minutes - about 28% higher than the W-132. As such, for localised and predictable fires, the design is outperformed by a fleet of smaller aircraft. This is expected as these are contrary to the use case of a large range and mutual international aid centred design that this aircraft adheres to.

8.4.3. Spanish Response Time and Water Drop Simulation

The simulation developed for and used in Section 3.3 can also be used to validate the design and demonstrate the additional performance gain across Spain from the incorporation of the W-132 into their fleet. In the Spanish fleet the W-132 would serve as a replacement for the CL-415 and thus the validation will be conducted by comparing results using the CL-415 against using the W-132. As can be seen in Figure 8.5 and Figure 8.6 the W-132 reduces the mean risk score by two and a half minutes, and thus greatly improves the response time of the Spanish fleet to high risk areas. Finally Figure 8.7 and Figure 8.8 show that the W-132 triples the average impact score across Spain allowing

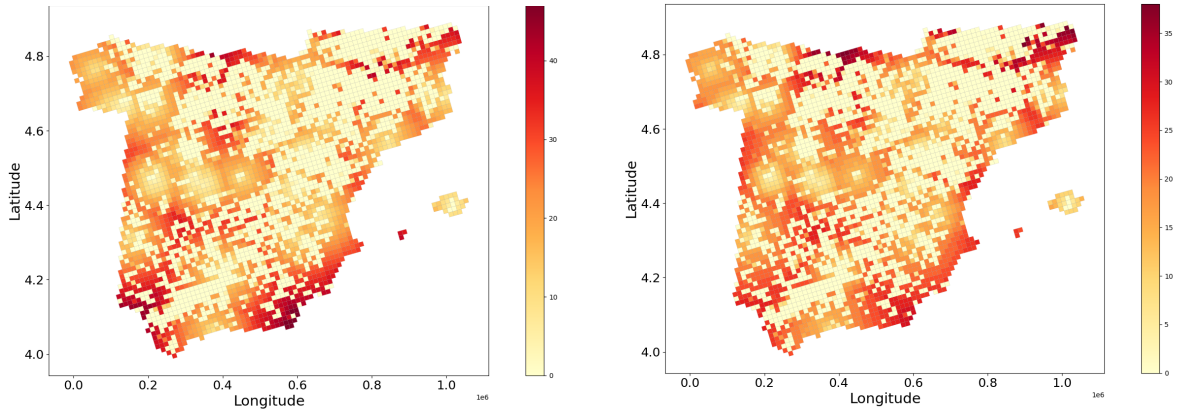

(a) *W-132* **(b)** *DHC-515*

Figure 8.5: *Comparison of Risk Score of Spain.*

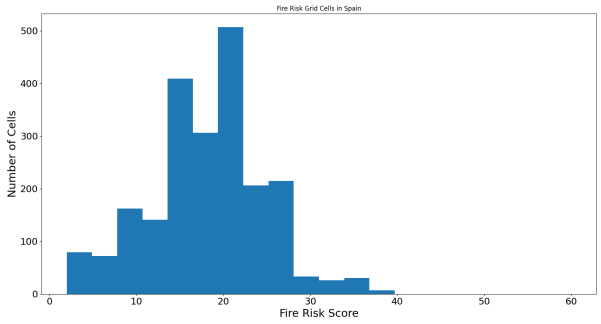

(a) *W-132 Mean Risk Score 17.3*

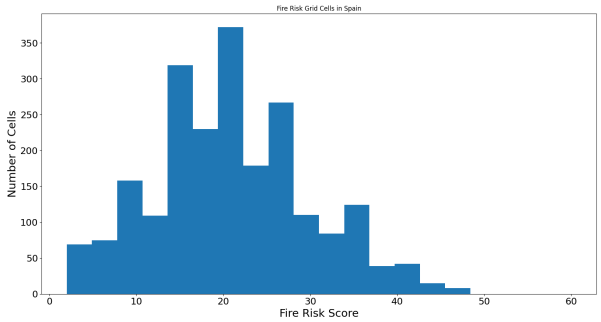

(b) *CL-415 Mean Risk Score 19.8*

Figure 8.6: *Histograms for Comparison of Risk Score Across Spain*

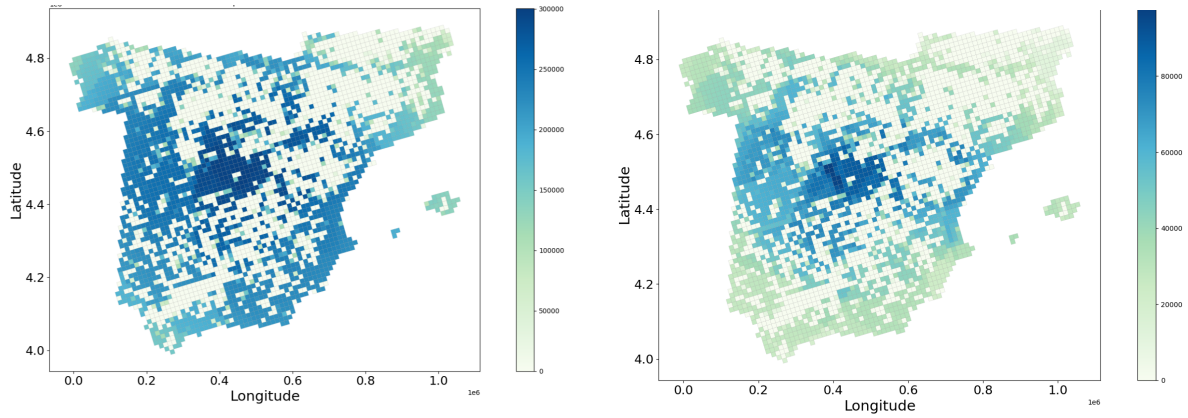

(a) *W-132* **(b)** *CL-415*

Figure 8.7: *Comparison of Impact Score of Spain.*

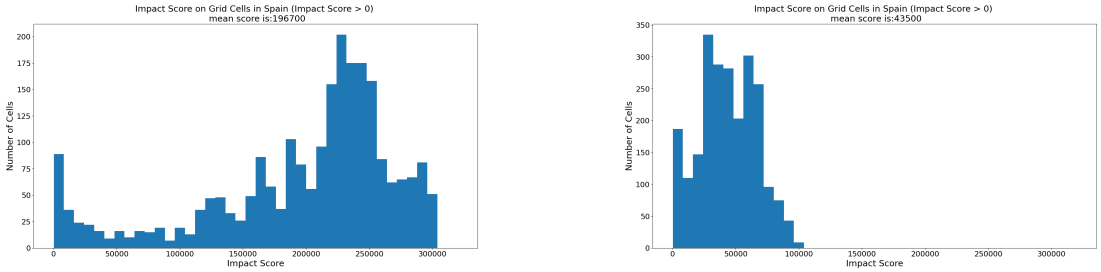

(a) *W-132 Mean Impact Score 196700* **(b)** *CL-415 Mean Impact Score 43500*

Figure 8.8: *Histograms for Comparison of Impact Score Across Spain*

9

Aircraft Subsystem Logistics

9.1. Requirements

Before explaining the design of the remaining subsystems, the requirements associated with it must be recalled. This is shown in Table 9.1.

Table 9.1: *Requirements of the remaining subsystems*

Requirement ID	Description	Compliance	Verification Method
REQ-LOG-1	The aircraft shall be capable of IFR flight	✓*	Analysis, not verified
REQ-LOG-2	The navigation system shall be equipped with an flight aid systems	✓*	Inspection, not verified
REQ-LOG-3	The onboard computer shall provide firefighting related data	✓*	Demonstration, not verified
REQ-LOG-4	The aircraft shall communicate with ground control and nearby aircraft	✓*	Demonstration, not verified
REQ-LOG-5	The communication system shall allow communication in extreme conditions	✓*	Demonstration, not verified
REQ-LOG-6	The aircraft shall measure environmental conditions	✓*	Demonstration, not verified
REQ-LOG-7	The aircraft shall measure system conditions	✓*	Demonstration, not verified
REQ-LOG-8	The hydraulic system shall operate within temperatures of up to 70 ^{o}C	✓*	Test, not verified
REQ-LOG-9	The aircraft shall have a safety mechanism in case of an emergency	✓*	Inspection, not verified

As can be seen, all requirements are expected to be complied with. This is explained in their respective hyperlinks. However due to the design maturity of these subsystems, they cannot be verified yet.

9.2. System Connectivity Diagrams

This section displays the hardware, software and data handling block diagrams as well as the communications flow diagram. These detail the connections and parts necessary for the complete functioning of the aircraft with itself and with external systems. All of these follow similar conventions to similar modern aircraft, with the added necessity of water tank integration systems.

9.2.1. Hardware Block Diagram

The hardware block diagram details the aircraft system infrastructure, the connections between them and the flows of information and material connecting them. The blocks of the diagram are separated in the following types :

- **Data Gathering Systems** : These are the external measurement and processing units which aim to provide the necessary information regarding every aspect of the aircraft position, attitude and conditions in order to ensure appropriate decision making of the pilot and automatic flight control system. The flows of these systems are mostly data flows into the flight management computer as they provide their data to the rest of the aircraft, and electrical flows from the APU as some require power to operate.
- **Cockpit Controls** : These are the mechanical devices the pilot can interact with. Depending on their type, they feed their inputs to the fly-by-wire control system if they relate to the mechanical actuation of the aircraft, or into the flight management system for the other controls.
- **Avionic Systems** : These are the core systems of the aircraft and serve as the logistical centre points. These subsystems receive data from the entire aircraft, compute the necessary flight course of action through the autopilot, and translate these into mechanical instructions. As such, these take information from the measuring instruments and pilot inputs and flow into the entire aircraft.
- **Landing Gear Subsystems** : These are the subsystems that relate to the deployment and functioning of the landing gears. As such, these mostly relate to the hydraulic actuation of the landing gear sealing and deployment mechanism, as well as their breaks.
- **APU Subsystems** : The APU serves as the main power of the aircraft. The aircraft is comprised of 2 independent main electrical circuits, one for the avionics and light displays, covered by the APU, and the engines, which have a dedicated battery.
- **Flight Control Surfaces** : These are the flight control surfaces that the pilot and autopilot can interact with to create the appropriate trajectory and ensure stability. These are all hydraulically actuated.
- **Lifeline and Comfort Systems** : These systems relate to the consistent functioning of the aircraft and pilot. As this aircraft is unpressurised, there is no pressurisation system; instead, it relies on an oxygen system for unbreathable atmospheric levels. The anti-icing system ensures regulation compliance; however, it should not be critical, as forest fires do not typically occur in subzero temperatures. These are all controlled through the flight management computer.
- **Lighting Systems** : These are standard lighting instruments required by regulations for proper ground communication. These require electricity from the APU and are controlled from the cockpit.
- **Engine Subsystems** : This represents the entire engine management subsystems, from the fuel and electricity units to the individual functions of the necessary components for the functioning of the engine. In addition to the conventional components of an engine, an electrical subsystem is appended on as this is a hybrid engine system. This engine is controlled hydraulically through the fuel pumps and digitally through the PPMS.
- **Hydraulic System** The hydraulic system is responsible for the actuation of every mechanical subsystem, as such it receives input from the fly-by-wire control system. This system is responsible for the movement of the flight control surfaces, pumps, landing gear and water system.

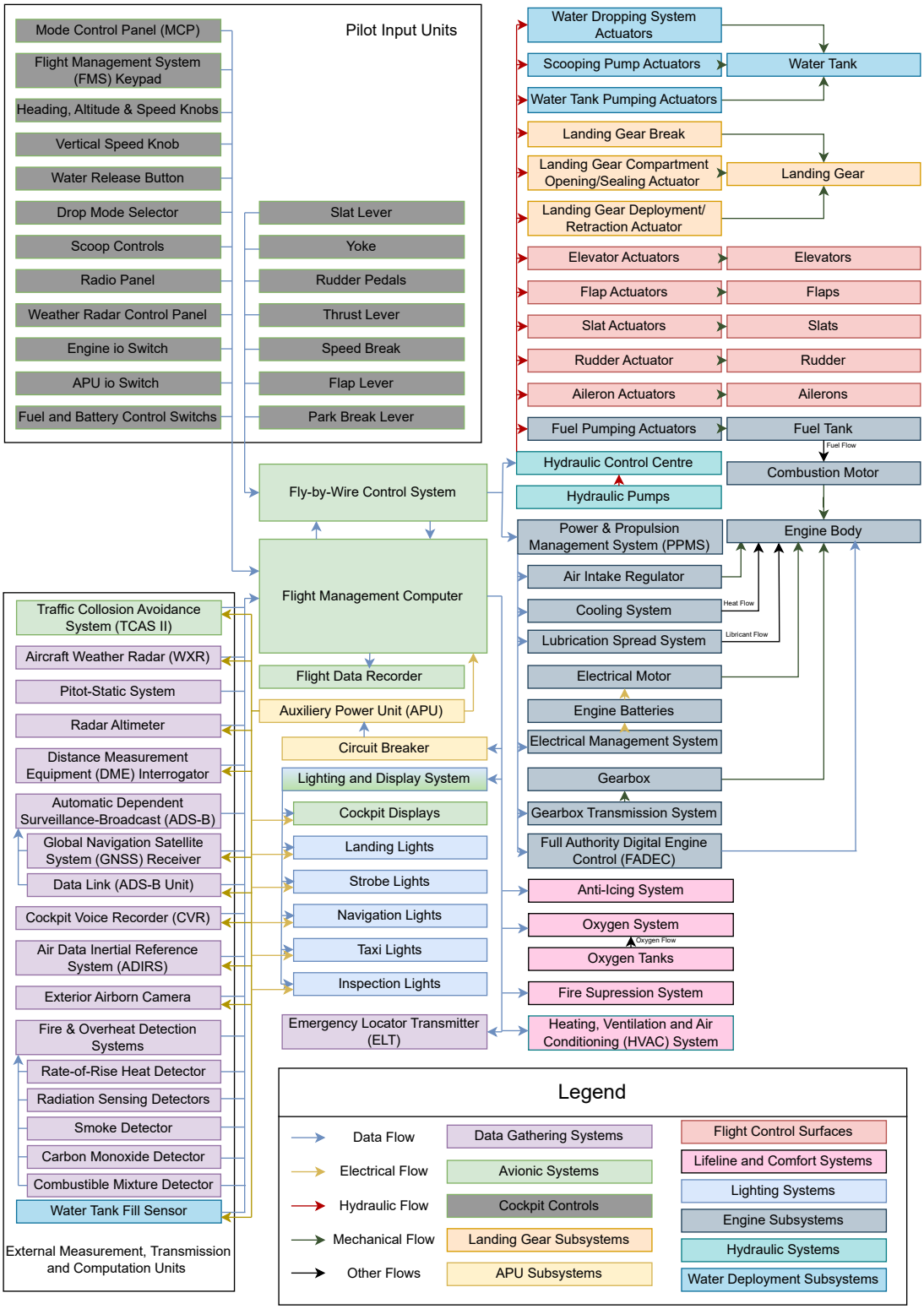

Figure 9.1: *Hardware Block Diagram*

9.2.2. Software Block Diagram

The software block diagram describes the primary software necessary for the functioning of the aircraft and their interconnectivity. The same subsystems as for the hardware block diagram are present with some further precision for clarity, and there is also an absence of certain as they do not explicitly require any software.

As it can be seen, most of the software is connected through the flight management system, which serves as the core of the aircraft computational node. This system receives inputs from the data measuring instruments and the fly-by-wire control system and is responsible for the processing and commanding of the output subsystems. This system works in tandem with the fly-by-wire control system through the autopilot to ensure consistency across the entire system.

The other outputs of the flight management system are primarily visual outputs, non-actuated flight system control and data logging. The visual outputs are used to communicate decisions and status to the pilot and the exterior. Non-actuated flight controls mostly relate to electrical and engine control as well as life-support systems such as the ECS. Data logging is done to monitor the wellbeing of the aircraft for maintenance, crash logs and pilot information.

As it can be seen, the aircraft uses many modern avionic system as these are majorly beneficial in firefighting mission. This is because these missions require rapid and informed decision making and as such conveying all the necessary information to the pilot is a priority of the avionic systems.

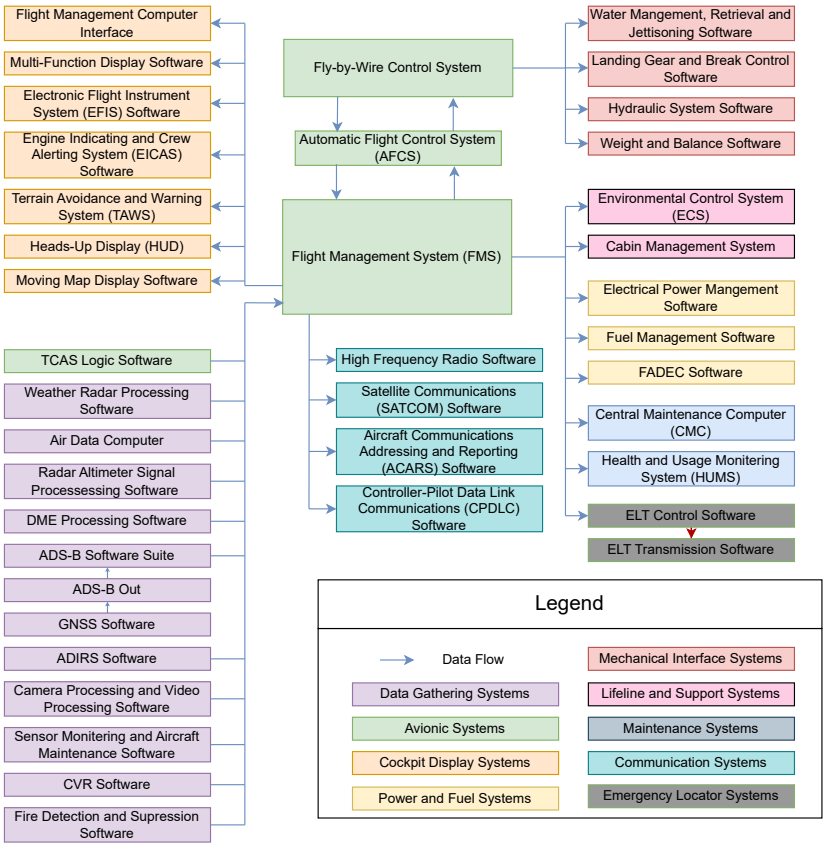

Figure 9.2: *Software Block Diagram*

9.2.3. Data Handling Block Diagram

This diagram shows the data transfer relations between the subsystems of the aircraft as well as the main communication and processing speeds and the unit storage spaces.

As it can be seen, the interconnected data transfer speeds are in the order of 100Mbps, this is because the aircraft is designed to utilise a modern Ethernet-like connected system. This is to allow for the lowest amount of latency between the reception of the data and its transfer to the pilot, this system also allows for higher data packets transfer such as external cameras to allow the pilot to make better informed decisions.

Similarly, modern high speed processing units are used to further reduce the critical time required to convey information to the pilot. This also allows for quicker autopilot and TCAS II decision making to reduce the probability of catastrophic failures due to unforeseen collisions.

This system utilises many redundant components as failure of any of these systems would result in disastrous consequences as it could greatly reduce the amount of data the pilot can utilise or even completely incapacitate the aircraft. As such many of these processing, memory and transfer units are present in multiple copies to cross validate and continue functioning in case of failure of one of them. An example of this is the use of 3 flight management computers, each connected to their own sensor and detection systems. This allows for voting logic to overwrite any faulty data and prevent failure. These units also have redundancy in their processor units, allowing for a fail-safe approach whereas the failure of any of these components can be ignored until the end of the mission. A similar concept is applied to the storage units and the inter-system connections. This is further accentuated along critical data paths, for example, through the use of 3 distinct main data transfer bus each with multiple sets of wiring. All of these approaches should ensure that failure of any of these components should not affect the airworthiness of the aircraft.

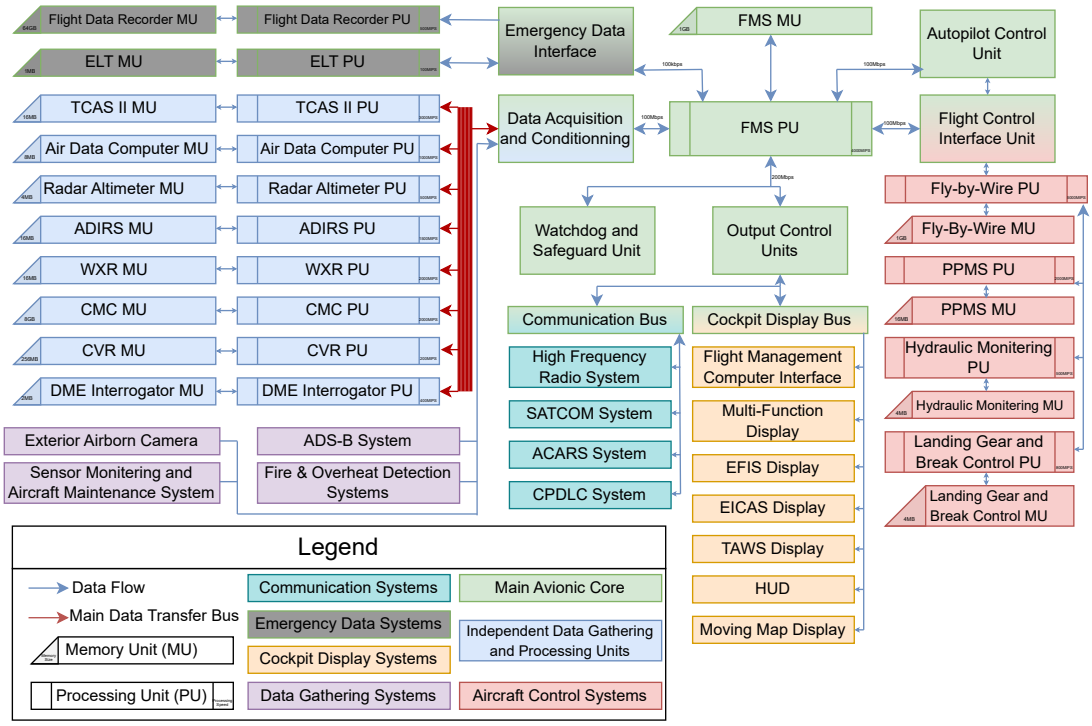

Figure 9.3: *Data Handling Block Diagram*

9.2.4. Communication Flow Diagram

The communication flow diagram shows transfer of data in and out of the system. This data is both explicit, with purposeful data such as radio communications and pilot inputs, as well as implicit with external conditions data assumed to be a communication point. This is done so that the entire flight loop can be analysed and the aircraft computational system can be isolated from exterior influence.

The pilot is not considered part of this system as this diagram only shows the deterministic part of the flight system. As such, the pilot commands and the visual outputs for the pilot are considered to be input and outputs.

From the diagram, it can be seen that the aircraft receives external data from its instrumentation, ground communications and the pilot. All of these are connected through the flight management system which also serves as the output processing centre, distributed into satellite and radio telecommunication as well as visual indications.

Overall, this system is similar to conventional aircraft, with the addition of redundancy in the communication devices. This is because communication is imperative in firefighting missions as obtaining precise and exact information on the location of the fire, the terrain and water body locations can greatly increase the successfulness of a mission.

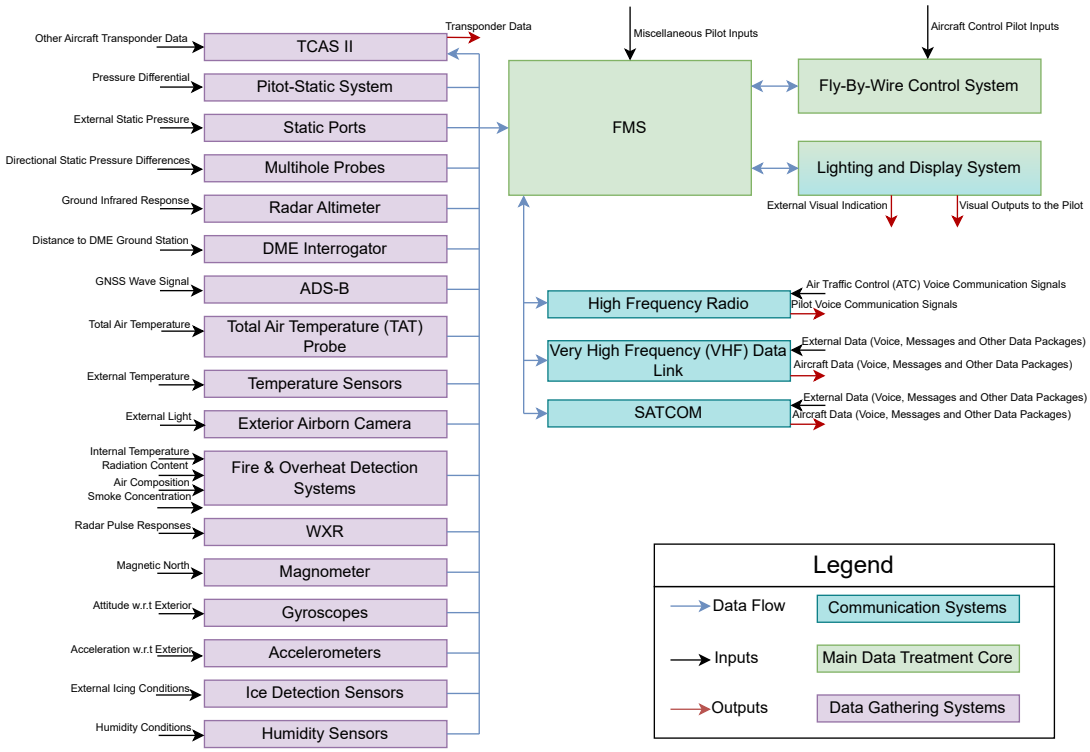

Figure 9.4: *Communication Flow Diagram*

9.2.5. Electrical Block Diagram

The electrical block diagram shows the main electrical systems along with their components and relations. There are 3 main electrical loops here, the main one with the avionics and instrumentation of the aircraft connected to the main power generator and the APU, the electrical motor system which is not linked to the rest of the system and the ELT which is designed to be completely independent so as to be operational during or after emergencies.

These systems also have integrated breakers so as to be able to cut power in cases of emergencies. The main electrical system runs using the engine driven generator during most of the operating life, the APU exists so as to provide emergency power in case the main power source becomes unavailable due to engine failure or simply because the aircraft is grounded. The flight data recorder, external lights and fire detection & suppression systems all use the main power source during regular flight, however these are all equipped with emergency power sources in the form of battery as these are critical systems and must be operational during emergencies.

The electrical engine system is a critical part of the electrical system as it represents the highest voltage and power transfers within the aircraft, however due to these, the system is simple so as to limit the amount of failure points. As such, this system is mainly composed of the batteries, the engine and the energy management system which controls the electrical flows between them.

The emergency locator transmitter must operate during and after major failure of the aircraft, furthermore as it is a low power consumption system, it can be completely supplied by a battery. It is therefore completely independent to the rest of the electrical system.

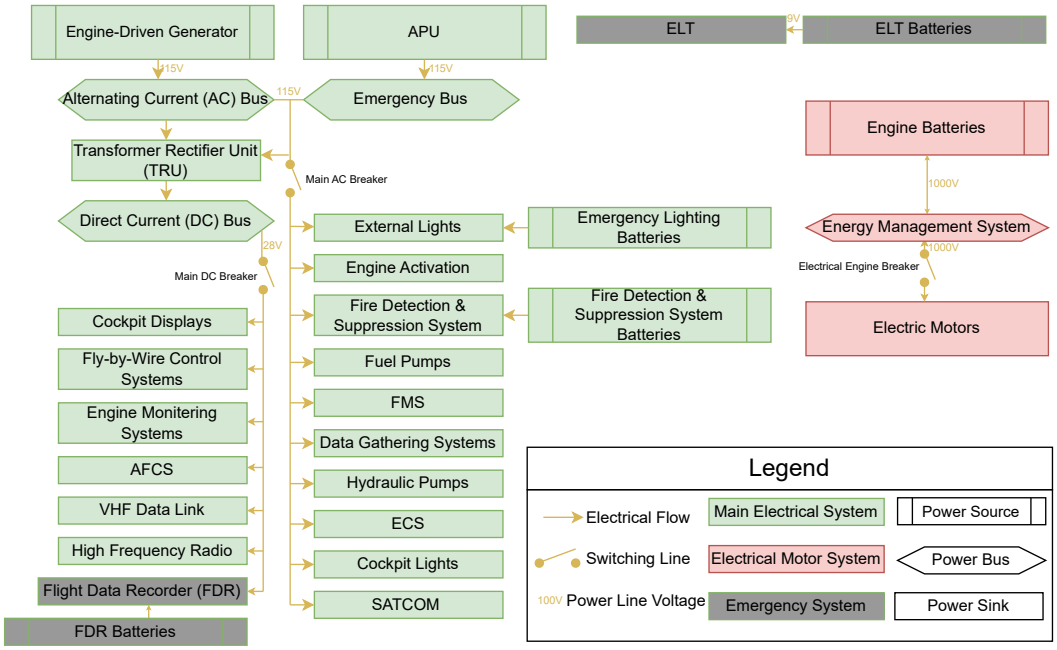

Figure 9.5: *Electrical Block Diagram*

10

Risk Assessment, Contingency Management and RAMS

In this chapter, a technical assessment and contingency management of potential project risks is carried out. Section 10.1 provides the main technical risks that might pose threats to the mission's success and their respective mitigation processes. Subsequently, Section 10.2 focuses on the derived requirements from the contingency management. Then, Section 10.4 demonstrates the redundant methods of the aircraft. Moreover, Section 10.5 demonstrates the availability of the aircraft in the current European market. Section 10.6 and Section 10.7 assess the maintenance and safety of different subsystems throughout the aircraft.

10.1. Risk Analysis and Contingency Management

This section carries out a technical risk assessment with the aim of identifying the most mission constraining risks. To properly analyse possible risks, the mission was divided into 7 different phases; Taxiing, Take Off, Cruise, Water Collection Manoeuvrer, Fire Approach, Payload Drop and Landing, whereas risks were derived within each phase. Each risk is given an ID, which is created by following the structure of [R-ABC-#], where the first letter R differentiates these risks from requirements that are phrased as follows: [REQ-ABC-#]. The three letters [ABC] are chosen based on the phase name. Finally, the # demonstrates the numbering of the requirement within each phase. The mitigation processes that are carried out to reduce the level of these risks are also addressed. These either reduce the risk's severity or its likelihood. Certain risks however, are accepted as they do not pose sufficient threats to the success and efficacy of the mission to allocate time and resources for their mitigation. Each of the risks are ranked in terms of likelihood and severity. Likelihood is based on the following criteria: unlikely, possible, highly possible and inevitable. The same logic can be applied for the severity with inconvenience, problematic, critical and catastrophic. The mitigation processes reduce either criteria and their effect is visually depicted in Figure 10.2. Table 10.1 demonstrates the risks and mitigation processes. The colour coding of the table is divided into green, orange and red which represent whether the risk has been mitigated, reduced or accepted, respectively.

Table 10.1: *Risk Analysis Across Flight Phases and Allocated Mitigation Processes*

ID	Risk	Mitigation Process
Taxiing		
R-TAX-1	Taxiing curve radius is too slim and aircraft is unbalanced leading to roll over	Ensure that main landing gear arrangement should lead to a turnover angle of at least 55°
R-TAX-2	Tire puncture	Carry out daily tire pressure maintenance procedures

ID	Risk	Mitigation Process
R-TAX-3	Miscommunications with control towers	Require minimum 1500 hour piloting experience to carry out missions to evade communication problems [87]
Take Off		
R-TOF-1	One engine becomes inoperative	Aircraft shall be able to take-off with only one engine
R-TOF-2	Take off distance is too short for certain airports	Ensure airports around mission have long enough take off distances
R-TOF-3	Cross wind during take off exceeds the nominal requirement	Aircraft structure is capable of sustaining 1.5 x the nominal cross wind requirement
R-TOF-4	Control Surfaces Malfunction	Implement both slats and double slotted flaps in case one malfunctions the other still provides extra lift to take off appropriately
R-TOF-5	Obstacle interference (Mountains, forests, uncanny environment)	Ensure missions take off with no payload and approach water source on the way
Cruise		
R-CRS-1	High unexpected wind gust loads due to adverse weather conditions	Risk accepted in Figure 6.3.
R-CRS-2	Loss of IFR instrumentation	Require minimum 1500 hour piloting experience to carry out missions and be able to properly go about VFR [87]
CRS-3	Electrical system overload or fault	Use system coolers and detectors to prevent this from occurring
Water Collection Manouver		
R-WCM-1	Water collection actuators do not properly open before reaching water	Carry out consistent actuator lubrication processes before take off
R-WCM-2	Water impact exceeds acceptable loading	Pilot aborts approach if safe contact with the water is not feasible - pilot training
R-WCM-3	Water intake gets blocked due to water debris such as wood, fish, algae, flora	Install debris filter while maintaining flow rate and design dual intakes for redundancy
R-WCM-4	Aircraft approaches water incorrectly and sinks deeper than expected	Pilot aborts approach if safe contact with the water is not feasible
R-WCM-5	Not enough speed to carry out take off safely	Carry out water approach with a speed of 1.5 x minimum required to take off again
R-WCM-6	Landing gear is exposed to water	Create a sealed landing gear compartment and place landing gear at a minimum height of **2.7** m to prevent water from entering
R-WCM-7	Unintentional asymmetrical fill of tanks negatively affecting CG	Implement effective and modern automatic control systems to atomize control surface reactions
R-WCM-8	Engine salt water ingestion or spray	Place the engines above the wing to create enough water clearance to prevent water contact
R-WCM-9	Collision with boats	Carry out an obligatory visual analysis of water source and potential obstructions

ID	Risk	Mitigation Process
R-WCM-10	Tank structure disrupted due to tank pressure	Conservatively design tank structure to sustain 1.5 x the expected loads.
Fire Approach		
R-FAH-1	Turbulence and gust loads due to hot air columns cause instability or structural failure	Design load tolerant structure using 1.5 safety factor
R-FAH-2	Smoke of fire leads to VFR reduction	Ensure IFR flight
R-FAH-3	Increased temperatures lead to malfunction of electrical systems	Add internal cooling systems that prevent overheating of electrical systems
R-FAH-4	Engine efficiency reduced due to smoke or fire debris	Electrically powered system implemented into engines to aid in case of power shortage
R-FAH-5	Lift and thrust reduced due to increased temperatures and reduced density	Fly at altitudes at least 45.72 meters above the highest vegetation
R-FAH-6	Material failure due to increased temperatures	Use Al-1%Mg-1.1%Si-0.8%CoNi heat resistant aluminium alloy that prevents any potential heat from causing material failure
R-FAH-7	Fire approach is not correctly calculated, leading the aircraft to catastrophic temperatures	Always maintain a maximum distance of 45.72 meters above the largest vegetation using control systems limiting closeness based on fire strength
R-FAH-8	Airframe structure failure due to higher stresses caused by higher loadings than expected	When designing the airframe structure a safety factor of 1.5 will be used at all times to ensure no loads surpass the maximum load capacity
Payload Drop		
R-PLD-1	Instantaneous changes in fire magnitude and wind direction	Risk accepted
R-PLD-2	Malfunction in payload actuators	Maintenance between every mission ensuring proper functioning
R-PLD-3	Incorrect drop timing and location due to GPS errors or human error (pilot misjudgement)	Implement automated drops with sensors
R-PLD-4	Induced instability and uncontrollability due to a sudden CG change during the payload release	Design releasing payload system to distribute payload evenly and symmetrically. Implement effective and modern automatic control systems
R-PLD-5	Water Dispersion due to excessive altitude water drop	Respect requirement to fly only 45.72 meters above largest vegetation but try to approach fire as much as possible with this in mind
Landing		
R-LNG-1	Control Surfaces malfunctions	Wing designed to be capable of landing without HLDs
R-LNG-2	Brake overheating or failure on landing due to higher temperature exposures during mission	Implement further cooling systems in the landing gears

ID	Risk	Mitigation Process
R-LNG-3	MTOW landing if full payload is retained due to mission abort or malfunction	Requirement for brakes to allow for landing distance 1.25 only of nominal landing distance

Using all of these risks a risk map can be created demonstrating the effect of the mitigation processes. Figure 10.2 demonstrates a risk map which is useful to visually determine whether certain risks still pose significant threats to the mission and thus require further mitigation action. The risk map is colour coded to portray the significance of every risk. The darker coloured sections define the higher level risks. The x-axis is the severity of the risk (i.e. how strongly it impacts the project) and the y-axis is the likelihood (i.e. how likely it is to occur).

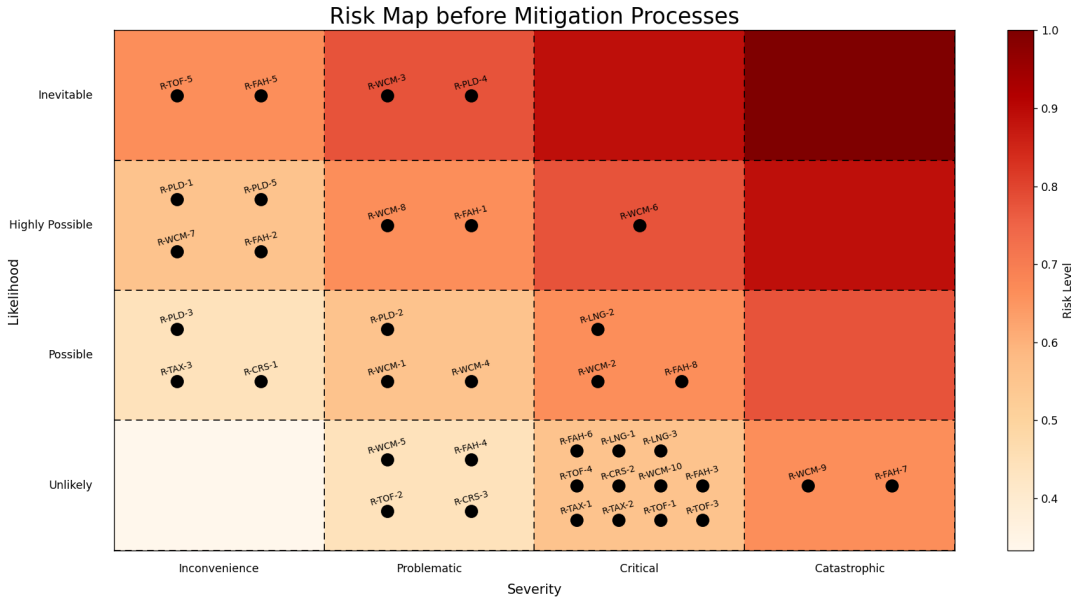

Figure 10.1: *Risk Map Before Mitigation Processes*

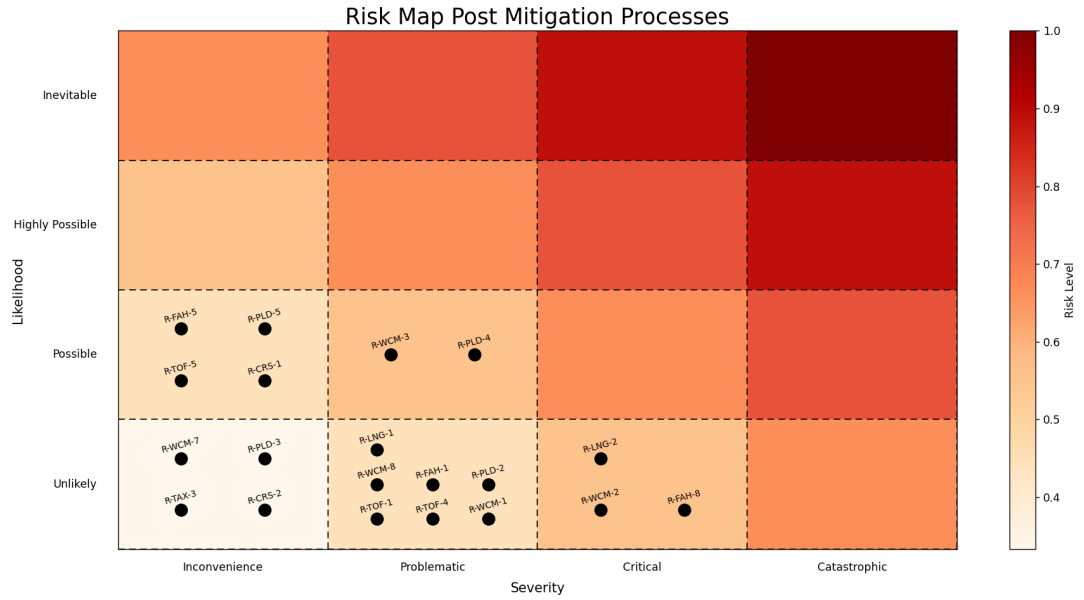

Figure 10.2: *Risk Map Post Mitigation*

10.2. Requirement Derivation

The majority of risks have been mitigated throughout the contingency management. These mitigation processes lead to a certain amount of requirements that create a constraining design space for the W-132. These are listed as follows;

- **REQ-OPS-10** - The aircraft shall not fly below 45.72 meters above largest vegetation
- **REQ-OPS-11** Pilot shall have a minimum of 1500 flight hours
- **REQ-PROP-8** - Landing distance at MTOW shall not exceed 1.25x the nominal landing distance
- **REQ-PROP-9** Aircraft shall be able to take off with one engine inoperative
- **REQ-FUS-12** Aircraft structure shall be capable of sustaining loads 1.5 x higher than the limit load factor
- **REQ-UCA-5** Main landing gear shall have a maximum turnover angle of 55°
- **REQ-UCA-6** - Landing gear shall be placed at a minimum height of 2.7 meters
- **REQ-RAMS-4.1** - Aircraft tank actuators shall be maintained every 100 flight hours
- **REQ-RAMS-4.2** Aircraft payload actuators shall be lubricated at least every 200 flight hours

The design was revisited to ensure that these requirements were complied with. For future recommendations, more detailed analysis into the specific mitigation processes could be carried out to fully mitigate more of the potential risks. Also, more lower level risks might arise throughout the mission that despite not posing significant threats to the aircraft itself, they might reduce the overall success of the mission. Thus, these could be addressed in a more extensive continuation of this project.

10.3. RAMS Requirements

Before analysing the reliability, availability, maintenance and safety of the system, the requirements that drive these operations must be defined. These are as follows:

Table 10.2: *Requirements regarding RAMS*

Requirement ID	Description	Compliance	Verification Method
REQ-RAMS-1	The aircraft shall have a failure rate equal or lesser than comparable aircraft	✓*	Demonstration, not verified
REQ-RAMS-2	The aircraft shall have a durability equal or greater than comparable aircraft	✓*	Demonstration, not verified
REQ-RAMS-3	The aircraft shall have a time-to-repair equal or less than comparable aircraft	✓*	Demonstration, not verified
REQ-RAMS-4	All subsystems shall undergo routine maintenance tasks	✓	Demonstration, not verified
REQ-RAMS-5	Critical subsystems shall include redundancy	✓	Analysis, verified

The first three requirements have not been verified yet, as a specific failure rate, durability, and time-to-repair have not been determined. When performing the RAMS analysis, the assumption is that

the aircraft will be produced, manufactured, and assembled. When this is done, further analysis can be carried out to determine the specific values for these aspects.

10.4. Reliability

Reliability indicates how likely the aircraft is to perform the firefighting mission without failure. A reliable aircraft is fundamental to ensure safety, efficiency and continuity throughout the mission. It depends heavily on the redundancy of different critical components. For instance, different subsystems might present different reliability challenges. This is heavily linked to the mitigation processes that have been carried out to improve the aircraft's reliability. The reliability can be qualitatively assessed based on the redundancy of individual systems. Table 10.3 provides the different systems that have applied redundant techniques and what section in the report they can be found in.

Table 10.3: *Systems Redundancy*

System	Redundancy	Section
Propulsion System	The propulsion system is hybrid electric. It feeds power through the main combustion engines but is complemented by additional power from batteries. In case of engine inoperative or increased thrust requirements, this system becomes redundant	Section 6.5
HLDs	The wings have slats on them to aid in providing more lift during the low velocity manoeuvres. This extra lift provides the aircraft with the capacity to fly at slightly lower speeds if needed	Subsection 6.6.3
Empennage	The vertical tail area is around 12% larger than the minimum requirement thanks to the implementation of the dorsal and ventral fin, ensuring directional stability	Subsubsection 6.8.3.4
Payload Tanks	The payload is divided into two different tanks which are connected via 2 3 way T-valves in case of scooping mechanisms failures. Also, the individual tanks are divided into 5 compartments to prevent shifts in CG from water movement and at the same	Subsection 6.10.1
Piloting	W-132 has the capacity for 2 pilots making flight redundant in case of control loss from one of them.	[-]
Avionics	Processing, memory and transfer units are present in multiple copies to cross validate and continue functioning in case of one failure	Subsection 9.2.3

Table 10.3 demonstrates the redundant systems that have been implemented into the W-132. For future applications, more redundancy could be applied to certain subsystems such as the primary flight controls, electrical systems and the payload dropping mechanism.

10.5. Availability

Availability refers to the indication that ensures that a system, resources, or services remain accessible, functional, and ready to be used at a given time and conditions. In the context of firefighting, this aspect is crucial as a slight delay on an emergency response can lead to a greater spread of the fire. For this reason determining the availability of the W-132 is imperative, especially during intense fire seasons, as emergency calls happen on irregular bases, and response time is a crucial factor.

The W-132 will be integrated into some already existing European fleets. The hybrid powertrain present in the W-132 design is a key design aspect that influences the aircraft's availability. The warming up time of the engines is greatly reduced by the use of the hybrid powertrain. This system allows the aircraft to be ready for takeoff much quicker, as the conventional engines do not need as long to warm up because the electrical batteries will assist them during take-off. This is a key feature that will differentiate the W-132 from the existing firefighting aircraft, as it will be able to be in the air much faster than the rest of the fleet.

Moreover, the W-132 is a scooper aircraft, which means that the aircraft will be available within the fire area for a longer period than other aircraft that would have to go back to base to refuel and refill the tanks between each drop. Additionally, the W-132's range and fuel efficiency will allow for longer missions without the need for refuelling as often as current aircraft.

Maintenance procedures are another factor that affects the availability of the W-132. These procedures are essential to ensure the correct functionality of the aircraft and prevent any failures that would drastically reduce its availability. However, the maintenance procedures also influence its availability, but they can be performed at strategic moments so that it does not influence the mission times. The big maintenance checks will be performed during the off-peak fire season in winter, as most aircraft will be stationed at the bases. During wildfire season, regular checks will be performed to identify any possible issues.

10.6. Maintenance

Different subsystems of the aircraft have different maintenance requirements, thus, 5 different essential subsystems were analysed; Engine, Landing Gear, Wing, Empennage and Floater. Within the engine the Hot Section Inspection (HSI), compressors and the blades are analysed. HSI includes the combustion chamber, fuel nozzles and turbines. For the landing gear, the struts and tires were analysed. Additionally, an overhaul maintenance constraint was added to dismantle the entire landing gear, which is an intrusive procedure. Intrusive procedures refer to the disassembling or opening up of parts while non intrusive procedures are less costly and more regular. The maintenance of the wing is divided into the HLDs and its internal structure. Due to the lack of data on HLD maintenance requirements it is assumed that they shall be maintained every 300 - 600 flight hours based on CL-415 data. Lastly, it is assumed that the elevators and rudder, i.e tail control surfaces generally carry out the same types of maintenance procedures as wing HLDs. Thus, the same maintenance flight hours are required. The maintenance procedures can be found in Table 10.4.

Table 10.4: *Subsytem Maintenance, FH = Flight Hours, FC = Flight Cycles*

Subsystem	Internal system	Maintenance	Units	Additional Maintenance
Engine	HSI	2000 [88]	FH	Routine Visual, Borescope, Functional and Operational Checks 100 - 500 flight hours
	Compressors	6500[88]	FH	
	Blades			
Landing Gear	Struts	50[89]	FH	Tire pressure checks before flight
	Tires	150 - 400 [90]	FH	
	Overhaul	15000 - 20000 [89]	FC	
Wing	HLDs	300 - 600	FH	Periodic heavy inspections are carried out
	Structure	[-]	[-]	
Empennage	Elevators	300 - 600	FH	Periodic heavy inspections are carried out
	Rudder	300 - 600	FH	
Floater	Structure	100 - 300[91]	FH	Detailed Structural Inspections every 1000 - 2000 flight hours

To more thoroughly analyse the maintenance of the aircraft, in depth fatigue analysis could be carried out in a future extension of the project. This would allow for estimates of the wing's lifetime and fatigue failure rates. This could be applied to other subsystems for more precise estimates of maintenance requirements.

10.7. Safety

Safety is a critical aspect that has to be considered during the design process of the aircraft. To do this, the critical functions of the aircraft have to be identified and assessed. This must be considered not only for the safety of the aircraft but also for the safety of the people, infrastructure, and environments that can be influenced by the mission.

In the case of aerial firefighting missions, safety becomes a crucial aspect as unconventional manoeuvres are carried out and are operated in harsh and challenging environments, which comes hand in hand with an increase in risks. Moreover, the design of this type of aircraft is unconventional, due to the nature of the mission. This design has to include design aspects that take into account the before mentioned aspects, which for a commercial airliner would not be taken into account.

The safety assessment is closely linked to the risk assessment that was discussed in Section 10.1 and thus, the severity levels used to asses the critical safety functions used will be the same four: "Inconvenience", "Problematic", "Critical", and "Catastrophic".

System	Failure	Severity level and Consequences	Mitigation Measure
Battery	Failed charging	Inconvenience: Pilots are unable to use extra battery power during certain stages of the mission, which require of that extra power	Establish battery charging time and check battery level when the battery has finished charging
	Unexpected battery fire	Catastrophic: Mid-flight fire can cause catastrophic failure of main subsystems	Battery is housed in a firewall, and cooling systems and PCM are used
Engine	Engine failure	Moderate: One of the two conventional engine becomes inoperative	Regular checks for maintenance of the engine. In case of failure, return back to base with electrical assistance
	Propeller blade fails	Critical: One of the blades of the propeller fails or detaches from the engine	Regular checks on the propeller system to check for cracks or fatigue failures
Water system	Water tank leakage	Moderate: Water in the tank leaked, so CG will shift irregularly	Regular checks on the water tanks to check for cracks or fatigue failures
	Blocked water intake	Moderate: Water tanks are filled irregularly and CG will shift irregularly	Check the water intakes after every mission

Continued on next page

System	Failure	Severity level and Consequence	Mitigation Measure
Landing Gear	Landing gear failure	Critical: Belly landing has to be performed with extreme caution	Regular checks on the landing gears to check for cracks or fatigue failures
	Landing gear puncture	Moderate: Perform landing manoeuvre with extreme caution	Check tire pressures before take-off and regular tyre changing to prevent punctures
Structures	Overheating from fire	Critical: The structures or subsystems could fail if certain temperatures are surpassed	Material choice and keep required clearance with the fire
	Structure failure	Catastrophic: The structure is not able to withstand loads from manoeuvre	A safety factor was used during design for the structure to withstand all manoeuvre loads

11

Cost Analysis and ROI

This chapter outlines the methodology used to estimate the total cost of the aircraft, from development to production and operational phases. The analysis is based on Raymer's cost-estimating relationships (CERs) and integrates corrections for technological, economic, and geographical factors through the use of fudge factors.

One of the key system-level requirements guiding this analysis is **REQ-SYS-2:** *The total cost of the aircraft subsystems shall be less than $56 million.*

This requirement serves as a cost ceiling, influencing design decisions, material selection, and production strategies. The goal of the following sections is to evaluate whether the proposed aircraft design is likely to meet this constraint.

11.1. Cost Analysis

11.1.1. Method

Throughout the present chapter, Raymer's cost analysis method [1] was used, using a "top-down" statistical method, namely the "cost-estimating relationship" (CER). CERs work by estimating labour hours and applying a *wrap rate* consisting of *hourly rates*, averages for different labour costs. As seen in Figure 11.1, the life-cycle cost is divided into six main components, however, only three are approached in this section. GSE&IS is a military parameter, special construction is not taken into account because the aircraft is assumed to be built in existing facilities, then, disposal costs are ignored as they are negligible compared to operations and maintenance (O&M) costs.

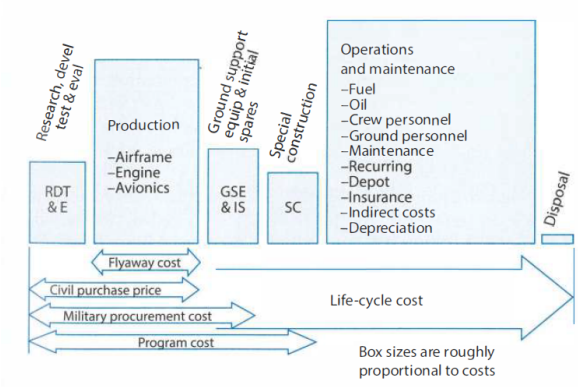

Figure 11.1: *Elements of life-cycle cost*

11.1.2. Development and Production Costs

For the research, development, test and evaluation and the flyaway (production) costs, Raymer makes use of the DAPCA IV method from RAND. This statistical method, well known and respected

in the industry, was originally designed for military aircraft and thus tends to overestimates for other types of aircraft, it is also based on aluminium aircraft whereas the W-132 is mostly made out of carbon fibre, moreover the latest iteration of the method provides costs in $2012, not $2025. To fix these shortcomings, a common method for better accuracy is to use "fudge factors" that "corrects" the estimations.

The carbon fibre fudge factor is within the recommended range provided by Raymer for graphite-epoxy materials, Europe funding fudge factor is not used in the present analysis but will be talked about more in Subsection 11.2.3. As said earlier, DAPCA IV tends to overestimates for non-military aircraft, so a 0.9 fudge factor is used upon recommendation of Raymer, inflation is based on values extracted for the month of September 2012 compared to May 2025, as to get definitive values, as opposed to $2035 predictions, using US Bureau of Labor Statistics data[1].

Table 11.1: *Fudge Factors*

Fudge Factors	**Value**
Carbon Fiber	1.2
Europe funding	1
DAPCA overestimation	0.9
Inflation $2012/$2025	1.39

Continuing, instead of using the OEW, Raymer recommends adopting the *Airframe Unit Weight* (AUW) for better accuracy in cost analysis. This represents the aircraft's weight excluding all components that are simply purchased and integrated, i.e., the parts the manufacturer buys and "bolts onto" the custom-designed structure. In Table 11.2, it can be seen that the AUW is equal to 76% of the OEW, whih corresponds with expected values from Raymer.

Table 11.2: *AUW Definition*

Item	**Weight (kg)**
OEW	21,098
Engines	670
Batteries	3925
Elec motor	136
Avionics	100
Rotors	227
Tires	59
AUW	15,955
AUW/OEW	0.76

Two values were not calculated using the DAPCA method, both propulsion systems and avionics are estimated using off-the-shelf parts.

[1] bls.gov

Table 11.3: *Engine Subsystems Cost*

Item	Cost (M$2025)
Avionics (Collins Pro Line Fusion®)	5,33 [2]
WE 3000	∼2.1
Wright electric Motor	3-6
Batteries	0.13

The propulsion system was then calculated to be (using a value of $3 million for the electric motor) 2· *WE 3000 Cost* + 2· *Wright Motor Cost* + *Batteries Cost* = *10.3 M$2025*

With these values on hand, the RDT&E and flyway cost come from following DAPCA IV statistical equations resulting in the following table. A production quantity of twenty aircraft in five years was assumed, or a production rate of one aircraft every three months. This assumption is sensible since that is approximately the time it requires to produce one CL-415[3].

Table 11.4: *Total RDT&E and Production Costs (Rounded)*

Parameter	Value (hr)	Wrap rate ($2012)	Cost ($2012)	Cost ($2025)
Engineering Hours	1,821,000	115.00	209,483,000	262,063,000
Tooling Hours	1,193,000	118.00	140,780,000	176,115,000
Manufacturing Hours	1,852,000	108.00	200,000,000	333,600,000
Quality Control Hours	246,000	98.00	24,137,000	40,261,000
Development Support Cost	-	-	30,495,000	50,866,000
Flight Test Cost	-	-	8,344,000	13,918,000
Manufacturing Materials Cost	-	-	69,393,000	115,748,000
Engine Costs	-	-	-	206,960,000
Avionics Costs	-	-	-	5,325,000
Non-recurring Costs	-	-	-	502,963,000
Recurring Costs	-	-	-	701,894,000
RDT&E + Production costs	-	-	-	1,204,856,000

In Table 11.4, the non-recurring costs refer to engineering hours, tooling hours, development support cost and flight test cost, the rest is recurring costs.

11.1.3. Cost per Unit

To estimate a cost per unit, the learning curve shall be looked into. When producing an aircraft, an improvement in production time can be observed. According to the amount of time and money invested in designing production facilities and flows, this can have a massive impact on manufacturing hours as seen in Figure 11.2. A conservative 90% learning curve percentage was chosen because the current aircraft is unlikely to be produced in large quantities or in a dedicated, custom-built factory as it is a conventional design, aside from its hybrid propulsion system.

[2] skiesmag.com, Avionics Cost
[3] globalmilitary.net

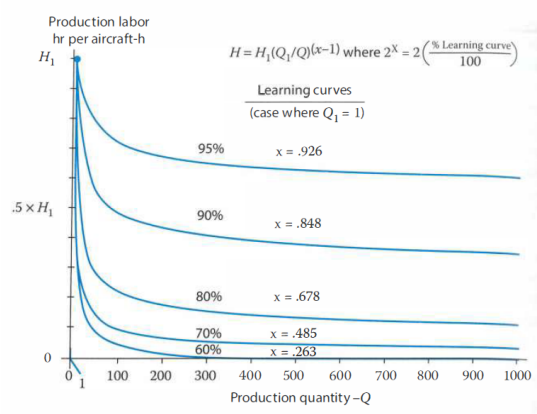

Figure 11.2: *Production Learning Curve*

Finally, recurring costs and non recurring costs, were inputted to calculate estimated costs per unit , as can be seen from Figure 11.3 the values become asymptotic above 20 M$2025 (22.9 M$2025, at 2500 units) when production achieve maximum efficiency from the learning curve and where non-recurring costs are reduced to negligible numbers.

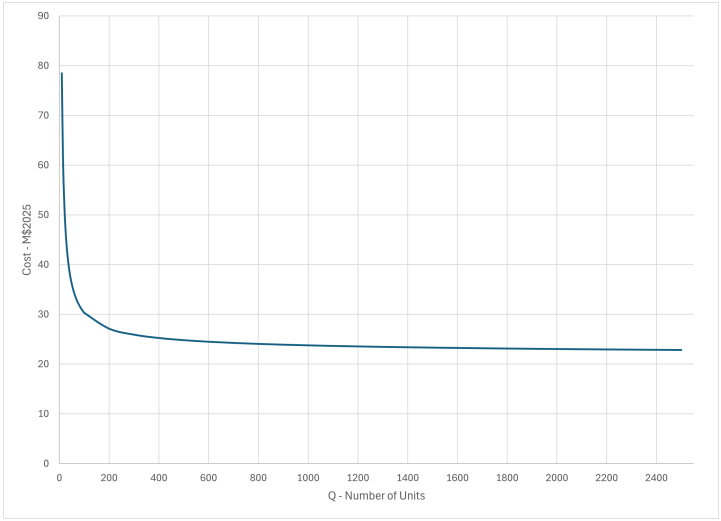

Figure 11.3: *Cost per Unit Produced*

11.1.4. Sensitivity

The cost per unit at 2500 units from the previous section can be used to measure the sensitivity of the cost analysis according to different actions that could prove to be changing.

Table 11.5: *Cost analysis sensitivity analysis*

Action	Cost Difference
Increasing OEW by 20%	10.8% increase
no DAPCA overestimation fudge factor	0.1% increase
Half production rate: 2 aircraft/yr	11.2% increase

This shows a relatively robust method for cost analysis with the final values, as the cost behaves predictably with relation to changes in its inputs with little changes.

11.1.5. Margins

Finally it is needed to look at margins. As seen in Table 11.3, the Wright electric motor has a $3-6 million range. Furthermore, fudge factors in Table 11.1 are also part of ranges, especially carbon fibre, which is said to have a 1.1-1.8 range according to Raymer. Add to that the uncertainty of designing for hybrid-electric engine, this led to a margin analysis, where very optimistic and very conservative values were chosen, it resulted in a conservative **20% margin** to be taken when looking at the RDT&E and production costs.

11.2. Return On Investment

Return on Investment (ROI), refers to the ratio between the net profit earned from the aircraft program and the total costs invested in its development and production—including RDT&E, tooling, certification, and manufacturing.

The following section first defines a number of unit to be made and makes use of the ROI and corresponding break-even point to find a reliable market price for the W-132, around $50 million. Finally, it explores the idea of a possible EU investment opportunity that would reduce cost as much as $1 million per unit.

11.2.1. Projected Production Size

As shown in the market analysis in **SECTION**,Europe and the European Union, through its RescEU initiative, are expected to be the first buyers of the W-132 aircraft. As a strategic investment in strengthening aerial firefighting capacity across member states, RescEU would likely acquire around five units out of the initial batch of 20 aircraft scheduled for delivery by 2035. Beyond RescEU, the W-132 presents strong market potential for both public agencies and private operators seeking to modernize their aerial firefighting fleets, particularly as many are still relying on the ageing cl-415, which is becoming increasingly costly and inefficient to maintain.

The remaining 15 aircraft from the initial production run could be delivered to a mix of private firefighting companies operating globally, or to national and regional authorities in fire-prone areas such as Southern Europe, the United States, and parts of Australia or South America. In addition, a second production phase aims to deliver 20 more units by 2040, further supporting the replacement of legacy fleets and contributing to a more resilient global aerial firefighting capacity. This phased rollout allows the manufacturer to gradually scale up production while adapting to feedback from early users.

11.2.2. Price per Unit and ROI

An expected 40 units makes for a cost per unit of 38,922,934 $2025 exactly. Different mark-up factors are explored, keeping under the requirement and looking at the best ROI while keeping a reasonable enough value such that the W-132 would still be interesting to buy in comparison to its competitors. This shows that a markup of 30% would be best, resulting in a market price of 50,600,000 $2025, which is compliant with REQ-SYS-2. This analysis is shown in Table 11.6

Table 11.6: *Price analysis*

Mark-up	Cost ($2025)	Price ($2025)	Break Even Point (units)
10%	38,922,000	42,815,000	39
20%	38,922,000	46,707,000	29
30%	38,922,000	50,600,000	23
40%	38,922,000	54,492,000	19

In Figure 11.4, the return on investment profile of the 30% mark-up can be seen. At a rate of production of one aircraft per six months, after ten years and forty aircraft built, a 20% profit can be observed.

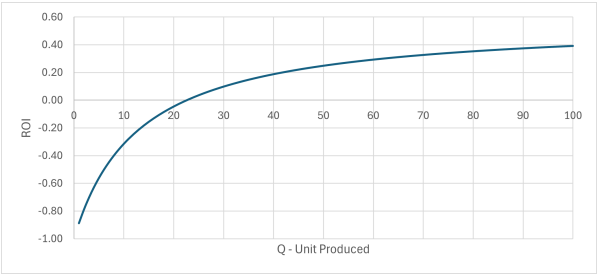

Figure 11.4: *ROI for 30% Markup*

11.2.3. European Funding Opportunity

The European Union has a strong strategic interest in boosting its wildfire response capabilities, especially as climate change increases the frequency and severity of such events across the continent. Contributing 10% of the RDT&E costs for a hybrid-electric turboshaft firefighting aircraft would align well with existing EU priorities. Programs like the European Defence Fund (EDF) or RescEU already support collaborative projects in aerospace and dual-use technologies, including efforts focused on energy resilience and environmental transition. At the same time, the EU is heavily investing in green aviation through initiatives like Clean Aviation under Horizon Europe, which specifically funds hybrid-electric and hydrogen-powered aircraft, indicating both a financial and strategic interest in sustainable aerospace.

This level of EU support could serve as essential funding for the design phases. In line with past EU practices, such as co-financing other such projects, this approach would reduce development risk, support European autonomy in a key area, and contribute to various climate goals, making the proposed 10% investment both reasonable and aligned with long-term EU objectives. Thus, a way to measure the impact of such an investment opportunity is to make use of the *European funding fudge factor* mentioned earlier in Table 11.1. Putting it to 0.9, results in a decrease of more than $50 millions in RDT&E costs and a $1 million dollar decrease in the cost per unit. A non-negligible advantage in the competitive world of firefighting aircraft manufacturing.

11.3. Operation and Maintenance Costs

The following direct operation and maintenance costs found in Table 11.7 were calculated using Raymer unless, stated otherwise. Values for euros-to-dollar conversion and jet fuel A price for Netherlands were extracted on the 18/06/2025. All dollars are in $2025.

Table 11.7: *Operation and Maintenance Costs*

Parameter	**Min**	**Max**
Flight Hours (h/yr)	300	500
Fuel (kg/h)	-	777
Jet Fuel A ($/h)	-	1150.26
Maintenance hours (MMH/FH)	20	40
Maintenance Technician (€/hr) [92]	195	255
Maintenance Cost ($/FH)	4,485	11,730
Material Maintenance ($/FH)	-	920
Crew Salary , 2 people ($/FH)	-	624
Insurances ($/FH)	143	865
DOC ($/FH)	7,323	15,290
DOC ($/yr)	2,196,000	7,645,000

12

Future Development

This chapter focuses on the subsequent steps required after the preliminary design of Waffle-132, which are clearly visualized through a Development Logic Diagram and a Future Gantt Chart, as well as a manufacturing, assembly and integration plan.

12.1. Project Design and Development Logic

As can be seen in Figure 12.1, the Development Logic Diagram is divided in five phases (Phase VI to Phase X) following the previous five phases performed since the beginning of the DSE. These follow from the detail design to the end-life of the aircraft.

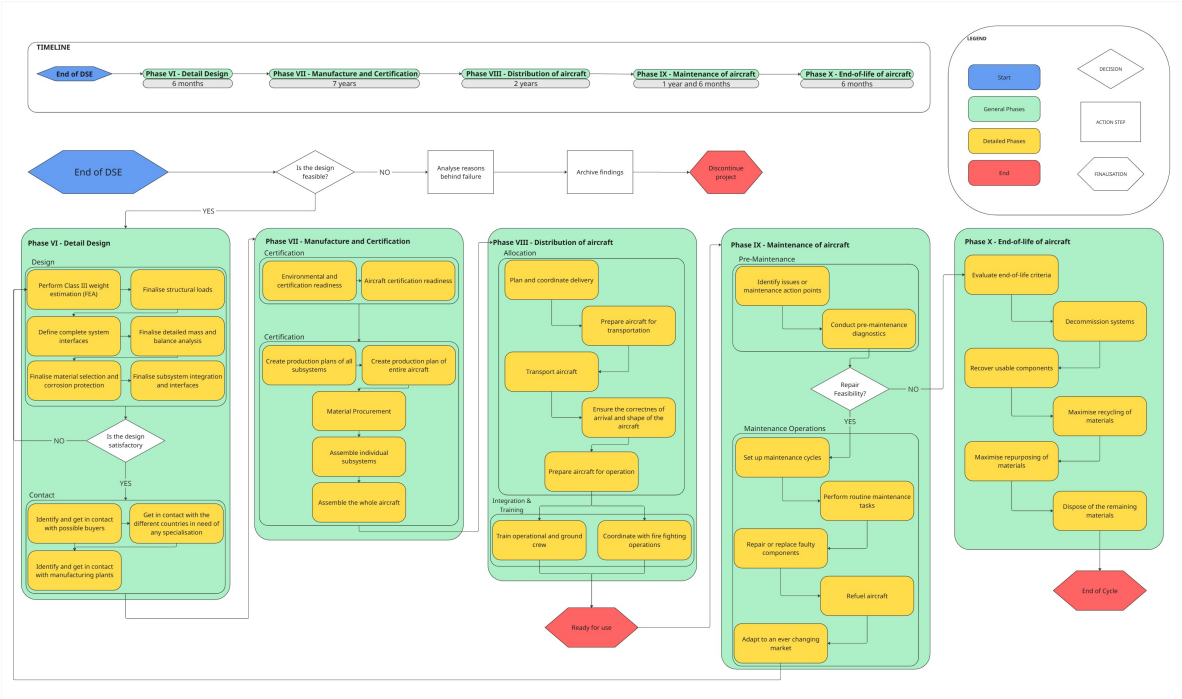

Figure 12.1: *Project Design and Development Logic*

12.2. Post-DSE Project Gantt Chart

In the same way as for the Development Logic Diagram, the next steps are divided in five phases. However, the essence of the Gantt Chart is to focus on end and start dates, as well as the total timeline of how the entire aircraft design process will unfold if it were to be manufactured and sent into service. As can be seen in Figure 12.2, it also captures part of the process that is essential, such as the certification or the maintenance of such aircraft.

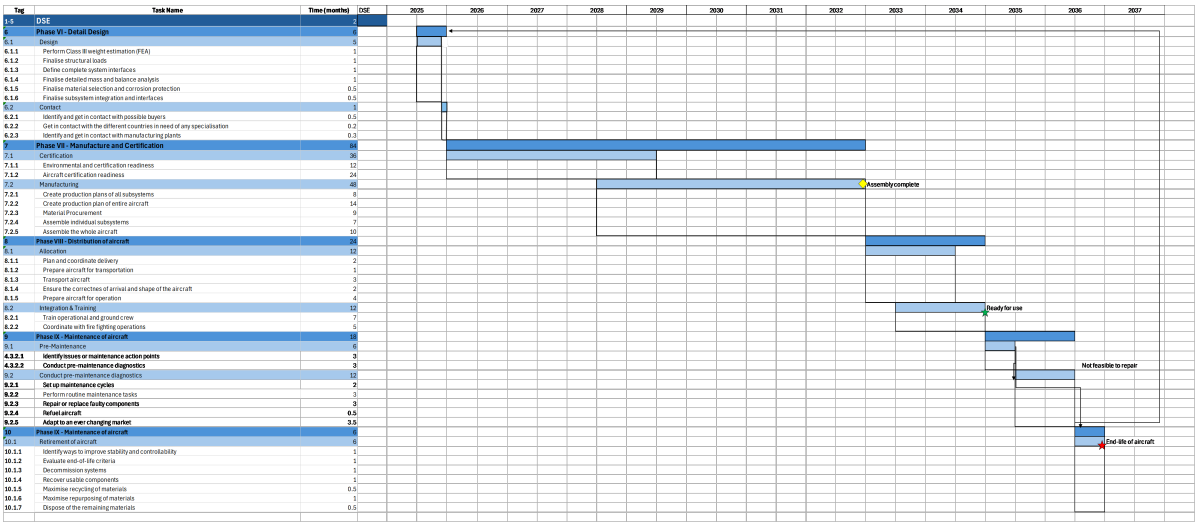

Figure 12.2: *Post-DSE Gantt Chart*

12.3. Manufacturing, Assembly, Integration Plan

This section builds upon Phase VII of Section 12.1, detailing further the different steps, and aspects to consider for the manufacturing, assembly and integration of the W-132. Considering the market for this aircraft, a small production run should be considered for the W-132. The manufacturing and assembly of the W-132 can therefore be benchmarked against that of aircraft such as the CL-415, of which a total of 95 units have been produced to date. This provides a reference point for the production volume of the W-132, which, although initially designed for the European market, could also be deployed in other regions worldwide.

Considering the scope of this report, only the main elements of the manufacturing, assembly and integration plan will be shown, without diving deep in the procedures and requirements for each of these aspects.

Design for manufacturing, assembly, and maintenance was considered throughout the current design phase, but will require further refinement in future iterations. This is essential to reduce long-term production costs, assembly complexity and simplify the in-service maintenance. An example of decisions taken with manufacturing in mind, is the spar thickness size which was set to not go below a certain value.

Subsection 12.3.1 presents the manufacturing plan, analysing potential production facilities, and the manufacturing techniques applicable to the various components. In Subsection 12.3.2 the plan for integrating all the different components and subsystems is presented. The critical aspects to consider during the assembly is the proper sequencing of the assembly of the different aircraft parts and systems. The next steps following the assembly are also shown there.

12.3.1. Manufacturing

The strategy to manufacturing is mostly driven by the low production volume of the aircraft. Hence, the manufacturing approach should be focused on being flexible, with low-rate production methods minimizing cost while still meeting the aerospace quality and certification compliance.

A similar production facility could be built, with a similar functioning to the assembly line of the CL-415, built in the Viking Air facilities [93]. The most important aspect is that the aircraft shall not entirely be manufactured in one single place. Taking advantage of the dense European network of roads, rail lines, and airports, the assemblies could be located in places where the expertise is the

highest, or in places where raw materials are present. This allows for more time and cost efficient manufacturing of the aircraft. Due to the low production volume of the aircraft, some subsystems could be delegated to external companies, such that no large investment would be required for some parts of the aircraft requiring very specific technologies. Collaboration could be done with other aircraft manufacturers to take advantage of their facilities. The fuselage or wing, made with composites could take advantage of the existing materials from Airbus's facilities. The engine could be bought from external companies like Rolls-Royce, which could be manufacturing both the batteries as well as the engine, and its propellers.

12.3.2. Assembly Planning

Figure 12.3 shows the chronological order of the assembly. There, the big assemblies like the wing, fuselage and empennage are assembled separately from each other. Whenever assembling these subparts, priority should be given to get the structural parts of the assemblies or the aircraft done first. Adding subsystem to the wing when the whole wing box is not yet finished could result in the failure of the whole assembly.

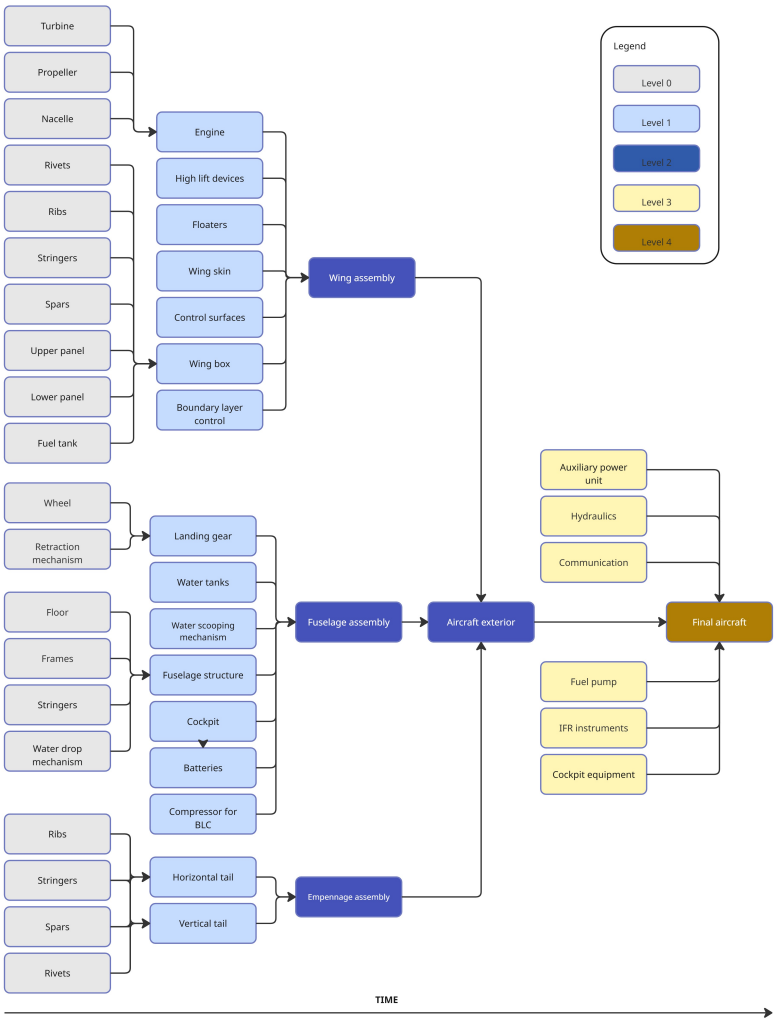

Figure 12.3: *Assembly Chronological Planning*

13

Conclusion

This report aimed to detail the design of an optimised wildfire-fighting aircraft and assess its feasibility. This was done by first determining the driving requirements through the analysis of a complete functional breakdown. These were then explored more in depth through a market analysis, an operations and logistics analysis and a sustainability study.

An extensive design of the aircraft was then performed by taking into account all of these requirements with particular focus on the design of the propulsion system, wing, empennage and fuselage. This led to the creation of a non-pressurised carbon fibre composite based aircraft utilising electrical hybrid engines to aid in high load manoeuvres, an after-body empennage for stability as well as a boundary layer control system to increase the performance of the wings. This produced a design with the following notable parameters :

Table 13.1: *W-132 Performance parameters*

Parameter	Value	Unit	Parameter	Value	Unit
Maximum take-off weight	39780	kg	Mission range	688	km
Operational Empty Weight	20760	kg	Ferry range	2450	km
Payload weight	13200	L	Scooping Distance	1300	m
Cruise speed	741	km/h	Empty take-off distance	1300	m
Stall speed	120	km/h	Full take-off distance	1800	m

So as to ensure the correctness of the values and performance benchmarks of the aircraft, verification and validation of the system was then performed. This was conducted by performing verification of the design code and their method and by carrying out the validation of the design through the use of the numerical tools provided by the Colossus Grand Challenge and an optimised flight route simulation.

An in depth analysis of the aircraft subsystem logistics was implemented so as to analyse the equipment within the aircraft and its relations. This revealed the importance of the use of modern avionics to optimise mission success and reduce the likelihood of failure. Further analysing of these risks was then done to establish contingency plans and assess the reliability of the design. This culminated into an analysis of the cost of the aircraft to determine a coherent sell price of 50.6M$ for a break even point of 23 aircraft sold.

This entire process made evident that the design is not only feasible but also extremely competitive and could establish itself as the large firefighting aircraft industry benchmark. It is therefore urged to finalise the design, set up production and establish distribution to ensure timely market entry.

Bibliography

[1] Raymer, D. P., *Aircraft Design: A Conceptual Approach*, 6th ed., AIAA, Reston, VA, 2018.

[2] Cuenca, O., "EU announces 2024 firefighting fleet," https://www.airmedandrescue.com/latest/news/eu-announces-2024-firefighting-fleet, May 2024. Accessed: 2025-04-25.

[3] Chalabi, W., "The Vehicle Routing Problem for Aerial Firefighting," Msc thesis, Delft University of Technology, April 2023. URL http://repository.tudelft.nl/, defended publicly on 24 April 2023.

[4] Embraer, "C-390 Millennium," Tech. rep., ????

[5] McDonnell Douglas, ""MD-80 Series Airplane Characteristics for Airport Planning" ," 1989.

[6] Irkut Corporation, " "The Be-200 Multipurpose Amphibious Aircraft". ," 2008.

[7] Jackson, P., "Jane's all the World's Aircraft," *Jane's Publishing Group*, 2004, pp. 360–361.

[8] ShinMaywa, ""Performance of the State-of-the-Art US-2: US-2 Specifications"," 2005.

[9] Gabbert, B., "In Europe, balancing firefighting and war fighting," , 2022. URL https://wildfiretoday.com/in-europe-balancing-firefighting-and-war-fighting/.

[10] "Los Incendios Forestales en España," Tech. rep., Ministerio de Agricultura, Pesca y Alimentación, 2018. URL https://www.miteco.gob.es/content/dam/miteco/es/biodiversidad/temas/incendios-forestales/iiff_2018_tcm30-521614.pdf.

[11] "Les moyens aériens et terrestres," , 2025. URL https://www.securite-civile.interieur.gouv.fr/nous-connaitre/nos-missions/moyens-aeriens-et-terrestres.

[12] "Top 5 Firefighting Helicopters: Aerial Giants in Wildfire Suppression," , 2025. URL https://www.fairlifts.com/helicopter-services/firefighting/top-5-firefighting-helicopters-aerial-giants-in-wildfire-suppression/.

[13] "Specifications and Performance," https://firebossllc.com/specifications-and-performance/, 2025. Accessed June 18, 2025.

[14] Natural Earth, "Natural Earth Data," https://www.naturalearthdata.com/, 2025. Accessed June 18, 2025.

[15] OurAirports, "Airport Data," https://ourairports.com/data/, 2025. Accessed June 18, 2025.

[16] Ministerio para la Transición Ecológica y el Reto Demográfico, G. d. E., "Los medios aéreos de extinción de incendios forestales," , 2025.

[17] European Commission, Joint Research Centre (JRC), "Copernicus Emergency Management Service: Fire Risk Viewer," , 2025. URL https://forest-fire.emergency.copernicus.eu/apps/fire.risk.viewer/, accessed: 2025-05-21.

[18] European Commission, Joint Research Centre (European Forest Fire Information System), "EFFIS Wildfire Risk Data," GeoTIFF/CSV, accessed via EFFIS Wildfire Risk Viewer, 2025. URL https://effis.jrc.ec.europa.eu, archived dataset from EFFIS as component of Copernicus Emergency Management Service.

[19] pas Sorcier, C., "Comment éviter les feux de forêts ?" , 2023. URL https://youtu.be/_5l4r1EHc2w, accessed: 2025-05-19.

[20] WinAir, "Everything that You Need to Know about the Canadair CL-415," , 2018. URL https://winair.ca/blog/everything-need-know-canadair-cl-415/, accessed: 2025-05-02.

[21] California Air Resources Board, "Detailed Analysis for Indirect Land Use Change," Tech. rep., California Air Resources Board, Sacramento, CA, 2014. URL http://www.arb.ca.gov/fuels/lcfs/lcfs.htm.

[22] Jeremy M. B. Smith and The Editors of Encyclopædia Britannica, "Temperate forest: Biological productivity," Encyclopædia Britannica Online, n.d. URL https://www.britannica.com/science/temperate-forest/Biological-productivity.

[23] National Airtanker Study Committee, "National Study of (Large) Airtankers to Support Initial Attack and

Large Fire Suppression: Final Report Phase 2," Tech. rep., USDA Forest Service and U.S. Department of the Interior, Washington, DC, November 1996.

[24] Raymer, D., *Aircraft Design: A Conceptual Approach, Sixth Edition*, 2018. doi:10.2514/4.104909.

[25] Roskam, J., *Airplane Design. Part V: Component Weight Estimation*, DARcorporation, 1985.

[26] Roskam, J., *Airplane Design. Part III: Layout Design of Cockpit, Fuselage, Wing and Empennage*, DARcorporation, 1986.

[27] Roskam, J., *Airplane Design. Part IV: Layout Design of Landing Gear and Systems*, DARcorporation, 1986.

[28] Shawon, M. H., Chao, H., Rhudy, M., Johansen, T. A., Tian, P., Flanagan, H. P., and Goyer, J., "Vertical Wind Velocity Estimation during UAS Fire Plume Encounters," *AIAA Science and Technology Forum and Exposition (SciTech) 2025*, American Institute of Aeronautics and Astronautics (AIAA), Orlando, FL, USA, 2025. doi:10.2514/6.2025-1624, presented Jan 6–10, 2025.

[29] Desai, A., Heilman, W. E., Skowronski, N. S., and Banerjee, T., "Features of turbulence during wildland fires in forested and grassland environments," *Agricultural and Forest Meteorology*, Vol. 338, 2023, p. 109501. doi:10.1016/j.agrformet.2023.109501.

[30] Avincis, "Canadair CL-415 Specifications Flyer," Technical flyer, Avincis, November 2024. URL https://www.avincis.com/wp-content/uploads/2024/11/A4-CL-415-Specifications-Flyer-Low-Res.pdf, low-resolution PDF from Avincis website.

[31] Rokhsaz, K., Kliment, L. K., and Nelson, J. A., "Flight Loads Analysis of CL-415 Scoopers," *AIAA Aviation 2022 Forum*, 2022. doi:10.2514/6.2022-4015, flight data from a fleet of four CL-415 aircraft recorded between 2015 and 2019, analyzed to develop flight loads spectra.

[32] Khan, M. H., Tucci, V., Lamberti, P., Longo, R., and Guadagno, L., "Lithium-Based Batteries in Aircraft," *Engineering Proceedings*, Vol. 90, No. 1, 2025. doi:10.3390/engproc2025090039, URL https://www.mdpi.com/2673-4591/90/1/39.

[33] Wright Electric, "Motor," , 2023. URL https://www.weflywright.com/motor.

[34] Federal Aviation Agency (FAA), "TYPE CERTIFICATE DATA SHEET NO. E00008CH," Tech. Rep. E00008CH_Rev_5, DEPARTMENT OF TRANSPORTATION FEDERAL AVIATION ADMINISTRATION, aug 2018. Revision 5.

[35] Finger, D. F., Braun, C., and Bil, C., "An initial sizing methodology for hybrid-electric light aircraft," *2018 Aviation Technology, Integration, and Operations Conference*, 2018, p. 4229.

[36] De Vries, R., Brown, M., and Vos, R., "Preliminary sizing method for hybrid-electric distributed-propulsion aircraft," *Journal of Aircraft*, Vol. 56, American Institute of Aeronautics and Astronautics Inc., 2019, pp. 2172–2188. doi:10.2514/1.C035388.

[37] European Aviation Safety Agency, "Type-Certificate Data Sheet: Pratt Whitney Canada PW150 series," Tech. Rep. EASA.(IM).E.049, European Aviation Safety Agency (EASA), ????

[38] Fintech.Aero, "PW150 Engine Values," , 2023.

[39] HeliHub.com, "Rolls-Royce Awarded $26M Contract for 12 AE1107C Engines," *HeliHub.com*, 2021. URL https://www.helihub.com/2021/04/08/rolls-royce-awarded-26m-contract-for-12-ae1107c-engines/.

[40] International Civil Aviation Organization (ICAO), "ICAO Environmental Report 2016," Tech. rep., International Civil Aviation Organization, Montreal, Canada, 2016. URL https://www.icao.int/environmental-protection/Documents/ICAO%20Environmental%20Report%202016.pdf.

[41] European Union Aviation Safety Agency, "Study on the Societal Benefits of Electric Aviation," https://www.easa.europa.eu/en/downloads/135219/en, 2021. Accessed: 2025-06-16.

[42] European Union Aviation Safety Agency (EASA), and Pratt & Whitney Canada, "Type-Certificate Data Sheet No. IM.E.041 for Engine PW100 Series Engines," Tech. Rep. IM.E.041, European Union Aviation Safety Agency, dec 2023. URL file://./EASA.IM_.E.041_TCDS_Issue_7.pdf, issue 07.

[43] Gudmundsson, S., *General Aviation Aircraft Design Applie Methods and Procedures*, Butterworth-Heinermann, 2022.

[44] Bojdo, N., and Filippone, A., "A comparative study of helicopter engine air particle separation technologies," *38th European Rotorcraft Forum 2012, ERF 2012*, Vol. 2, 2012, pp. 1276–1289.

[45] European Union Aviation Safety Agency (EASA), "Type-Certificate Data Sheet: IM.E.017 for Pratt and Whitney Canada Corp. PW206 PW207 Series Engines," Tech. Rep. IM.E.017, Issue 08, European Union Aviation Safety Agency, Cologne, Germany, aug 2022. URL https://www.easa.europa.eu/downloads/7769/en.

[46] Pratt Whitney, "Certified Pre-Owned," https://www.prattwhitney.com/en/services/pwc-engine-services/technical-engineering/certified-pre-owned, 2024. Accessed: 16 June 2025.

[47] Brelje, B. J., and Martins, J. R. R. A., "Electric, hybrid, and turboelectric fixed-wing aircraft: A review of concepts, models, and design approaches," *Progress in Aerospace Sciences*, Vol. 104, 2018, pp. 1–19. doi:10.1016/j.paerosci.2018.06.004.

[48] Friedrich, C., and Robertson, P. A., "Hybrid-electric propulsion for aircraft," *Journal of Aircraft*, Vol. 52, No. 1, 2015, pp. 176–189. doi:10.2514/1.C032613.

[49] Kim, H. D., Brown, G. V., and Felder, J. L., "Distributed turboelectric propulsion for hybrid wing body aircraft," Tech. Rep. NASA/TM-2008-215234, NASA, 2008. URL https://ntrs.nasa.gov/api/citations/20080045140/downloads/20080045140.pdf.

[50] Gohardani, A. S., Doulgeris, G., and Singh, R., "Challenges of future aircraft propulsion: A review of distributed propulsion technology and its potential application for the all electric commercial aircraft," *Progress in Aerospace Sciences*, Vol. 47, No. 5, 2011, pp. 369–391. doi:10.1016/j.paerosci.2010.09.001.

[51] Roskam, J., *Airplane Design, Part III: Layout Design of Cockpit, Fuselage, Wing and Empennage: Cutaways and Inboard Profiles*, DARcorporation, 2002.

[52] ShinMaywa, "US-2 connects Sea, Air, and Land," , 2023. URL https://www.shinmaywa.co.jp/english/products/aircraft/amphibian/us2/.

[53] of Canada, D. H. A., "CL-415 Specifications," , 2024. URL https://dehavilland.com/viking/firefighting/specifications.

[54] A. Elham, G. L. R. A. C., F. Oliviero, "Aerospace Design System Engineering Elements," , 2024.

[55] ShinMaywa, "Performance of the State-of-the-Art US-2," , 2023. URL https://www.shinmaywa.co.jp/english/products/aircraft/amphibian/us2/capability.html.

[56] Roskam, J., *Airplane Design, Part II: Preliminary Configuration Design and Integration of the Propulsion System*, DARcorporation, 1997.

[57] Avincis, "CANADAIR CL-415 Specifications," https://www.avincis.com/wp-content/uploads/2024/11/A4-CL-415-Specifications-Flyer-Low-Res.pdf, 2023. Accessed: 2025-05-08.

[58] Ma J, Z. Y. W. Y. Z. K., Du H, "Experimental study on the flow control mechanism of blowing flap," *Sage Journals*, 2025.

[59] Scholz, D., "Definition and discussion of the intrinsic efficiency of winglets," *ResearchGate*, 2018.

[60] Chicken, S. H., "Conceptual Design Methodologies for Waterborne and Amphibious Aircraft," Phd thesis, Cranfield University, Cranfield, UK, 1999.

[61] Torenbeek, E., *Advanced Aircraft Design: Conceptual Design, Analysis and Optimization of Subsonic Civil Airplanes*, John Wiley & Sons, Chichester, UK, 2013.

[62] Megson, T., *Aircraft Structures for Engineering Students*, 7th ed., Butterworth-Heinemann, 2021.

[63] Airfoil Tools, "NACA 4412 Airfoil Details," http://airfoiltools.com/airfoil/details?airfoil=naca4412-il, n.d. Accessed: 2025-06-17.

[64] *Composite Materials Handbook, Volume 1: Polymer Matrix Composites - Guidelines for Characterization*

of Structural Materials, U.S. Department of Defense, 2002, Chap. 6.8.4, pp. 6–116–6–128. Section on Shear Properties. Conservative shear strength value estimated at 60 MPa.

[65] Inc., A. T., "Pilot's Operating Handbook and FAA Approved Airplane Flight Manual," Tech. rep., FAA, 2023. URL https://es.scribd.com/document/809539182/AirTractor-at-802-AFM?, accessed: 2025-06-16.

[66] Roskam, J., *Airplane Design, Part V: Component Weight Estimation*, DARcorporation, 2002.

[67] Spreeman, K. P., "DESIGN GUIDE FOR PITCH-UP EVALUATION AND INVESTIGATION AT HIGH SUBSONIC SPEEDS OF POSSIBLE LIMITATIONS DUE TO WING-ASPECT-RATIO VARIATIONS," , 1961. URL https://ntrs.nasa.gov/api/citations/19630003100/downloads/19630003100.pdf.

[68] et al., P. B., "Empannage Statistics and Sizing Methods for Dorsal Fins," , 2013. URL https://www.fzt.haw-hamburg.de/pers/Scholz/Aero/AERO_TN_TailSizing_13-04-15.pdf.

[69] Skybrary, "Hypoxia (OGHFA BN)," , 2021. URL https://skybrary.aero/articles/hypoxia-oghfa-bn.

[70] Federal Aviation Administration, "Beware of Hypoxia," , 2015. URL https://www.faa.gov/pilots/training/airman_education/topics_of_interest/hypoxia.

[71] Zhou, J., Zhou, X., Cong, B., and Wang, W., "Convective heat transfer coefficient of steel member in localized fire condition," 2023. doi:10.6084/m9.figshare.22215712.v1, URL https://figshare.com/articles/conference_contribution/Convective_heat_transfer_coefficient_of_steel_member_in_localized_fire_condition/22215712.

[72] Lavanya, K. V., Venkatesh, and Kashinath, S. V. H., "Experimental Investigation of the Fatigue Behavior of Fiber-Reinforced Composites under Cyclic Loading Conditions," *International Journal for Research in Applied Science and Engineering Technology (IJRASET)*, Vol. 12, No. 6, 2024. doi:10.22214/ijraset.2024.65482, URL https://doi.org/10.22214/ijraset.2024.65482.

[73] Mazlan, S., Yidris, N., Koloor, S. S. R., and Petrů, M., "Experimental and Numerical Analysis of Fatigue Life of Aluminum Al 2024-T351 at Elevated Temperature," *Metals*, Vol. 10, No. 12, 2020. doi:10.3390/met10121581, URL https://www.mdpi.com/2075-4701/10/12/1581.

[74] Ma, Y., Yan, J., and Elham, A., "Initial weight estimation of twin-fuselage configuration in aircraft conceptual design," *Proceedings of the Institution of Mechanical Engineers Part G Journal of Aerospace Engineering*, Vol. 237, 2022. doi:10.1177/09544100221095370.

[75] Wrigley, S., "Hard Landing Within Limits," , 2020. URL https://fearoflanding.com/accidents/accident-reports/hard-landing-within-limits/.

[76] Hu, X., and Liu, S., "Numerical Investigation of Wave Slamming of Flat Bottom Body during Water Entry Process," *Mathematical Problems in Engineering*, Vol. 2014, No. 1, 2014, p. 821689. doi:https://doi.org/10.1155/2014/821689, URL https://onlinelibrary.wiley.com/doi/abs/10.1155/2014/821689.

[77] NEXCOMB, "Why Should You Choose Aluminium Honeycomb Panels over Solid Aluminium Panels?" , 2024. URL https://nexcomb.com/why-should-you-choose-aluminium-honeycomb-panels-over-aluminium-panels.

[78] OpenStax, "University Physics I: Mechanics, Sound, Oscillations and Waves," 2023. doi:10.6084/m9.figshare.22215712.v1, URL https://phys.libretexts.org/Bookshelves/University_Physics/University_Physics_%28OpenStax%29/Book%3A_University_Physics_I_-_Mechanics_Sound_Oscillations_and_Waves_%28OpenStax%29/14%3A_Fluid_Mechanics/14.03%3A_Fluids_Density_and_Pressure_%28Part_2%29.

[79] ZIMMERMAN, M., and KRUITHOFF, D. M., "Aerial fire suppression system," , 2018. URL https://patents.google.com/patent/WO2018030999A1/en.

[80] Gleim Aviation, "FAR/AIM: Subpart B—Flight Operations," , 2025. URL https://www.gleim.com/aviation/faraim/index.php?fullTextNum=135B&srsltid=AfmBOop8cI8ieIZsHyYp8c-WmGKIIzpf1jPepFdscuW9jFC93k4IWuej, accessed June 13, 2025.

[81] Vos, R., and Hoogreef, M., "Landing Gear and Empennage Design," https://brightspace.tudelft.

nl, n.d. Lecture slides, Aerospace Design and Systems Engineering Elements I.

[82] Defence Research and Development Organisation (DRDO), "Technology Acquisition Compendium," , Sep. 2019. URL https://www.drdo.gov.in/drdo/sites/default/files/inline-files/TA_Compendium_New-23.09.2019.pdf, accessed: 2025-06-16.

[83] Janes Information Group, "Bombardier 415," https://janes.migavia.com/can/bombardier/bombardier-415.html, n.d. Accessed: 2025-05-02.

[84] Kliment, L. K., Rokhsaz, K., and Nelson, J., "Study of CL-415 Usage in Forest Service Operation," *AIAA AVIATION 2022 Forum*, 2022, p. 4014.

[85] Gubisch, M., "Analysis: Aircraft retirement wave poses challenges for recyclers," *FlightGlobal*, 2018. URL https://www.flightglobal.com/analysis/analysis-aircraft-retirement-wave-poses-challenges-for-recyclers/127188.article.

[86] Olloqui, C. I., Azoulay, E., Ruano, J. P., Zarraga, D. D., Comenge, M., García, N. N., Caron, S., Valle, M. C., Hasler, D. J., and Verstraete, S., "Optimized Wildfire Fighting Aircraft: DSE - Midterm Report," Tech. rep., Delft University of Technology, May 2025. Group 19, AE3200 Design Synthesis Exercise.

[87] Academy, H. A., "How to Become a Fire Helicopter Pilot," , n.d. URL https://blog.flyhaa.com/blog/how-to-become-a-fire-helicopter-pilot, accessed June 12, 2025.

[88] Rolls-Royce, "AE 1107C," , 2025. URL https://www.rolls-royce.com/products-and-services/defence/aerospace/transport-tanker-patrol-and-tactical/ae-1107c.aspx, accessed: 2025-06-16.

[89] Federal Aviation Administration, "AC 20-106: Aircraft Inspection for the General Aviation Aircraft Owner," , 1978. URL https://www.faa.gov/documentLibrary/media/Advisory_Circular/AC_20-106.pdf, accessed: 2025-06-16.

[90] Jet-Bed, "How Long Do Airplane Tires Last?" https://www.jet-bed.com/how-long-do-airplane-tires-last, Aug. 2024. Accessed: 2025-06-16.

[91] Viking Air Limited, "Manual Status List – CL-215/215T/415/415MP," , 2020. URL https://www.vikingair.com/sites/default/files/manual-status-list-_cl_aircrafts_sep-2020.pdf, accessed: 2025-06-16.

[92] HANGAR 901 Aircraft Maintenance GmbH, "Pricelist Aircraft Maintenance Services," , jan 2025. URL https://hangar901.aero/wp-content/uploads/2025/02/H901-PRICE-LIST-Issue-11_JAN-2025_H901.pdf, issue 11.

[93] Viking Air Limited, "Viking Air Limited Quality System & Company Profile," Company profile document (PDF), Dec. 2015. URL https://www.vikingair.com/sites/default/files/Company_Profile.pdf, revision date: December 2015; Sidney, British Columbia, Canada.

A

Appendix A

A.1. Functional Flow Diagram and Functional Breakdown Structure

Pre-Operation

FUN-5.4: Maximise recycling of materials
FUN-5.5: Maximise repurposing of materials

FUN-1: Design Aircraft

FUN-1.1: Define Mission and System Requirements
- FUN-1.1.1: Identify Stakeholder objectives — All
- FUN-1.1.2: Characterize operational environment — Design
- FUN-1.1.3: Specify payload and drop requirements — Payload
- FUN-1.1.4: Determine mobility and endurance requirements — Propulsion
- FUN-1.1.5: Establish autonomy and control level — Control operations
- FUN-1.1.6: Define safety and regulatory constraints — Safety & Certification

FUN-1.2: Generate Conceptual Designs
- FUN-1.2.1: Identify driver constraints — System
- FUN-1.2.2: Assess technological risks — All
- FUN-1.2.3: Define possible aircraft configurations — Design
- FUN-1.2.4: Evaluate Operational Compatibility — Operation
- FUN-1.2.5: Construct design option tree — All

FUN-1.3: Perform Trade off
- FUN-1.3.1: Define evaluation criteria — All
- FUN-1.3.2: Collect comparative data of all designs — Design
- FUN-1.3.3: Conduct qualitative and quantitative analysis — Design

FUN-1.4: Select Baseline Design Concept
- FUN-1.4.1: Review all conceptual design options` — Design
- FUN-1.4.2: Verify compliance with key mission requirements — System
- FUN-1.4.3: Discard options — System

FUN-1.5: Perform Preliminary Design
- FUN-1.5.1: Define major subsystems — System
- FUN-1.5.2:Develop initial geometry and layout — Design
- FUN-1.5.3: Perform Class I Weight estimation — System
- FUN-1.5.4: Perform Class II Weight estimation — System

Difference of OEW between Class I and II estimation <1%?
- YES → FUN-1.6: Develop Detailed Design
- NO → FUN-1.5.5: Perform changes in the design — System

FUN-1.6: Develop Detailed Design
- FUN-1.6.1: Finalize airframe and structural design — Structure
- FUN-1.6.2: Finalize propulsion and energy systems — Propulsion
- FUN-1.6.3: Finalize flight control and avionics — Control Operations
- FUN-1.6.4: Complete system design drawings — Design

FUN-1.7: Verify and Validate Design
- FUN-1.7.1: Perform unit tests — All
- FUN-1.7.2: Perform system tests — All
- FUN-1.7.3: Evaluate requirement coverage — All
- FUN-1.7.4: Perform sensitivity study — Simulation

Is verification successfull?
- NO → FUN-1.1: Define Mission and System Requirements
- YES → Is validation successfull?

Is validation successfull?
- NO → FUN-1.1: Define Mission and System Requirements
- YES → FUN-1.8: Review and Approve Final Design

FUN-2: Manufacture Aircraft

FUN-2.1: Procure Components and Materials
- FUN-2.1.1 : Identify Required Materials and Components — Materials
- FUN-2.1.2: Select Suppliers — Materials
- FUN-2.1.3 : Order Materials and Components — Materials
- FUN-2.1.4: Inspect Incoming Materials — Materials

FUN-2.2: Manufacture Aircraft Structures
- FUN-2.2.1 : Manufacture Propulsion System — Manufacturer
- FUN-2.2.2 : Manufacture Lift Providing System — Manufacturer
- FUN-2.2.3 : Manufacture Aircraft Fuselage Section — Manufacturer
- FUN-2.2.4: Manufacture Control Surfaces — Manufacturer
- FUN-2.2.5: Manufacture Landing Gear — Manufacturer
- FUN-2.2.6: Manufacture Wing-tip Floats — Manufacturer
- FUN-2.2.7: Manufacture Boundary Layer Control Device — Manufacturer
- FUN-2.2.8: Apply Surface Treatment On All Elements — Manufacturer

FUN-2.3: Assemble Aircraft
- FUN-2.3.1 : Join Wing, Aircraft Body, Propulsion System and Control Surfaces — Manufacturer
- FUN-2.3.2: Install Landing Gear Structures — Manufacturer
- FUN-2.3.3: Perform Structural Integrity Checks — Structure

FUN-2.4: Integrate Systems
- FUN-2.4.1 : Integrate Firefighting-specific Structural Modules — Manufacture
- FUN-2.4.2: Install Avionics and Flight Control Systems — Manufacture
- FUN-2.4.3: Integrate Control System for Payload Release (Pilot interface) — Manufacture
- FUN-2.4.4: Connect Environmental and Safety Monitoring Instruments — Manufacture

FUN-2.5: Perform Quality Inspections and Certification Tests
- FUN-2.5.1 : Perform Certification Tests — Certification
- FUN-2.5.2: Test the Firefighting System — System
- FUN-2.5.3 : Perform Functional Tests of Integrated System — System

Malfunctions found due to tests?
- YES → FUN-1.6: Prepare for Delivery
- NO → FUN-2.5: Perform Quality Inspections and Certification Tests

FUN-1.6: Prepare for Delivery
- FUN-2.6.1 : Paint Aircraft and Apply Markings — Manufacture
- FUN-2.6.2: Install Documentation Package and Labels — Manufacture

FUN-3: Distribute Aircraft

FUN-3.0: Allocation and Integration to use case
- FUN-3.1.1: Assign country-specific packages — Logistics
- FUN-3.1.2: Integrate aircraft into EU-level emergency response plans — Logistics

FUN-3.1: Plan and coordinate delivery
- FUN-3.1.1: Identify delivery mode and timeframes — Logistics
- FUN-3.1.2: Asses regulations — Logistics
- FUN-3.1.3: Select transport method — Logistics
- FUN-3.1.4: Schedule delivery timeline — Logistics

FUN-3.2: Prepare aircraft for transportation
- FUN-3.2.1: Determine aircraft configuration needs — Transport
- FUN-3.2.2: Isolate and secure systems — Transportation
- FUN-3.2.3: Protect aircraft surfaces — Transportation
- FUN-3.2.4: Package components — Transportation
- FUN-3.2.5: Load onto transport vehicle — Transportation

FUN-3.3: Transport aircraft
- FUN-3.3.1: Secure components during transit — Transportation
- FUN-3.3.2: Track shipment status — Logistics
- FUN-3.3.3:Confirm arrival at destination — Logistics

FUN-3.5: Train operational and ground crew
- FUN-3.5.1: Develop training program — Trainer
- FUN-3.5.2: Train flight crew — Trainer
- FUN-3.5.3: Train ground crew — Trainer
- FUN-3.5.4: Evaluate crew proficiency — Trainer

FUN-3.4: Prepare aircraft for operation
- FUN-3.4.1: Inspect aircraft upon arrival — Manufacture
- FUN-3.4.2: Reassemble dissasembled aircraft — Manufacture
- FUN-3.4.3: Conduct systems check — System
- FUN-3.4.4: Test flight systems — System

FUN-4: Operate aircraft

Legend
- Level 0
- Level 1
- Level 2
- Level 3
- Process timeline
- DECISION
- FUN-X.X.X: Function — Subsystem

FUN-3.5: Train operational and ground crew

Operation

FUN-4: Operate aircraft

FUN-4.1: Deploy aircraft

FUN-4.1.1 : Brief pilots and crew on fire mision — Trainer

FUN-4.1.2 : Check all systems work correctly — Ground

FUN-4.1.3 : Prepare the aircraft at the launch site — Ground

FUN-4.1.4 : Taxi to runway — Ground

FUN-4.1.5: Take-off — Aircraft

FUN-4.1.6: Maintain directional control on ground — Aircraft

FUN-4.1.7: Provide enough lift and thrust — Aircraft

FUN-4.1.8: Maintain stability and attitude control — Aircraft

Necessary flight conditions met?

YES

NO

FUN-1.5: Perform Preliminary Design

FUN-1.6: Develop Detailed Design

FUN-1.7: Verify and Validate Design

FUN-4.2: Manoeuvre aircraft

FUN-4.2.1: Execute entry manoeuvres — Pilot

FUN-4.2.2: Maintain aerial positioning — Pilot

FUN-4.2.3: Perform pre-drop alignment manoeuvres — Pilot

FUN-4.2.4: Initiate drop exit manoeuvres — Pilot

FUN-4.2.5: Perform low-altitude scooping manoeuvres — Pilot

FUN-4.2.6: Perform evasive & emergency manoeuvres — Pilot

FUN-4.2.7: Stabilise due to wind and smoke — Pilot

FUN-4.2.8: Coordinate with other aircraft — Pilot

FUN-4.2.9: Avoid terrain and obstacles — Pilot

FUN-4.3: Cruise

FUN-4.3.1: Monitor environmental and system conditions — System

FUN-4.3.2: Maintain situational awareness — System

FUN-4.3.3: Communicate with ground control — Communication

FUN-4.3.4: Communicate with other aircraft from the fleet — Communication

FUN-4.3.5: Communicate with satellite & UAV's — Communication

FUN-4.3.6: Optimise route and speed — Control Operations

FUN-4.3.7: Stabilise subsystems — System

FUN-4.4: Collect Water

FUN-4.4.1: Identify suitable water source — Pilot

FUN-4.4.2: Navigate to water source — Pilot

FUN-4.4.3: Assess wind, wave, and terrain conditions at water source — Pilot

Safe to scoop?

NO

YES

FUN-4.4.4: Position aircraft for water collection — Pilot

FUN-4.4.5: Deploy collection mechanism — Pilot

FUN-4.4.6: Fill water tank — System

FUN-4.4.7: Monitor water collection — System

Enough quantity?

NO

YES

FUN-4.4.8: Retract collection system — Pilot

FUN-4.4.9: Depart towards fire zone — Pilot

YES

FUN-4.5: Approach Fire

FUN-4.5.1: Confirm safe approach conditions — System

FUN-4.5.2: Assess terrain and fire propagation conditions — Operations

FUN-4.5.3: Assess airspace & environmental constraints — Operations

FUN-4.5.4: Generate optimal path to fire zone — Operartions

FUN-4.5.5: Detect & avoid enroute hazards — Operartions

FUN-4.5.6: Identify fire front and designate target area — Operartions

FUN-4.5.7: Communicate with mission control & allied ground or air assets — Pilot

FUN-4.5.8: Align aicraft with final drop position — Pilot

FUN-4.5.9: Validate safety parameters & authorise drop — Operartions

All steps confirmed to be correct?

NO

YES

FUN-4.6: Extinguish Fire

FUN-4.6.1: Assess Drop Conditions — Operartions

FUN-4.6.2: Confirm drop zone alignment — Pilot

FUN-4.6.3: Ensure final stabilation — Pilot

FUN-4.6.4: Calculate offset drop point — Operartions

FUN-4.6.5: Initiate payload release — Pilot

FUN-4.6.6: Monitor drop execution — Operartions

FUN-4.6.7: Execute post-drop exit manoeuvre — Pilot

Is all fire estinguished?

YES

NO

FUN-4.7: Perform Landing

FUN-4.7.1: Coordinate with Ground Operations — Communication

FUN-4.7.2: Configure Aircraft for Landing (firefighting-specific) — System

FUN-4.7.3: Perform Approach to Landing Site — Pilot

FUN-4.7.4: Land Aircraft Safely with Remaining Payload — Pilot

FUN-4.7.5: Taxi aircraft to hangar — Ground

FUN-4.7.6: Secure Aircraft Post-Landing — Ground

FUN-4.8: Perform aircraft maintenance

FUN-4.8.1: Identify issues or maintenance action points — Maintenance

FUN-4.8.2: Conduct pre-maintenance diagnostics — Maintenance

FUN-4.8.3: Perform routine maintenance tasks — Maintenance

FUN-4.8.4: Repair or replace faulty components — Maintenance

FUN-4.8.5: Refuel aircraft — Ground

Is the aircraft airworthy and ready for flight?

YES

NO

Post-Operation

FUN-5: Retire aircraft

FUN-5.1: Evaluate end-of-life criteria

FUN-5.1.1: Asses structurual integrity — Evaluation

FUN-5.1.2: Evaluate system performance — Evaluation

FUN-5.1.3: Analyse operational history — Evaluation

FUN-5.1.4: Review regulatory compliance — Evaluation

FUN-5.1.5: Evaluate potential for upgrade or extension — Evaluation

FUN-5.1.6: Asses environmental impact — Evaluation

FUN-5.1.7: Determine maintenance feasability — Evaluation

FUN-5.2: Decommission systems

FUN-5.2.1: Power down and isolate systems — Ground

FUN-5.2.2: Remove hazardous material — Ground

FUN-5.2.3: Disable propulsion and flight systems — Ground

FUN-5.2.4: Prepare systems for recovery, reuse or disposal — Ground

FUN-5.3: Recover usable components

FUN-5.3.1: Identify recoverable components — Evaluation

FUN-5.3.2: Disassemble and extract components — Ground

FUN-5.3.3: Clean, repair or refurbish components — Ground

FUN-5.3.4: Label and catalog components — Ground

FUN-5.3.5: Package components for storage/ transport — Ground

FUN-5.4: Maximise recycling of materials

FUN-5.4.1: Identify recyclable components — Ground

FUN-5.4.2: Dissasemble and extract components — Ground

FUN-5.4.3: Remove contamintants from components — Ground

FUN-5.4.4: Sort aircraft components by category — Ground

FUN-5.4.5: Process components for recycling — Ground

FUN-5.4.6: Send processed components to certified recyclers — Ground

FUN-5.5: Maximise repurposing of materials

FUN-5.5.1: Identify repurposable components — Ground

FUN-5.5.2: Evaluate alternate use cases — Ground

FUN-5.5.3: Modify or adapt components — Ground

FUN-5.5.4: Send modified components to new users — Logistics

FUN-5.6: Dispose of the remaining materials

FUN-5.6.1: Asses environmental risks — Ground

FUN-5.6.2: Select appropiate disposal method — Ground

FUN-5.6.3: Prepare components for disposal — Ground

FUN-5.6.4: Dispose components — Ground

FUN-5.6.5: Document disposal activities and impact — Documentation

FUN-2.2: Manufacture Aircraft Structures


FUN-1: Design aircraft
FUN-2: Manufacture aircraft
FUN-3: Distribute aircraft
FUN-4: Operate aircraft
FUN-5: Retire aircraft

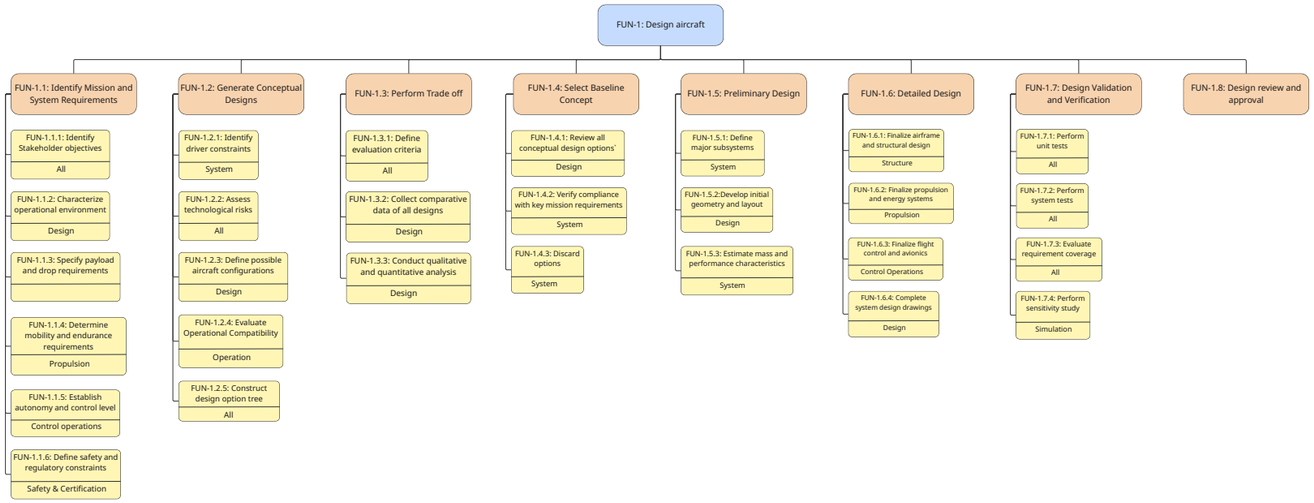
FUN-1: Design aircraft
FUN-1.1: Identify Mission and System Requirements
FUN-1.1.1: Identify Stakeholder objectives
All
FUN-1.1.2: Characterize operational environment
Design
FUN-1.1.3: Specify payload and drop requirements
FUN-1.1.4: Determine mobility and endurance requirements
Propulsion
FUN-1.1.5: Establish autonomy and control level
Control operations
FUN-1.1.6: Define safety and regulatory constraints
Safety & Certification
FUN-1.2: Generate Conceptual Designs
FUN-1.2.1: Identify driver constraints
System
FUN-1.2.2: Assess technological risks
All
FUN-1.2.3: Define possible aircraft configurations
Design
FUN-1.2.4: Evaluate Operational Compatibility
Operation
FUN-1.2.5: Construct design option tree
All
FUN-1.3: Perform Trade off
FUN-1.3.1: Define evaluation criteria
All
FUN-1.3.2: Collect comparative data of all designs
Design
FUN-1.3.3: Conduct qualitative and quantitative analysis
Design
FUN-1.4: Select Baseline Concept
FUN-1.4.1: Review all conceptual design options'
Design
FUN-1.4.2: Verify compliance with key mission requirements
System
FUN-1.4.3: Discard options
System
FUN-1.5: Preliminary Design
FUN-1.5.1: Define major subsystems
System
FUN-1.5.2:Develop initial geometry and layout
Design
FUN-1.5.3: Estimate mass and performance characteristics
System
FUN-1.6: Detailed Design
FUN-1.6.1: Finalize airframe and structural design
Structure
FUN-1.6.2: Finalize propulsion and energy systems
Propulsion
FUN-1.6.3: Finalize flight control and avionics
Control Operations
FUN-1.6.4: Complete system design drawings
Design
FUN-1.7: Design Validation and Verification
FUN-1.7.1: Perform unit tests
All
FUN-1.7.2: Perform system tests
All
FUN-1.7.3: Evaluate requirement coverage
All
FUN-1.7.4: Perform sensitivity study
Simulation
FUN-1.8: Design review and approval

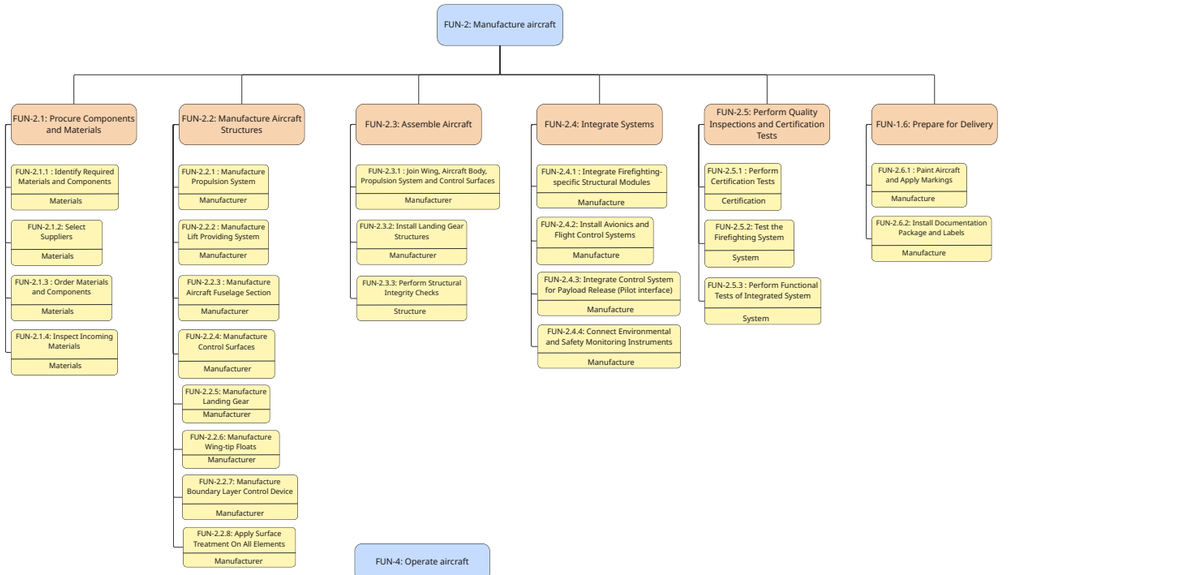
FUN-2: Manufacture aircraft
FUN-2.1: Procure Components and Materials
FUN-2.1.1 : Identify Required Materials and Components
Materials
FUN-2.1.2: Select Suppliers
Materials
FUN-2.1.3 : Order Materials and Components
Materials
FUN-2.1.4: Inspect Incoming Materials
Materials
FUN-2.2: Manufacture Aircraft Structures
FUN-2.2.1 : Manufacture Propulsion System
Manufacturer
FUN-2.2.2 : Manufacture Lift Providing System
Manufacturer
FUN-2.2.3 : Manufacture Aircraft Fuselage Section
Manufacturer
FUN-2.2.4: Manufacture Control Surfaces
Manufacturer
FUN-2.2.5: Manufacture Landing Gear
Manufacturer
FUN-2.2.6: Manufacture Wing-tip Floats
Manufacturer
FUN-2.2.7: Manufacture Boundary Layer Control Device
Manufacturer
FUN-2.2.8: Apply Surface Treatment On All Elements
Manufacturer
FUN-2.3: Assemble Aircraft
FUN-2.3.1 : Join Wing, Aircraft Body, Propulsion System and Control Surfaces
Manufacturer
FUN-2.3.2: Install Landing Gear Structures
Manufacturer
FUN-2.3.3: Perform Structural Integrity Checks
Structure
FUN-2.4: Integrate Systems
FUN-2.4.1 : Integrate Firefighting-specific Structural Modules
Manufacture
FUN-2.4.2: Install Avionics and Flight Control Systems
Manufacture
FUN-2.4.3: Integrate Control System for Payload Release (Pilot interface)
Manufacture
FUN-2.4.4: Connect Environmental and Safety Monitoring Instruments
Manufacture
FUN-2.5: Perform Quality Inspections and Certification Tests
FUN-2.5.1 : Perform Certification Tests
Certification
FUN-2.5.2: Test the Firefighting System
System
FUN-2.5.3 : Perform Functional Tests of Integrated System
System
FUN-1.6: Prepare for Delivery
FUN-2.6.1 : Paint Aircraft and Apply Markings
Manufacture
FUN-2.6.2: Install Documentation Package and Labels
Manufacture

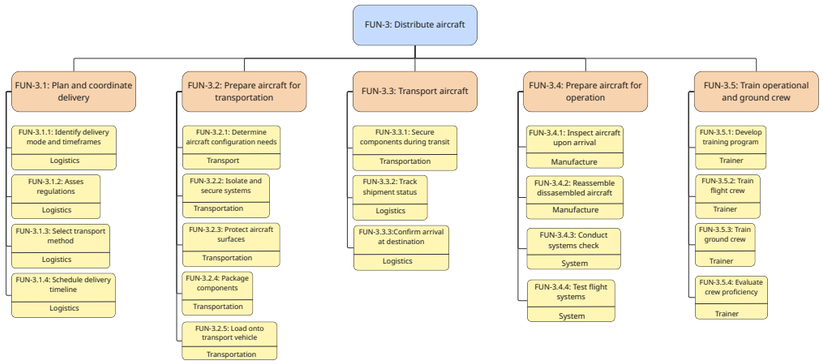
FUN-3: Distribute aircraft
FUN-3.1: Plan and coordinate delivery
FUN-3.1.1: Identify delivery mode and timeframes
Logistics
FUN-3.1.2: Asses regulations
Logistics
FUN-3.1.3: Select transport method
Logistics
FUN-3.1.4: Schedule delivery timeline
Logistics
FUN-3.2: Prepare aircraft for transportation
FUN-3.2.1: Determine aircraft configuration needs
Transport
FUN-3.2.2: Isolate and secure systems
Transportation
FUN-3.2.3: Protect aircraft surfaces
Transportation
FUN-3.2.4: Package components
Transportation
FUN-3.2.5: Load onto transport vehicle
Transportation
FUN-3.3: Transport aircraft
FUN-3.3.1: Secure components during transit
Transportation
FUN-3.3.2: Track shipment status
Logistics
FUN-3.3.3:Confirm arrival at destination
Logistics
FUN-3.4: Prepare aircraft for operation
FUN-3.4.1: Inspect aircraft upon arrival
Manufacture
FUN-3.4.2: Reassemble dissasembled aircraft
Manufacture
FUN-3.4.3: Conduct systems check
System
FUN-3.4.4: Test flight systems
System
FUN-3.5: Train operational and ground crew
FUN-3.5.1: Develop training program
Trainer
FUN-3.5.2: Train flight crew
Trainer
FUN-3.5.3: Train ground crew
Trainer
FUN-3.5.4: Evaluate crew proficiency
Trainer

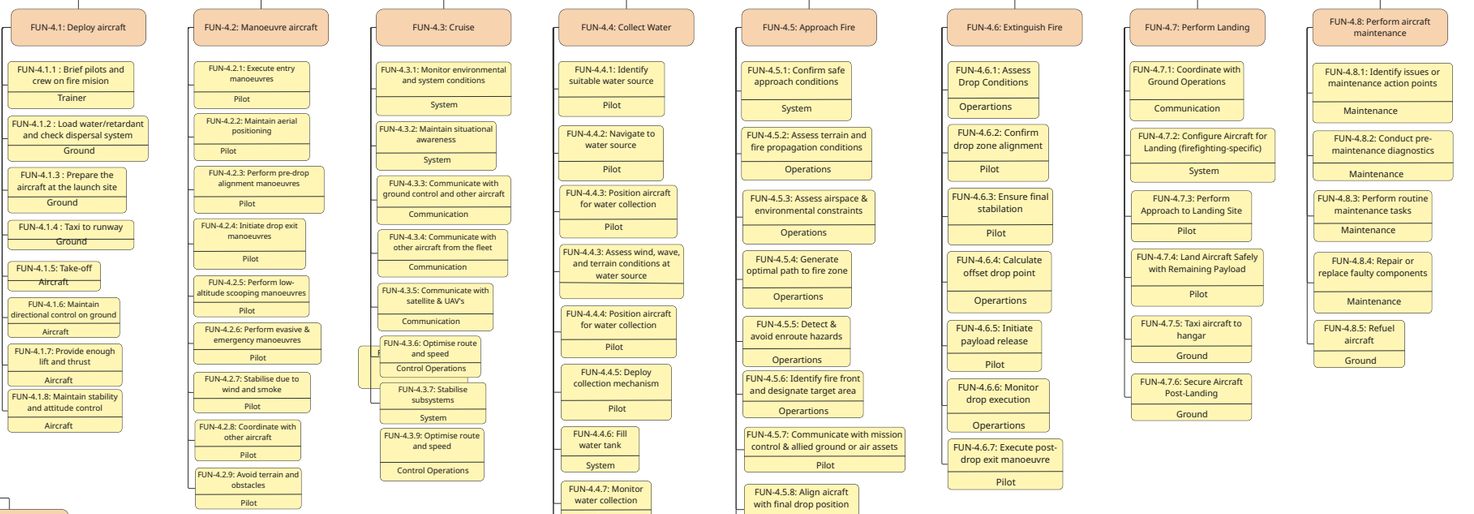
FUN-4: Operate aircraft
FUN-4.1: Deploy aircraft
FUN-4.1.1 : Brief pilots and crew on fire mision
Trainer
FUN-4.1.2 : Load water/retardant and check dispersal system
Ground
FUN-4.1.3 : Prepare the aircraft at the launch site
Ground
FUN-4.1.4 : Taxi to runway
Ground
FUN-4.1.5: Take-off
Aircraft
FUN-4.1.6: Maintain directional control on ground
Aircraft
FUN-4.1.7: Provide enough lift and thrust
Aircraft
FUN-4.1.8: Maintain stability and attitude control
Aircraft
FUN-4.2: Manoeuvre aircraft
FUN-4.2.1: Execute entry manoeuvres
Pilot
FUN-4.2.2: Maintain aerial positioning
Pilot
FUN-4.2.3: Perform pre-drop alignment manoeuvres
Pilot
FUN-4.2.4: Initiate drop exit manoeuvres
Pilot
FUN-4.2.5: Perform low-altitude scooping manoeuvres
Pilot
FUN-4.2.6: Perform evasive & emergency manoeuvres
Pilot
FUN-4.2.7: Stabilise due to wind and smoke
Pilot
FUN-4.2.8: Coordinate with other aircraft
Pilot
FUN-4.2.9: Avoid terrain and obstacles
Pilot
FUN-4.3: Cruise
FUN-4.3.1: Monitor environmental and system conditions
System
FUN-4.3.2: Maintain situational awareness
System
FUN-4.3.3: Communicate with ground control and other aircraft
Communication
FUN-4.3.4: Communicate with other aircraft from the fleet
Communication
FUN-4.3.5: Communicate with satellite & UAV's
Communication
FUN-4.3.6: Optimise route and speed
Control Operations
FUN-4.3.7: Stabilise subsystems
System
FUN-4.3.9: Optimise route and speed
Control Operations
FUN-4.4: Collect Water
FUN-4.4.1: Identify suitable water source
Pilot
FUN-4.4.2: Navigate to water source
Pilot
FUN-4.4.3: Position aircraft for water collection
Pilot
FUN-4.4.3: Assess wind, wave, and terrain conditions at water source
FUN-4.4.4: Position aircraft for water collection
Pilot
FUN-4.4.5: Deploy collection mechanism
Pilot
FUN-4.4.6: Fill water tank
System
FUN-4.4.7: Monitor water collection
System
FUN-4.4.8: Retract collection system
Pilot
FUN-4.4.9: Depart towards fire zone
Pilot
FUN-4.5: Approach Fire
FUN-4.5.1: Confirm safe approach conditions
System
FUN-4.5.2: Assess terrain and fire propagation conditions
Operations
FUN-4.5.3: Assess airspace & environmental constraints
Operations
FUN-4.5.4: Generate optimal path to fire zone
Operartions
FUN-4.5.5: Detect & avoid enroute hazards
Operartions
FUN-4.5.6: Identify fire front and designate target area
Operartions
FUN-4.5.7: Communicate with mission control & allied ground or air assets
Pilot
FUN-4.5.8: Align aicraft with final drop position
Pilot
FUN-4.5.9: Validate safety parameters & authorise drop
Operartions
FUN-4.6: Extinguish Fire
FUN-4.6.1: Assess Drop Conditions
Operartions
FUN-4.6.2: Confirm drop zone alignment
Pilot
FUN-4.6.3: Ensure final stabilation
Pilot
FUN-4.6.4: Calculate offset drop point
Operartions
FUN-4.6.5: Initiate payload release
Pilot
FUN-4.6.6: Monitor drop execution
Operartions
FUN-4.6.7: Execute post-drop exit manoeuvre
Pilot
FUN-4.7: Perform Landing
FUN-4.7.1: Coordinate with Ground Operations
Communication
FUN-4.7.2: Configure Aircraft for Landing (firefighting-specific)
System
FUN-4.7.3: Perform Approach to Landing Site
Pilot
FUN-4.7.4: Land Aircraft Safely with Remaining Payload
Pilot
FUN-4.7.5: Taxi aircraft to hangar
Ground
FUN-4.7.6: Secure Aircraft Post-Landing
Ground
FUN-4.8: Perform aircraft maintenance
FUN-4.8.1: Identify issues or maintenance action points
Maintenance
FUN-4.8.2: Conduct pre-maintenance diagnostics
Maintenance
FUN-4.8.3: Perform routine maintenance tasks
Maintenance
FUN-4.8.4: Repair or replace faulty components
Maintenance
FUN-4.8.5: Refuel aircraft
Ground

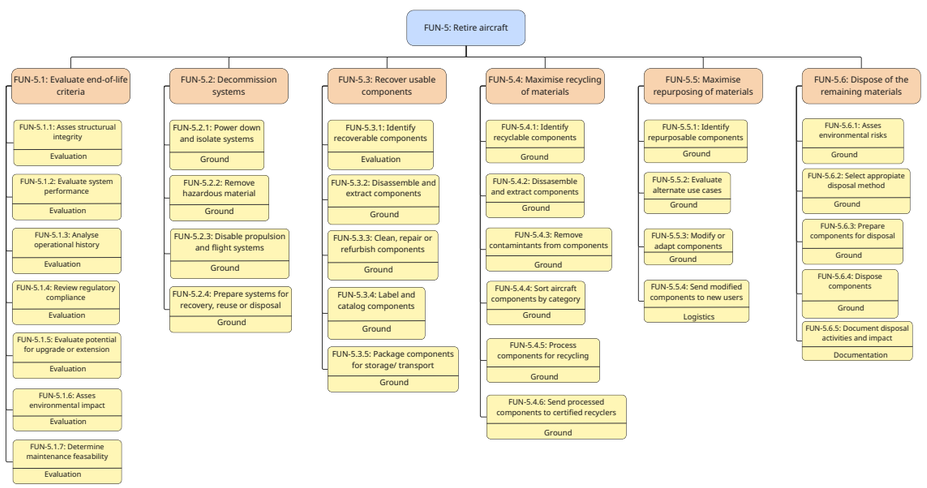
FUN-5: Retire aircraft
FUN-5.1: Evaluate end-of-life criteria
FUN-5.1.1: Asses structurual integrity
Evaluation
FUN-5.1.2: Evaluate system performance
Evaluation
FUN-5.1.3: Analyse operational history
Evaluation
FUN-5.1.4: Review regulatory compliance
Evaluation
FUN-5.1.5: Evaluate potential for upgrade or extension
Evaluation
FUN-5.1.6: Asses environmental impact
Evaluation
FUN-5.1.7: Determine maintenance feasability
Evaluation
FUN-5.2: Decommission systems
FUN-5.2.1: Power down and isolate systems
Ground
FUN-5.2.2: Remove hazardous material
Ground
FUN-5.2.3: Disable propulsion and flight systems
Ground
FUN-5.2.4: Prepare systems for recovery, reuse or disposal
Ground
FUN-5.3: Recover usable components
FUN-5.3.1: Identify recoverable components
Evaluation
FUN-5.3.2: Disassemble and extract components
Ground
FUN-5.3.3: Clean, repair or refurbish components
Ground
FUN-5.3.4: Label and catalog components
Ground
FUN-5.3.5: Package components for storage/ transport
Ground
FUN-5.4: Maximise recycling of materials
FUN-5.4.1: Identify recyclable components
Ground
FUN-5.4.2: Dissasemble and extract components
Ground
FUN-5.4.3: Remove contamintants from components
Ground
FUN-5.4.4: Sort aircraft components by category
Ground
FUN-5.4.5: Process components for recycling
Ground
FUN-5.4.6: Send processed components to certified recyclers
Ground
FUN-5.5: Maximise repurposing of materials
FUN-5.5.1: Identify repurposable components
Ground
FUN-5.5.2: Evaluate alternate use cases
Ground
FUN-5.5.3: Modify or adapt components
Ground
FUN-5.5.4: Send modified components to new users
Logistics
FUN-5.6: Dispose of the remaining materials
FUN-5.6.1: Asses environmental risks
Ground
FUN-5.6.2: Select appropiate disposal method
Ground
FUN-5.6.3: Prepare components for disposal
Ground
FUN-5.6.4: Dispose components
Ground
FUN-5.6.5: Document disposal activities and impact
Documentation

Legend

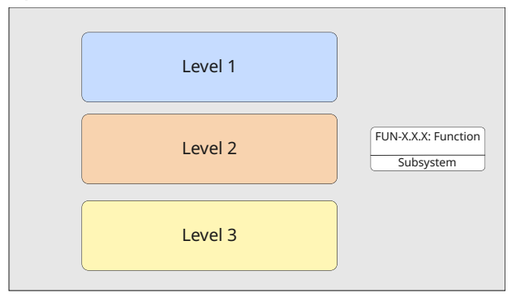
Level 1
Level 2
Level 3
FUN-X.X.X: Function
Subsystem

B

Verification Methods

Table B.1: *Explained Verification Methods of Requirements*

REQ-	Verification Method	REQ-	Verification Method
MIS-1	Range calculated through mission performance models	MIS-2	Conduct a battery-less ferry flight
MIS-3	Estimated from cruise speed and mission planning	MIS-4	Cost evaluated through subsystem cost breakdown
MIS-5	Aircraft speed profile analysed with 620 km/h capability	MIS-6	Mission loading and operational performance analysed.
OPS-1	Simulation will be made to optimise scheduling	OPS-2	Compliance will be checked by EU officers
OPS-3	Compliance will be checked by EU officers	OPS-4	Damage to local infrastructure will be analysed after missions
OPS-5	Damage to communities will be analysed after missions	OPS-6	Runway availability and range capabilities covers entire EU area
OPS-7	Lake sizes inspected against scooping system requirements	SUS-1	An analysis of emissions per mission has been done
SUS-2	A database of potentially dangerous water sources will be made	SUS-3	Compliance will be shown through operational demonstration
SUS-4	Testing on the retardant will be made to ensure biodegradability	SUS-5	A database of potentially dangerous water sources will be made
SYS-1	Verified against technology readiness levels	SYS-2	Cost evaluated through subsystem cost breakdown
SYS-3	Manufacturing origin will be inspected	SYS-4	Verified via performance and weight assessment
SYS-5	Design inspected for sealing and water avoidance features	SYS-6	Materials inspected for corrosion resistance
PROP-1	Verified via fuel system sizing	PROP-2	Verified through performance specifications and sizing
PROP-3	Will be estimated with performance modelling software	PROP-4	Engines will be tested in a control environment
PROP-5	Verified using take-off performance calculations	PROP-6	Will be demonstrated during a controlled test flight
PROP-7	Will be demonstrated during a controlled test flight	AER-1	Effect of ailerons will be analysed with flow simulation software
AER-2	Effect of ailerons will be analysed with flow simulation software	AER-3	Effect of ailerons will be analysed with flow simulation software
AER-4	Flight tests carried out with roll angle sensors	AER-5	Verified through trade-off analysis of airfoil geometries

Continued on next page

REQ-	Verification Method	REQ-	Verification Method
AER-6	More in-depth simulation will be made to evaluate this	AER-7	Verified via structural load case simulations
S&C-1	Verified by CG excursion analysis	S&C-2	Verified by CG range calculations
S&C-3	S&C calculation will be repeated considering for an extreme environment	EMP-1	Controlled test flights will prove compliance
EMP-2	Controlled test flights will prove compliance	EMP-3	Dynamic stability simulations will be conducted
EMP-4	Effect of rudder and elevator will be analysed with advanced software	EMP-5	Effect of rudder and elevator will be analysed with flow simulation software
EMP-6	Effect of rudder and elevator will be analysed with flow simulation software	EMP-7	Flight tests carried out with pitch angle sensors
EMP-8	Flight tests carried out with yaw angle sensors	FUS-1	Cockpit layout complies with visual flight rules
FUS-2	Cockpit dimensions fit 2 pilots	FUS-3	Placement and shielding inspected
FUS-4	Amphibious aircraft design guidelines followed	FUS-5	Fuel flow rate at inlet will be simulated
FUS-6	Structure analysed for given loading scenario	FUS-7	Structure analysed for given loading scenario
FUS-8	Visual inspection of paint application	FUS-9	Structure analysed for given loading scenario
FUS-10	Flow rate estimated with known scoop geometries	FUS-11	Inspect the presence of a scooping mechanism and its functionality
TANK-1	Drop will be cancelled in a test flight	TANK-2	Volume and structural calculations
TANK-3	Controlled slosh tests will be conducted	TANK-4	Cg will be measured due to tank filling
TANK-5	Oxygen payload estimated for given mission	TANK-6	Visual inspection of modular components
UCA-1	Loading of nose landing gear analysed	UCA-2	Hydrodynamic simulation will be conducted
UCA-3	Load analysis on landing gear conducted	UCA-4	Load analysis on landing gear conducted
LOG-1	Perform systems analysis on avionics and sensors	LOG-2	Inspect presence of flight aid systems
LOG-3	Demonstrate requirement by turning on the computer	LOG-4	Simulate on ground communication during mission
LOG-5	Communication will be demonstrated in extreme environments	LOG-6	Environmental conditions will be measured in test flight
LOG-7	System conditions will be measured in test flight	LOG-8	Test hydraulic endurance at given temperatures
LOG-9	Verify presence of firewalls, ventilation.	RAMS-1	Failure rates demonstrated after initial missions
RAMS-2	Maintenance requirements demonstrated after initial missions	RAMS-3	Time to repair demonstrated after initial missions
RAMS-4	Demonstration	RAMS-5	Systems analysed to ensure they are redundant

C

Appendix C

Task	David	Eliot	Marcos	Dario	Jorge	Simon	Syméon	Max	Cesar	Nico
Executive Overview										
Introduction										
Functional Analysis Overview										
Market Gap and Analysis										
Operations and Logistics										
Sustainability										
Aircraft Estimation Method										
Class 1 and 2 Estimations										
V-N Analysis										
Propulsion System										
Wing Group/Aerodynamic Analysis										
Wing Structure										
Stability and Control										
Empennage Design										
Fuselage Design										
Undercarriage										
Final Design and Budgets										
Verification										
Validation										
Aircraft Subsystem Logistics										
Risk Analysis and RAMS										
Cost Analysis and ROI										
Future Developement										
Conclusion										
CATIA Empennage										
CATIA Engine										
CATIA Floaters										
CATIA Fuselage (exterior and interior), Wing, Winglets, Scooping Mechanism and Assembly										